The electrical potential as a gauge of photosynthetic performance in plant chloroplasts: a patch-clamp study

De elektrische potentiaal als een graadmeter van de fotosynthese in chloroplasten van planten: een patch-clamp studie

Promotor   : dr. W.J. Vredenberg
                hoogleraar in de plantenfysiologie,
                met bijzondere aandacht voor de fysische aspecten
Co-promotor   : dr. J.F.H. Snel
                universitair docent bij de vakgroep Plantenfysiologie

Tijmen van Voorthuysen

The electrical potential as a gauge of photosynthetic performance in plant chloroplasts

A patch-clamp study

Cover shows a view through a light microscope of a *Peperomia metallica* chloroplast sucked onto the tip of a tapered open-ended glass patch-pipette. This is the experimental arrangement of the patch-clamp method which allows with relative ease the detection of light-induced potentials and currents. These electrical signals are a vestige of the photosynthetic activity at the chloroplast thylakoid membrane. Magnification 420x. (photograph taken by Hans Dassen).

STELLINGEN

I

De afleiding van een lag-fase in de electrogene reacties van de Q-cyclus in spinazie chloroplasten is onbetrouwbaar wanneer de vervalkinetiek van het electrische veld niet ondubbelzinnig is bepaald en geen rekening wordt gehouden met een snel dissiperende fractie van het electrische veld.

A. B. Hope and D. B. Matthews (1987), Aust. J. Plant Physiol. 14: 29-46
Dit proefschrift

II

De impliciete veronderstelling dat veranderingen in het electrische geleidingsnetwerk van de chloroplast geen significante rol spelen bij electrofysiologische metingen blijkt vaak onterecht. Het verdient aanbeveling geleidingsveranderingen consequent mee te nemen bij de bestudering van electrogene verschijnselen in de fotosynthetische membraan aan de hand van electrofysiologische metingen.

Dit proefschrift

III

Bij theorievorming gebaseerd op metingen aan chloroplastsuspensies wordt onvoldoende rekening gehouden met een mogelijk grote spreiding tussen individuele chloroplasten van een gemeten grootheid rond de gemiddelde waarde zoals die aan het licht komt met de patch-clamp methode.

Dit proefschrift

IV

De 15-voudig grotere magnitude van de theoretisch berekende thylakoïdspanning volgens modellering van vrije energietransductie in chloroplasten door O. van Kooten (1988) zou beter overeenkomen met de praktijk indien bij microelectrode metingen rekening wordt gehouden met het spanningsdelereffect zoals is afgeleid voor de patch-clamp methode.

O. van Kooten (1988), proefschrift Landbouwuniversiteit Wageningen
Dit proefschrift

V

Het voorkomen van bepaalde chemische verbindingen in planten hoeft niet altijd op een noodzakelijkheid voor de plant zelf te berusten.

"High na de aanval", Volkskrant 8 februari 1997

VI

De beste zorg voor het milieu zou in veel gevallen geen zorg moeten zijn.

VII

Nadenken over het file probleem is zinvol, maar je moet er niet te lang bij hoeven stilstaan.

VIII

Het gelijktijdig nastreven van flexibilisering van het arbeidsproces en vermindering van de drukte op de Nederlandse autosnelwegen toont ontegenzeglijk dat niet alles bereikbaar kan zijn.

IX

In onze op geld gebaseerde samenleving zal een volledige emancipatie van vrouw en man beter haalbaar worden door invoering van een volwaardige geldelijke beloning van zorg- en opvoedkundige taken.

"Betaalde moeders", De Volkskrant, 5 april 1997

X

Het educatieve computerspel SIMEARTH laat zien dat een samenleving spaakloopt wanneer beoefening van academische wetenschappen en cultuur wordt veronachtzaamd. Politiek Den Haag zou eerst spelletjes met de computer moeten spelen, vervolgens pas met de maatschappij.

Stellingen bij het proefschrift "The electrical potential as a gauge of photosynthetic performance. A patch-clamp study".

Wageningen, 3 juni 1997.   Tijmen van Voorthuysen

Voorwoord

De fysica van electrische verschijnselen is ontegenzeglijk verbonden met veel biologische processen, te denken valt aan de redox reacties in de ademhalingsketen of de electrostatische interacties die een rol spelen bij de driedimensionale vorm van eiwitmoleculen. In dit proefschrift wordt heel direct gekeken naar electrische signalen - stromen en spanningen - die in het plantencelorganel de chloroplast worden opgewekt onder invloed van licht. De beschreven patch-clamp methode staat het toe om deze lichtgeïnduceerde electrische verschijnselen te meten waaruit een beter begrip ontstaat over de wijze waarop de plant zonlicht vastlegt in energierijke bouwstoffen zoals glucose. De patch-clamp methode is een welkome aanvulling voor het biofysisch onderzoek naar de fotosynthese. Zeker in een tijd waarin samenwerking tussen wetenschappelijke disciplines sterk wordt bevorderd verdient het aanbeveling ook open te staan voor nieuwe toepassingen van de methode.

Voor degenen die proefschriften graag diagonaal lezen heb ik het hier extra aantrekkelijk gemaakt door invoering van korte samenvattingen in de hoofdstukken 3 tot en met 8. Bij het zoeken naar een volgende samenvatting doorkruis je gewild of ongewild toch alle bladzijden waardoor je en passant een behoorlijke indruk krijgt van het geheel, inclusief de figuren.

Hou je van puzzelen dan is een a(o)io baan een prachtige tijdsbesteding. Hou je van geld, dan niet. Ik hou meer van het eerste en heb het promotieonderzoek altijd met veel plezier gedaan. Daarbij heb ik me goed thuis gevoeld op de vakgroep. Electrofysiologie bleek een prima recept om fysische- en wiskundige methoden toe te passen op biologische systemen.

Voor menig idee en enthousiaste discussies ben ik mijn promotor Wim Vredenberg veel verschuldigd. Wim, je gaf me vaak interessante wegwijzers mee op mijn wetenschappelijke reis. Maar ook de niet minder belangrijke steun voor mijn levensreis ben ik niet vergeten. Voor meer wetenschappelijke degelijkheid kon ik prima terecht bij mijn co-promotor Jan Snel. Jouw kritische kennis van de fotosynthese en de biofysica hebben het fundament van mijn werk duidelijk verstevigd. Het biofysica clubje is zeker niet compleet zonder mijn goede vriend en collega Hans Dassen te noemen. Jouw Limburgse gastvrijheid, en niet te vergeten van Lenny natuurlijk, heeft mij altijd zeer goed gedaan. En bovendien, aan jouw ongedwongen wetenschappelijk visie kan menig a(o)io nog een puntje zuigen.

For a real state-of-the-art Russian electrophysiology I'll like to thank Alex(ander) Bulychev for his pleasant cooperation. Alex, I remember you as an unpretentious man who skills are not only restricted to successful experimental sciences but also extend to successful bowling and skating.

Naast kennis ontvangen heb ik ook kennis mogen uitdragen aan onder meer twee doctoraalstudenten, Martijn Jordans en Robert Huberts. Ik schrik 's nachts nog wel eens wakker met de vraag: schrikt Martijn nog wel eens wakker met de vraag: **!SPIKE?!**. Martijn, in hoofdstuk 5 kun je lezen wat nu de stand van zaken is. Gelukkig was Robert's gemoedstoestand minder onderhevig aan dit ongetwijfeld interessante fenomeen. Wilma, jou wil ik bedanken voor de ondersteuning bij de niet al te sprankelende P515 experimenten. Corine, ik wens jou veel sterkte toe bij de laatste zware loodjes van het proefschrift. Paul, jij vormt nu de harde kern van de electrofysiologie op onze vakgroep en ook jou wens ik nog veel onderzoeksplezier toe. Ja, Victor, samen (up)dates doornemen zal wel minder worden. Ik wens je heel veel plezier in je nieuwe baan. En als ik jou, de lezer, vergeten ben, je naam zal me misschien nog wel te binnen schieten, maar toch alvast bedankt. Tot slot denk ik aan de fijne momenten met Mariëtte.

Tijmen

CONTENTS

Abstract

The earliest events in the energisation of the photosynthetic membrane upon light capture are the formation of a transmembrane electrical potential ($\Delta\psi$) and a transmembrane proton gradient (ΔpH). In this thesis $\Delta\psi$ is employed for the study of the bioenergetics of chloroplast photosynthesis and its regulation by ΔpH in the shade adapted plant peperomia (*Peperomia metallica*) and the high-light adapted plant spinach (*Spinacia oleracea*). Electrochromism (P515) was used and a patch-clamp method was developed yielding two complementing tools for the detection of $\Delta\psi$. The patch-clamp method enables the detection of relatively large light-induced currents (photocurrents) or potentials (photopotentials) of a single *P. metallica* chloroplast. An electrical equivalent scheme is introduced incorporating amongst others the thylakoid membrane resistance and capacitance and an access resistance which, at least partly, is supposed to be associated with low (lateral) conductance phases of thylakoid lamellae. The light-induced electrical responses reflect the operation of the photosynthetic current-generators and the way generated current is distributed throughout the chloroplast conductance network. Simultaneous measurements of light- and current-induced responses allow the separation of electrogenic events from changes in chloroplast conductances. A kinetically well defined slow secondary phase (R1/Q) could be distilled from the flash-induced photocurrent/-potential which is related to the turnover of the cyt. *bₒf* complex (Q-cycle). Generally, the rise of R1/Q was sigmoidal. This biphasic rise is modelled by a consecutive reaction scheme with two relaxation times of 13 and 28 ms which likely reflect the oxidation of plastoquinol and reduction of plastoquinone at the lumen and stroma membrane/water interface of the *bₒf* complex, respectively. A P515 fraction (R1/RCf) of about 20 % is inadequately stabilised in dark-adapted spinach chloroplasts and decays rapidly with a relaxation time of 1 - 2 ms. A fast dissipation of $\Delta\psi$ as generated by photosystem (PS) II is suggested to cause R1/RCf. It is hypothesised that adequate charge stabilisation depends on efficient energy coupling between PS II and the cyt. *bₒf* complex which is only guaranteed in superclusters composed of both protein complexes. Energisation causes a suppression of about 50 % of PS II-dependent charge separation which is dark reversible with a relaxation time of about 20 s and is likely induced by the low lumenal pH created by light-driven proton pumping. The results are best explained by a reaction center quenching model in which a fraction of PS II centers exhibits a rapid charge recombination. Flash-induced changes in chloroplast conductances are first demonstrated. The seal conductance decreases transiently upon a brief flash with a minimum of 0.3 - 5 % at 50 - 200 ms after the flash and a slow relaxation in 1 - 10 s. It is proposed that an important part of the conductance changes is intimately associated with changes in the lateral conductances of thylakoids, in particular those of the narrow spaced grana thylakoids.

Keywords membrane potential, patch-clamp method, photosynthesis, electrogenesis, Q-cycle, photosystem II, *Peperomia metallica, Spinacia oleracea*, energisation.

📖 Abbreviations

A_{thyl}	surface area of thylakoid membrane
ATP	adenosine triphosphate
ADP	adenosine diphosphate
b_h	high potential b-heme of the cyt. b_6f complex
b_l	low potential b-heme of the cyt. b_6f complex
bleb	osmotically swollen thylakoid
BSA	bovine serum albumin
β	amplitude of slow potential rise upon current-injection of sealed chloroplast
Chl	chlorophyll
C_M	membrane capacitance (nF)
C_{spec}	specific membrane capacitance
cyt. b_6f	cytochrome b_6f complex
DBMIB	2,5-dibromo-3-methyl-6-isopropyl-p-benzoquinone
2,6-DCBQ	2,6-dichloro-p-benzoquinone
DCCD	dicyclohexylcarbodiimide
DCMU	3-(3,4-dichlorophenyl)-1,1-dimethylurea
DQH_2	duroquinol
$\Delta\psi$	transmembrane electrical potential
$\Delta\mu_{H^+}$	transmembrane electrochemical potential of protons
ΔpH	transmembrane proton gradient
EDTA	ethylenediaminotetraacetate
ETC	electron transport chain
F_0	minimal dark level of chlorophyll fluorescence
F_A, F_B, F_X	acceptors of PS I
Fd	ferredoxin
FeCy	ferricyanide
FeS	Rieske iron-sulfur protein
FNR	ferredoxin-NADP$^+$ oxidoreductase
FR	far-red light
g_{seal}	seal conductance
HEPES	4-(2-hydroxyethyl)-1-piperazineethanesulfonic acid
I_{comm}	command current
I_P	initial amplitude of flash-induced photocurrent
$I_P(t)$	light-induced current (photocurrent)
LHC	light harvesting complex
MES	2-(N-morpholino)-ethanesulfonic acid
NADP$^+$	nicotinamide-adeninedinucleotide (oxidised)
NADPH	nicotinamide-adeninedinucleotide (reduced)
OEC	oxygen evolving complex

p	relative measure of decrease in field dissipation relaxation time
P515	absorbance change at 518 nm
P680	reaction center chlorophyll of photosystem II
P700	reaction center chlorophyll of photosystem I
PAR	photosynthetically active radiation
PC	plastocyanin
Pheo	pheophytin, primary electron acceptor in photosystem II
P_i	phosphate anion
PMS	N-methylphenazonium methosulfate
PQ	plastoquinone
PQ^-	plastosemiquinone
PQH_2	plastoquinol
PS	photosystem
Q_A	primary quinone electron acceptor of photosystem II
Q_B	secondary quinone electron acceptor of photosystem II
q_E	energy-dependent quenching parameter
q_N	non-photochemical quenching parameter
q_P	photochemical quenching parameter
Q/RC-ratio	ratio of charges displaced by Q-cycle and by PS I and II reaction centers upon a single-turnover flash
Q_n-site	plastoquinone reduction and proton uptake site of the cyt. b_6f complex near the stroma membrane/water interface
Q_p-site	plastoquinol oxidation and proton release site of the cyt. b_6f complex near the lumen membrane/water interface
R1/Q	Reaction 1/Q associated with secondary charge separation involving cyt. b_6f turnover
R1/RC	Reaction 1/RC associated with primary charge separation
$R1/RC_f$	Reaction $1/RC_f$, P515 component with a slow relaxation associated with primary charge separation
$R1/RC_S$	Reaction $1/RC_S$, P515 component with a fast ms relaxation associated with primary charge separation
R_A	access resistance
R_L	leak resistance
R_M	membrane resistance
R_S	seal resistance
R_T	tip resistance
RC	reaction center
$t_{1/2}$	half-time; time after flash at which amplitude is half the initial amplitude
τ_1, τ_2	relaxation times describing the sigmoid rise of R1/Q in flash-induced photocurrent/-potential
τ_{CC}	voltage relaxation time of whole-thylakoid configuration under current-clamp
τ_D	diffusion-driven membrane relaxation time

τ_M	native diffusion-driven membrane potential relaxation time
TMPD	N,N,N',N'-tetramethylphenylene-diamine
Tyr_Z	tyrosine Z, primary donor of $P680^+$
V_0	initial level of potential output response of seal upon current-injection
V_h	holding potential
V_M	initial value of single-turnover flash-induced thylakoid membrane potential ($\equiv V_M(t=0)$)
$V_M(t)$	thylakoid membrane potential
V_P	initial amplitude of flash-induced photopotential ($= V_P(t=0)$)
$V_P(t)$	light-induced potential (photopotential)
V_{SS}	steady-state potential of patched chloroplast upon current-injection
V_T	potential of patch pipette upon current-injection

Chapter 1   General introduction

Why do plants look green? One of the common questions asked to a photosynthesis researcher. This small interrogative sentence highlights two important aspects of experimental sciences in general and photosynthesis research in particular. The first aspect is the way we look at matters, the second is the result of this 'looking' action. Figure 1-1 shows an electron microscopic picture of a chloroplast from *Peperomia metallica*, the plant species which was routinely used for the measurements described in this thesis. With electron microscopy the fast travelling electrons serve to produce an image of the internal thylakoid structure of the chloroplast and the outcome is definitely not green, contrary to how a chloroplast looks like under normal day light. Thus, with different methods the same entity apparently may look different.

Fig. 1-1   Electron microscopic picture of a *Peperomia metallica* chloroplast. GL, grana lamellae; SL, stroma lamellae; E, envelope membrane; SG, starch grain.

This thesis is mainly concerned with the detection of the transmembrane electrical field or potential ($\Delta\psi$) which is generated when the photosynthetic apparatus is illuminated. The two experimental tools used for probing $\Delta\psi$ are electrochromism and a modified patch-clamp method. Again, the results obtained with both tools (Fig. 1-2) show mutual agreements and disagreements. The combination of both methods will certainly provide an improved understanding of energy regulation and associated (electrogenic) processes in the photosynthetic membrane. What can we 'see' with this patch-clamp method? First, it provides a direct proportional measure of the electrical field which results from photosynthetic charge separation. Second, low conductance phases in the extended and many times folded thylakoids inside the chloroplast (Fig. 1-1) are sensed. Any alterations in the organisation of the thylakoids, including ion redistributions and structural changes, may be sensed with the method. The patch-clamp method then provides a new, supplementary experimental tool for 'looking' at the bioenergetic processes of photosynthesis besides to the more established techniques like chlorophyll fluorescence, absorption spectroscopy or light scattering.

The study of the highly efficient processes of photosynthesis is promising as a guidance for designing artificial systems for efficient energy conversion of solar radiation into electrical power (Byrd *et al.* 1996). Can we use the electrical power of chloroplasts? Disregarding any technological obstacles it can be deduced from the results of Chapter 3 that a single patch-clamped chloroplast can produce a steady-state current (I) of about 50 pA in continuous light which flows through a pipette resistance (R_T) of about 5 MΩ. The associated energy (U) follows from the relationship,

$$U = \int_0^\infty R_T \cdot I^2(t) \cdot dt$$

So, with an energy output of 1.25 10^{-14} Watt the photosynthetic micro power-plant produces 4.5 10^{-11} J in one hour. Not less than about 10^{16} chloroplasts, covering a surface area of 5.8 square kilometer of *P. metallica* leaves, need then be arranged in parallel to run a household appliance like a coffee machine.

Solar energy is efficiently captured by the photosynthetic pigments in the antennae of photosystem (PS) I and II, mainly chlorophyll *a* and *b*, after which a cascade of reactions finally produces the useful energy-rich molecule glucose. The 'light'-reactions generate ATP as an energy-storage molecule and NADPH as reducing power. The two products subsequently serve as the fuel to run the 'dark'-reactions of the Calvin-Benson cycle. The energetic link between photosynthetic electron transport and ATP formation is the transmembrane electrochemical potential of protons ($\Delta\mu_{H^+}$). The proton electrochemical potential is composed of the energetically equivalent transmembrane proton gradient (ΔpH) and $\Delta\psi$ (Junesch and Gräber 1991). Since the transmembrane electrical potential is relatively small during continuous illumination (Vredenberg and Tonk 1975, Admon *et al.* 1982) the largest contribution to $\Delta\mu_{H^+}$ comes from ΔpH (Rottenberg *et al.* 1972) and $\Delta\psi$ plays just a minor role in photosynthetic energy transduction. Why then study $\Delta\psi$ in chloroplasts?
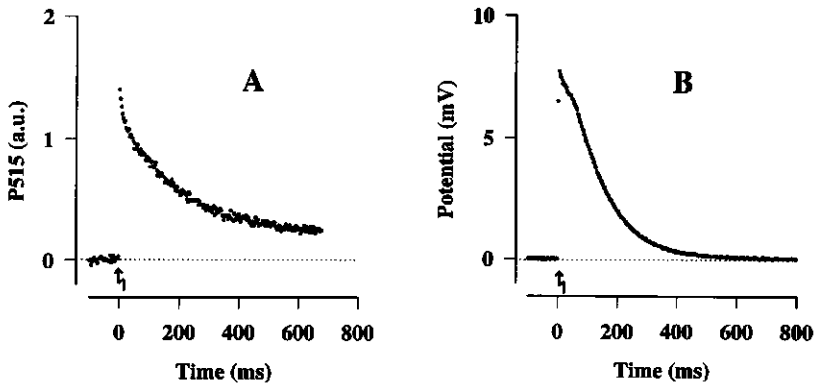
Fig. 1-2   Agreements and disagreements in the detection of the transmembrane electrical potential in
P. metallica chloroplasts by electrochromism (**A**) and the patch-clamp method (**B**). A single-
turnover light flash produces a rapid initial rise caused by primary charge separation in PS I
and II reaction centers followed by a slow discharge of the electrical field due to ion fluxes
across the membrane.

The transmembrane electrical field can act, though, as a gauge of ongoing energy
transduction. The activity of the photosystems, especially of photosystem II (Chapter 6),
and of the Q-cycle involving the cyt. b_6f complex (Chapter 4) were followed by flash-
induced potential generation. Information about membrane permeability and ion fluxes
across the membrane is contained in the discharge of the electrical field (Fig. 1-2, Junge
and Witt 1968, Bulychev and Vredenberg 1976a). The electrical field may also act as a
regulator of photosynthetic energy transduction. The rates of radical pair formation as
well as charge stabilisation and charge recombination in the photosynthetic reaction
center (RC) are slightly controlled by the membrane potential (Meiburg *et al.* 1983, Leibl
et al. 1989, Dau and Sauer 1992). The transmembrane potential also regulates electrically
triggered conformational changes of the ATP synthase (Junge 1970, Gräber *et al.* 1977).
The local electrical field arising from charge separation in the reaction centers was
discussed to affect adjacent ATP synthases thereby having control over a localised energy
coupling (Skulachev 1982). The lipid microviscosity was found to increase with applied
membrane potentials which might reduce lateral and rotational motion of membrane
proteins (Corda *et al.* 1982). Finally, a transmembrane electrical potential may alter the
electrogenic reactions in or at the cyt. b_6f complex (Bouges-Bocquet 1981, Van Kooten *et
al.* 1983, Hope and Rich 1989).

Three main topics will now be discussed in more detail. The first topic will cover a
diversity of electrogenic reactions occurring in the photosynthetic membrane. This will
place the patch-clamp method and the achieved results in a broader context. In addition
this survey will add to our knowledge about electrogenic processes to be anticipated

3

while interpreting the subjects described in this thesis. The second topic, the structural organisation of the thylakoid membrane, will have relevance amongst others for the light-induced conductance changes. The last topic is the role of protons in photosynthesis. This will be helpful in understanding the energisation-dependent suppression of the flash-induced electrical potential which is discussed in Chapter 6.

The field of photosynthesis research covers many subjects ranging from the fast spectroscopic studies on exciton migration in the photosynthetic antennae to the biochemical pathways of carbon fixation. Here some latest reviews are suggested which were most extensively used for this thesis: Structure, function and organisation of photosystem I (Golbeck 1992, Chitnis *et al.* 1995); Structure, function and organisation of the cytochrome *b₆f* complex (Hope 1993, Cramer *et al.* 1996); Structure, function and organisation of photosystem II and its chlorophyll *a* fluorescence (Dau 1994); The chloroplast ATP synthase (Ort and Oxborough 1992, van Walraven and Bakels 1996); Proton conductivity and proton exchange between bulk and membrane surface (Gutman and Nachliel 1995); Cyclic photophosphorylation and electron transport (Bendall and Manasse 1995); Photosynthetic control revised (Foyer *et al.* 1990).

1.1 The electrogenic events in photosynthesis

Within less than 3 ps after light capture by the antennae system or light-harvesting complex (LHC) the excitation energy or exciton is equilibrated throughout the main pool of chlorophyll pigments (Holzwarth *et al.* 1993). The antennae of higher plant PS I and II exhibit several trimeric LHC II moieties (Fig. 1-3) (Kühlbrandt and Wang 1991, Dreyfuss and Thornber 1994). When the exciton visits the primary donor (P) of the reaction center this pigment molecule is raised to the excited state (P*) which has a finite probability to ignite primary charge separation between P and an acceptor molecule (A). The excitation energy is thus trapped in the reaction center. The trapping time involves reversible processes like exciton transfer between the antenna pigments and the primary donor, formation of P*, and formation of the charge separated state P⁺A⁻ (Trissl and Leibl 1989). Due to ionic movements in the aqueous phases along both sides of the membrane and to polarisation of the membrane dielectricum the local charge separated state is rapidly delocalised within about 0.1 - 10 μs (Fowler and Kok 1974, Witt 1979).

The bulk-to-bulk electrical potential ($\Delta\psi_{DA}$) resulting from charge transfer between a donor (D) and an acceptor (A) within a membrane is given by the total charge transferred (q), often equal to the elementary charge unit, divided by the capacitance (C_M) of the membrane. The membrane capacitance of biological membranes per unit surface area is usually assumed to be 1 μF cm⁻² (Vredenberg 1976). If the charge is transferred within the membrane, along a charge-transfer distance vector ($\vec{d}_{DA}$) that is smaller than the total thickness (D_M) of the membrane, $\Delta\psi_{DA}$ must be weighted with the distance component parallel to the membrane normal, a unity vector ($\hat{n}$) perpendicular to the membrane. In addition, the measured potential is proportional to the number of active

reaction centers (N) and must be weighted with the average dielectric constant of the membrane (ε_M) in which the reaction takes place (Höök and Brzezinski 1994):

$$\Delta \psi_{DA} = \frac{N \cdot q}{C_M} \cdot \frac{(\vec{d}_{DA} \cdot \vec{n}) / \varepsilon_{DA}}{D_M / \varepsilon_M} = \Delta \psi_0 \cdot \frac{d_{DA}}{\varepsilon_{DA}} \cdot \frac{\varepsilon_M}{D_M} \qquad (1\text{-}1)$$

ε_{DA} is the effective (protein) dielectric constant around the donor D and acceptor A and $\Delta \psi_0$ is the potential difference associated with the transfer of one charge in each reaction center across the entire membrane.

Each electron transport reaction or the transport of a cation/anion through the membrane can be analysed by a lateral and a transverse electrogenic component. Here, electrogenic reactions will be discussed as reactions which contribute to a *transmembrane* electrical potential, hence only the transverse component is considered. Electrochromic changes in the visible spectral region and at a wavelength of 443 nm which are associated with the oxygen-evolving system when it is clocked through its oxidation states are not related to a transmembrane electrical potential but to local uncompensated charges (Saygin and Witt 1985). Ergo, they are not considered here.

Several techniques are at hand for detecting electrogenic events in the functional photosynthetic membrane. Electrochromism, a dipole property of pigments, was first applied for the detection of the transmembrane electrical field in the photosynthetic membrane by Witt (1967). Electroluminescence was discovered by Arnold and Azzi (1971) and is the chlorophyll luminescence resulting from electrical field-induced charge recombination. A more direct measurement of the electrical potential during prolonged illumination became possible by the introduction of the open-ended microelectrode technique for impalement of single *P. metallica* chloroplasts by Bulychev *et al.* (1971, 1972). Fast electrogenic reactions with picosecond time resolution in oriented reaction centers preparations is accomplished by the photovoltage technique first described by Fowler and Kok (1974). The extrinsic optical probe oxonol VI was first used in spinach thylakoids to supplement for single-turnover and continuous illumination (Schuurmans *et al.* 1978). At last, the patch-clamp technique introduced by Bulychev's group was initially developed to study photosynthetic ion currents as a function of a clamped membrane potential (Bulychev *et al.* 1992).

Table 1-1 presents an overview of electrogenic events in the photosynthetic membrane.

Table 1   Electrogenic events in the thylakoid membrane and membrane fragments of plant chloroplasts.

Electrogenic event	Time (s)	Material	References
charge separation P700⁺A₀ (22 ps), P700⁺A₁ (50 ps)	10^{-12}	Synechocystis sp. - PS II-deficient mutant	Hecks et al. (1994)
trapping of P680⁺Pheo⁻ (50–100 ps)		barley - PS I-deficient mutant; pea - PS II membranes	Trissl and Leibl (1989); Leibl et al. (1989)
charge stabilisation P680⁺Q$_A$ (300–450 ps) (550 ps)		pea - PS II inactivated blebs; pea - PS I membranes	Trissl et al. (1987); Leibl et al. (1989)
back reaction in RC II (0.8 - 1.2 ns)	10^{-9}	pea - PS II membranes	Leibl et al. (1989)
primary charge separation PS I and PS II (< 20 ns, electrochromism)			Wolff et al. (1969)
re-reduction P680⁺ by Tyr Z (29 ns)		pea - BBY membranes	Pokorny et al. (1994)
primary charge separation PS I and PS II (electrochromism)	10^{-6}	spinach - intact and broken chloroplasts	Junge and Witt (1968), Schliephake et al. (1968), Schapendonk et al. (1979)
F$_B$ (F$_X$) → F$_A$ (30 μs)		spinach - PS I particles	Sigfridsson et al. (1995)
charge recombination A₁(F$_X$) → P700 (330 μs)		spinach - PS I particles	Sigfridsson et al. (1995)
reteduction of Z⁺ by S-states (0.1 ms)		spinach - blebs	Vos et al. (1991)
protonation of Q$_B^{2-}$ (0.2 - 0.8 ms)		spinach - reconstituted PS II core; cyanobacteria - PS II particles	Höök and Brzezinski (1994); Mamedov et al. (1994)

Process	Time scale	System	References
primary charge separation PS I and PS II (electrophysiology)	10^{-3}	peperomia - single intact chloroplasts	Vredenberg (1976), Vredenberg et al. (1995a)
reduction of b_h in b_6f complex (4-5 ms) in reducing conditions		spinach - thylakoids	Jones and Whitmarsh (1985), Kramer and Crofts (1994)
re-oxidation b-cytochromes/proton uptake from stroma at Q_n-site (~4 ms)		spinach – thylakoids	Jones and Whitmarsh (1985)
proton movement stroma to Q_p-site in reducing conditions (20 ms)		algae - intact cells	Joliot and Joliot (1986)
Q-cycle with two electrogenic steps (13 and 28 ms)		peperomia - single intact chloroplasts	van Voorthuysen et al. (1996b)
trans-membrane ion fluxes (H^+, K^+, Mg^{2+}, Cl^-)		spinach - chloroplasts / peperomia - chloroplasts in situ / spinach - chloroplasts/thylakoids	Junge and Witt (1968), Bulychev and Vredenberg (1976a), Bulychev et al. (1980), Schapendonk et al. (1979)
H^+ dissipation through ATP synthase (200 - 300 ms)	1	pea - intact chloroplasts	Ooms et al. (1991)
ATP hydrolysis steady-state electrogenesis / light-induced steady-state electrogenesis		spinach - ATP synthase / spinach - thylakoids / lettuce - chloroplasts / peperomia - chloroplasts in situ	Shahak et al. (1982), Schuurmans et al. (1978), Admon et al. (1982), Vredenberg and Tonk (1975), Bulychev et al. (1976)

This table only includes reactions which were concluded from techniques that directly reflect the creation and decay of an electrical (membrane) potential. References cited were selected by the criterion that they contain kinetic information of electrogenic processes. The vertical time scale is shown for illustrative purposes only.

Primary charge separation in photosystem I and II

The primary structure of photosystem I (Fig. 1-3) and the overall mechanism of PS I functions are remarkably conserved among cyanobacteria, green algae and plants (Golbeck 1992). The monomer of PS I, with a total M_r of 340 K including 100 (cyanobacteria) or 200 (plant) antenna chlorophylls, contains the primary donor P700 probably a chlorophyll *a* dimer (Krauss *et al.* 1993, Evans and Nugent 1993). The primary acceptor of PS I (A_0) is generally believed to be a monomeric chlorophyll *a* molecule although unequivocal evidence for its existence is still scarce (Holzwarth *et al.* 1993). The secondary electron acceptor A_1 is a phylloquinone molecule (vitamin A). The following electron acceptors are the three iron-sulfur clusters F_X, F_b and F_A and finally the soluble PS I acceptor ferredoxin (Fig. 1-3).

The primary charge separation in PS I is essentially trap-limited, even though exciton transfer time and charge separation time are in relative close succession (Holzwarth *et al.* 1993). Two fast electrogenic steps of 22 ps and 50 ps (Fig. 1-3, ❶ and ❷) are involved in PS I charge separation from P700 to A_1 as detected by the photovoltage technique (Hecks *et al.* 1994). Assuming a homogeneous dielectric within the RC, the electron transfer between A_0 and A_1 spans only a small part (20 ± 8 %) of the distance P700-A_1, see Fig. 1-3 (Hecks *et al.* 1994). Some agreement of these figures has been found with X-ray analysis of PS I core crystals (Krauss *et al.* 1993): distance A_0-A_1 suggests only 13 % electrogenicity and A_0 is indeed located at a great distance from P700. The modelling of electroluminescence data on spinach blebs (Vos and van Gorkom 1990) gave very different results and showed that charge separation in PS I occurred with at least 3 electrogenic electron transfer steps (with dielectrically weighted distance in percentage): P700 to A_0 (30 %), A_0 to A_1 (50 %) and A_1 to F_A (20 %) (Fig. 1-3, ❸ for the latter step). These figures are less plausible and inconsistent with the crystal structure data (Krauss *et al.* 1993). F_A and F_B are located on the polypeptide *PsaC* protruding out of the membrane and are thus exposed to a local dielectric constant which is significantly higher than that inside the lipid membrane (Hecks *et al.* 1994). Although the electrogenicity of charge transfer between F_B and F_A is therefore expected to be small (see eq. 1-1) a 30 µs component ascribed to this process was observed by Sigfridsson *et al.* (1995) (Fig. 1-3, ❹). Upon chemical reduction of F_A and F_B a 330 µs electrogenic phase was observed which is assigned to charge recombination from A_1 or F_X to P700 (Sigfridson *et al.* 1995).

The PS II core complex consists of the proteins CP43, CP47, D1, D2, the α and β subunits of cytochrome b_{559}, and the lumen-faced proteins 17 kDa, 24 kDa and 33 kDa (Fig. 1-3). The charge separated state P680⁺Pheo⁻ is stabilised on the acceptor side by further electron transfer to the bound quinone Q_A and exchangeable quinone Q_B and on the donor side by electron donation from the oxygen-evolving complex via Tyr$_Z$, a Tyr-161 residue of the D1 protein (Debus *et al.* 1988).

The electrogenicity of primary charge separation in PS II also involves two main steps. Within a trapping time of 50 - 100 ps the radical pair P680⁺Pheo⁻ is formed which will proceed by forward electron transfer to the state P680⁺Q_A⁻, the charge stabilisation reaction taking about 300 - 500 ps (Trissl *et al.* 1987, Leibl *et al.* 1989, Trissl and Leibl 1989). The pheophytin is located approximately halfway P680 and Q_A with dielectrically

weighted distances of $d_{P680-Pheo} = 58 \pm 8$ % and $d_{Pheo-Qa} = 42 \pm 8$ % (Fig. 1-3, ❺ and ❻) (Trissl and Leibl 1989). These distances can be expected from the homology between the RC's of purple bacteria and PS II (Michel and Deisenhofer 1988).

The rereduction of $P680^+$ by Tyr_Z (Fig. 1-3, ❼) is probably electrogenic but of a quite small magnitude and it was argued to be less than 10 % of the total transmembrane charge separation (Trissl *et al.* 1987). Recently, Pokorny *et al.* (1994) found a 29 ns component ascribed to rereduction of $P680^+$ by Tyr_Z in their photovoltage experiments which represented 16 % of the total electrogenicity of $P680^+Q_A^-$. Electron transfer from the OEC to Tyr_Z is without (Höök and Brzezinski 1994) or, as an electroluminescence study demonstrated, with a only small amount (5 %) of electrogenicity scaled on the charge separation $P680^+Q_A^-$ (Vos *et al.* 1991). The rate of this reaction was about 10 ms^{-1} if the OEC was in the S_2 state (transition $Z^+M^{2+} \rightarrow ZM^{3+}$) (Vos *et al.* 1991).

Electron transfer from Q_A to Q_B is likely to have an insignificant contribution to the transmembrane electrical field as can also be concluded from the lateral orientation of the two quinones (Fig. 1-3). Indeed, in the PS II reaction center of spinach the electrogenicity for the reaction $Q_A^-Q_B \rightarrow Q_AQ_B^-$ is less than 5 % (Höök and Brzezinski 1994) or below detection limits (Vos *et al.* 1991). The subsequent proton uptake from the stromal phase upon protonation of Q_B^{2-}, proceeding with a time constant of 0.8 ms, amounts about 4 - 5 % of the total charge separation voltage (Fig. 1-3, ❽) (Höök and Brzezinski 1994). In bacterial reaction centers this electrogenicity was about 2 - 3 times larger with a time constant of 0.4 ms (Dracheva *et al.* 1988). Mamedov *et al.* (1994) showed that in the cyanobacterium *Anacystis nidulans* the dismutation of Q_A^- and Q_B^- and subsequent protonation of Q_B^{2-} gives an additional electrogenic phase with a relaxation time of 0.27 ms at pH 7.0 and an amplitude of 4 % of the fast electrogenic phase associated with the formation of $P680^+Q_A^-$. Both amplitude and relaxation times were unaffected in the pH-range 6 - 8.5 (Mamedov *et al.* 1994).

Electrogenicity involving cytochrome b_6f turnover (Q-cycle)

The cytochrome b_6f complex consists of four main subunits (Fig. 1-3): cytochrome b_{563} (24 kDa) accommodating the low (b_l) and high (b_h) potential b-hemes, cytochrome f (31 kDa), the Rieske iron-sulfur center (20 kDa) and a subunit IV (19 kDa) (Hope 1993). Although a complete data set on the amino-acid sequences of the four subunits exists the total molecular structure of the cytochrome b_6f complex in the membrane has not been elucidated yet (Hope 1993) and Fig. 1-3 shows a hypothetical arrangement of the proteins. The cyt. b_6f complex, operating as a redox link in linear electron flow between PS II and PS I and involved in PS I-dependent cyclic electron flow, shows two specific sites for interaction with plastoquinone. A quinol oxidation site (Q_P-site) located at the lumenal interface is well characterised through the specific inhibition by DBMIB, stigmatellin and 2-iodo-6-isopropyl-3-methyl-2',4',4'-trinitrodiphenylether (DNP-INT) of the slow electrochromic phase, and of cyt. b_{563} and cyt. f reduction (Jones and Whitmarsh 1988, Hope 1993). At the opposite site of the membrane a quinone reduction site (Q_n-site) is proposed where plastoquinone is reduced concomitantly with proton uptake from the stroma. Convincing evidence for this site is, however, still sparse (Hope and Rich

1989, Hope 1993). The inhibitors 2-*n*-heptyl-4-hydroxyquinoline *N*-oxide (HQNO) and 2-*n*-nonyl-4-hydroxyquinoline *N*-oxide (NQNO) are thought to act specifically with the Q_n-site (Jones and Whitmarsh 1988, Rich *et al.* 1991).

Velthuys (1978) has shown that a slow electrogenic event was involved with intersystem electron transfer from PS II to PS I which was coupled to proton release in the lumen upon plastoquinol oxidation. The slow electrogenic event is likely to arise from a transmembrane charge displacement, either an outward directed movement of an electron, or inward directed movement of a proton. Most customarily the slow electrogenic event is modelled as a Q-cycle as was originally formulated for the mitochondrial bc_1 complex (Mitchell 1976). In the traditional Q-cycle model a first electron upon PQH_2 oxidation at the Q_p-site is diverted laterally to the high potential chain comprising the photooxidised FeS and cyt. *f*, and the second electron is diverted transversally to a low potential chain comprising the two *b*-hemes. Subsequent oxidation of a second PQH_2 molecule results in reduction of both *b*-hemes which is followed by PQ reduction with concomitant proton uptake at the Q_n-site. The electrogenicity is then mainly associated with the charge transfer reaction between b_l and b_h: charges on the high potential b_h are located nearer to the stroma interface, probably about halfway across the membrane, than on the low potential b_l which is located at the lumenal membrane/water interface (Robertson and Dutton 1988, Kramer and Crofts 1994).

The slow electrochromic phase, the so-called slow phase b of the P515 response, has been taken as evidence for the Q-cycle electrogenicity as observed in algae (Joliot and Delosme 1974) and plant chloroplasts (Velthuys 1978). The rise of the slow P515 phase regularly proceeds with a relaxation time of 3 - 20 ms in spinach and pea chloroplasts (Girvin and Cramer 1984, Jones and Whitmarsh 1985, Hope and Matthews 1987, Ooms *et al.* 1989). Similarly, in the presence of DQH_2 and DCMU, a reducing poise suitable for inducing Q-cycle activity (Ooms *et al.* 1989), a 7 ms slow phase b was observed in pea thylakoids (Hope *et al.* 1992). The kinetics and extent of the slow P515 phase are related to the ambient redox potential (Hope and Matthews 1987). For whole-chain electron transport at relatively oxidising conditions the half-time for the slow P515 phase was 18 - 20 ms but decreased to 3 - 5 ms at a relatively low ambient potential, i.e. under reducing conditions in the presence of duroquinol (Hope and Matthews 1987). This redox dependency is likely responsible for the light stimulation of the Q-cycle (see Chapter 4 of this thesis, Velthuys 1978) which shows that a reductant, probably plastoquinol, is required. The amplitude of the slow P515 phase was measured to be constant from -200 mV up to about +80 mV followed by a sheer drop to about zero for higher ambient redox potentials (Girvin and Cramer 1984).

To resolve the true magnitude of the electrogenicity of reactions associated with the slow electrogenic turnover of the b_6f complex takes more effort than for PS I and II. Most studies agree on an electrogenicity of 60 - 80 % for the reduction of b_h and it is likely that the two *b*-hemes are separated by 60 - 80 % of the dielectrically weighted distance across the membrane (Fig. 1-3, ❾) (Jones and Whitmarsh 1985, 1988, Robertson and Dutton 1988, Kramer and Crofts 1994). The deposition of protons in the lumen at the Q_p-site upon plastoquinol oxidation and the concomitant electron transfer

to h are probably non-electrogenic processes (Robertson and Dutton 1988).

The group of Jones and Whitmarsh has proposed that the slow electrogenic step associated with b_6f turnover measured in the presence of DQH_2 and DCMU is composed of at least two consecutive reactions (Jones and Whitmarsh 1985). In their model electron transfer between the two b-hemes accounts for 70 % electrogenicity while 30 % is related to the Q_n-site (Fig. 1-3, ❾ and ❿, respectively), the latter either caused by the oxidation of cyt. b_{563} or by proton uptake from the stroma or both (Jones and Whitmarsh 1986, 1988). In contrast, Hope and Rich (1989) reasoned that in pea chloroplasts proton uptake at the Q_n-site is probably non-electrogenic.

The slow phase of P515 can occur even when both b-hemes are fully reduced, e.g. for sufficient dark-adapted *Chlorella* cells under anaerobic conditions (Joliot and Joliot 1986) or in the presence of dithionite (Bouges-Bocquet 1981). With a half-time of only 2 - 10 ms for the slow P515 rise the extent of the electrogenic step under these conditions was as high as 1.2 - 1.5 charges transferred through the membrane per charge transferred by the PS I charge separation reaction (Bouges-Bocquet 1981, Joliot and Joliot 1986). Surely, this must exclude a direct coupling between the electrogenic step and cyt. b_{563} reduction. Therefore, electrogenic H^+ movement (Fig. 1-3,⓫) was postulated to explain the results (Girvin and Cramer 1984, Joliot and Joliot 1985, 1986). Moreover, a rapid oxidation of cyt. b_{563} was observed followed by a slow dark reduction (Girvin and Cramer 1984, Joliot and Joliot 1986). The oxidation of cyt. b_{563} was thought to be initiated by the oxidation of heme h by a semiquinone bound to the Q_p-site which was formed after first oxidation by photooxidised Rieske-iron. This may then be followed by electrogenic movement of a proton from the negative stromal phase to the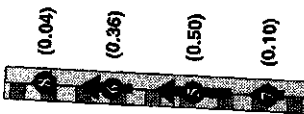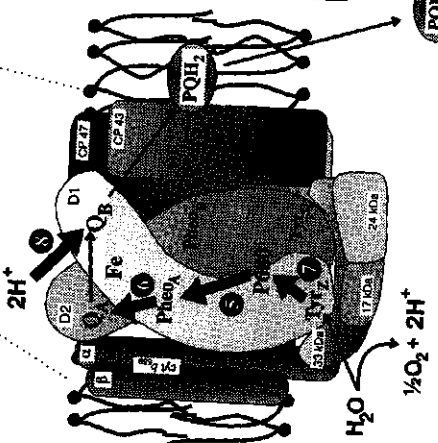 Q_p-site (Joliot and Joliot 1985, 1986). This model implies the presence of a transmembrane proton channel at or through the cyt. b_6f complex (Joliot and Joliot 1985, 1986).

Fig. 1-3 (next pages). The thylakoid membrane of chloroplasts is the site of several electrogenic reactions which are indicated by a bold arrow (⬆). (**Upper part**) The thylakoid grana-stroma organisation. Open arrows (⇧) indicate proton uptake and release reactions. The proton stoichiometry shown is based on the travelling of two electrons through the electron transport chain, including a Q-cycle. The membrane-spanning protein complexes PS I, PS II and the cyt. b_6f complex participate in linear electron flow. The ATP synthase complex couples the light-induced electrochemical proton gradient with phosphorylation of ADP and P_i into ATP. (**Lower part**) The polypeptide organisation of PS I was derived essentially as in Golbeck (1992) and Chitnis *et al.* (1995). The polypeptide organisation of PS II was derived essentially as in Dau (1994) and Govindjee and van Rensen (1993). The polypeptide organisation of the cyt. b_6f complex is a hypothetical model based on the properties of the individual subunits (Hope 1993). The polypeptides of the PS II and cyt. b_6f complex are designated by their molecular weight (kDa) or by *PsaA*, etc. for the PS I complex. The distances normal to the membrane associated with most of the electrogenic steps discussed in the text are based on dielectrically weighted distances.
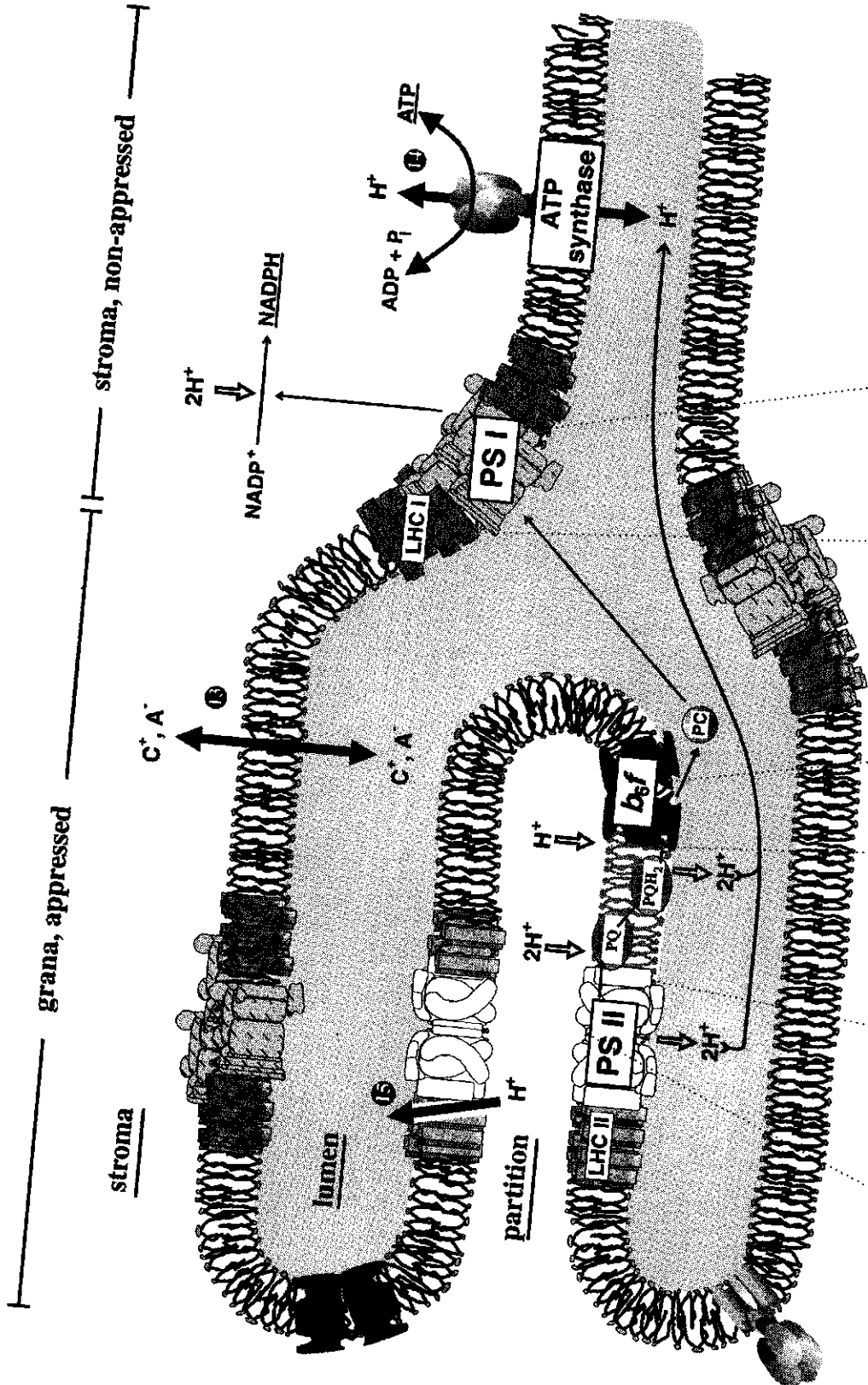
Photosystem II
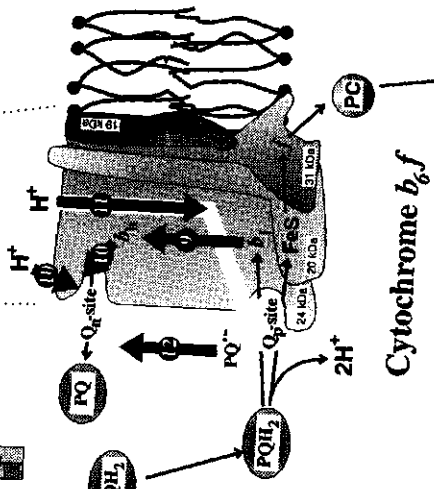
Cytochrome b_6f

Photosystem I

$2H^+$

H_2O

$\frac{1}{2}O_2 + 2H^+$

(0.04)
(0.36)
(0.50)
(0.10)

POH_2

POH_2

PQ

$PQ^{\cdot-}$

$2H^+$

Q_n-site

Q_p-site

H^+

H^+

19 kDa

31 kDa

24 kDa

20 kDa

FeS

PC

PC

$2H^+$

NADPH

Ferredoxin

FNR

F_A
F_B
F_X
A_1
A_0

P700

PC

(0.20)
(0.16)
(0.64)
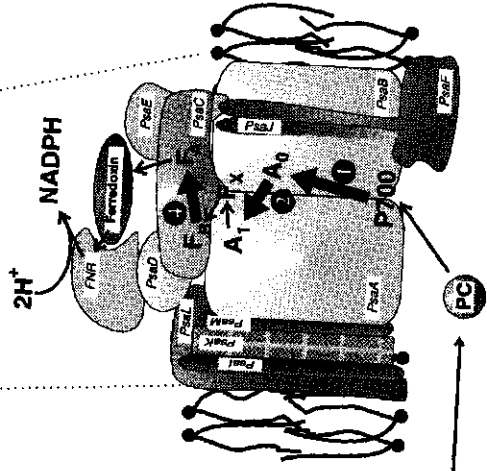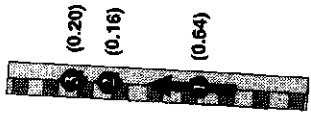
In a recent alternative view the substantial slow electrogenic phase under reducing conditions is proposed to originate from an electrogenic reorientation or transverse movement of a semiquinone anion (PQ⁻) from its interaction with the Q_p-site to the Q_n-site (Fig. 1-3, ⑩). The semiquinone anion likely moves in its deprotonated charged form. This is generally modelled as a semiquinone(SQ)-cycle mechanism of cyt. b_6f turnover (Wikström and Krab 1986, Joliot and Joliot 1994). The electrogenic movement of a semiquinone between the domains of the Q_p-site and Q_n-site was discussed for mitochondrial cyt. bc_1 complexes (Rich and Wikström 1986) and for *Chlorella* algae under reducing conditions (Joliot and Joliot 1994). In *Chlamydomonas reinhardtii* cells under reducing conditions the HQNO-sensitive part of the slow phase b of P515 showed an initial lag of about 1 - 2 ms whereas the HQNO-insensitive part, with a rise time of about 5 ms, was without an initial lag (Fernández-Velasco *et al.* 1995). The HQNO-insensitive signal was argued to reflect the transverse movement of the semiquinone radical generated at the Q_p-site to the Q_n-site, since this process should not involve the Q_n-site where HQNO is thought to bind. The HQNO-sensitive phase would then be the result of electron transfer from heme b_1 to the Q_n-site. Clearly, the transfer of a semiquinone needs to be localised in order not to allow equilibration of the highly reactive radical with the PQ-pool. Energetically, the electrogenic movement of the semiquinone anion from site p to n would be made feasible by its stronger binding to the latter (Joliot and Joliot 1992). This leaves the question whether or not there is a special channel for facilitated semiquinone movement.

Ion fluxes and ATP synthesis/hydrolysis

The final product of the electrogenic reactions discussed so far is a transmembrane electrical field $\Delta\psi$. Reports on the magnitude of this field in a single-turnover light flash range from 10 - 35 mV (Vredenberg and Tonk 1975, Schapendonk and Vredenberg 1977) to 50 mV (Schliephake *et al.* 1968) and even as high as 135 mV (Zickler *et al.* 1976). The patch-clamp method, which will be extensively discussed in Chapter 3, settles down to 40 ± 20 mV for the single-turnover thylakoid potential (Vredenberg *et al.* 1995a, Chapter 3). The formation and decay of the electrical field has been extensively studied with the microelectrode technique on *P. metallica* chloroplasts in relation to transmembrane fluxes of K^+, Mg^{2+} and H^+ and their diffusion potentials (Bulychev *et al.* 1972, Vredenberg and Tonk 1975, Bulychev and Vredenberg 1976a, Vredenberg and Bulychev 1976, Bulychev *et al.* 1976, Bulychev *et al.* 1980, Van Kooten *et al.* 1986).

In the dark there is thermodynamic equilibrium of cations (C^+) and anions (A^-) across the membrane and all electrochemical potentials of ions j (j = K^+, H^+, Mg^{2+} and Cl^-) are zero: $\Delta\mu_j = 0$. The light-activated electrogenic proton pumping moves the system out of equilibrium and a compensating transversal flux of ions along their respective electrochemical gradients commences (Fig. 1-3, ⑥) (Vredenberg 1976). The flux of an ion j is determined in a first approximation (for small $\Delta\psi$) by its charge (z_j), the transmembrane potential $\Delta\psi$ and by the ion conductance g_j (Goldman 1943, Vredenberg 1976). The ion conductance equals the product of the concentration difference of the ion across the membrane (Δc_j) and the membrane permeability coefficient (P_j) of ion j. A

specific chloride conducting channel has been detected in patch-clamp studies with thylakoid blebs (Schönknecht *et al.* 1988). The total membrane conductance (g_M) is the algebraic sum of the individual ion conductances and has its main contribution from K^+ in the dark at pH = 7.0. The potassium ion is abundant in chloroplasts (100 - 300 mM, Vredenberg 1976) and has a relatively high permeability coefficient ($P_K \sim 10^{-8}$ cm s^{-1}, Vredenberg 1976). Although the permeability coefficient of the proton is a 1000-fold larger ($P_H \sim 10^{-5}$, Vredenberg 1976) the contribution of this cation to the overall membrane conductance at pH 7.0 is negligible but may become increasingly dominant upon acidification of the lumen (Vredenberg 1976). Membrane conductances can be calculated from the membrane decay relaxation time ($\tau_M = C_M/g_M$) associated with the dissipation of the electrical field after light-off assuming a constant membrane capacitance C_M (Bulychev and Vredenberg 1976a, Vredenberg 1976).

Proton transport catalysed by the ATP synthase is an electrogenic process (Fig. 1-3, ⬤) in both directions of synthesis and hydrolysis (Admon *et al.* 1982) and contributes to the overall membrane conductance (Ooms *et al.* 1991). The decay rate constant of the P515 response attributed to the proton conductance through the ATP synthase was found to be 2 - 5 s^{-1} (Ooms *et al.* 1991). The chloroplast ATP synthase, composed of nine different subunits (Boekema *et al.* 1988, van Walraven and Bakels 1996), is a latent enzyme and requires $\Delta\mu_{H+}$ -dependent conformational changes to become active (van Walraven and Bakels 1996). By thiol modulation, *in vivo* taken care for by thioredoxin, less $\Delta\mu_{H+}$ is required. In the absence of a ΔpH ATP-hydrolysis may promote $\Delta\psi$ well above 120 mV (Crimi *et al.* 1995).

An electrogenic proton backflow around PS II was postulated by Jahns *et al.* (1988) (Fig. 1-3, ⬤). The parallel inhibition by DCCD of q_E quenching (Ruban *et al.* 1992a) and of proton release from PS II (Jahns *et al.* 1988) led to the hypothesis of a putative proton channel in the LHC II protein complexes (Horton *et al.* 1994). The inhibition of proton release from PS II by DCCD showed good correlation with a strong acceleration of the decay of the flash-induced electrochromic bandshift into the ms time domain. This might indicate an electrogenic short-circuiting of the PS II proton pump through which a fraction of protons released at the OEC funnels back to the plastoquinone reduction site of PS II.

1.2 Structural organisation of thylakoids

The thylakoid membrane probably constitutes a single membrane enclosing the inner membrane space or lumen and separating the lumen from the outer membrane space or stroma (Fig. 1-3). Thylakoids show the unique ability to form closely spaced regions of appressed thylakoids called grana which are laterally separated from the stroma or non-appressed thylakoids (Fig. 1-1, 1-3). The stromal spaces inside the grana are referred to as stroma partitions or simply partitions (Junge and Polle 1986, Junge 1989). The peripheral domain of grana thylakoids are stroma-exposed membranes and constitutes the margins and two end membranes (Albertsson 1995). The negative surface charge of thylakoids is

presumably of importance in grana formation as was described by the surface-charge theory of Barber (1982). Allen (1992) proposed that molecular recognition between (phosphorylated) proteins plays an essential role. Other factors like steric hindrance (Stys 1995) and a positively charged polypeptide on the light harvesting complex of PS II may be involved in stacking (Mullet and Arntzen 1980). Whatever cause, stacking is associated with a lateral segregation of protein complexes, e.g. of PS I and PS II (Briantais *et al.* 1984). The consequences of this typical chloroplast membrane behaviour for functional and structural organisation and for the electrical behaviour will now be addressed.

Structural and functional organisation of PS I, PS II and the cyt. b₆f complex

A remarkable consistency is found in the relative amount of grana membranes (including margins and end membranes) and stroma lamellae in chloroplasts: for 10 different plants, including Peperomia, the amount of stroma lamellae is 20 ± 3 % (Albertsson 1995). The number of paired membranes per granum increases from 5 to 20 for sun to shade leaves, respectively (Anderson *et al.* 1988, Albertsson 1995). The thylakoid margins, which also contain cyt. *b₆f* complexes, PS I complexes and ATP synthases, are certainly not negligible and the marginal area could represent as much as 20 - 38 % of the non-appressed domain (Anderson 1992). The structural domain organisation of thylakoids has probably its functional match in regulating the proportion of linear and cyclic electron flow. The margins enriched in PS I are likely involved in linear electron flow while stroma PS I is involved in cyclic electron transport.

Dynamic regulation of light energy utilisation is essential for plants and the composition of the thylakoid membrane protein complexes may vary according to changes in environmental conditions. Shade and low-irradiance plants have decreased amounts of cyt. *b₆f* complexes on a chlorophyll basis compared to sun and high-irradiance plants (Anderson *et al.* 1988). Typically, the cyt. *f*/P700 ratios are 0.33 - 0.5 for shade and low-irradiance plants, compared to ratios near 1 for sun and high-irradiance plants. The ratio (PS I + PS II)/cyt. *f* increases slightly when going from sun to shade conditions (Anderson 1992).

Photosystem I most likely occurs in a monomeric and trimeric form imbedded in the stroma lamellae (Fig. 1-3) (Boekema *et al.* 1987, Kruip *et al.* 1994). The monomer-dimer equilibrium has been hypothesised to be related to state transitions (Kruip *et al.* 1994). Photosystem II seemingly shows a dimeric organisation (Fig. 1-3) in native thylakoid membranes as was first shown for the thermophillic cyanobacterium *Synechococcus* (Rögner *et al.* 1987) and later also for barley (Peter and Thornber 1991), spinach (Boekema *et al.* 1995) and maize (Santini *et al.* 1994), but the oligomeric structure is still contentious considering the Holzenburg's group claim of a monomeric PS II (Holzenburg *et al.* 1993, Holzenburg *et al.* 1994). The dimeric organisation was discussed to correlate with thylakoid stacking (Rögner *et al.* 1996). In this view grana thylakoids harbour the dimeric and functional form of PS II while the stroma lamellae exclusively contain monomeric PS II. The functional relationship of this heterogeneous distribution with phosphorylation of LHC II and with state transitions is still under investigation (Kruip *et al.* 1994).

The cyt. b_6f complex (M_r 230 kDa) has been discussed to be most likely a structural and functional dimer, both in grana and stroma lamellae (Romanowska and Albertsson 1994, Huang et al. 1994, Chain and Malkin 1995). Nevertheless the monomeric unit seems to be capable of electron transport (Rich et al. 1991). The dimerisation of the complex might provide a regulatory mechanism in adjusting the rates of linear versus cyclic electron transport (Cramer et al. 1991, Bendall and Menasse 1995). In this view the b_6f dimer is located in the grana thylakoids operating in linear electron flow from PS II to PS I whereas the monomeric unit is located in the stroma thylakoids operating in cyclic mode (Kruip et al. 1994, Bendall and Menasse 1995, Rögner et al. 1996). Direct visualisation by immunogold-labelling has demonstrated that cyt. b_6f complexes are almost evenly distributed over both appressed and non-appressed regions with a slight tendency for somewhat more b_6f complex in the grana (Olive et al. 1986, Vallon et al. 1986, Anderson 1992). Besides its function in linear and cyclic electron flow the cyt. b_6f complex has a pivotal function in the regulation of balanced light excitation energy distribution between PS II and PS I because its redox state governs the activation of the LHC II kinase involved in state transitions (Knaff 1990, Anderson 1992).

Several studies have emerged concerning functional clusters of protein complexes in the thylakoid membrane. A functional supercluster consisting of 2 PS II centers and 1 cyt. b_6f complex was concluded from the biphasic reduction of P700 and cyt. b_{563} (Joliot and Joliot 1992); a molar ratio PS II : cyt. b_6f of 2 : 1 (Yu et al. 1993) is in line with this conclusion. In these PS II - cyt. b_6f clusters restricted diffusion of 4 - 6 molecules of PQ, which is the fraction PQ rapidly (25 - 60 ms) reduced by PS II (Joliot et al. 1992), couples electron flow between PS II and the cyt. b_6f complex (Joliot and Joliot 1992). A second supercomplex consisting of cyt. b_6f and PS I (plus Fd-NADP reductase) was postulated by Laisk et al. (1992). They concluded that plastocyanin (PC) does not evenly transfer electrons from cyt. f to P700 but that PC is rather confined to a particular b_6f - PS I supercomplex. Kinetic consideration of the biphasic reduction kinetics of P700$^+$ corroborates on the existence of two pools of plastocyanin, one closely complexed with cyt. b_6f and P700 and the other mobile (Haehnel et al. 1980). Finally, a localised protonic coupling between the cyt. b_6f complex and the ATP synthase was concluded from the stimulatory effect of the local anaesthetic procaine on photophosphorylation (Laasch et al. 1993).

Compartmentation and the consequences for ionic mobilities
The grana-stroma membrane organisation likely causes compartmentation. The physical-chemical properties in the compartments may differ in some fundamental respects from free aqueous solutions: i) a charge gradient between different compartments is highly feasible: laterally, between subcompartments from stroma to inner grana and transversely between top and bottom lumens or stroma partitions of the grana (Becker et al. 1978, Osváth et al. 1994); ii) the effective dielectric constant at the membrane/water interface of the aqueous layer between phospholipid membranes is always smaller (about 40) than that of bulk water (Gutman et al. 1992). As a result the electrostatic interactions on the surface of the phospholipid membrane are intensified (Gutman and Nachliel 1995); iii)

the rotational and translational motion of molecules including water at the membrane/water interface is slowed down (Raghavan *et al.* 1992, Steinhoff *et al.* 1993). Nesbitt and Berg (1982) observed a light-induced increase in the hindrance of a spin-label which they related to approaching thylakoid membranes and the hindrance likely resides in the aqueous lumenal phases. Most interestingly, a dynamic simulation of water between dilauroylphosphatidylethanolamine bilayers showed that the translational and rotational diffusion of the water molecule might be enhanced in the middle between two layers over that of water in the bulk (Raghavan *et al.* 1992).

The diffusion of the proton in the narrow environments between phospholipid membranes is not dramatically retarded but equal or only somewhat slower than in free water (Gutman and Nachliel 1995). The intermembrane water provides the protons with an efficient diffusion matrix where the proton propagates by the same Grotthuuss mechanism, a rapid exchange of covalent and hydrogen bonds between the water molecules, as in the bulk water. Moreover, there is also no clear evidence for an acceleration of proton diffusion at the lipid/water interface of an artificial bilayer (Gutman *et al.* 1992) or of the thylakoid membrane (Polle and Junge 1989). Of course proton buffers, either mobile or fixed to the membrane surface, will retard the diffusion of the protons (Junge and McLaughlin 1987). In the artificial membrane model composed of a phosphatidylcholine/water interface the mobility of anions and cations was shown to be hindered, after a maximum value, when two opposing membranes are substantially suppressed (Rigaug and Gary-Bobo 1977, Benyoucef *et al.* 1978).

Conductivity measurements to examine the electrical properties of the membrane/water interface are notoriously difficult to perform (Gutman and Nachliel 1995). Some groups found a slight (less than 10 %) increase in the conductance which was attributed to monolayer formation (Morgan *et al.* 1991, Sakurai and Kawamura 1989). Menger *et al.* (1989) examined the problem by using an alternating measuring current in order to prevent polarisation artefacts, which is believed to be a more trustworthy method, and found that a decrease in conductance occurred. This may be related with a lower conductivity of the hydration layer with respect to the water/air interface and it was concluded that surfaces of biological membranes, in the absence of carriers, serve as poor conduits for ion movement (Menger *et al.* 1989). Experimental results from membranes with imbedded proteins, representing an improved model system for the highly proteinuous thylakoid membrane, are presently unavailable. However, recent patch-clamp results on the thylakoid membrane of *P. metallica* chloroplasts have demonstrated the potential importance of light-induced changes in lateral conductances of thylakoid lamellae (Vredenberg *et al.* 1995b, van Voorthuysen *et al.* 1997). In the presence of ammonium a close correlation has been found between light-induced swelling of thylakoids, as concluded from electron microscopy, and an increase in chloroplast conductances (W. J. Vredenberg, A. A. Bulychev, V. K. Opanasenko, personal communication).

1.3 The role of protons in energy transduction and its regulation

Photosynthetic electron transport is accompanied by proton pumping from external to internal phases which creates the transthylakoid proton-motive-force. Three proton uptake sites at the stroma membrane/water interface can be discerned (Fig. 1-3): the plastoquinone reduction site of PS II or Q_B binding niche, the Ferredoxin-NADP-Reductase (FNR) site of PS I and the Q_n-site of the cyt. b_6f complex (cyclic electron transport only). Protons are released in the thylakoid lumen at two sites: the OEC of PS II and the plastoquinol oxidation site Q_p of the cyt. b_6f complex (Fig. 1-3). In the dark-adapted state a proton gradient of about one unit may already exists across the thylakoid membrane due to a Donnan potential (Van Kooten 1988). The lumenal pH *in vivo* will probably not decrease below pH 5.0 during illumination (ΔpH hardly exceeds 2.7 units) in chloroplasts of the intact leaf (Schönknecht *et al.* 1995). Lower values of lumen pH should be feasible with isolated chloroplasts and thylakoids.

Proton regulation of electron transport is exerted at two distinct levels: an effect on PS II efficiency and an effect on the rate of intersystem electron flow as determined by plastoquinol oxidation at the cyt. b_6f complex. Regulation appears as a compulsory phenomenon inasmuch as excess light energy is detrimental for the photosynthetic apparatus.

The proton as a mediator between redox energy and chemical energy
In C_3 photosynthesis the Calvin-Benson cycle consumes three molecules of ATP and two molecules of NADPH for each CO_2 molecule fixed (Calvin 1962), which demands an ATP/NADPH ratio of 1.5 for the photosynthetic electron transport. C_4 photosynthesis is less efficient in ATP consumption and requires 5 or 6 ATP molecules per CO_2 fixed (Furbank *et al.* 1990, Bendall and Manasse 1995). How the right balance of the ATP/NADPH ratio is furnished by the 'light'-reactions is therefore a fundamental and essential issue.

When considering linear electron flow from water to $NADP^+$ only, two electrons are needed for the reduction of $NADP^+$ and the travel of these two electrons through the photosynthetic electron transport chain deposits 4 H^+ in the lumenal phase. For a H^+/ATP ratio of 3, which is a commonly accepted value with which the ATP synthase works (Davenport and McCarty 1984, Ooms *et al.* 1991), the 'light'-reactions then supply an ATP/NADPH ratio of 1.33. A higher H^+/ATP ratio of 4 has been claimed for spinach chloroplasts (Rumberg and Berry 1995) and spinach leaves (Gerst *et al.* 1994) which would lower the ATP/NADPH ratio to 1. Certainly, the ATP produced by linear electron flow appears insufficient to drive carbon fixation and alternative electron pathways are required to supply the extra ATP. The increase of the ATP/NADPH ratio can be realised through: i) cyclic PS I-dependent phosphorylation involving Fd (Schürmann *et al.* 1971, Heber *et al.* 1978, Bendall and Manasse 1995), ii) a secondary electrogenic loop or Q-cycle (Heber and Walker 1992, Gerst *et al.* 1994, Bendall and Manasse 1995) and iii) the Mehler reaction (Schreiber and Neubauer 1990), electron transport from water to O_2 or, in the presence of ascorbate, faster electron flow to

monodehydroascorbate (MDA) (Forti and Elli 1995).

The H^+/e^- ratio for linear electron transport from water to $NADP^+$ may be either 2 or 3, depending on whether or not a Q-cycle operates at the level of the cytochrome b_6f complex (Heber and Walker 1992). A H^+/e^- ratio of 2 in spinach and pea thylakoids was concluded by Davenport and McCarty (1984) and would exclude a Q-cycle. Recently, in spinach leaves the H^+/e^-- ratio associated with linear electron transport is suggested to be 3 (Gerst *et al.* 1994). A H^+/e^- ratio of 3 implies the existence of an obligatory Q-cycle in accordance with the ideas of Rich (1988) and most recent evidence strongly supports this idea (Bendall and Manasse 1995). On the other hand, the involvement of the Q-cycle may be facultative, with decreasing coupling efficiency at increasing light intensities (Moss and Bendall 1984).

Coupling between redox reactions and ATP synthesis through a delocalised proton flow is a well accepted concept for free energy transduction in chloroplasts. That a bulk $\Delta\mu_{H^+}$ is indeed capable of phosphorylation is evidenced by the fact that an artificially imposed $\Delta\mu_{H^+}$ is competent in ATP formation (Junesch and Gräber 1991). However, it has been suggested that resistive pathways between sources (PS II, cyt. b_6f) and sinks (ATP synthases) may exist in thylakoids which may cause local deviations of the proton-motive-force (Haraux and de Kouchkovsky 1983, Sigalat *et al.* 1985). It is suggested that the exchange of protons between the bulk phase and a hypothetical membrane phase is energetically hindered (Sigalat *et al.* 1985). In the narrow thylakoid partitions and lumenal phases protons are extensively buffered which results in a hindered proton diffusion and a loss of proton-motive-force of about 0.2 pH units was therefore predicted (Polle and Junge 1986, Junge and Polle 1986, Junge 1989).

Energy-dependent down-regulation of photosystem II

Illumination has a large impact on the quantum efficiency of light utilisation in photosystem II which can be observed e.g. as a reduction in efficiency of O_2 evolution (Weis and Lechtenberg 1989, Horton *et al.* 1989, Genty *et al.* 1990, Rees and Horton 1990). With an increase in light intensity an increasing fraction of the excitation energy is dissipated as heat, and accordingly less energy will be available for photochemistry. The very same dissipation mechanism quenches the variable chlorophyll *a* fluorescence emitted by PS II which is quantified by the so-called non-photochemical fluorescence quenching (q_N). A substantial part of q_N is related to the built-up of the transthylakoid pH gradient and is dark reversible with a half-time of about 40 s: the energy-dependent fluorescence quenching (q_E) (Krause *et al.* 1982). We have to consider that q_N and PS II quantum efficiency show a strong energisation-dependent regulation *in vivo* in a narrow pH range around $\Delta pH = 2.5$ (Schönknecht *et al.* 1995).

Energy-dependent quenching has been considered to be associated with antenna quenching, in relation to de-epoxidation of xanthophylls (zeaxanthin formation) and structural changes in the LHC II, and with reaction center quenching.

Reaction center quenching, generally observed *in vitro*, is sensitive to the PS II donors ascorbate or diphenylcarbazide (DPC) and does not lead to a significant quenching of the

minimal (dark) fluorescence yield (F_o) (Crofts and Horton 1991, Krieger *et al.* 1992). This type of quenching starts when the pH in the lumen decreases below 5.5 which causes a slowing-down of the reactions at the PS II donor side (Schlodder and Meyer 1987, Krieger and Weis 1992). The donor-side limitation increases the life-time of the strong oxidant $P680^+$ and recycling of electrons from the PS II acceptor side to the impaired donor side will be stimulated. Charge recombination between Q_A^- and $P680^+$ (Weis and Berry 1987, Krieger and Weis 1992) or a futile electron cycle around PS II involving cyt. b_{559} (Schreiber and Neubauer 1987, 1990, Krieger and Weis 1992) were proposed to be responsible for this back cycling. The impairment of the PS II donor side upon a low pH was shown to have consequences for the PS II acceptor side as well. An increase in the redox potential of Q_A from -80 mV (active PS II) to +40 mV (inactive PS II) was correlated with calcium release from the OEC (Krieger *et al.* 1993), a process known to be accompanied with PS II donor-side inactivation (Boussac *et al.* 1992). Interestingly, the reverse process of photoactivation of oxygen evolution in inactivated PS II was associated with a return of the Q_A redox potential from +110 mV to -80 mV, again demonstrating the close relationship between Q_A redox state and OEC activity (Johnson *et al.* 1995). Whether or not reaction center quenching occurs *in vivo* is still disputed, since it is uncertain that the pH in the thylakoid lumen attains a sufficiently low value to induce Ca^{2+} release and concomitant inactivation of the OEC (Foyer *et al.* 1990, Johnson and Krieger 1994).

Antenna quenching is redox insensitive and leads to significant quenching of F_o (Rees *et al.* 1990). A close correlation between leaf zeaxanthin content and the amount of non-photochemical quenching has led to the conclusion that zeaxanthin acts as a direct quencher of excitation energy in the PS II antennae (Demmig *et al.* 1987, Demmig-Adams 1990). Zeaxanthin and pH likely act synergistically and are both required for energy dissipation *in vivo* (Demmig-Adams and Adams 1996). There appears, however, not always to be an obligatory requirement for zeaxanthin in q_E formation (Noctor *et al.* 1991, Ruban *et al.* 1993).

The model of Horton and his collaborators also assumes that energy dissipation takes place in the LHC II (Horton *et al.* 1991, Horton and Ruban 1992). A low pH in the thylakoid lumen leads to the formation of a quenching state of aggregated LHC II (Horton *et al.* 1991, Ruban and Horton 1992, Ruban *et al.* 1992b). The parallel inhibition by antimycin A of LHC II aggregation (Ruban *et al.* 1992b) and of q_E (Oxborough and Horton 1987, Noctor *et al.* 1993, Ruban *et al.* 1994) supports this view. A localised proton gradient with protonation of specific groups of lumenal exposed LHC II residues would trigger the quenching. Recently, the protonation of the minor, proximal antenna proteins has been proposed to be a key step in the induction of energy dissipation (Horton *et al.* 1994, Crofts and Yerkes 1994). The function of zeaxanthin would be to promote quenching. It is suggested that the carotenoid acts as a quencher amplifier, implying that a lower ΔpH is required for the same q_E development (Rees *et al.* 1989, Noctor *et al.* 1991, Goss *et al.* 1995). The observed light-activation of q_N (it needs a lower ΔpH) is based on this concept (Rees *et al.* 1989, Noctor *et al.* 1991, Johnson *et al.* 1994). The physico-chemical properties of zeaxanthin were suggested to cause conformational

changes of the LHC II via changes in the detergent-like properties of bound LHC II xanthophylls (Horton and Ruban 1992, Horton *et al.* 1994).

Antenna quenching and reaction center quenching might very well co-exist with the former prevailing *in vivo* and the latter prevailing *in vitro*. Mohanty and Yamamoto (1995, 1996) nicely showed in spinach chloroplasts that de-epoxidised xanthophylls in the presence of ascorbate are involved in q_N but if ascorbate was omitted, i.e. without de-epoxidation, non-photochemical quenching is still prevalent and is reaction center type. The reaction center quenching was strictly depended on the pH. With an ascorbate content between 12 - 25 mM in chloroplasts *in vivo* (Foyer *et al.* 1983) reaction center quenching is expected to be suppressed while antenna quenching is stimulated. The effect of dibucaine revealed that antenna quenching is more related to sequestered protons (localised) but needs a delocalised proton gradient for the obligatory violaxanthin de-epoxidation conversion (Mohanty and Yamamoto 1995, 1996). Reaction center quenching requires a delocalised proton gradient. The mechanisms involved in non-photochemical quenching may be different in some of its fundamental aspects for different plant species (Johnson *et al.* 1994).

Photosynthetic control
The main constraint of electron flow is generally considered at the plastoquinol oxidation site of the cyt. b_6f complex which is referred to as 'classical' photosynthetic control (Siggel 1976, Bendall 1982, Foyer *et al.* 1990). The decreased plastoquinol oxidation rate is reflected by a decrease in electron donation rate to oxidised cytochrome f and $P700^+$ (Siggel 1976, Foyer *et al.* 1990, Nishio and Whitmarsh 1993). Of importance is the consideration whether or not this type of control dominates *in vivo*. The pH-dependent control of PS II photochemistry was argued to be of primary importance for controlling photosynthetic electron flow *in vivo* (Foyer *et al.* 1990). A support for this conclusion was found in the constant half-time ($t_{1/2}$) for $P700^+$ reduction over a wide range of irradiances in leaves under normal atmospheric conditions (Harbinson and Hedley 1989, Laisk and Oja 1994). At a high constant irradiance, corresponding to a high q_N, control of linear electron flow is mainly at the cyt. b_6f complex when the availability of the acceptor CO_2 was varied in sunflower leaves (Laisk *et al.* 1992). This shows that photosynthetic control at the PQH_2 oxidation site becomes increasingly significant under limited availability of electron acceptors (CO_2, O_2) (Harbinson *et al.* 1990, Laisk and Oja 1994). At lower CO_2 concentrations membrane energisation and associated built-up of ΔpH by cyclic PS I-dependent electron flow may increase which is likely involved in the modulation of non-photochemical energy dissipation in PS II (Katona *et al.* 1992, Heber and Walker 1992).

It appears that the well-known saturation curve of CO_2 fixation versus irradiance is caused by a limitation within the electron transport chain itself, at the PS II site for low irradiances and at the cyt. b_6f site for high irradiances, rather than within the Calvin-Benson cycle (Foyer *et al.* 1990). Were it for a limitation of the enzymatic reactions of the Calvin-Benson cycle an accumulation of reducing equivalents would bring about photosynthetic control at the level of plastoquinol oxidation at the cyt. b_6f complex. This is generally not observed under normal atmospheric conditions.

1.4 Outline of this thesis

The study presented in this thesis illustrates the use of the electrical potential in exploring the bioenergetics of chloroplast photosynthesis.

Chapter 2 describes the cultivation of the sample plants, *P. metallica* and *S. oleracea*, and the preparation of chloroplasts. This is followed by the technical details of the techniques and methods used.

Chapter 3 presents a thorough analysis of the patch-clamp method. This covers introduction to the whole-thylakoid configuration, the current-injection technique, light-induced responses, analytical derivation of formulas of the electrical equivalent scheme, a numerical example, statistics and an analysis of error.

Chapter 4 illustrates the parallel use of current- and flash-induced patch-clamp responses in acquiring a kinetically well resolved electrogenic Q-cycle in a single *P. metallica* chloroplast. The generally observed sigmoid rise and the occasionally observed high extent of the Q-cycle are two striking features found for cyt. *b₆f* turnover in *P. metallica*.

Chapter 5 describes a fast 1 ms decay component generally observed in the P515 response. Most evidence relates this component to a fraction of photosystem II-dependent charge separation which is inadequately stabilised and quickly dissipated by a charge recombination reaction.

Chapter 6 describes a reversible suppression of photosystem II-dependent charge separation upon energisation in *P. metallica* and *S. oleracea*. Most evidence suggests that lumenal acidification causes a reversible inactivation of photosystem II in analogy with the reaction center quenching model of chlorophyll *a* fluorescence.

Chapter 7 gives a first report on (the kinetics of) changes in the chloroplast conductance network induced by a single-turnover of the reaction centers. The conductance changes are discussed in relation to alterations in low conductance phases of chloroplast thylakoids, notably those of the narrow spaces in grana thylakoids.

Chapter 8 closes this thesis with a general discussion about agreements and disagreements between P515 and patch-clamp data. Some reflections are given on the regulation of the Q-cycle in *P. metallica* and on the mechanism of non-photochemical energy dissipation in PS II. Finally, some suggestions for future research are presented.

Chapter 2   Materials and methods

2.1 Plants: description and cultivation

Peperomia, *Peperomia metallica*

The *Peperomia* (Gr., from peperi, pepper, etc. and homoios, resembling, referring to its resemblance to the closely allied genus Piper, the same of peppers) *metallica* species is a succulent, shade-adapted herb with silvery red-green leaves originally found in Peru (Linden and Rodigus 1892), see Fig. 2-1. The metallica species has about 3 to 5 relatively large chloroplasts of approximately 20 μm diameter (Fig. 1-1) in its mesophyll cells that makes it particular suitable for electrophysiological experiments. Routinely, chloroplasts were isolated from plants grown in a laboratory-built climate cabinet of which the growth conditions are summarised in Table 2-1. The low light conditions specifically stimulate the development of thin leaves containing large chloroplasts and reduced amounts of anthocyanin. Plants were grown from top cuts which were planted in the growing soil after dipping the stalk in some cytokinin to induce root formation.

It is judicious to realise that *P. metallica* may own some properties essentially different from the more regularly used high-light adapted plants like spinach or pea. Shade plants have less cyt. b_{559}, cyt. b_{563}, cyt. f and plastoquinone per unit chlorophyll, while the P700 content is unaltered (Anderson *et al.* 1988). Furthermore, Peperomia species may show a transient photosynthetic metabolism from C_3 photosynthesis to Crassulacean acid metabolism (CAM) photosynthesis, a temporal separation of C_3 and C_4 metabolism, as was found for *P. camptotricha* during leaf development from young to mature leaves (Nishio and Ting 1987, Ting *et al.* 1994).

Fig. 2-1   Six months old *P. metallica* plant.

Table 2-1 Growth conditions of *Peperomia metallica* (cabinet) and *Spinacia oleracea* (phytotron).

		Peperomia metallica	*Spinacia oleracea*
light conditions			
	type of light	fluorescent + bulb lamp	HPI + Philinea (Philips)
	intensity (PAR)	1.0 W m^{-2}	75 W m^{-2}
	day/night	12/12 hours	8.5/15.5 hours
air temperature			
	day	24 - 26 °C	19 - 20 °C
	night	19 - 21 °C	18 °C
relative humidity		80 - 90 %	60 - 65 %
soil composition		compost : river sand = 1:1	compost : river sand = 1:1

PAR = Photosynthetically Active Radiation.

Table 2-2 shows data on the Chl a/b ratio of *P. metallica* for three conditions. The Chl a/b ratio was lower when grown under low light and full-grown leaves showed a lower Chl a/b ratio than young leaves under identical light conditions. A relatively low Chl a/b ratio might indicate a relatively high ratio of LHC II over reaction center complexes which will enhance the efficiency of light capture (Anderson *et al.* 1988, Sailaja and Rama Das 1995). This is possibly also related to a higher degree of thylakoid stacking.

Table 2-2 Two properties of *Peperomia metallica* chloroplasts.

	growth conditions	Chl a/b ratio	F_V/F_M
young leaves	cabinet, 1 W m^{-2}	2.57 ± 0.05	n.d.
full-grown leaves	cabinet, 1 W m^{-2}	2.33 ± 0.05	0.813± 0.010
full-grown leaves	green house, 10 - 50 W m^{-2}	2.77 ± 0.05	n.d.

The Chl a/b ratio was determined spectrophotometrically on 10 leaves according to Bruinsma (1963). The PS II quantum efficiency (F_v/F_M) was determined as described in § 2.5. n.d. = not determined.

Spinach, *Spinacia oleracea* L.

Spinach is a typical high-light adapted plant. Spinach was grown on 60 x 40 cm^2 trays in a phytotron of which the growth conditions are given in Table 2-1. Four weeks after sowing the spinach plants received additional nutrients (Osmocote, N-P-K = 15-17-13 plus 2 units of Mg). Leaves from 3 to 5 weeks old plants were used for chloroplast isolation.

2.2 Sample preparation: isolated chloroplasts and infiltrated leaves

Peperomia, *Peperomia metallica*

Isolation of intact Peperomia chloroplasts was done by cutting a leaf with a razor blade in standard isolation medium containing 300 mM sorbitol, 50 mM KCl, 0.5 mM MgCl$_2$,

0.1 - 0.5 % (mg/ml) Bovine Serum Albumin (BSA) and 10 mM HEPES/KOH, pH 7.5. The sliced preparation with free chloroplasts was transferred into a 2-ml measuring chamber. Hence, per definition the experimental bath solution is identical to the isolation medium. As a regular rule, the chloroplasts were dark adapted for about 5 minutes prior to starting a measurement.

Leaves from two types of plants were used for chloroplast isolation (Fig. 2-2). Young leaves contained regular, bright light-green chloroplasts. Full-grown leaves were composed of several layers of mesophyll cells containing more darkened chloroplasts and often starch grains were visible.

Young intact *P. metallica* leaves were used for the spectrophotometric methods (P515, fluorescence and P700). The signal-to-noise ratio of the P515 response was improved by using infiltrated leaves as obtained by applying a vacuum for 5 minutes to the leaves submerged in standard isolation medium. For reasons of comparison *P. metallica* leaves used for fluorescence and P700 measurements were also infiltrated.
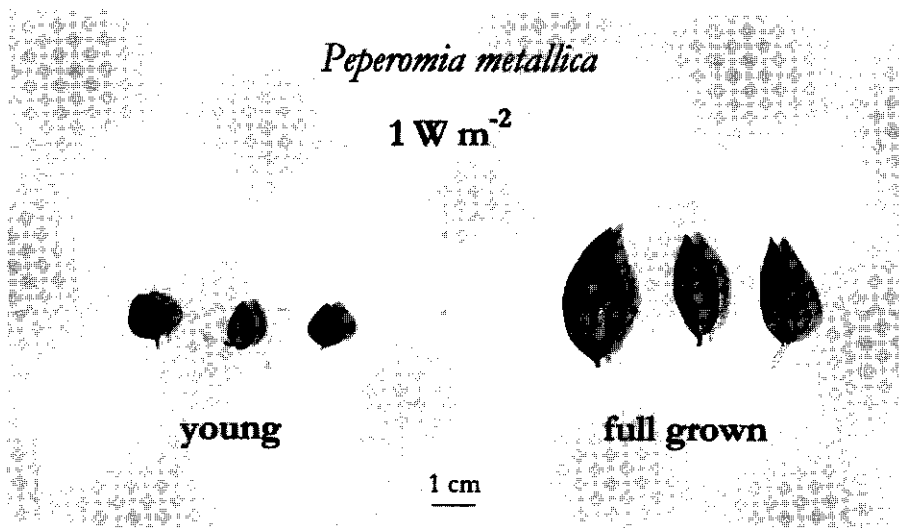
Fig. 2-2 Two types of leaves were used for isolation of *P. metallica* chloroplasts. Young leaves were picked from scanty, 2 months old plants (not shown). Full-grown leaves were picked out of the 4 upper leaves of the 6 months old plants (Fig. 2-1).

Spinach, *Spinacia oleracea* L.

Isolation of intact spinach chloroplasts was done in a cold room at 3 - 4 °C and under safe dim green light (20 µmol m^{-2} s^{-1}). Twenty grams of spinach leaves were harvested and washed once with tap water and once with demineralised water. After removing the veins the leaves were cut into 5 mm sections which were transferred into an Omnimixer (Sorvall, Connecticut, USA) containing 50 ml isolation medium (Table 2-3). After three

Table 2-3 Media used for preparation of intact spinach chloroplasts.

	Isolation medium	Resuspension medium
sorbitol	0.3 M	0.3 M
NaCl	10 mM	
MgCl$_2$	1 mM	1 mM
MnCl$_2$	1 mM	1 mM
EDTA	2 mM	2 mM
KH$_2$PO$_4$	0.5 mM	0.2 mM
ascorbate*	2 mM	
cystein*	4 mM	
BSA*		1 mg ml^{-1}
MES buffer	50 mM	
HEPES buffer		50 mM
	pH 6.1 - 6.3	pH 6.7 - 6.8

Substances marked with an asterisk (*) were freshly added.

short bursts of the Omnimixer at maximum speed the homogenate was filtered through two layers of cheese cloth. The filtered suspension was spinned down in a MSE Chillspin centrifuge at 900 g for 50 s. The supernatant was decanted leaving the chloroplasts containing pellet which was washed once carefully with a few drops of resuspension medium (Table 2-3). The pellet was then resuspended in 50 ml resuspension medium and again spinned down at 900 g for 50 s. The nearly clear supernatant was decanted and the remaining pellet was resuspended in a small volume of resuspension medium which was stored on ice for further use.

This isolation procedure yielded a preparation of 80 - 90 % intact chloroplasts as determined by ferricyanide reduction (Heber and Santarius 1970). The chlorophyll content was determined spectrophotometrically (Bruinsma 1963). Experiments were mostly done with intact chloroplasts diluted in assay medium (Table 2-4, a 1:1 mixture of double assay medium and break medium) to a final chlorophyll concentration of 10 - 25 µg ml^{-1}. If broken chloroplasts were required a fraction of the isolated chloroplast suspension was dissolved in break medium for 1 minutes on ice. Thereafter an equal

Table 2-4 Assay medium for spinach chloroplasts.

	double assay medium	break medium
sorbitol	0.66 M	
NaCl	20 mM	
MgCl$_2$	2 mM	4 mM
MnCl$_2$	2 mM	
EDTA	4 mM	
KH$_2$PO$_4$	1 mM	
HEPES buffer	100 mM	50 mM
	pH 7.5	pH 7.5

volume of double assay medium was added. For measuring the pH dependency of the amplitude of the P515 response, spinach thylakoids were incubated for 5 minutes in the same assay medium (Table 2-4) but with HEPES buffer replaced by a mixture of 25 mM HEPES and 25 mM MES and adjusted to the desired pH with KOH or HCl.

For *in vivo* measurements spinach leaves were infiltrated with assay medium (Table 2-4) similarly as done for *P. metallica* leaves.

The inhibitors, redox mediators and ionophores used for the experiments were purchased from Sigma, except for DBMIB. The concentration of ethanol never exceeded 0.5 %, unless indicated otherwise.

2.3   Electrophysiological measurements

Two electrophysiological techniques (Fig. 2-3) were employed: classical microelectrode impalement and a modified patch-clamp method (Vredenberg *et al.* 1995a). Both electrophysiological techniques were done on essentially the same set-up. A microscope, a micromanipulator supporting the amplifier head-stage and pipette, and a superfusion device were mounted onto a vibration-free supporting table, which permitted electrical recordings from one chloroplast during tens of minutes (impalement) or up to several hours (patch-clamp). The patch-clamp technique is more stable with regard to mechanical vibrations since both pipette and chloroplast cannot move independently.

The use of an inverted microscope IM (Zeiss, Oberkochen, West Germany) enabled easy sample manipulation with illumination (flash and continuous light) coming from above. Magnification was 200 to 630 times.

The MO 303 micromanipulator (Narashige, Tokyo, Japan) is a manual, hydraulic manipulator allowing controlled X-Y-Z movements. The micromanipulator was mounted onto the microscope table which guaranteed a stable and rigid measuring configuration.

A superfusion Drug Application Device DAD-12 (Adams & List Associates, New York, USA) was used in combination with the patch-clamp technique and permits the successive application of chemicals to the same single chloroplast. As such, this combination offers a unique experimental tool.

Illumination was provided by an incandescent light source (variable light intensity) equipped with an electromechanical shutter or by a xenon flash-lamp (General Electric FT-230) with 8 µs discharge time. Single-turnover flashes and continuous light were directed to the chloroplast through flexible light guides.

Measurements were performed at room temperature.

2.3.1   Microelectrode impalement

Microelectrode impalement was done in chloroplasts *in situ* in thin leaf sections of *P. metallica* which were clamped to the bottom of a cuvette. Microcapillary glass electrodes made from Clark borosilicate glass GC200TF (Clark instruments, Reading, UK) with

internal filament were pulled with a BB-CH puller (Mecanex, Geneve, Switserland) or a Palmer puller (Palmer, London, UK) and had tip diameters of less than 0.5 µm. Pipettes were backfilled with 0.5 M KCl solution and had a typical tip resistance of 20 - 80 MΩ. Electrical potentials were recorded with a high impedance microelectrode amplifier VF 102 (Bio-Logic, Claix, France) connected through an Ag-AgCl silver wire electrode to the pipette's KCl solution. The reference was placed into the bath solution. The amplifier output was either displayed on a digital oscilloscope (Tektronix, Oregon, USA) or on a chart recorder.

2.3.2 Patch-clamp technique

Patch-pipettes prepared from Clark borosilicate glass GC200TF or GC150TF (Clark instruments, Reading, UK) with internal filaments were fire-polished and back-filled with standard isolation medium (§ 2.2). The filling solution was preliminary filtered through Millipore filters. The tip resistance (2 - 20 MΩ) of the pipette was voltage-independent. The capacitance of the pipette was relatively small and was consequently not compensated for. A single chloroplast was sucked onto the pipette and additional suction created the so-called whole-thylakoid configuration, discernible by the appearance of light-induced responses, in which the electrode and reference have a low conductance access (Fig. 2-3, resistance R_A) to the thylakoid membrane (see Chapter 3). The success rate for seal formation and associated light-induced responses (whole-thylakoid configuration) was somewhat higher for chloroplasts isolated from full-grown leaves than from young leaves. The input (seal) resistance of the patched chloroplast in this configuration varied from 4 to 50 MΩ. Giga-ohm seals were not achieved which is interpreted as being due to relatively large leakage currents.

Electrical potentials and currents were detected with an EPC-7 patch-clamp amplifier (List Electronics, Darmstadt-Eberstadt, Germany) in current-clamp or voltage-clamp mode, respectively. In both measuring modes the responses were filtered electronically by a 10 kHz low-pass Bessel filter. Square pulses used for current-injection were obtained from a pulse generator (Tektronix, Oregon, USA). Visual inspection of electrical responses was done on a digital oscilloscope (Tektronix, Oregon, USA).

Values of the potential recorded in current-clamp mode correspond to the potential of the electrode inside the pipette tip with respect to the external reference electrode placed in the bath. By convention, under voltage-clamp the inward currents (currents flowing into the pipette) are represented by a negative sign. The time resolution of the photopotential response under current-clamp was limited to 1 - 3 ms by an as yet unresolved multiphasic rise. In voltage-clamp the time response was at its lowest limit of about 0.2 - 0.5 ms. Responses measured in either voltage-clamp or current-clamp have identical information contents (see Chapter 3).

For real time recording of the chloroplast seal conductance a sine-wave voltage (rms amplitude 1 or 3.5 mV, 100 Hz) was applied to the electrode in voltage-clamp and the output modulated current was fed into an EG&G 2510 lock-in amplifier (EG&G,
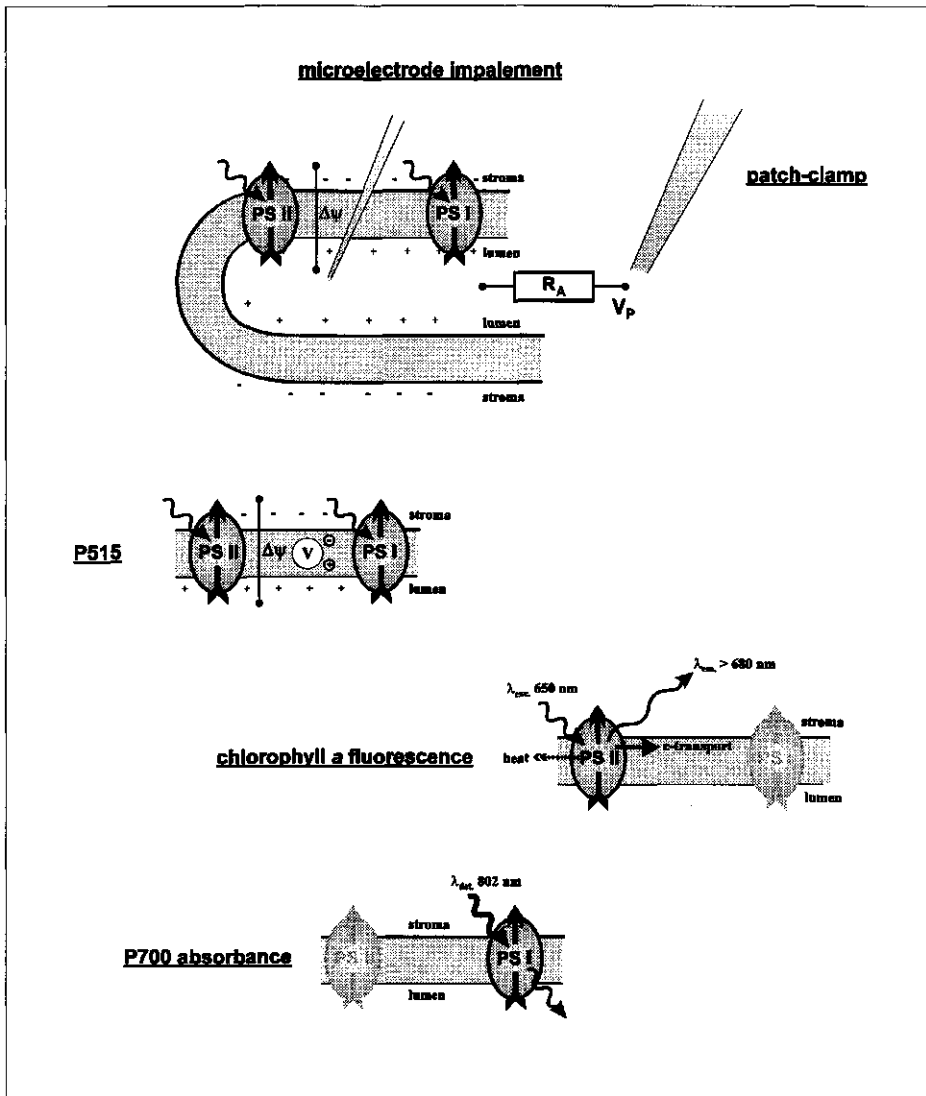
Fig. 2-3 Pictograms of employed techniques. Large upward arrows indicate light-induced charge separation in the reaction centers. Wavy arrows indicate in- and outgoing photons.

Princeton Applied Research, Princeton, USA). Consequently, the output signal was proportional to the seal conductance (inversely proportional to the seal resistance). The time constant of the lock-in amplifier was set to 100 or 300 ms; this setting limited the time response in the onset phase of the conductance changes.

2.4 Electrochromism (P515)

Flash-induced electrochromic absorbance changes (Fig. 2-3, P515) were measured using a modified Aminco Chance spectrophotometer (American Instruments, Maryland, USA) (Snel 1985). Weak green measuring light with a peak emission at 518 nm and a bandwidth of 13.8 nm was provided by a tungsten lamp powered by an Oltronix B32-20R power supply. The transmitted measuring beam was detected by a photomultiplier shielded by a filter combination consisting of a Balzers DT Cyan, a Corning CS4-96 and a Schott BG39 filter. This was a modified P515 filter combination which resulted in an improved signal-to-noise ratio but introduced a small flash artefact. As a consequence, the first 0.25 ms of the response after the flash firing were discarded. The photomultiplier output was fed into a home-built amplifier allowing for compensation of the dark output, a 200 or 500 times signal amplification and signal filtering.

Red saturating single-turnover flashes were generated by a FT-230 Xenon flash lamp (General Electric, Albany, New York) with a flash duration of 8 μs and filtered by a Schott RG645 filter. Red continuous actinic light used for pre-illumination of chloroplasts was provided by a tungsten-halogen lamp (Philips, The Netherlands) filtered by a Schott RG610 filter. Far-red light used for P700 oxidation was provided by a tungsten-halogen lamp (Philips, The Netherlands) filtered by a Schott RG715 filter and a Calflex heat filter. Both flash and continuous light were guided to the cuvette using flexible optical fibers.

Experiments were performed at 10 or 20 °C.

2.5 Chlorophyll *a* fluorescence

Chlorophyll *a* fluorescence yield (Fig. 2-3) was measured with a Pulse Amplitude Modulated (PAM) fluorometer (Walz, Effeltrich, Germany) (Schreiber 1986, Schreiber *et al.* 1986). Pulse-modulated (1.6 kHz) weak red light used for excitation was provided by a 650 nm light-emitting-diode (LED). A DT-Cyan short-pass filter in front of the LED removed long wavelength emissions of the LED. The modulated fluorescence response was detected by a photodiode shielded by a Schott RG9 long-pass filter. Red actinic illumination (175 μmol m^{-2} s^{-1}) was provided by a Fiber Illuminator FL101 (Walz, Effeltrich, Germany) filtered by a Schott RG610 filter. Saturating light pulses of 400 ms duration were supplied by a FL103 Saturation Pulse Lamp (Walz, Effeltrich, Germany) for quantification of photochemical and non-photochemical quenching. Photochemical (q_P) and non-photochemical (q_N) quenching coefficients were calculated essentially in accordance with Van Kooten and Snel (1990) except for the assumption that quenching of F_o could be neglected,

$$q_P = (F_M' - F)/(F_M' - F_o) \qquad (2\text{-}1)$$
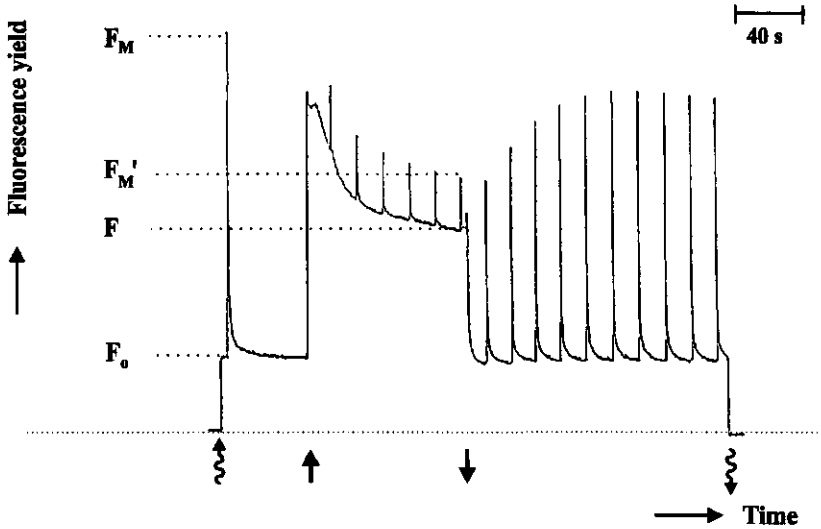
Fig. 2-4 Chlorophyll fluorescence yield of an infiltrated *P. metallica* leaf induced by 2 minutes red actinic illumination (175 μmol m^{-2} s^{-1}). Saturating light pulses of 400 ms were given before (F_M), during and after (F_M') illumination to resolve photochemical and non-photochemical quenching components. F is the quasi steady-state level of fluorescence. F_o is the fluorescence yield in the dark. Solid arrows denote switching actinic light on and off; wavy arrows denote turning on and off the modulated weak measuring light.

$$q_N = 1 - (F_M' - F_o)/(F_M - F_o) \tag{2-2}$$

(refer to Fig. 2-4 for a definition of the symbols used). The quantum efficiency of photosystem II in the dark-adapted state was calculated as,

$$F_v/F_M = (F_M - F_o)/F_M \tag{2-3}$$

Experiments were performed at room temperature.

2.6 P700 measurement

The light-induced formation of the P700$^+$ cation radical (Fig. 2-3) was monitored in the P515 sample chamber by measuring the absorbance increase around 820 nm with a modified PAM fluorometer (Walz, Effeltrich, Germany) in the reflection mode (Schreiber *et al.* 1988). Pulse-modulated light pulses (100 kHz) were provided by a 802 nm LED and the absorbance response was detected by a photodiode. Both LED and photodiode were shielded by a Schott RG780 long-pass filter to prevent interferences with visible light. The maximum amount of oxidisable P700 was determined by applying a far-red

light pulse which was obtained from an incandescent lamp filtered by a Schott RG715 long-pass filter plus a Balzer Calflex heat filter. The final photon flux density of the far-red light was 15 μmol m^{-2} s^{-1}. It was verified that the far-red light intensity was saturating. Experiments were performed at room temperature.

2.7 Creation of a dark ΔpH by ATP hydrolysis

A transmembrane pH gradient in spinach thylakoids was created in the dark by hydrolysis of externally added ATP catalysed by a pre-activated ATP synthase. The activation of the ATP synthase was done by illuminating a thylakoid sample (10 μg Chl ml^{-1}) with white actinic light (410 μmol m^{-2} s^{-1}) for 30 s in the presence of 10 mM dithiothreitol (DTT) and 0.1 mM methylviologen. At 60 s after the activating illumination 0.2 mM ATP was added to start the hydrolysis.

The formation and decay of the ΔpH was followed by 9-aminoacridine (9-AA) fluorescence quenching recorded on a DW2000 spectrophotometer (SLM Aminco, American Instruments, Maryland, USA). The 9-AA fluorescence was detected in dual beam mode as a virtual increase in transmission with λ_1 serving as the excitation wavelength and with λ_2, the reference, set at 900 nm. The 9-AA was excited at 390 nm (= λ_1) with a bandwidth of 15 nm. Fluorescence light was detected around 450 nm by the built-in photomultiplier tube shielded by a combination of a Corning CS4-96, a Schott GG435, a Balzers DT Cyan and a Balzers B51 filter.

The fluorescence quenching of 9-AA (8 μM) was calibrated according to the method described in Lohse *et al.* (1989) using a standard phosphate potential of 29,50 kJ mol^{-1} (Rosing and Slater 1972) appropriate for our experimental conditions. The dark created ΔpH continued for periods longer than 15 minutes which allowed ample time for averaging of P515 responses.

Experiments were performed at 10 °C.

2.8 Data acquisition

For all described methods but ATP hydrolysis the analogue output was digitised using an analogue-digital converter 1401 *Plus* intelligent interface (Cambridge Electronic Design, Cambridge, UK). Process control, data capture and data analysis were accomplished by the program MEAM 1.0 or MEAS 1.1 (Lovoan, Wageningen, The Netherlands) running under MS-DOS on a personal computer. Light-induced conductances changes were either monitored directly on a chart recorder or digitised using the 1401 *Plus* interface. For recording the decay and formation of the ΔpH by 9-AA fluorescence quenching the data processing and process control were accomplished by the software provided with the DW2000 spectrophotometer.

Chapter 3   Patch-clamp method for electrical field detection in single chloroplasts

The patch-clamp technique was initially developed to resolve discrete changes in conductances associated with ionic currents through small patches of membranes from muscle or nervous cells (Neher and Sakmann 1976). One of the advantages of this electrophysiological technique is the possibility to clamp the membrane patch at a constant voltage. This advantage was used by Bulychev *et al.* in 1992 to study light-induced currents in the photosynthetic membrane as a function of an externally applied voltage. They demonstrated large light-induced currents in a single isolated *P. metallica* chloroplast. True voltage clamping of the membrane was, however, not met in their experiments, since high seal resistances appeared unfeasible. Even today, high seal resistances have not been realised and substantial leakage currents are still present. Nevertheless, large light-induced currents can easily and accurately be measured which was one of the reasons to pursue the development of the patch-clamp technique. This resulted in a firm quantitative description of the method with the prospect of calculating the thylakoid voltage generated by a single-turnover of the reaction centers and the total patched thylakoid area of a single chloroplast (Vredenberg *et al.* 1995a). This chapter describes the basics of the technique, its limitations and prospects.

3.1 Classical impalement versus patch-clamp technique

Microelectrode impalement has been considered a rather destructive technique (Racker 1976, Junge 1977). This prejudice concerns the internal membrane distortions and is more or less based on intuitive grounds. Certainly, a consideration of the relative dimensions of electrode tip (internal diameter about 200 nm) and intermembrane spacing of thylakoids (about 5 nm) is illustrative, but illusory. Giving the self-sealing properties of membranes we might expect that the damage made upon microelectrode injection is restored to some extent (Van Kooten 1988). An acceptable estimation of the impalement damage is provided by a judgement of the speed at which a transmembrane potential is dissipated. A too large acceleration of the potential decay after a single-turnover flash compared to the decay rate of the native thylakoid membrane, e.g. as obtained from the decay of Reaction R1/RC of the P515 response, points to too much leakage and the

A. Impalement

Light pulse Light flash

B. Patch-clamp

Current-clamp:
POTENTIALS

Voltage-clamp:
CURRENTS
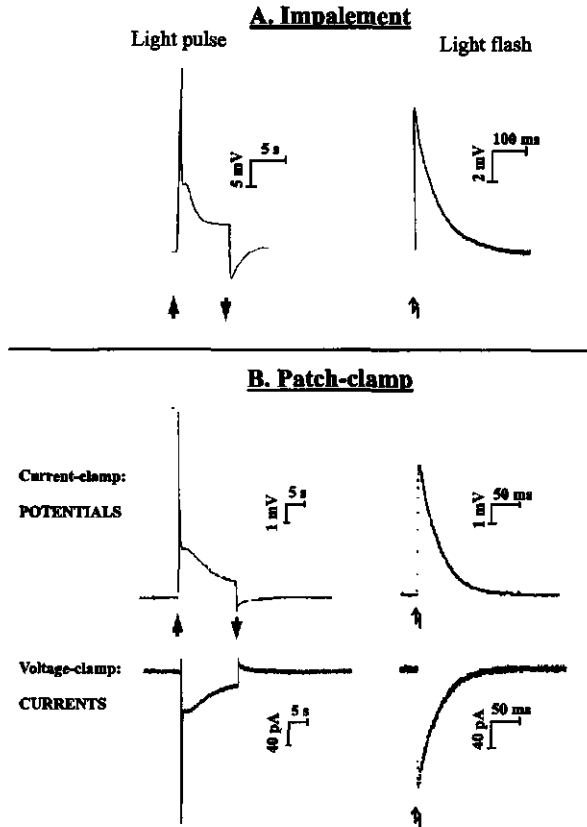
Fig. 3-1 Picture gallery of light-induced responses in *P. metallica* chloroplasts as detected with two alternative techniques: (A) microelectrode impalement and (B) patch-clamp method. Representative response patterns are shown which are not necessarily interrelated. Notice different sensitivities between A and B. The flash-induced response in A was taken from Bulychev and Vredenberg (1976a).

particular impaled chloroplast should be discarded. However, many impaled chloroplasts showed acceptable decay relaxation times. In Fig. 3-1A a representative response monitored with impalement is shown upon continuous illumination (left) and upon a single-turnover light flash (right).

This semi-quantitative assessment of dissipative pathways induced upon impalement is one of the corner stones in the more qualitative approach of the patch-clamp method. Here, a quantification of the relative increase in the field dissipation rate allows insight into the chloroplast network resistances and their impact on the measured responses. Typical patch-clamp responses are shown for comparison in Fig. 3-1B. In general, the profiles of the patch-clamp signals are essentially congruent to those of impalement. The same is true for the patch-clamp current responses which agree well with patch-clamp potential responses. Two striking differences with impalement are the lower amplitude of the photopotential and its usual faster relaxation kinetics. The more suppressed amplitude
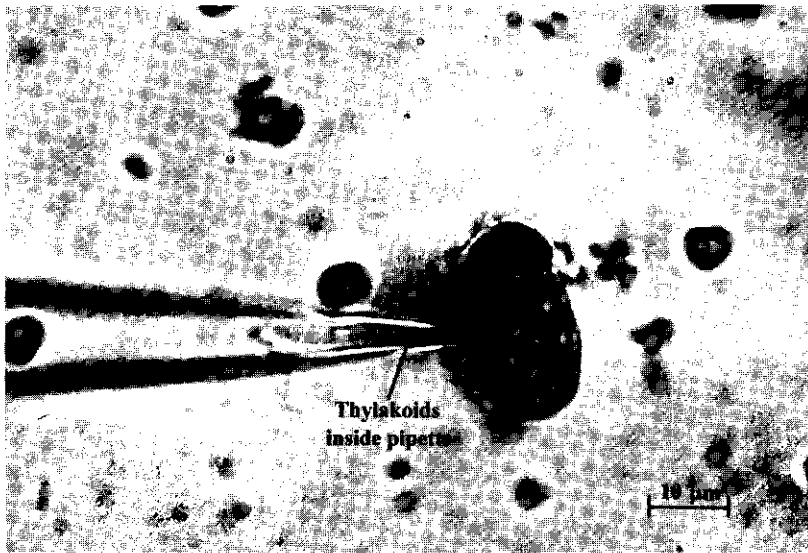
Fig. 3-2 Light microscopy of a single *P. metallica* chloroplast (right) sucked onto a patch-pipette (left).

might have been anticipated since the pipette's tip is more distant to the sites of potential generation in the membrane than the tip of the impaled microelectrode. Light-induced electrical currents originating at the thylakoid membrane must then travel over a longer distance with likely more loss of potential. The faster relaxation kinetics of the patch-clamp technique is caused by the presence of relatively large leakage currents which were disregarded with the impalement technique merely by selecting flash-induced responses with a satisfactory slow decay (Van Kooten 1988). The response time of the three responses increases in the following order: photocurrent > photopotential > impalement.

The patch-clamp method has some advantages over impalement. Experimentally, the method is less sensitive to mechanical vibrations and electrical contact is not rapidly lost. This allows for longer experimentation times ranging from half-an-hour up to several hours. The success rate of making positive contacts is significantly higher than for impalement. At last, the K^+ concentration of the pipette filling solution can be kept low in order to avoid contamination of K^+ in the chloroplast's interior.

In the patch-clamp method a *P. metallica* chloroplast is sucked onto the tapered end of a patch-pipette (Fig. 3-2) and a configuration is easily established in which light-induced currents or potentials can be measured (Fig. 3-1B). Inferred from the polarity of the responses, the electrode is in electrical contact with the thylakoid lumen. However, current is not rapidly dissipated in voltage-clamp mode (Fig. 3-1B) which implies that the pipette tip and reference must have a finite conductance access to the thylakoid membrane. This configuration will be defined as the 'whole-thylakoid configuration'. For this configuration it is assumed that the membrane patches of envelope and thylakoid inside the pipette are permeabilised.

Chapter 3

3.2 Analytical treatment of the whole-thylakoid configuration

Flash-induced patch-clamp responses are generally non-linear. A slowly relaxing tail of the photopotential has been reported and suggested to be related to flash-induced changes in the chloroplast network conductance(s) (Vredenberg *et al.* 1995a). Additionally, secondary electrogenic events (van Voorthuysen *et al.* 1996b, Chapter 4) cause non-linear decay kinetics. Therefore, to improve our understanding of the chloroplast impedance network independently from other phenomena a current-injection technique is employed.

3.2.1 Potential response upon current-injection

The electrical properties of the patch-clamped chloroplast were routinely determined by a current-injection technique in current-clamp mode (Fig. 3-3). With this technique the potential response upon a square current pulse of amplitude I_{comm} is monitored of the patch-pipette and of the patch-clamped chloroplast after establishing the whole-thylakoid

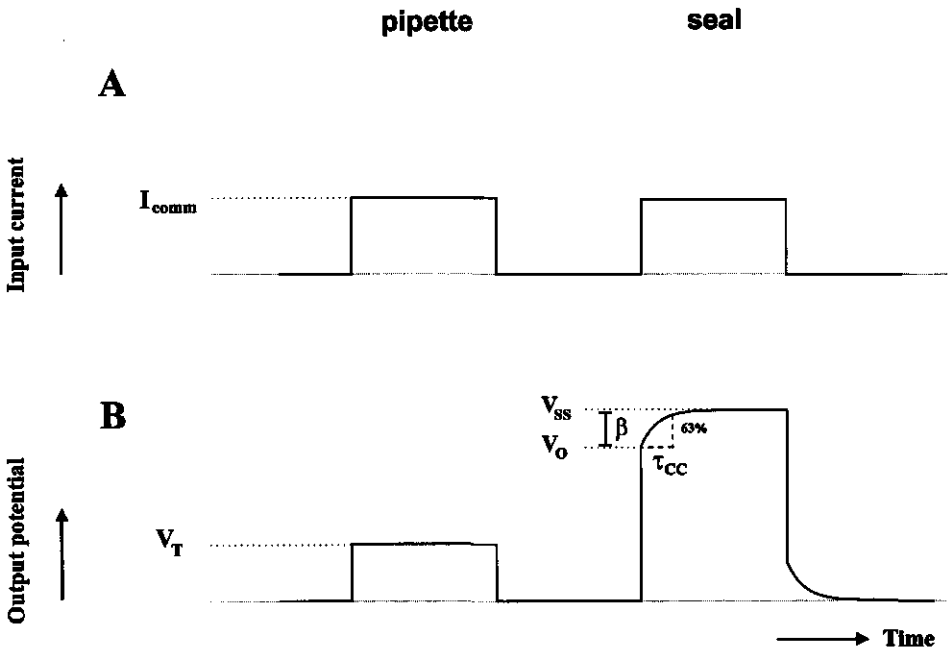**Fig. 3-3** Definition of parameters of the current-injection technique. (A) Input current injected into the pipette tip in the absence (left) and presence (right) of a patched chloroplast. (B) Output potential profiles measured during the current-injection sequence in A. The secondary slow rise of the seal potential response is described by a single exponential function with amplitude β and relaxation time τ_{CC}.

configuration. When the unit of I_{comm} is taken as nA the potential responses in mV directly correspond to resistances in $M\Omega$. Likewise, expressing capacitances in nF and resistances in $M\Omega$ allows relaxation times to be expressed in ms.

The response of the pipette tip exhibits linear ohmic behaviour which results in a square potential output response (neglecting a limited initial rise) of amplitude V_T (Fig. 3-3B). The pipette tip resistance (R_T) can then be calculated according to,

$$\mathbf{R_T} = \frac{\mathbf{V_T}}{\mathbf{I_{comm}}} \qquad\qquad [M\Omega] \qquad (3\text{-}1)$$

After a chloroplast has been contacted and a seal has formed the injected current pulse leads to a higher instantaneous potential (V_0) followed by a small, but distinct slow rise to a steady-state level (V_{SS}) (Fig. 3-3B). The resistance corresponding to this level will be defined as the seal resistance ($R_{Seal} = V_{SS} / I_{comm}$). Assuming the whole-thylakoid configuration the secondary slow rise likely originates from the charging of the thylakoid membrane capacitance. The slow rise kinetics can be satisfactorily described by a single-exponential function characterised by a relaxation time (τ_{CC}) and amplitude (β). Thus, three independent parameters, in addition to V_T, are retrieved from the current-injection technique, i.e. V_{SS}, β ($= V_{SS} - V_0$) and τ_{CC}.
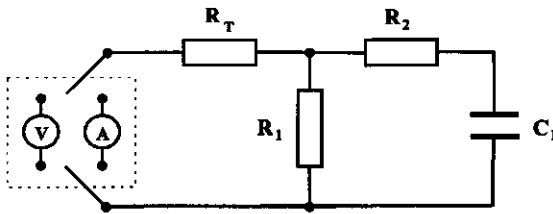
Fig. 3-4 The simplest electrical equivalent scheme concluded from the electrical characterisation of the patch-clamped chloroplast with the current-injection technique (Fig. 3-3). The two symbols in the dashed box indicate the configuration of the EPC-7 patch-clamp amplifier under voltage-clamp (A, current-to-voltage converter) or current-clamp (V, high input impedance voltage buffer) mode.

The simplest electrical scheme which can account for the potential profiles of Fig. 3-3 is shown in Fig. 3-4. Next to the pipette tip resistance R_T the scheme introduces three independent variables, namely two resistances (R_1 and R_2) and one capacitance (C_1). The values of these three variables are calculated according to,

$$R_1 = \frac{V_{SS} - V_T}{I_{comm}} \qquad\qquad [M\Omega] \qquad (3\text{-}2)$$

$$R_2 = \frac{(V_{SS} - V_T) \cdot (V_{SS} - V_T - \beta)}{\beta \cdot I_{comm}} \qquad [M\Omega] \qquad (3\text{-}3)$$

$$C_1 = \frac{\beta \cdot I_{comm} \cdot \tau_{CC}}{(V_{SS} - V_T)^2} \qquad [nF] \qquad (3\text{-}4)$$

3.2.2 Native membrane relaxation time deduced from P515

A quantitative assessment of the increased field dissipation caused by the (as yet unknown) damage produced upon making electrical contact with the thylakoid membrane is given by comparing τ_{CC} with the field dissipation relaxation time of the intact, native thylakoid membrane. The native diffusion-driven relaxation time (τ_M) cannot easily be retrieved from the patch-clamp technique (but see § 3.4). Therefore an independent technique is used, in our case the flash-induced electrochromic absorbance bandshift (P515).

The flash-induced P515 response of a Peperomia leaf shows the multiphasic pattern observed in other leaves and chloroplasts (Vredenberg 1981). The decay is biphasic, with a rapid phase, attributed to the decay of the transmembrane potential (Reaction 1/RC),
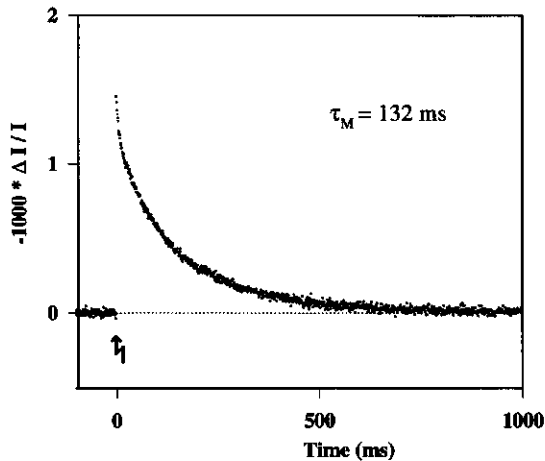
Fig. 3-5 P515 response in the last flash of a train of ten (flash frequency 5 Hz) measured in dark-adapted young leaves (Fig. 2-2) of *P. metallica*, after correction for a contribution (approx. 30 %) of a slow phase Reaction 2 (Schapendonk 1980, Vredenberg 1981). The decay occurs with a relaxation time of 132 ms, attributed to Reaction 1/RC. Average of 500 flash trains given at a rate of 0.03 Hz. Time resolution 1 ms. The leaves were infiltrated with standard isolation medium as described in § 2.2. t = 20 °C.

and a much slower phase attributed to localised electrical membrane effects (Reaction 2) (Ooms *et al.* 1991). Peperomia leaves were given a train of ten flashes, fired at a frequency of 5 Hz, to saturate Reaction 2. The tenth flash was then analysed with a two-exponential function having decay times of 132 ms and 730 ms and amplitudes of 70 % and 30 % for R1/RC and R2, respectively. Figure 3-5 shows the net Reaction 1/RC response upon the last flash. Apparently, the native membrane relaxation time τ_M of *P. metallica* chloroplasts in leaves infiltrated with standard isolation medium (control) is about 132 ms (Table 3-1). This value will be accepted as the default value for τ_M. Care should be taken when experimental conditions are employed other than the dark-adapted control state, e.g. upon light treatment or upon addition of ionophores. In principle, for every new condition the native membrane relaxation time should be determined again. For the case of nigericin this was done on young leaves infiltrated with standard isolation medium supplemented with 1 μM of the ionophore (Table 3-1). The presence of nigericin caused a deceleration of the decay, indicating a lower ion permeability of the thylakoid membrane. Such could have been caused by a decrease of the internal [K+] upon nigericin-facilitated equilibration with the medium K+ (50 mM).

Table 3-1 The native membrane relaxation time (τ_M) of *P. metallica* chloroplasts.

Condition	τ_M (ms)
control, young leaves	132 ± 8[†] (default)
1 μM nigericin, young leaves	230 ± 50[‡]

Leaves were infiltrated with standard isolation medium (§ 2.2). [†]*The indicated error denotes the 99 % confidence interval of the Levenberg-Marquardt fit algorithm of 1 measurement.* [‡]*Indicated error is the SE of N = 4 measurements.*

The single-exponential field dissipation can be described electrically by the scheme shown in Fig. 3-6. It is composed of the membrane resistance (R_M) and the membrane capacitance (C_M). The native membrane relaxation time can then be written as,

$$\tau_M = R_M \cdot C_M \qquad\qquad \text{[ms]} \qquad (3\text{-}5)$$
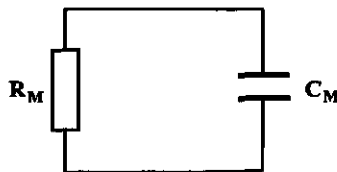

Fig. 3-6 Electrical equivalent scheme of the native thylakoid membrane. R_M - membrane resistance and C_M - membrane capacitance.

3.2.3 Electrical equivalent scheme of the whole-thylakoid configuration

The relative increase of the field dissipation can now be quantified as,

$$p = \frac{\tau_{CC}}{\tau_M} \qquad\qquad 0 < p < 1 \qquad\qquad [\text{-}] \qquad\qquad (3\text{-}6)$$

The simplest electrical scheme which can account for both the current-injection and P515 responses of Figs 3-3 and 3-5 is shown in Fig. 3-7. Current leakage along the pipette rim is represented by a leak resistance (R_L). A low conductance access of the electrode and reference to the thylakoid membrane is represented by an access resistance (R_A). A more elaborate discussion of R_A is postponed to § 3.5 and Chapter 7. As can now be appreciated, the scheme of Fig. 3-4 is only a zero-order approximation of the whole-thylakoid scheme (Fig. 3-7) in the limiting case when the current through R_M can be neglected ($R_M / (R_A + R_L) \rightarrow \infty$) and p approaches zero (i.e. $R_A + R_L \rightarrow 0$). This approximation is best met for small τ_{CC}. We may therefore write,

$R_1 = R_L^{(0)}$ - 0th order approximation of R_L

$R_2 = R_A^{(0)}$ - 0th order approximation of R_A

$C_1 = C_M^{(0)}$ - 0th order approximation of C_M

For a finite $0 < p < 1$ the values of R_L, R_A, R_M and C_M can be deduced by equating the relationships describing the extent and kinetics of the potential profiles upon current-injection, and τ_M for both electrical schemes Figs 3-4 and 3-7. This analysis (not shown) results in the following set solutions,

$$R_L = R_L^{(0)} \cdot \frac{1 - p \cdot R^{(0)}}{1 - p} = R_L^{(0)} \cdot [1 + (1 - R^{(0)}) \cdot (p + p^2 + ...)] \quad [\text{M}\Omega] \qquad (3\text{-}7)$$

$$R_A = R_A^{(0)} \cdot \left[1 - p \cdot R^{(0)} \right] \qquad\qquad\qquad\qquad [\text{M}\Omega] \qquad (3\text{-}8)$$

$$R_M = \frac{\left(R_L^{(0)} + R_A^{(0)} \right)}{p} \cdot \left[1 - p \cdot R^{(0)} \right]^2 \qquad\qquad [\text{M}\Omega] \qquad (3\text{-}9)$$

$$C_M = \frac{C_M^{(0)}}{\left[1 - p \cdot R^{(0)} \right]^2} = C_M^{(0)} \cdot [1 + 2 \cdot p \cdot R^{(0)} + 3 \cdot p^2 \cdot (R^{(0)})^2 + ...] \qquad [\text{nF}] \quad (3\text{-}10)$$
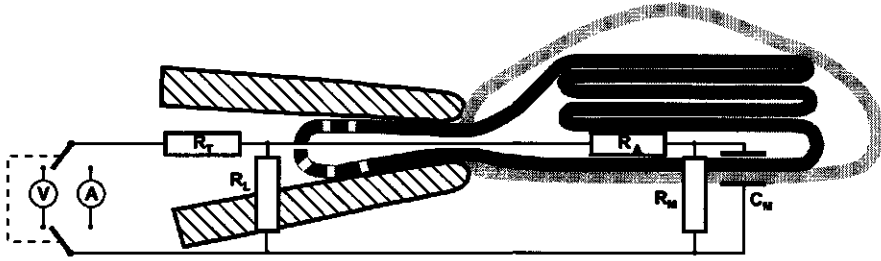
Fig. 3-7 Electrical equivalent scheme of the whole-thylakoid configuration. R_T - tip resistance, R_L - leak resistance along rim of pipette, R_A - access resistance to thylakoid membrane, R_M - membrane resistance and C_M - membrane capacitance. Other symbols as in Fig. 3-4. Original drawing made by J. F. H. Snel.

$$\text{with} \quad R^{(0)} = \frac{R_A^{(0)}}{R_A^{(0)} + R_L^{(0)}}$$

The expressions for R_L, R_A, R_M and C_M have been derived explicitly as a function of p, to elucidate the dependency of those quantities on τ_M and to allow for a series expansion in p ($<$ 1) of equations 3-7 through 3-10. This is necessary because τ_M is derived from an independent method and introduces the largest uncertainty because there is no one-to-one dependent relationship between patch-clamp and P515 data. A brief examination shows that R_L, R_A and C_M are increasingly better determined when p approaches zero which is the case for responses with fast decays ($\tau_{CC} \rightarrow 0$).

The set of equations 3-2 through 3-10 can be combined to yield more convenient expressions as a function of the measured variables $\{V_T, V_{SS}, \beta, \tau_{CC}, \tau_M\}$,

$$R_L = \frac{\alpha}{I_{comm}} \cdot [1 + \frac{1}{\gamma}] \qquad R_A = \frac{\alpha}{I_{comm}} \cdot [1 + \gamma]$$

$$R_M = \frac{\tau_M}{I_{comm}} \frac{\beta}{\tau_{CC}} \cdot [1 + \gamma]^2 \qquad C_M = \frac{\tau_{CC} \cdot I_{comm}}{\beta} \cdot [1 + \gamma]^{-2}$$

$$\text{with } \alpha = V_{SS} - V_T - \beta \text{ and } \gamma = \frac{\alpha}{\beta} \cdot (1 - \frac{\tau_{CC}}{\tau_M})$$

The surface area (A_{thyl}) of the extended patched thylakoid can be calculated from the membrane capacitance and from the specific capacitance of biological membranes (C_{spec} = 10^7 nF m^{-2}) (Vredenberg 1976),

$$A_{thyl} = \frac{10^{12} \cdot C_M}{C_{spec}} \qquad\qquad [\mu m^2] \qquad (3\text{-}11)$$

43

(the factor 10^{12} allows the surface area to be expressed in μm^2 when C_M is expressed in nF) and C_{spec} in nF m^{-2}.

Summary 1

Patch-clamping the giant chloroplasts of P. metallica allows large light-induced currents or potentials to be measured. The electrode is likely in electrical contact with the thylakoid lumen: the so-called 'whole-thylakoid configuration'. Probing the whole-thylakoid configuration with a square current pulse shows that the thylakoid membrane is charged with a field dissipation relaxation time τ_{CC} which is smaller than the field dissipation relaxation time τ_M of the native thylakoid membrane as probed by P515. This difference along with the potential response upon current-injection allows for a quantification of the electrical pathways of the whole-thylakoid configuration which includes an access resistance to the thylakoid membrane, the membrane resistance and the membrane capacitance.

3.2.4 Light-induced responses

The light-induced potential or photopotential ($V_P(t)$) at any time t is not directly equal to the transthylakoid potential but rather a derived response, depending on both the activity of the current generators (e.g. PS I, PS II, Q-cycle) and on the way this current is attenuated in the chloroplast network. Using the scheme of Fig. 3-7 the measured $V_P(t)$ can be translated back to the voltage generated at the site of creation, i.e. the transthylakoid voltage ($V_M(t)$). Considering Fig. 3-7 V_M is attenuated by the voltage-divider made up of R_A and R_L and we can write,

$$V_M(t) = \frac{R_L + R_A}{R_L} \cdot V_P(t) \qquad \text{[mV]} \qquad (3\text{-}12)$$

This transformation is depicted in Fig. 3-8, upper part. It is implicitly assumed that the electrical resistance network responds in a linear fashion to the current. This is, however, only roughly true as light-induced resistance changes have been reported (van Voorthuysen *et al.* 1997, see Chapter 7).

Transformation (3-12) holds true when considering V_M in the patch-clamped chloroplast only. However, by making electrical contact with the thylakoid membrane the rate of field dissipation has been increased by a factor p^{-1} for which the relatively high leakage current (low seal) is essentially responsible. Since the potential level reflects the balance between light-driven electrogenic (proton) currents and passive ion leaks we may anticipate that in the native intact thylakoid membrane, or when having a sufficient high seal resistance, the light-evoked transmembrane potential would have been better retained. Consequently, a higher potential level during continuous illumination *in vivo* is predicted. Nevertheless, when considering the initial amplitude of the flash-induced potential response ($V_P(t = 0)$, or simply defined as V_P) transformation 3-12 would suffice
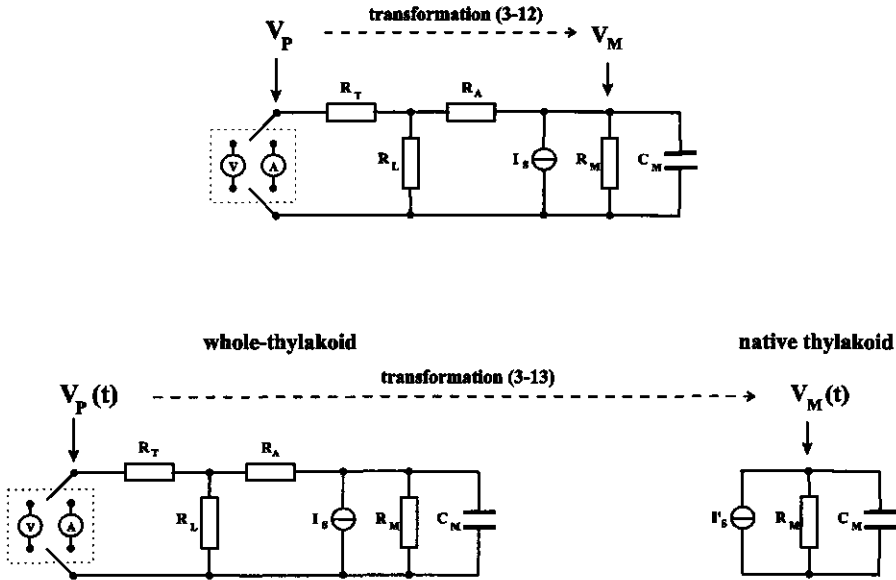
Fig. 3-8 Depiction of two ways for transforming the photopotential (V_P) to the thylakoid membrane voltage (V_M): accounting for the attenuation by the voltage-dividing network only (top) or accounting for both voltage-dividing network and increased field dissipation (bottom). The currents I_S or $I_S`$ represent the active light-driven current generators (PS I, PS II, Q-cycle). Other symbols the same as in Figs 3-4 and 3-7.

for calculating V_M at the moment of flash firing, valid for both in the patch-clamped or *in vivo* situation.

To calculate the thylakoid voltage which would have been generated in the ideal case when the leakage current is negligible we have to account for both the accelerated dissipation and the attenuation by the voltage-divider,

$$V_M(t) = \frac{R_L + R_A}{R_L} \cdot \left[V_P(t) + e^{-t/\tau_M} \cdot \left(\frac{1}{\tau_{CC}} - \frac{1}{\tau_M} \right) \cdot \int_0^t V_P(t`) \cdot e^{t`/\tau_M} \cdot dt` \right] \text{ [mV]} \quad (3-13)$$

This general transformation is also depicted in Fig. 3-8. Transformation (3-13) has been derived (not shown) by considering the two differential equations associated with the whole-thylakoid configuration (Fig. 3-8, bottom, left) and with the simple $R_M C_M$ circuit (Fig. 3-8, bottom, right) of the native thylakoid. For both electrical schemes the potentials $V_P(t)$ and $V_M(t)$ can be related to a given current $I_S(t)$ and $I_S`(t)$, respectively, generated by the light-driven ion pumping. Assuming these pumps to operate independently of the prevailing membrane potential we may equate $I_S$ to $I_S`$ which allows V_M to be related to the measured photopotential V_P according to transformation (3-13).

Summary 2   *After quantification of the whole-thylakoid configuration with the current-injection technique the thylakoid transmembrane potential V_M can be calculated from the measured photopotential V_P response. V_P needs to be corrected for the voltage-dividing resistance network plus for the increased field dissipation rate. The latter correction can be omitted when considering the amplitude of a flash-induced response only.*

3.3 A numerical example

Figure 3-9 shows a representative example of the patch-clamp method for a particular chloroplast. The numerical data of this experiment are collected in Table 3-2. The values for V_T and V_{SS} were directly read from the potential profiles as defined in Fig. 3-3. An accurate measurement of V_{SS} is guaranteed when the pulse duration is taken sufficiently long with respect to the relaxation time τ_{CC} but in order to minimise polarisation effects short current pulses are required. If the desired precision of V_{SS} is more then 98 % the pulse duration must be at least 4 times larger than τ_{CC}. This condition is fulfilled for the chloroplast of Fig. 3-9 (τ_{CC} = 36 ms) which has been probed by a 200 ms pulse, a pulse
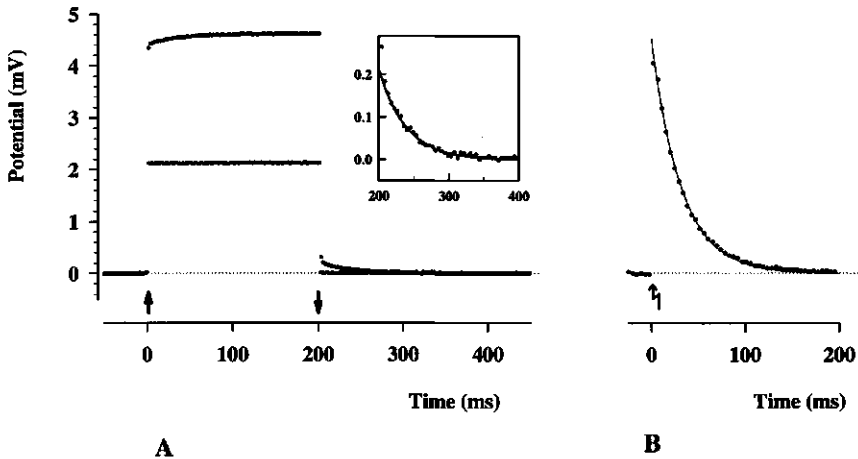
Fig. 3-9   (A) Profile of the potential response upon a 200 ms square current pulse (0.4984 nA) through the pipette of a patched *P. metallica* chloroplast. Horizontal line is potential response of pipette before seal formation. Average of 50 current-induced responses with 0.5 ms time resolution. Insert (data skip of 9, time resolution 5 ms) shows a magnification of the slow potential decay after current-off. The line is a single-exponential fit with 0.202 mV amplitude and 36 ms relaxation time. (B) Flash-induced photopotential of the same chloroplast. Line is a single-exponential fit with 4.6 mV amplitude and 32 ms relaxation time. Flash duration was 6 µs (half width). Dark adaptation approx. 5 minutes. Time resolution 5 ms.

duration most customarily used. The condition, however, fails for chloroplasts with τ_{CC} > 50 ms and in those cases V_{SS} can be predicted from an exponential analysis of the secondary slow rise (not shown). It can be proven that the charging and discharging kinetics are identical (Fig. 3-7). Here we used the current-off decay for the determination of τ_{CC} and β as the relaxation of the potential could be measured for extended periods without polarising the thylakoid membrane. The initial amplitude of the photopotential V_P is determined from an extrapolation to t = 0 of an exponential fit.

First, the values of R_T, R_1, R_2 and C_1 of scheme Fig. 3-4 were calculated (Table 3-2, middle part). Taking the default τ_M = 132 ms the relative acceleration of the field dissipation amounts p^{-1} = $(0.273)^{-1}$ which was subsequently used for calculating R_L, R_A, R_M and C_M according to formulas 3-7 to 3-10 (Table 3-2, lower part).

The relaxation time of the photopotential was found to be 32 ± 3 ms which is in close agreement with τ_{CC}. Based on the electrical scheme (Fig. 3-7) an equal field dissipation relaxation time is predicted for a current-induced and a flash-induced response: whether C_M is charged externally (current-injection) or internally (single-turnover charge separation) makes no difference with regard to the kinetics. Flash excitation of the photosynthetic machinery may, however, induce secondary electrogenic processes like a Q-cycle. Such secondary electrogenic events reveal themselves in photopotential profiles as an apparent slower potential decay, see for example Fig. 4-2 in the next chapter. The good match between τ_{CC} and the relaxation time of the photopotential indicates that

Table 3-2 Quantitative evaluation of the whole-thylakoid configuration of a single chloroplast.

	Current-injection			Flash-induced			P515		
V_T	2.129 ± 0.014	mV	V_P	4.6 ± 0.3	mV	τ_M	132 ± 8	ms
V_{SS}	4.610 ± 0.018	mV						
β	0.202 ± 0.018	mV						
τ_{CC}	36 ± 3	ms						
I_{comm}	0.4984 ± 0.0018	nA						
R_T	4.27 ± 0.03	MΩ						
R_1	4.98 ± 0.05	MΩ						
R_2	56 ± 6	MΩ						
C_1	0.59 ± 0.07	nF						
R_L	5.13 ± 0.05	MΩ	V_M	42 ± 4	mV			
R_A	42 ± 5	MΩ	Q	2.8 ± 0.3	10^8 e⁻			
R_M	$(1.3 ± 0.3)\ 10^2$	MΩ	ETCdens	$(1.33 ± 0.11)\ 10^3$	μm^{-2}			
C_M	1.05 ± 0.18	nF						
A_{thyl}	$(105 ± 18)\ 10^3$	μm^2						

The measured data (upper part) were taken from the experiment of Fig. 3-9. The errors indicated in the upper part designate the standard deviation or precision of the experimental measurements. The errors in the middle and lower part were calculated based on the rules for combination of standard deviations (see appendix A). The symbol e⁻ denotes the elementary charge ($1.6022\ 10^{-19}$ Coulomb). Q - total number of charges displaced. For calculating the ETC density (ETCdens) a PS II : PS I ratio of 1 was assumed.

secondary electrogenic events are absent in the experiment of Fig. 3-9. The calculated membrane potential of 42 mV (Table 3-2) upon a single-turnover of the reaction centers is in reasonable agreement with other data documented thus far (Vredenberg 1976, Schapendonk and Vredenberg 1977, Junge 1977). Based on the calculated membrane capacitance a total patched area of $1.05 \cdot 10^5$ μm^2 is calculated (Table 3-2, eq. 3-11). Assuming a spherical chloroplast of radius 10 μm (Fig. 3-2) the envelope surface area is amounts $1.25 \cdot 10^3$ μm^2 and the thylakoid area sensed by the pipette is then about 84 times larger than the chloroplast area. This is not inconsistent with the many times folded architecture of the thylakoid membrane (Fig. 1-1). The total number of charges (Q) (Table 3-2) displaced upon PS I and II turnover is calculated from the membrane capacitance and the thylakoid potential according to $Q = V_M \cdot C_M$. The electron chain transport density (ETCdens = Q/A_{thyl}) was calculated to be 1333 μm^{-2}, assuming a PS II : PS I ratio of 1. This is in reasonable agreement with the PS I and PS II particle densities as obtained by freeze-fracture studies on spinach, pea and barley (Haehnel 1984).

In relation to photosynthetic free energy transduction, mediated by $\Delta\mu_{H^+}$, it is interesting to reconsider the steady-state transmembrane potential during continuous illumination. In Fig. 3-10A a photopotential response upon 5 s illumination is shown of the same chloroplast as was used for Fig. 3-9 and whose numerical values of the model parameters

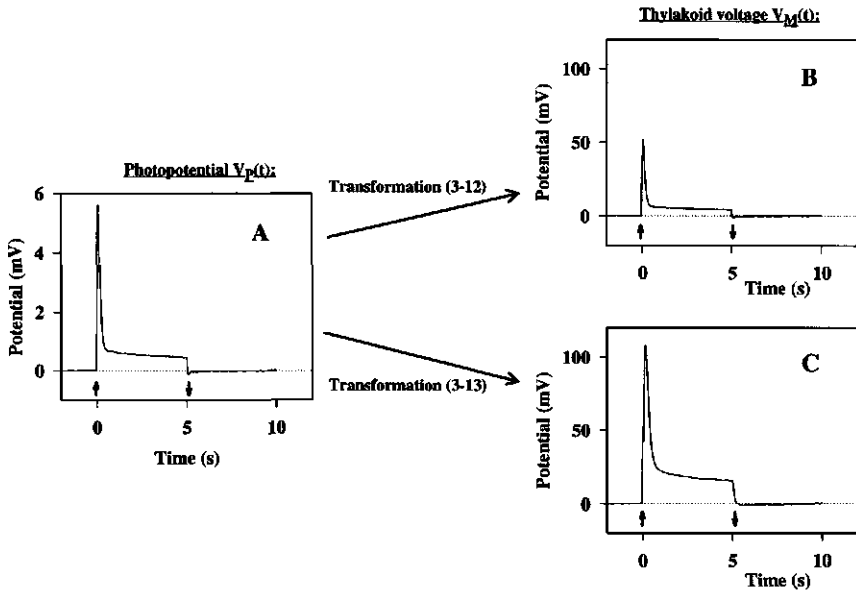**Fig. 3-10** Recalculation of the potential profile upon a 5 s light pulse (**A**) according to transformation 3-12 (**B**) or transformation 3-13 (**C**). Notice the difference in sensitivity between graph(s) on the left and on the right. The rapid potential undershoot at light-off seen in A and B is virtually absent in C because of an effective increase in response time by the integrating transformation 3-13.
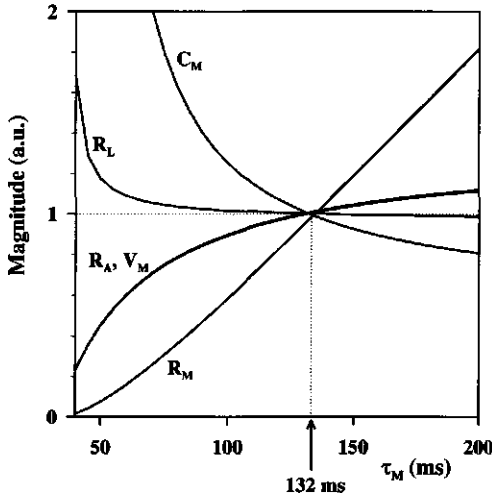
Fig. 3-11 Computed changes of R_L, R_A, R_M, C_M and V_M (normalised on their value at the default $\tau_M = 132$ ms) upon variation of the native relaxation dissipation time τ_M. Numerical values were taken from Table 3-2. The curves for R_A and V_M coincide.

are thus known (Table 3-2). The quasi steady-state potential detected by the electrode is about 0.5 mV (Fig. 3-10A). Correcting for the attenuation due to the voltage-dividing network (transformation 3-12) this will be about 9 times higher at the thylakoid membrane, i.e. 4.5 mV (Fig. 3-10B). When the light pulse would have been given to the same chloroplast in isolation, then having an intact native thylakoid membrane, it can be calculated (transformation 3-13) that the steady-state potential would have been about 20 mV (Fig. 3-10C). For a steady-state $\Delta pH = 2.5$ (Schönknecht *et al.* 1995) the energetic contribution of $\Delta\psi$ to $\Delta\mu_{H^+}$ is then about 12 %, still substantial smaller than the equivalent free energy of ΔpH.

The numerical solutions (Table 3-2) are based on transformations of measured data associated with some uncertainty. Four possible errors will be addressed here:

(1)   the assumptions underlying the model are incorrect;
(2)   the presumed value of τ_M is incorrect;
(3)   systematic errors;
(4)   random errors.

Some reflections on point (1) are postponed to § 3.5. In Fig. 3-11 are plotted normalised data of R_L, R_A, R_M, C_M and V_M calculated from the experimental values of Table 3-2 (middle part) and using a variable τ_M. From this graph we can learn that the precision in determining R_L, R_A, R_M, C_M and V_M decreases in the following order (from highest reliability to lowest reliability): $R_L \rightarrow R_A = V_M \rightarrow C_M \rightarrow R_M$.

In appendix A a short treatise is given covering the systematic and random experimental errors. Considering the results of Fig. 3-11 and those discussed in this paragraph and appendix A we can summarise the following rules of thumbs for working with the patch-clamp method (valid for whole-thylakoid configurations with $R_M > R_A >> R_L$):

49

- The patch-clamp method allows a reasonable estimation of the thylakoid voltage, of the thylakoid surface area (or membrane capacitance), of the ETC-density and of the access resistance. The latter has been proposed to contain information about conductive pathways within the chloroplast thylakoids (Chapter 7).
- The patch-clamp method is less suitable for monitoring (changes in) the thylakoid membrane resistance.
- Since the calculated model parameters are highly sensitive to errors in V_{SS} (Table A-1 of Appendix A) an accurate determination of V_{SS} is required.
- R_A and V_M are relatively insensitive to the relaxation times τ_{CC} and τ_M (Table A-1 of Appendix A).
- A large β predicts a relatively high V_P. Positive correlation found for $N = 36$ chloroplasts with a correlation coefficient of 0.781.
- Fast photocurrents are most suitable for an accurate determination of R_A, V_M and C_M (p approaches zero).

3.4 Statistics of the patch-clamp method

The path-clamp method is unique in its ability to study photosynthetic bioenergetics on a single chloroplast. It has the potential to study e.g. differences in V_M (proportional to the number of active reaction centers) among chloroplasts isolated from different leaf tissues. With regard to the *a priori* unknown value of τ_M a heterogeneity therein will, however, lead to mistakenly calculated answers.
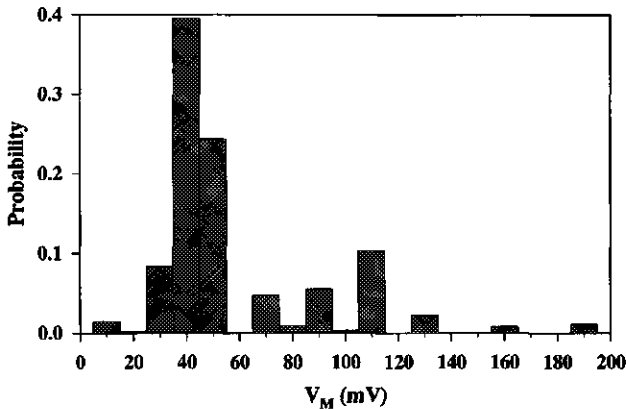

Fig. 3-12 Probability histogram of the single-turnover thylakoid membrane potential V_M. $N = 38$ observations. Calculated from current- and flash-induced potential responses assuming $\tau_M = 132$ ms (from P515). The share of each individual V_M to the probability was weighted according to its associated standard error.

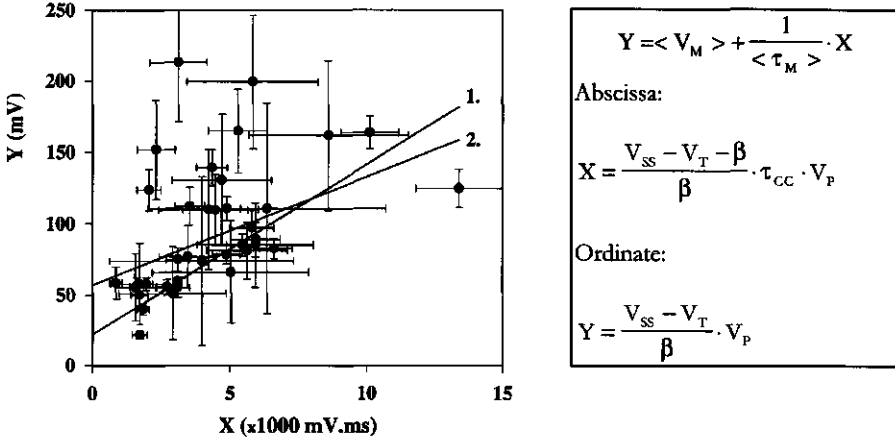The figure contains the following boxed equations on the right:

$$Y = <V_M> + \frac{1}{<\tau_M>} \cdot X$$

Abscissa:

$$X = \frac{V_{SS} - V_T - \beta}{\beta} \cdot \tau_{CC} \cdot V_P$$

Ordinate:

$$Y = \frac{V_{SS} - V_T}{\beta} \cdot V_P$$

Fig. 3-13 Determination of the average membrane potential $<V_M>$ and average native membrane relaxation time $<\tau_M>$ based on relationship 3-12. Data from $N = 38$ measurements. The meaning of the variables X and Y is explained in the box on the right.
　　Line 1: linear regression analysis according to the equation given in the box (top) giving
　　　　$<V_M> = 22.2 \pm 6.0$ mV and $<\tau_M> = 84 \pm 12$ ms.
　　Line 2: predicted relationship based on $\tau_M = 132$ ms and corresponding $<V_M> = 57$
　　　　mV as deduced in Fig. 3-12.

First, let us examine the variation in calculated membrane potentials V_M induced by a single-turnover flash. Figure 3-12 shows the spread in V_M calculated from current-induced and flash-induced potentials of $N = 38$ dark-adapted chloroplasts. A constant default $\tau_M = 132$ ms was used for the calculations. Evidently, thylakoid potentials ranging from 10 up to 190 mV have been calculated with a weighted average membrane potential ($<V_M>$) of 57 mV with a weighted standard deviation of 6 mV (weight according to standard error in individual V_M values). To patch a chloroplast with a V_M of about 40 mV has the highest probability.

In order to explore the unknown variation in τ_M relationship 3-12 was used for finding an average V_M and average τ_M ($<\tau_M>$). The results of this investigation are shown in Fig. 3-13. Thus, only patch-clamp data were used in calculating the variables X and Y (Fig. 3-13), without using another technique which demonstrates that in principle τ_M can be obtained from comparative patch-clamp measurements. In the situation that every individual chloroplast were to have a same τ_M and a same V_M all data points would fall on a single straight line. Line 2 (Fig. 3-13) was drawn based on $\tau_M = 132$ ms and $<V_M> = 57$ mV as obtained from Fig. 3-12. Apparently, there are a lot of exceptions and we therefore conclude that either the membrane potential or the native membrane relaxation time or both must show variations among different chloroplasts. A linear regression analysis using all $N = 38$ data points gave an average membrane potential of $<V_M> = 22$ mV and an average membrane relaxation time of $<\tau_M> = 84$ ms (line 1 in Fig. 3-13).

Summary 3   *With the patch-clamp method the thylakoid membrane potential V_M generated upon a single-turnover flash in a chloroplast with an presumed native membrane relaxation time of 132 ms is estimated to be 20 - 60 mV with 40 mV the most probable value. In addition, the thylakoid surface area (membrane capacitance), number of active reaction centers and the access resistance can be assessed. Variations in V_M as well as in τ_M among (populations of) chloroplasts between 20 % and 300 % are likely to exist. We therefore conclude that the patch-clamp method works best for studying relative changes in parameters of interest on the same chloroplast.*

3.5   On the nature of the access resistance R_A

An intriguing and important question remains to be addressed concerning the (physiological) interpretation of the access resistance R_A. In the most unbiased approach it includes any resistance encountered when going from electrode or reference to that moiety of the thylakoid membrane which is located outside the pipette (cf. Fig. 3-2). That the outside located thylakoids are responsible for the majority of the light-induced current is inferred from dimensional considerations of the extensive calculated surface area (Table 3-2). The R_A has been proposed to be related to a lateral resistance along the thylakoids and to a hindered exchange between the bulk phase and a hypothetical membrane phase (van Voorthuysen *et al.* 1997, see Chapter 7). Other possible contributions may come from the envelope resistance and the stromal and lumenal resistances, but need to be elucidated. Preliminary results on photocurrent measurements in the presence of NH_4Cl indicate that shrinkage and swelling of thylakoids are likely involved (W. J. Vredenberg, A. A. Bulychev, personal communication).

A partial, structural partitioning of R_A, however, might seem possible if a closer look is taken on the voltage-induced and flash-induced responses shown in Figs 3-14 and 3-15, respectively. These responses were measured under voltage-clamp as to optimise the temporal resolution in the first milliseconds; the signal-to-noise ratio is lower than in current-clamp mode. The voltage-induced response of the seal configuration (Fig. 3-14) shows two kinetically distinct phases: a slow phase of small amplitude which has an identical origin as the slow rise seen upon current-injection (§ 3.2.1), and a much faster phase below 1 ms (Fig. 3-14, B2). The respective relaxation times of these two phases, obtained from a two-exponential fit, are 13.2 and 0.35 ms. It should be emphasised that both phases are absent in the voltage response of the pipette alone (Fig. 3-14, A1 and A2).

The flash-induced response (Fig. 3-15) was also analysed with a two-exponential function giving relaxation times of 14.2 and 0.42 ms for a slow and a fast phase, respectively. These times show a close correspondence with the two relaxation times of the slow and fast phases detected upon voltage-injection and therefore likely have a common cause. A remarkable feature of the flash-induced photocurrent, regularly, but not always observed that clear, is its transient positive amplitude. A possible configuration which can account for these phenomena is shown as the extended electrical equivalent scheme (Fig. 3-16). Part of R_A ($R_A^{(1)}$) has been allotted to the thylakoid
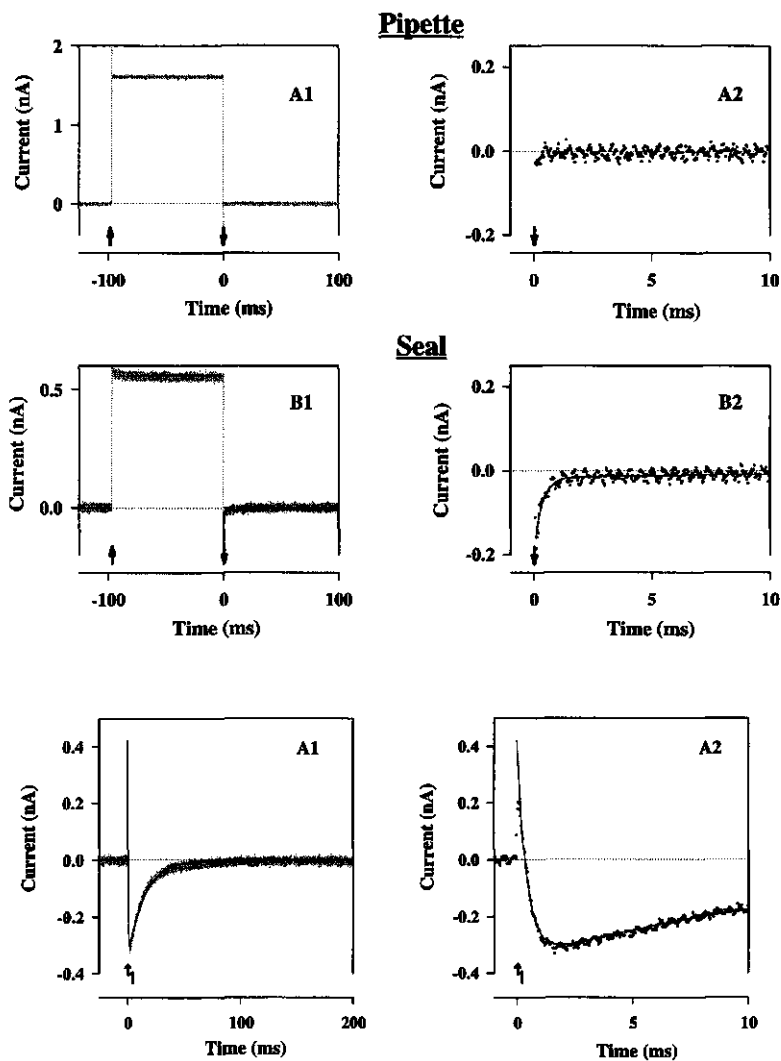
Pipette

Seal

Fig. 3-14 Current response of pipette (**A1** and **A2**) and seal (**B1** and **B2**) of a *P. metallica* chloroplast upon voltage-injection with a square pulse (9.1 mV, 100 ms). The graphs on the right show a magnified view of the potential-off response. Sample frequency 30 kHz. Electronic filter (EPC-7) 10 kHz. The solid line in graph B2 is a two-exponential fit with amplitudes of -0.017 and -0.17 nA and relaxation times of 13.2 and 0.35 ms for the slow and fast phase, respectively.

Fig. 3-15 Flash-induced photocurrent on a long (**A1**) and short (**A2**) time-range. Same chloroplast as used for Fig. 3-14. Sample frequency 30 kHz. Electronic filter (EPC-7) 10 kHz. The solid line in graph A2 is a two-exponential fit with amplitudes of -0.353 and +0.773 nA and relaxation times of 14.2 and 0.42 ms for slow and fast phase, respectively.

53

membrane portion inside the pipette tip while a remainder ($R_A^{(2)}$) is still allotted to low conductances more proximal to the thylakoid membrane outside the pipette tip. It must be understood that the resistance $R_A^{(1)}$ may still have contributions from all of the possible resistances summarised at the beginning of this paragraph and in addition from a (partial leaky) thylakoid membrane resistance. A contribution from the envelope membrane is, however, considered unlikely since the envelope is expected to be easily ruptured upon suction.

A capacitance (C'_M), with likely a main contribution from the thylakoid membranes in the tip, has also been included. The surface area of this portion is expected to be smaller than that associated with the extensive thylakoid membrane outside the tip. The non-zero initial amplitude is explained in this model by an unequal density of active charge separating reaction centers in thylakoids located in the tip and those located outside the tip, respectively.
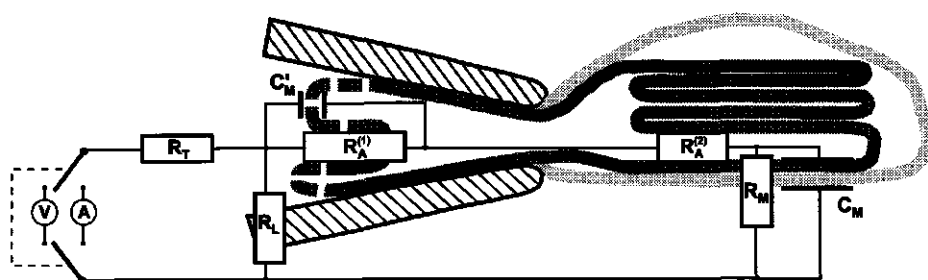
Fig. 3-16 Extended electrical equivalent scheme describing the biphasic kinetics of voltage-induced and flash-induced responses of Figs 3-14 and 3-15. Symbols the same as in Fig. 3-7 except for: $R_A^{(1)}$ - first component of access resistance R_A related to the portion of thylakoids inside pipette tip, $R_A^{(2)}$ - second component of R_A related to low conductances located more proximal to the thylakoid membranes outside the pipette tip, C'_M - (membrane) capacitance associated with portion thylakoids inside pipette tip.

The flash-induced response on a ms time-range is still well described by the standard scheme of the whole-thylakoid configuration discussed in § 3.2.3. On this time-scale the system behaves as it is in direct electrical access to the lumen: electrical charges pass undelayed through the thylakoid portion inside the tip. A physical transport of larger molecules should, however, not be an obligatory consequence and the thylakoid portion inside the tip may equally be closed on a spatial scale. When patch-clamp studies are to be done in relation to variations and modifications in chloroplast structure, the extended equivalent scheme deserves closer attention. The extended equivalent scheme becomes increasingly important when the ratio between thylakoids outside to thylakoids inside the tip decreases as will be the case for small chloroplasts like those from spinach and pea.

Experiments have been performed with the charged fluorescent dye Lucifer Yellow (LY) (data not shown) to explore any physical access of the pipette's interior to the thylakoid lumen. Unfortunately the results were not conclusive since contamination of

the stroma by LY, extending the fluorescence over the whole spherical chloroplast surface area, could not be discriminated for.

Summary 4

Part of the access resistance R_A may be associated with a thylakoid portion inside the tip of the pipette and is active in charge separation. This would explain the generally observed sub-ms rise kinetics and the occasionally observed non-zero initial amplitude of photocurrents. Different functional types of resistances are expected to be involved in R_A: (leaky) thylakoid membranes and lateral resistances. On a ms timescale the electrical behaviour of the patched chloroplast is as though there is direct contact with the thylakoid lumen. Accounting for the thylakoid portion inside the tip becomes increasingly important when patching small chloroplasts like those from spinach and pea.

3

Chapter 4 Secondary electrogenic transport in chloroplasts. Relation to Q-cycle

Light absorption by the light harvesting complexes of photosystem (PS) I and II results in the formation of the primary charge-separated state in the respective reaction centers within about 300 ps (Wasielewski *et al.* 1989, Hecks *et al.* 1994). The ensuing redox reactions, including those associated with proton binding and release at the thylakoid membrane interfaces, cause the formation of a transmembrane electrical potential and a proton gradient which serve as the electrochemical driving-force for the formation of ATP by the ATP synthase. In addition to the fast primary electrogenic events in the reaction centers a slow secondary electrogenic process involving the cyt. b_6f complex has often been discerned, having the same orientation as primary charge separation (Mitchell 1976, Bendall 1982, Jones and Whitmarsh 1988, Ooms *et al.* 1989). In this secondary electrogenic step, generally modelled as a Q-cycle (Mitchell 1976, Hope *et al.* 1992) and modifications thereof (Hope *et al.* 1992, Wikström and Krab 1986, Rich *et al.* 1992, Joliot and Joliot 1994), a difference in redox energy between two b-cytochromes is coupled to transversal electron transport from lumen to stroma (Hope 1993). Besides these two major electrogenic events other thylakoid membrane related processes might be operative and add to the light-induced transmembrane electrical field, e.g. ATP synthase activity (Van Kooten *et al.* 1986, Groth and Junge 1995).

The dispute of a functional Q-cycle in chloroplasts continues unabated. In general, the electrogenic nature of a Q-cycle concept is inferred from the kinetic correlation of the slow electrochromic phase of P515 with the turnover of the b_6f complex, strengthened by the suppression of this slow phase by specific Q_p-site inhibitors like DBMIB or stigmatellin (Jones and Whitmarsh 1988, Hope and Rich 1989, Kramer and Crofts 1994). The interpretation of the decay kinetics of the P515 response is, however, not unambiguous and is hindered by non-specific flash-induced absorbance changes taking place concurrently. This may lead to an incorrect estimation of the electrogenic reactions associated with the cyt. b_6f complex (Vredenberg 1996). For example, the slowly decaying phase of P515 defined as Reaction 2 (Vredenberg 1981, 1996), a non-electrogenic reaction, needs to be taken into account when extracting a Q-cycle-type component from the slow P515 phase (Ooms *et al.* 1989).

The Q-cycle concept was challenged by Furbacher *et al.* (1989), who found a too small redox potential difference between the two b-hemes to allow for efficient electron transfer in an operative Q-cycle. This was contradicted by Kramer and Crofts (1994),

who demonstrated the existence of rapid electron transfer between the quinol oxidising site (Q_p-site) and cyt. b_h as is demanded for by the Q-cycle mechanism. A more straightforward and independent technique will therefore be desirable to settle some of these controversies on the electrogenic steps within the cyt. b_6f complex.

Progress in the detection and analysis of light-induced thylakoid membrane potentials has been achieved recently by the introduction of a patch-clamp method (Bulychev *et al.* 1992, Vredenberg *et al.* 1995a, Chapter 3). With this method, the extent and relaxation kinetics of the flash-induced membrane potential can be measured on a single chloroplast. The patch-clamp method is particularly suitable for the study of light-induced electrical phenomena using single-turnover flashes because i) signal-averaging is not required considering the sufficient signal-to-noise ratio and ii) the electrical response is directly proportional to the thylakoid membrane potential, without interfering contaminations from non-electrogenic processes as in the P515 method (see Vredenberg 1981); see however Chapter 7.

This chapter reports on a secondary electrogenic event which results in a multiphasic photopotential response detected in single *Peperomia metallica* chloroplasts. Emphasis is laid on a detailed kinetic analysis of the slow electrogenic phase. The results are discussed in the light of existing Q-cycle models for b_6f turnover.

4.1 Deconvolution of photopotential/-current in R1/RC and R1/Q

The flash-induced changes in potential (photopotential) and current (photocurrent) were measured on single *P. metallica* chloroplasts in current-clamp and voltage-clamp mode, respectively. See Fig. 3-7 in Chapter 3 for a representation of the measuring configuration (whole-thylakoid configuration). The whole-thylakoid configuration of a particular chloroplast was characterised as described in § 3.3. Figure 4-1 shows that the current-off response is symmetrical to the current-on response. In order to minimise polarisation effects short current pulses had to be employed. As photopotential relaxation times as high as 120 ms were observed, we used the current-off response for the analysis of the decay kinetics as in this way the relaxation of the potential could be measured for extended periods without polarising the thylakoid membrane. For t > 15 ms the slow decay can be described satisfactorily with a single exponential function (Fig. 4-1C, curve I) to which a field dissipation relaxation time (τ_D) is assigned. For the particular chloroplast of Fig. 4-1 the calculation yields $\tau_D = 74$ ms. Single-exponential decay kinetics would thus be anticipated for a flash-induced response evoked by fast primary charge separation in PS I and PS II reaction centers.

Figure 4-1B shows the flash-induced photopotential response of the same chloroplast. After a fast initial rise a further slow increase in photopotential is evident and this is followed by a multiphasic decay. Hence, contrary to what is predicted from the results of the current-injection technique, the photopotential exhibits multiphasic kinetics (Fig. 4-1C, curve II). This observation leads to the conclusion that besides primary charge separation a secondary electrogenic event is involved. The photopotential relaxes from

A. Current-induced response:

B. Flash-induced response:
photopotential $V_p(t)$

C. Decay kinetics of 2 responses:

I. $\tau_D = 74$ ms

II. $\tau_D = 76$ ms
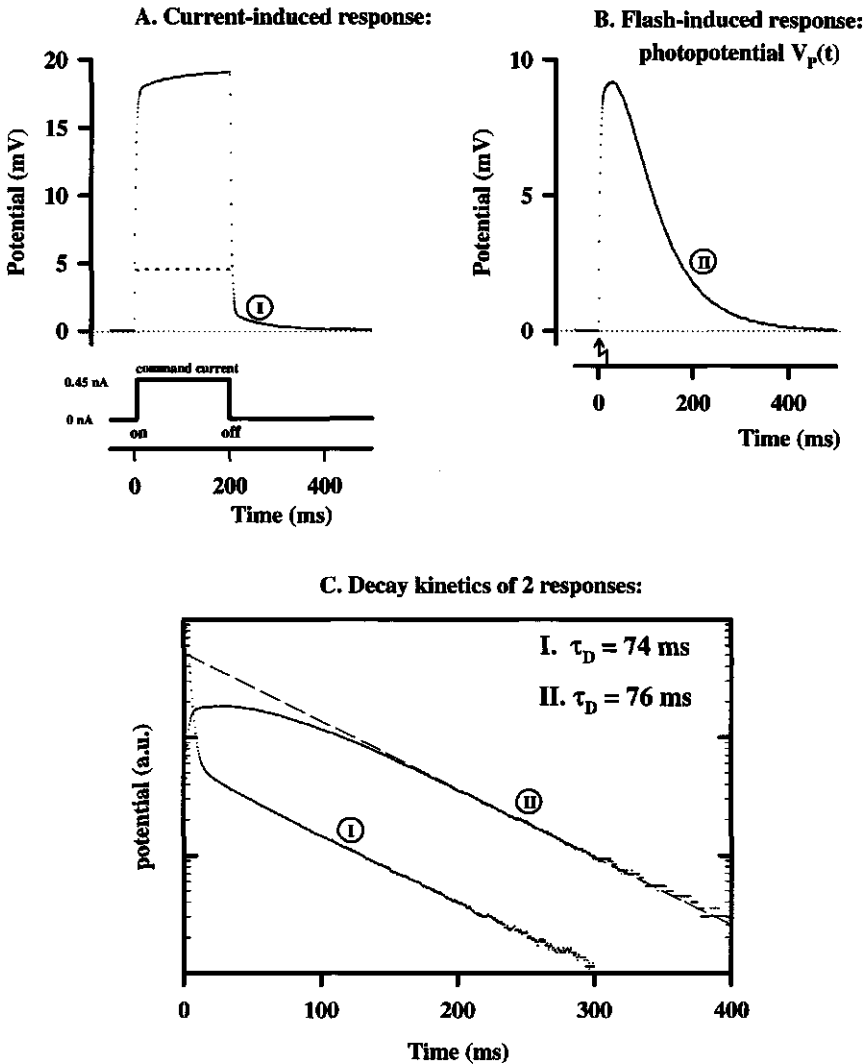
Fig. 4-1   Potential responses (current-clamp mode) of a patched *P. metallica* chloroplast in the whole-thylakoid configuration. (**A**) Response induced by a square current pulse of 200 ms duration and 0.45 nA amplitude. The horizontal dashed line indicates the potential response of the patch-pipette before seal-formation. For this particular experiment the following values were calculated (for method see Chapter 3): $R_T = 10.0$ MΩ, $R_L = 35.4$ MΩ, $R_A = 173$ MΩ, $R_M = 174$ MΩ, $C_M = 0.775$ nF, $V_M = 46$ mV. (**B**) Potential response induced by a saturating single-turnover flash. (**C**) Semi-logarithmic plot of the decay after current-off (curve I) and after the flash (curve II). The respective relaxation times for $t > 200$ ms of both decays are $\tau_D = 74$ ms and $\tau_D = 76$ ms.

59

about 200 ms onwards (Fig. 4-1C, dashed line) with a relaxation time of 76 ms which corresponds nicely with the relaxation time of the potential decay after current-injection. This close match strongly suggests that the tail of the photopotential is associated with the dissipation of the electrical field by currents through the load resistances. It must be stressed that the secondary rise of the flash-induced photopotential is more obvious in experiments where the chloroplast shows a response with $\tau_D > 50$ ms. This is the case when R_L or R_A are relatively high (high seal) compared with R_M and τ_D will approach the native membrane relaxation time τ_M ($p \to 1$, see § 3.2.3). In experiments with $\tau_D < 50$ ms, i.e. with relatively low seal resistances as in Vredenberg et $al.$ (1995a), the rise of secondary electrogenic events are masked by the fast field dissipation.

Both current and flash-induced responses (Figs 4-1A and B) were measured under current-clamp which allowed for a direct comparison of their field dissipation relaxation times. The current-clamp mode benefits from a good signal-to-noise ratio and from less interference of stray capacitance than the voltage-clamp mode but has a relatively poor time resolution. To improve the kinetic resolution in the first milliseconds, the flash-induced current response was measured in voltage-clamp mode on the same chloroplast (Fig. 4-2). Notice the similarity in the kinetics obtained for both measuring modes (Figs 4-1B and 4-2). The initial amplitude of the photocurrent ($I_P(0)$ or simply I_P) is -240 ± 10 pA. The relaxation time calculated from the decay of the photocurrent for t > 200 ms, about 68 ms, was found to be in close agreement with τ_D obtained by current-injection, provided that the slightly increased rate of field dissipation introduced by the tip resistance R_T (cf. Fig. 3-7) is taken into account. In a first approximation (method 1) the photocurrent ($I_P(t)$) of Fig. 4-2 was assumed to be a linear combination of two exponentials,

$$I_P(t) = a_I \cdot e^{-t/\tau_I} + a_{II} \cdot e^{-t/\tau_{II}} \qquad \text{[pA]} \qquad (4\text{-}1)$$

in which a_I and a_{II} are amplitudes of opposite sign and τ_I and τ_{II} are relaxation times with, by definition, $\tau_I > \tau_{II}$. Relaxation time τ_I is thus equal to the field dissipation relaxation time τ_D. The best values found for the photocurrent of Fig. 4-2, as obtained from a least-square fit using eq. 4-1, are: $\tau_I = 67.7$ ms, $\tau_{II} = 42.8$ ms, $a_I = -903$ pA, $a_{II} = 659$ pA. The initial amplitude of the photocurrent calculated from the bi-exponential fit is then $a_I + a_{II} = -244$ pA which is in close agreement with the amplitude directly read from the current profile. In order to give a physiological interpretation of this bi-exponential analysis we must realise that primary charge separation in the reaction centers should results in a fast initial rise with a subsequent dissipation of the electrical field governed by τ_D (Vredenberg 1976, Vredenberg et $al.$ 1995a). Therefore, a meaningful deconvolution of the bi-exponential fit will be the sum of a reaction called R1/RC, associated with fast primary charge separation in the reaction centers, and of a slow secondary reaction which we call R1/Q,

$$R1/RC(t) = (a_I + a_{II}) \cdot e^{-t/\tau_I} = I_P(0) \cdot e^{-t/\tau_D} \qquad \text{[pA]} \qquad (4\text{-}2)$$

$$R1/Q(t) = -a_{II} \cdot (1 - e^{-t/\tau_r}) \cdot e^{-t/\tau_D} \qquad \text{[pA]} \qquad (4\text{-}3)$$
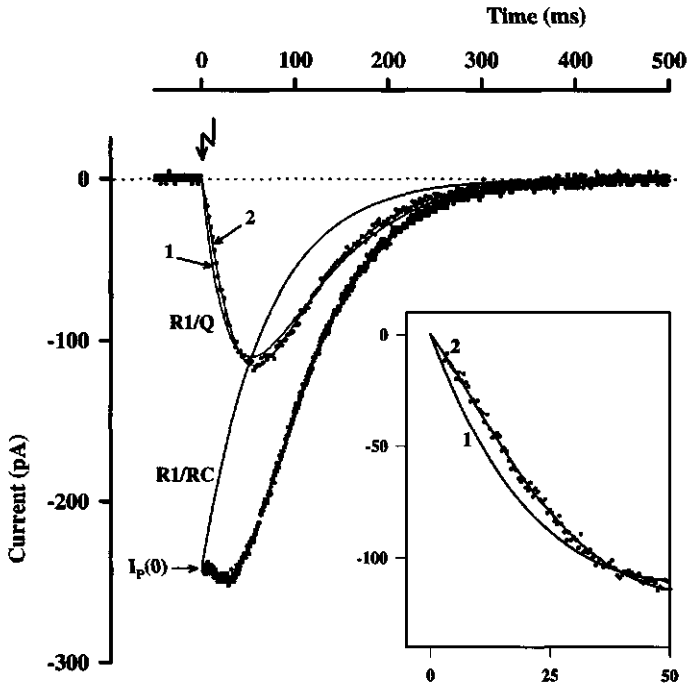
Fig. 4-2 Flash-induced photocurrent (voltage-clamp mode) measured on the same chloroplast as in Fig. 4-1. The overall response was deconvoluted into R1/RC and R1/Q. R1/RC is a single exponential function constructed from the initial amplitude $I_P(0)$ and the relaxation time taken from the current decay for t > 200 ms (see Fig. 4-1C). R1/Q (dots) was obtained by subtraction of the overall response with the constructed R1/RC (method 2). The solid lines 1 and 2 refer to the two analytical fits of R1/Q: 1, calculated from a bi-exponential fit of the overall photocurrent transient (method 1, eqs 4-2 and 4-3) and 2, analysis based on a partly consecutive reaction scheme shown in Fig. 4-6. Inset shows R1/Q on a shorter time-scale elucidating the sigmoid rise kinetics.

with $1/\tau_r = 1/\tau_{II} - 1/\tau_I$. Figure 4-2 shows R1/RC (solid line) and R1/Q (solid line 1) as calculated using eqs 4-2 and 4-3, respectively (method 1). The acronym R1/Q specifies the relation to a Q-cycle mechanism (Ooms *et al.* 1989), a notion which is supported by the inhibition of R1/Q by DBMIB (cf. Fig. 4-4B).

In a second, less constrained manner R1/Q is obtained as follows (method 2). Reaction R1/RC can be constructed as a single exponential function with an initial amplitude read from the photocurrent response at t = 0 and a field dissipation relaxation time τ_D given by the current-injection technique or, equivalently, by the relaxation time calculated from the tail of the photocurrent for t > 200 ms. Next, R1/Q is deduced as the difference between the measured curve and R1/RC (Fig. 4-2, R1/Q dots).

Assuming identical dissipation mechanisms, the area under the photocurrent traces allows a relative estimation of the number of charges separated by the two electrogenic

reactions R1/RC and R1/Q. A ratio Q/RC is introduced to quantify the contribution of R1/Q to the photocurrent/-potential. The Q/RC-ratio is defined as the number of charges displaced by R1/Q divided by the number of charges displaced by R1/RC (originating from both PS I and PS II). For the chloroplast of Fig. 4-2 the Q/RC-ratio is about 0.95.

Summary 1   *The multiphasic photocurrent can be deconvoluted into two electrogenic reactions: 1) R1/RC, associated with fast primary charge separation in PS I and PS II reaction centers, and 2) R1/Q, a slow secondary electrogenic reaction. The close agreement between the discharge relaxation time after current-injection and the decay relaxation time of the tail of the photocurrent (t > 200 ms) allowed for a well-defined deconvolution of the photocurrent into R1/RC and R1/Q. The number of charges translocated by R1/Q and R1/RC can be estimated from the area under the respective deconvoluted reactions from which a Q/RC-ratio is calculated.*

4.2   Characterising R1/Q as cyt. b_6f turnover

In the presence of the artificial electron donor duroquinol (DQH$_2$) a slow secondary rising phase appeared after partial inhibition of PS II-dependent plastoquinone reduction by DCMU (Fig. 4-3). Duroquinol has been shown to be a potent stimulator of Q-cycle
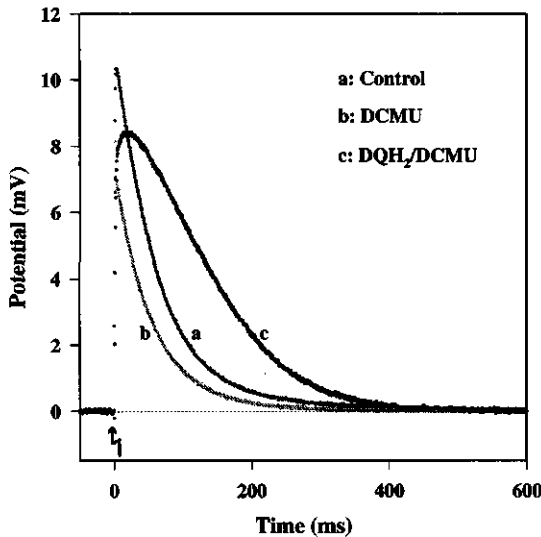

Fig. 4-3   Stimulation of R1/Q by duroquinol (DQH$_2$). Photopotentials on a first single-turnover flash of a dark-adapted (5 minutes.) *P. metallica* chloroplast. The chloroplast was given the following treatments: a) control, no additions, b) addition of DCMU (5 μM final concentration) and c) after subsequent addition of DQH$_2$ (1.5 mM final concentration).

activity in chloroplasts (Jones and Whitmarsh 1985, Ooms *et al.* 1989). Since oxidised duroquinone (DQ) can act as a competitive inhibitor at the Q_p-site, DQ and DQH_2 both compete for the same binding site: therefore sufficiently high concentrations DQH_2 are necessary, here 1.5 mM, also because DQH_2 is easily oxidised by O_2 present in the isolation medium (Kramer *et al.* 1994). Notice that R1/Q is virtually absent in the control response (Fig. 4-3). Addition of DCMU in the dark caused less than 50 % suppression of the amplitude upon a first flash in the dark. This shows that even in the presence of DCMU PS II reaction centers slowly re-open in the dark.

Two other characteristics of the slow rising phase were observed (data not shown): i) closure of PS I reaction centers in the presence of far-red background illumination eliminated R1/Q and ii) addition of 1 μM tentoxine, a specific blocker of the ATP synthase (Groth and Junge 1995), was without noticeable effect on R1/Q.

Addition of 2.5 μM DBMIB, an inhibitor of cyt. b_6f turnover (Trebst 1980, Rich *et al.* 1991), caused the disappearance of the secondary slow phase in a 5-flash sequence from flash 2 onwards (Fig. 4-4B).

4.3 Regulation of R1/Q by light

4

Flash illumination
It was observed that in the absence of DBMIB the extent of R1/Q increased in a sequence of 5 single-turnover flashes given with a flash frequency of 0.5 Hz to a dark-adapted chloroplast (Fig. 4-4A). Deconvolution of the responses using method 2 discussed
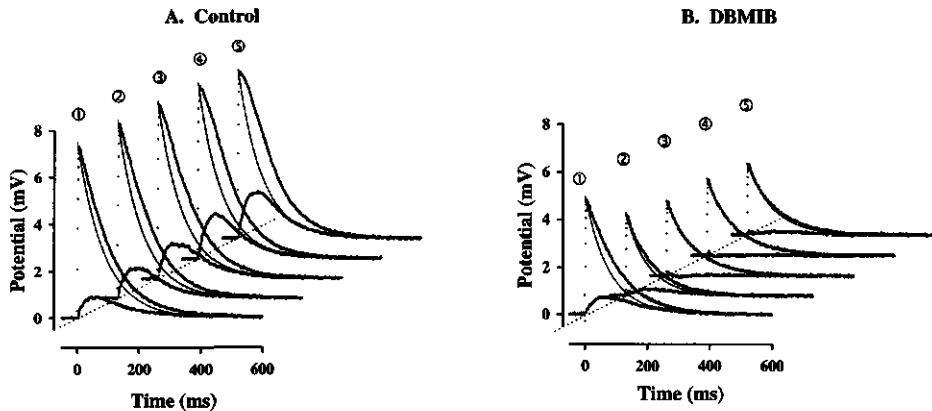
Fig. 4-4 Photopotentials measured on a single *P. metallica* chloroplast upon five saturating single-turnover flashes given with a flash frequency of 0.5 Hz. Deconvolution into R1/RC and R1/Q as in Fig. 4-2 using method 2: solid lines represent R1/RC, lower dotted curves represent R1/Q. After the recording of the control (A), the same chloroplast was immersed with medium supplemented with 2.5 μM DBMIB by the aid of a superfusion DAD-system (§ 2.3) (B). BSA was omitted from the standard isolation medium in this experiment to prevent non-specific adsorption of DBMIB onto BSA, thus preventing a lowering of the effective concentration of inhibitor.

in § 4.1 resulted in an *increase* of the Q/RC-ratio from 0.20 to 0.50 for flash numbers 1 to 5, respectively. This is most readily explained by an increase in the concentration of PQH$_2$ produced by PS II turnover of preceding flashes. The increased PQH$_2$ concentration will subsequently enhance the number of *bf* complexes with a bound PQH$_2$ at the Q$_p$-site prior to the flash. Contrary, in some chloroplasts which had a relatively high Q/RC-ratio upon a first flash, a *decrease* of the Q/RC-ratio was seen after a few single-turnover flashes (data not shown).

Continuous illumination
Reaction 1/Q was examined in relation to energisation of the thylakoid membrane by pre-illuminating a single *P. metallica* chloroplast for 2 minutes with continuous red actinic light. Before (dark) and at various times after pre-illumination the state of energisation was probed by monitoring the current response upon a single-turnover flash (Fig. 4-5A). In Fig. 4-5A the flash-induced photocurrents were deconvoluted according to method 2 of § 4.1, using a decay relaxation time τ_D as obtained from the tail of the photocurrents. The number of charges displaced by RC and Q-cycle were calculated from the area under the deconvoluted reactions. For a first-approximation quantification of the rise of R1/Q method 1 of § 4.1 was used to obtain τ_{II} (eq. 4-1).

The apparent extent and kinetics of the flash-induced photocurrents changed dramatically and in a complicated manner upon energisation, e.g. compare response 5 s after pre-illumination with the dark response before pre-illumination, and these effects were essentially dark reversible (Fig. 4-5A). Energisation bestows a 58 % suppression of the initial amplitude at 5 s after pre-illumination which can only partially be explained by an energisation-dependent suppression of PS II-dependent electrogenesis, a fully dark reversible process being completed within 60 s (van Voorthuysen *et al.* 1995, see Chapter 6). The remaining, slowly or non-reversible amplitude suppression as seen at 120 s after pre-illumination is likely caused by light-induced changes in the chloroplast network resistances (see Chapter 7). Under the experimental conditions used here an energisation-dependent increase in seal resistance was detected from which a concomitant energisation-dependent increase in the attenuation of the thylakoid voltage V$_M$(t) may be anticipated (eq. 3-12, Fig. 3-8, top). Part of the increased current attenuation can likely be attributed to an increase of the access resistance R$_A$ (van Voorthuysen *et al.* 1997, see Chapter 7). Inasmuch as charges displaced by both RC's and Q-cycle activity dissipate through the same chloroplast resistance network (Fig. 3-8) the energisation-dependent resistance changes will affect the calculated number of charges as generated by Q-cycle activity in an exact manner as those from RC's. For this moment the interference of resistance changes in estimating Q-cycle activity was circumvented by using the ratio Q/RC before and after pre-illumination (Fig. 4-5B). More refined analyses are needed to separate changes in chloroplast network resistances from changes in photosynthetic electrogenesis.

The Q/RC-ratio seems not much affected by pre-illumination (Fig. 4-5B). Caution has to be paid to the interpretation of the relatively long lag phase of R1/Q seen after pre-
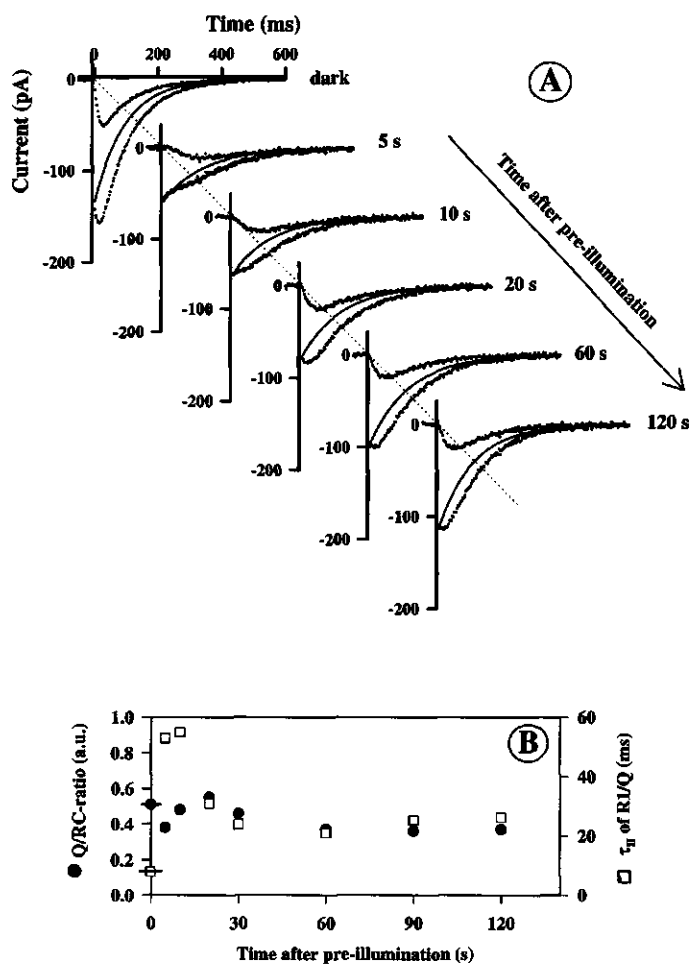
Fig. 4-5 **(A)** Effect of 2 minutes pre-illumination with red actinic light (RG610, 175 μmol^{-2} s^{-1}) on the flash-induced photocurrent. Single-turnover flashes were given before (dark) and at various times after (5, 10, 20, ..., 120 s) pre-illumination. The flash-induced responses were deconvoluted according to method 2 of § 4.1. **(B)** Changes in the Q/RC-ratio (left axis) and in the rise relaxation time τ_{II} of R1/Q (eq. 4-1) (right axis) of the photocurrents of part A. The photocurrents at 30 and 90 s after pre-illumination were omitted in part A. The dark values before pre-illumination of the Q/RC-ratio and τ_{II} are indicated by the horizontal lines through the corresponding symbols at the left y-axis.

illumination (Fig. 4-5A, responses 5 and 10 s) in which an interference of the fast ms-component Reaction 1/RC$_f$ as discussed in Chapter 5 can not *a priori* be excluded. Additionally, the temporarily, energisation-dependent decrease in the share of PS II charge separation to the amplitude of R1/RC causes an overestimation of the Q/RC-

ratio. Nevertheless, the small variations in the Q/RC-ratio suggest that the stoichiometry of charges translocated transversally and laterally in the cyt. *bₒf* complex is approximately independent of the state of thylakoid energisation and the Q-cycle is likely well coupled to linear electron transport as was rationalised by Rich (1988). The rate of the electrogenic steps in the *bₒf* complex is, however, much affected by energisation and shows a strong deceleration after pre-illumination. The rise of R1/Q as characterised by τ_{II} was about 8 ms in the dark, slowed down to 50 - 60 ms shortly after pre-illumination and levelled off within about 30 s to a quasi-stable value of about 20 ms (Fig. 4-5B). A much retarded rise may easily mask the true extent of R1/Q, yet our data suggests that although the apparent extent appears to be small, the calculated number of charges, i.e. the area under the current trace of R1/Q, displaced by the Q-cycle remains fairly constant. No interference from resistance changes as evoked by the pre-illumination is expected inasmuch as τ_{II} is a relaxation time independent of the discharge kinetics of the whole-thylakoid configuration (§ 4.1). The strong deceleration of R1/Q is likely caused by a restrained re-oxidation rate of PQH_2 at the Q_p-site of the cyt. *bₒf* complex due to the light-induced lumenal acidification.

4

S̲u̲mmary 2   *Reaction R1/Q most likely originates from electrogenic events involving cyt. bₒf turnover generally modelled as the Q-cycle. The (apparent) extent and rise kinetics of R1/Q on single-turnover flash excitation depends critically on the light history of the chloroplast. Successive flashes (0.5 Hz) may enhance Q-cycle activity. Pre-illumination (2 minutes) caused a dark-reversible 6 to 8-fold retardation of the rise of R1/Q. The number of charges displaced by the Q-cycle normalised on those displaced in the reaction centers was almost independent on the state of thylakoid energisation and suggests an obligatory role for Q-cycle operation in P. metallica.*

4.4 A detailed kinetic analysis incorporating a consecutive reaction

The bi-exponential fit of R1/Q (eq. 4-1) is a reasonable first approximation but deviates significantly from the data points, especially in the onset phase (Fig. 4-2, curve 1). Actually the rise of R1/Q seems to be sigmoid (Fig. 4-2, insert, dots) and we suggest that at least part of the slow charge separation proceeds according to a consecutive reaction sequence with two steps in the ms time domain. Therefore, the data of R1/Q were analysed with the help of the reaction schemes shown in Fig. 4-6; for a derivation of the analytical solutions see appendix B.

Two populations A1 and A2 of cyt. *bₒf* complexes are assumed to exist at the start of the flash which will produce the electrogenic products Q1 and Q2, respectively. An electrogenic product Q stands for the transmembrane potential (field) or equally for the number of charges separated by *bₒf* turnover. The formation of Q1, described by two reaction steps with rate constants k_1 and k_2, will exhibit a lag phase whereas Q2 formation, described by only a single reaction step with rate constant k_1, will proceed without a noticeable lag. Consequently, the rise kinetics of the secondary charge separation

sequence 1 **[fraction A1]**

$$A1 \xrightarrow{k_1} B1 \xrightarrow{k_2} C1 + Q1$$

$\downarrow k_D$ → **field dissipation**

sequence 2 **[fraction A2]**

$$A2 \xrightarrow{k_1} B2 + Q2$$

$\downarrow k_D$ → **field dissipation**

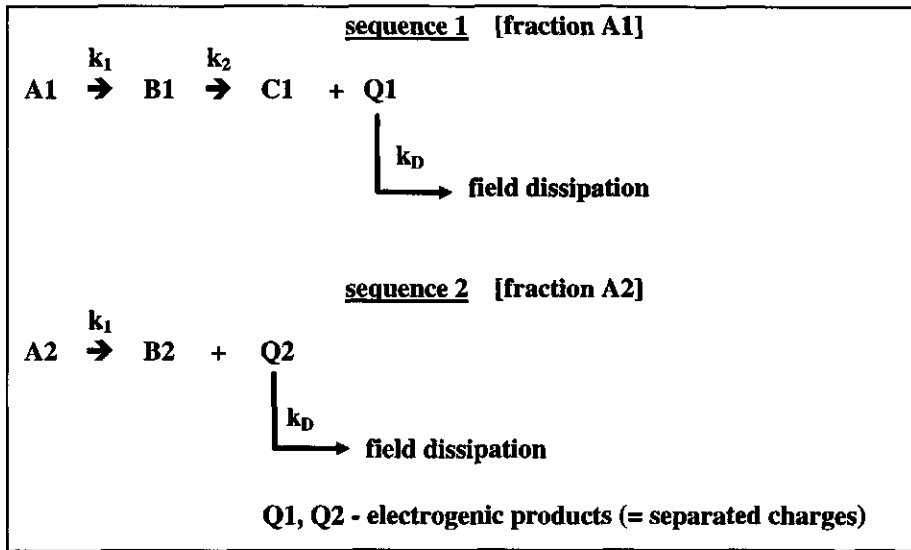**Q1, Q2 - electrogenic products (= separated charges)**

Fig. 4-6 Two reaction sequences used for describing the sigmoid rise of Reaction 1/Q. Sequence 1 is a consecutive reaction resulting in Q1 formation having an initial lag. Sequence 2 will give direct production of Q2.

4

evoked by the sum of the two $b_6 f$ populations will be an average of these two extremes. Figure 4-2 (R1/Q, curve 2) shows the fit of R1/Q based on the reaction sequences of Fig. 4-6 and the data are much better described by the inclusion of a consecutive reaction sequence. The relaxation times τ_1 and τ_2 corresponding to k_1 and k_2 are found to be 17.6 and 27.8 ms, respectively. The two kinetic rate constants k_1 and k_2 give a description of R1/Q which is independent of the rate of field dissipation and the variations in τ_D, observed when patching different chloroplasts, are thus eliminated. Table 4-1 presents a survey of the parameters characterising the kinetics and extent of R1/Q for 5 experiments on different *P. metallica* chloroplasts.

Table 4-1 Quantification of the slow electrogenic component R1/Q of 5 different *P. metallica* chloroplasts based on the model of Fig. 4-6.

	τ_1 (ms)	τ_2 (ms)	$A1_0$	$A2_0$	Q/RC-ratio
1	13.7	28.3	0.74	0.26	0.15
2	11.0	37.2	0.84	0.16	0.43
3 (Fig. 4-4A, flash 5)	16.4	28.6	0.76	0.24	0.50
4	6.3	15.2	0.55	0.45	0.74
5 (Fig. 4-2)	17.6	27.8	0.66	0.34	0.95

τ_1 and τ_2 are the relaxation times of R1/Q derived from a 3-exponential fit as discussed in appendix B. These two τ-values correspond to the rate constants k_1 and k_2 of the reaction schemes shown in Fig. 4-6. $A1_0$ and $A2_0$ are the initial fractions of the two cyt. $b_6 f$ populations.

Summary 3   *The sigmoid rise of R1/Q can be well modelled by two populations of cyt. b of complexes. In a first population the electrogenic reaction proceeds with a lag phase while in a second there is no lag phase. This is mathematically described by a combination of a consecutive reaction and a non-consecutive reaction, respectively. The two relaxation times describing the sigmoid rise are about 13 and 28 ms. The number of charges translocated by R1/Q shows large variations among different dark-adapted chloroplasts ranging from 0.15 to 0.95 charges per single charge separation in RC I plus RC II.*

4.5 Discussion

In this chapter a slow, light-driven, electrogenic reaction in the thylakoid membrane is discussed whose kinetics could be accurately determined. This was realised by using a current-injection technique which grants an objective determination of the field dissipation relaxation time τ_D associated with the dissipation of the transmembrane electrical field by ion fluxes. The unequivocal determination of τ_D can be considered an advantageous property of the patch-clamp method. The close similarity of relaxation times obtained with current-injection and flash-excitation (Fig. 4-1C) justifies the estimation of R1/RC from the initial amplitude of the flash-induced response and τ_D. Hence a proper kinetic definition of R1/Q can be obtained by subtraction of R1/RC from the overall signal. The implicit assumption made in these analyses is that the initial amplitude at $t = 0$ arises solely from R1/RC, which automatically sets the initial amplitude of R1/Q to zero. In voltage-clamp the initial amplitude can be fairly accurately determined within a time resolution of less than 1 ms. The close agreement between the initial amplitude values as calculated from an exponential fit and from a direct determination of the current data near $t = 0$ strongly suggests that the extent of primary charge separation is safely determined with the patch-clamp method within an error limit of about 5 %.

The initial retarded decay of the photopotential (photocurrent), sometimes even preceded by a slow rising phase, can originate in principle from the following processes:

1. Electrogenic steps involving the cyt. *bf* complex.
2. Electrogenic proton transfer driven by ATP hydrolysis catalysed by a flash-activated ATP synthase.
3. Non-linearity in the network impedance(s): resistance(s) or capacitance(s).

The sensitivity of the slow secondary rise to DBMIB, a potent Q_P-site inhibitor (Trebst 1980, Jones and Whitmarsh 1988, Rich *et al.* 1991), suggests that our results are best explained by electrogenic events involving the cyt. *bf* complex. The partial inhibition seen upon a first flash (Fig. 4-4B) suggests that reduced DBMIB has to be formed first, likely requiring PS II activity, before full inhibition of *bf* turnover results (Rich *et al.* 1991). The decrease of the initial amplitude of the photopotential accompanying the

inhibition of R1/Q (Fig. 4-4B) witnesses partial inactivation of PS II by competitive binding of DBMIB to the Q_B pocket (Trebst 1980, Velthuys 1981a) and of PS I inactivation as probably caused by a shortage of reducing equivalents at its donor side. The established blend of DCMU and millimolar amounts of DQH_2 (Jones and Whitmarsh 1988, Ooms *et al.* 1989, Rich *et al.* 1991, Kramer *et al.* 1994) is also for patch-clamp recordings a useful poise for conditioning of the Q-cycle (Fig. 4-3).

Hydrolysis of stromal ATP can create an electrical field with the same orientation as that evoked by primary charge separation: positive inside (Admon *et al.* 1982). For this to happen, the ATP synthase needs to be activated which might have resulted from the flash-induced transmembrane potential. Involvement of ATP hydrolysis is, however, unlikely because tentoxine addition was without effect on the slow rising phase.

A 1 - 5 % increase in the chloroplast network resistances has been reported under conditions of flash-excitation (Vredenberg *et al.* 1995b, van Voorthuysen *et al.* 1997, see Chapter 7). These resistance changes are only detectable if an offset current is applied which transforms a change in resistance into a slow change in electrical potential superimposed on the photopotential response. For our measuring conditions of zero current, potential changes related to changing network resistances can be neglected. Since the measured potential is a reflection of the thylakoid membrane potential attenuated by a voltage-divider $R_L/(R_A + R_L)$ (Fig. 3-7), an alteration of the photopotential profile by changing network resistances might, however, be anticipated even at zero current. The attenuation factor will shift to a new value in the event that one or both resistances R_A and R_L change after the flash. It can be calculated, based on scheme Fig. 3-7, that such an effect will have little impact on the photopotential kinetics unless unreasonably large changes in R_A or R_L are assumed. Such an assumption can be considered unlikely. A similar rationale holds for flash-induced changes in the thylakoid membrane capacitance. Furthermore, the relatively slow kinetics of the flash-induced resistance changes (van Voorthuysen *et al.* 1997, see Chapter 7) are quite distinct from those of R1/Q. We therefore conclude that resistance and capacitance changes are not involved in the multiphasic relaxation of the photocurrent/-potential at zero holding potential/current and the phenomenon is best explained by a slow secondary electrogenic step.

Thylakoid energisation clearly has a strong impact on the kinetics and apparent extent of the Q-cycle in *P. metallica* (Fig. 4-5). The 6- to 8-fold increase of the relaxation time τ_{II} is probably related to the light-induced acidification of the lumen which slows down the electron donation from PQH_2 to the b_6f complex because the reaction is associated with H^+ release in the lumen (Siggel 1976, Bendall 1982, Foyer *et al.* 1990). The recovery of τ_{II} in the dark contains a reversible and an irreversible component (Fig. 4-5B). The reversible energisation-dependent increase in τ_{II} might very well be related to the transthylakoid pH. The transmembrane proton equilibration after pre-illumination occurs with a half-time of about 5 s (Bilger *et al.* 1988, van Voorthuysen *et al.* 1995) which compares well with the half-time of about 10 s for the recovery of τ_{II} (Fig. 4-5B). Slowly or non-reversible changes in network resistances (Chapter 7) are an unlikely cause for the non-reversible phase since they will only affect the field relaxation kinetics while leaving τ_{II} unperturbed: charging the thylakoid membrane by primary or secondary charge

separation is independent of the membrane capacitance. Since the rate-limiting step for cyt. b_6f turnover has been discussed to be within the b_6f complex itself (Joliot and Joliot 1992), the cyt. b_6f complex may then have undergone an irreversible energisation-dependent change, e.g. by conformational alterations, which affects the redox potential and/or distances of redox components involved. Alternatively, the localised environment at the membrane/water interface may be in a slow equilibrium with the bulk phase and the localised pH at time 120 s after pre-illumination may still be significantly different from that after prolonged dark adaptation. In this first analysis of the energisation-dependent changes in R1/Q the number of charges displaced by b_6f activity seems fairly constant (Fig. 4-5B). Further experiments and especially a more refined analyses are needed in which an accurate separation can be realised of energisation-dependent changes in chloroplast resistances (notably of R_A), PS II-dependent charge separation (Chapter 6), the fast ms component $R1/RC_f$ (Chapter 5) and in the number of charges displaced by R1/Q.

One of the characteristics of the slow electrogenic phase as measured with the patch-clamp technique is its sigmoid rise. This S-shaped rise might suggest that in one fraction of b_6f complexes the electrogenic step occurs with an apparent lag and in a second population without. Such a typical behaviour was also noticed by Fernández et al. (1995) who discriminated a lag in the slow P515 phase by its sensitivity to 2-n-heptyl-4-hydroxyquinoline N-oxide (HQNO) suggesting that the electrogenicity associated with the re-oxidation of heme b_h at the Q_n-site proceeds indeed with sigmoidal rise kinetics. A proper physiological assignment of the rate constants k_1 and k_2 found from the mathematical analysis (Table 4-1) cannot be given as yet. One reasonable interpretation would be that k_1 and k_2 are related to the oxidation of PQH$_2$ at the Q_p-site and to the reduction of PQ at the Q_n-site, respectively. The two reaction sequences (Fig. 4-6) are based on this interpretation. Cytochrome b_6f complexes with reduced b_h and oxidised h are expected to give an electrogenic phase corresponding to the oxidation of the b-hemes associated with reduction of PQ at the Q_n-site (k_2). This reaction can, however, occur only after a non-electrogenic reduction of oxidised heme h upon PQH$_2$ oxidation (k_1). When both b-hemes are in their oxidised state the oxidation of PQH$_2$ at the Q_p-site will immediately induce a slow electrogenic phase corresponding to reduction of heme b_h (k_1). The relaxation times of about 13 and 28 ms (Table 4-1) for k_1 and k_2, respectively, compare reasonably well with results from others (Hope et al. 1992, Pace et al. 1992, Laisk and Oja 1995) and differences might be related to the local environment in the P. metallica chloroplasts (e.g. pH, quinol concentration, ambient redox potential) used in our study.

From a thermodynamical point of view the PQ-pool with a redox midpoint potential of about +110 mV (Golbeck and Kok 1979) would be more rapidly reduced than heme b_h with a midpoint potential of about -45 mV (Kramer and Crofts 1994). So, it is expected that photocurrents with a small contribution of R1/Q, indicating only a few b_6f complexes with a bound PQH$_2$ molecule, should be short in the fraction b_6f complexes with b_h reduced, i.e. a small fraction $A1_0$. This is, however, not observed (Table 4-1). To

untangle this paradox we should realise that the reactions at the Q_n-site leading to reduction of b_h need not necessarily be in thermodynamic equilibrium with the PQ-pool and a protein-bound quinone or semiquinone near the Q_n-site might have redox properties fundamentally different from free-diffusing quinones. An EPR signal in spinach chloroplasts under oxidising conditions, lasting for several hundreds of milliseconds, has been interpreted as evidence for a semiquinone located at the stromal membrane interface (Pace *et al.* 1992). Considering the redox midpoint potential of about -165 mV for the PQ^-/PQ couple (Rich and Bendall 1980) heme b_h may become partially reduced when it has a bound PQ^-. This might be a possible explanation for the relatively high calculated concentrations $A1_0$ of b_6f complexes with retarded electrogenicity in dark *P. metallica* chloroplasts (Table 4-1).

Other explanations for the sigmoid rise might be an oxidation of b_6f complexes by two different pools of plastocyanin (Haehnel *et al.* 1980, Laisk *et al.* 1992). In this scenario one pool, in close proximity of PS I and the cyt. b_6f complex, is expected to exhibit an instantaneous onset of secondary potential rise whose kinetics is determined by PQH_2 oxidation. The other, less tightly associated pool, will give a retarded potential rise with a lag time controlled by the average diffusion time of the mobile plastocyanin from PS I to a b_6f complex.

Our results show that flash-induced turnover of the cyt. b_6f complex in *P. metallica* chloroplasts may translocate as high as about 2 charges per single turnover of the reaction centers. A semiquinone (SQ)-cycle mechanism might be a possible explanation for high Q/RC-ratios (Wikström and Krab 1986, Joliot and Joliot 1994). A prerequisite for full SQ-cycling is the pre-reduction of both low and high potential *b*-hemes in the dark which would require a considerable low ambient redox potential of at least -200 mV (Joliot and Joliot 1994, Kramer and Crofts 1994). If both *b*-cytochromes would have undergone a dark reduction, the prevailing ambient redox potential inside the *P. metallica* chloroplasts apparently warrants this pre-reduction. Unfortunately, the preparation of suspensions of intact *P. metallica* chloroplasts for biochemical characterisation remains a daunting task at this time and consequently the redox state of the *b*-hemes in *P. metallica* in relation to light history or local conditions is unknown.

Alternatives for the apparent high Q/RC-ratios (Table 4-1) may be considered. Double turnovers of PS I during the flash may cause an apparent increase of the Q/RC-ratio which would lead to an overestimation of the Q-cycle activity. However, since PS I and cyt. b_6f turnover are stoichiometrically coupled by a one-to-one relationship the apparent Q/RC-ratio can never exceed 2/3 when all PS I centers make a double turnover and assuming that there are equal concentrations of PS I and PS II. The approximately 5 % uncertainty in the initial amplitude will cause no more than about 10 % uncertainty in the calculated Q/RC-ratio. Therefore Q/RC observations of < 0.75 could still be explained with the traditional Q-cycle concept assuming double turnovers of PS I but chloroplasts having a larger extent of secondary charge separation suggest the existence of a fundamentally different type of cyt. b_6f turnover. A second alternative concerns the redox state of Q_A. When the PQ-pool becomes more reduced the fraction

of PS II centers with reduced Q_A will also increase as was discussed by Diner (1977): Q_A reduction increased from 10 % to 50 % upon a change of the PQ-pool redox state from 50 % to 90 %. We should consider, therefore, a smaller share of PS II charge separation to the total initial amplitude of the photocurrent/-potential under more reducing conditions. The Q/RC-ratio would then be overestimated. Thirdly, when the dielectrically weighted distance between donor D (e.g. cyt. b) and acceptor A (e.g. cyt. b_h) in the cyt. b_6f complex is larger than the dielectrically weighted distance associated with primary charge separation in PS I and II, the transmembrane electrical field associated with R1/Q may effectively be larger. This only holds true when the charges of the b_6f complex are still residing on D and A and when the field associated with PS I and II charge separation is delocalised. The latter field has then a dielectrically weighted distance D_M/ε_M (see eq. 1-1). A higher dielectrically weighted distance associated with Q-cycle than with PS I and II charge separation may happen when the dielectric environment ε_{DA} between D and A is substantially lower than the average dielectric constant ε_M of the membrane (eq. 1-1). The cyt. b_6 polypeptide with four membrane-spanning α-helices is reported to be one of the most hydrophobic polypeptides of the cyt. b_6f complex (Cramer *et al.* 1992). A low dielectricum might also be provided by the three small hydrophobic subunits constituting the cyt. b_6f complex (Cramer *et al.* 1992).

Summary 4   *Alternative explanations for the origin of R1/Q like flash-induced ATP hydrolysis or changes in the chloroplast network resistances seems unlikely and most evidence points to a Q-cycle activity of the cyt. b $_6$f complex. The sigmoid rise of R1/Q, characterised by a k_1 of about $(13)^{-1}$ ms^{-1} and a k_2 of about $(28)^{-1}$ ms^{-1}, might be associated with immediate PQH$_2$ oxidation at the lumen interface and a retarded PQ reduction at the Q $_n$-site, respectively. The large extent of R1/Q as found for some chloroplasts is difficult to reconcile with the traditional Q-cycle but might be explained by a semiquinone (SQ)-cycle model. This would, however, presume full reduction of both b-cytochromes in the dark.*

Chapter 5   Fast field decay/changes associated with photosystem II activity

The efficiency of converting primary charge separation into a proton electrochemical gradient and the transport of electrons partakes in the overall efficiency of photosynthetic energy transduction of light into ATP and NADPH. For that purpose, an adequate stabilisation of the primary charge separated state is indispensable. Charge recombination reactions in photosystem II will lower this efficiency. These reactions may cover a wide span of time scales: i) A direct back-reaction between Q_A^- and P680$^+$ as evidenced by 50 μs luminescence has been proposed to occur upon a PS II donor-side limitation (Schreiber and Neubauer 1989, 1990, Krieger *et al.* 1992). An alternative pathway of recombination between Q_A^- and P680$^+$ may involve intermediate redox moieties like the intrinsic PS II cytochrome b_{559} (Satoh *et al.* 1990) or a carotenoid (Velthuys 1981b). ii) A back-reaction between Q_A^- and the S_2 state in several hundreds of ms (Robinson and Crofts 1983, Vermaas *et al.* 1984). iii) A back-reaction of Q_B^- with the S_2 state in about 22 s (Robinson and Crofts 1983). Additionally, it has been postulated that a localised, electrogenic back shuttling of protons from lumen to stroma may occur through the LHC II pigment-protein complex on a ms time scale (Jahns *et al.* 1988, Horton *et al.* 1994).

Charge stabilisation might very well depend on association of protein complexes which creates the possibility of efficient reactant channelling, i.e. of plastoquinone. Functional clusters consisting of 4 PS II units and 2 cyt. b_6f units have been proposed to exist (Joliot and Joliot 1992, Joliot *et al.* 1992) and appear essential for efficient energy coupling mediated by only a few restricted plastoquinone molecules. Macro-structural rearrangements therein are likely to perturb this coupling, not in the last place because of concomitant changes in (local) ambient redox potential, pH and dielectric properties. Structural changes in PS II leading to long range effects were suggested to occur as reflected by a donor-side induced shift of the Q_A redox midpoint potential (Krieger *et al.* 1993, Andréasson *et al.* 1995, Johnson *et al.* 1995). Such a change in redox midpoint potential will affect redox equilibria involving Q_A, particularly the $Q_A^-Q_B \Leftrightarrow Q_AQ_B^-$ equilibrium.

In this Chapter we report on a fast ms dissipation of the transmembrane electrical potential created by photosystem II-dependent charge separation. This was detected by the electrochromic bandshift at 518 nm in spinach chloroplasts. The results point to an electrogenic dissipation of charges in the electron transfer pathway between Q_A and the

cyt. *b₆f* complex. It is hypothesised that a macro-structural association of PS II and cyt. *b₆f* protein complexes is a prerequisite for stabilisation of the charge separated state of photosystem II.

5.1 Definition of a fast P515 component: R1/RC$_f$

A comprehensive description of the electrochromic part of the P515 response incorporates two electrogenic components and one non-electrogenic component (Ooms *et al.* 1989, Ooms 1990, Vredenberg 1996). The two electrogenic components, abbreviated by R1/RC and R1/Q, are attributed to primary charge separation in PS I and PS II and to secondary charge separation in the cyt. *b₆f* complex (Q-cycle), respectively. The non-electrogenic component (Reaction 2) is believed to be associated with localised proton domains (Ooms 1990, Ooms *et al.* 1991). The initial unresolved rise of the electrochromic part of P515 can be entirely attributed to the amplitude of R1/RC since both R1/Q and R2 have a slow rise with a relaxation time (τ) of more than 25 ms (Ooms 1990). In addition to these three electrochromic components a non-electrochromic component (Reaction 3) of the P515 response was discerned in Ooms (1990) with a rather flat 480 - 520 nm absorbance difference spectrum and a strong retarded relaxation into the time domain of seconds.

Figure 5-1A shows a representative flash-induced difference response at 518 nm in the first 40 ms after a single-turnover flash measured in intact spinach chloroplasts with a sampling time of 20 µs and a response time of 0.05 ms (calculated as $1/2\pi f$ with f the frequency of the electronic filter). The first 0.25 ms were discarded for reasons
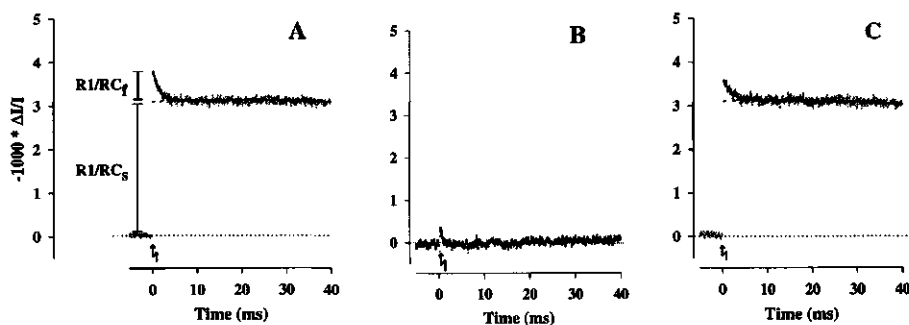
Fig. 5-1 Flash-induced difference response at 518 nm of intact spinach chloroplasts (20 µg ml⁻¹). (A) control. A single-exponential fit of R1/RC$_f$ resulted in an amplitude of 0.78 (a.u.) and a relaxation time of 1.4 ms. The initial amplitude of R1/RC$_S$ was found to be 3.09 (a.u.) as obtained by extrapolation to t = 0 of P$^{(2)}$(t) as described in the text. (B) Presence of 10 µM valinomycin. (C) Difference between responses A and B. R1/RC$_f$ amplitude 0.55 (a.u.) and relaxation time 1.9 ms; initial amplitude of R1/RC$_S$ is 3.11 (a.u.). Experimental conditions: assay medium as given in Table 2-4, average of 50 sweeps with a dark time of 5 s. Electronic filter 3 kHz, sample frequency 50 kHz. t = 10 °C.

discussed in § 2.4. On this time-scale a fast phase with ms decay kinetics can readily be distinguished which makes it kinetically distinct from the aforementioned four P515 components. For the time being this fast ms-component will be defined as a fraction of R1/RC and abbreviated by Reaction $1/RC_f$, suggesting its intimate relationship with primary charge separation as supported by its unresolved initial rise within a time of less than 0.25 ms. To make a clear distinction with $R1/RC_f$ the remainder of R1/RC will be abbreviated here by $R1/RC_S$, emphasising its relatively slow decay. Thus, we may write symbolically,

$$R1/RC = R1/RC_S + R1/RC_f \qquad \text{(initial amplitudes)}$$

For further quantitative analyses the following procedure was employed. The smallest relaxation time reported for both rise and decay of the three components R1/RC ($\equiv$ $R1/RC_S$), R1/Q and R2 is about 25 ms: the rise time of R1/Q (Ooms *et al.* 1989, Ooms 1990). The unresolved initial rise of P515 of less than 20 ns (Wolff *et al.* 1969) is not considered because this is far below our detection limits. Therefore, the relaxation times associated with $R1/RC_S$, R1/Q and R2 are substantially slower than the relaxation time associated with the decay of $R1/RC_f$ which is according to the data of Fig. 5-1A and to similar data of different preparations in the 1 - 3 ms time range. Accordingly, the sum of $R1/RC_S$, R1/Q and R2 was approximated in the time range 10 - 40 ms by a second order polynomial ($P^{(2)}(t)$) which was subsequently extrapolated to $t = 0$ to obtain the initial amplitude of $R1/RC_S$. The polynomial approximation has no physiological meaning whatsoever but merely serves as a base-line correction for a further analysis of $R1/RC_f$. This was done by subtracting $P^{(2)}(t)$ from the original data after which the remaining signal was fitted to a single-exponential function in the time-range 0 - 10 ms. The amplitude of $R1/RC_f$ was either taken as the difference between the total initial amplitude of the P515 response and the amplitude of $R1/RC_S$ or as the amplitude found from the exponential fit. It might be argued against this kinetic approach that several, as yet unknown processes may interfere with the ms-component. The aim of this chapter is to (partially) resolve this puzzle. Table 5-1 shows representative data of reaction $R1/RC_f$ for spinach chloroplasts under three different conditions and for Peperomia chloroplasts *in vivo*.

Table 5-1 Representative data of the fast P515 component $R1/RC_f$.

Species	Condition	Reaction $R1/RC_f$		Reaction $R1/RC_S$
		τ (ms)	A (a.u.)	A (a.u.)
Spinach	broken chloroplasts, 10 °C	1.5	0.22	0.78
	intact chloroplasts, 10 °C	1.5	0.20	0.80
	in vivo, 20 °C	1.0	0.06	0.94
Peperomia	*in vivo*, 20 °C	5	0.15	0.85

Amplitudes (A) are given as a fraction of the total initial amplitude. τ - dark decay relaxation time. In vivo designates infiltration of leaves with medium (see § 2.2).

5.2 Identifying the electrochromic nature of R1/RC$_f$

To estimate the electrical field related contribution to R1/RC$_f$ spinach chloroplasts were uncoupled by 10 μM valinomycin (Fig. 5-1B). It was verified that a concentration of 10 μM was saturating with regard to the collapse of the P515 response. A residual sub-millisecond 518 nm absorbance change was persistent (Fig. 5-1B). The cause of this residue has not been studied in detail because of the limited time resolution of our set-up. It is likely composed of a remaining accelerated field dissipation and of absorbance changes related to the formation and decay of carotenoid triplets whose response has been extended because of the tail of the flash (Eckert and Renger 1980). The original trace was corrected for the fast residual fraction (Fig. 5-1C). The relaxation time obtained from an exponential fit to the valinomycin-corrected response (Fig. 5-1C) was found to be somewhat larger than of the uncorrected response (Fig. 5-1A) but became more or less equal when the fit interval started at t > 0.5 ms. From Fig. 5-1 it is concluded that at least 60 % of R1/RC$_f$ is related to a delocalised transmembrane electrical field.

A substantial electrochromic origin of R1/RC$_f$ was concluded from the flash-induced difference spectrum of the amplitude of R1/RC$_f$ recorded between 460 - 530 nm (Fig. 5-2A). The amplitude of R1/RC$_f$ was obtained as the difference between P$^{(2)}$(t = 0) (see § 5.1) and the total initial amplitude. The spectrum of R1/RC$_S$ (S$_{R1/RC_S}$) has also been included (Fig. 5-2B) to recall the characteristics of an electrochromic spectrum (Junge 1977, Witt 1979). The spectrum of R1/RC$_f$ (S$_{R1/RC_f}$) shows resemblance to that of S$_{R1/RC_S}$ but appears to be shifted upwards by an approximately constant positive absorbance
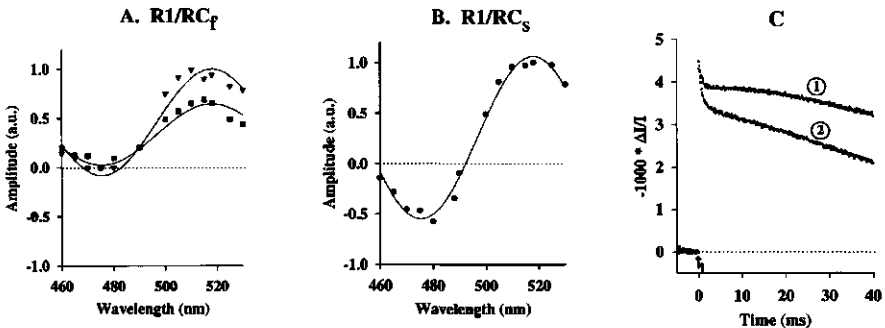

Fig. 5-2 (A) Flash-induced difference spectrum of R1/RC$_f$ on a first (■) and a second (▼) flash separated by 100 ms. Amplitudes were normalised on the highest amplitude of the second flash in the measured wavelength interval. A fit of the spectra of flash 1 and 2 according to eq. 5-1 gave the following partition into an electrochromic and a non-electrochromic fraction, respectively: 1st flash, 63 % and 37 %; 2nd flash, 72 % and 28 %. (B) Flash-induced difference spectrum of the amplitude of R1/RC$_S$. Amplitudes were normalised on the highest amplitude in the measured wavelength interval. Notice that the sensitivity of the abscissa of graph A is higher than for graph B because the amplitude of R1/RC$_f$ is smaller than of R1/RC$_S$. (C) Representative responses at 518 nm upon a first (①) and a second (②) flash separated by 100 ms demonstrating the increase of R1/RC$_f$ in the second flash. Experimental conditions the same as for Fig. 5-1 except for the sample frequency which was set to 10 kHz.

change. To give the notion a more quantitative basis the spectrum of R1/RC$_f$ was presumed to be composed of an electrochromic part, congruent to that of R1/RC$_S$, and a non-electrochromic part of unknown shape,

$$S_{R1/RC_f}(\lambda) = \alpha . S_{R1/RC_S}(\lambda) + S_{unknown}(\lambda) \tag{5-1}$$

with λ the wavelength of the measuring light and S$_{unknown}$ the unknown difference absorption spectrum of an (as yet) unidentified origin; α is a scaling factor. Since the spectrum of R1/RC$_S$ (Fig. 5-2B) could not be satisfactorily described by the first derivative of a single Gaussian absorbance band a general algorithm was employed to obtain an adequate analytical description of S$_{R1/RC_S}$ which is shown by the sine-shaped line in Fig. 5-2B. In a first approximation the unidentified spectrum was assumed to be constant (S$_{unknown}(\lambda)$ = constant). Subsequently the data of Fig. 5-2A were fitted according to eq. 5-1 with the unknown constant and the scaling factor α as free fit parameters. This analysis yielded a 63 % electrochromic contribution to R1/RC$_f$ on a first flash. The electrochromic fraction was found to increase to about 72 % upon a second flash given 100 ms after the first (Fig. 5-2A). This increase can be mainly attributed to a larger extent of R1/RC$_f$ on the second flash (Fig. 5-2C).

A close correlation between the valinomycin-insensitive residue (Fig. 5-1B) and the non-electrochromic part of R1/RC$_f$ seems not unlikely. This would suggest that the non-electrochromic part of R1/RC$_f$ has faster decay kinetics (Fig. 5-1B) than the electrochromic part (Fig. 5-1C). Therefore, the 1 - 2 ms decay is most probably explained by a fast electrogenic discharge of the transmembrane electrical field.

The question arose whether the ms component represented a fraction of damaged (leaky) thylakoids as was suggested in Schönknecht et al. (1990). For this to be true both PS I and PS II-dependent charge separation should contribute to R1/RC$_f$ in proportion to their relative presence in the thylakoid membrane. This expectation is based on the notion that the highly organised thylakoid structure most probably constitutes a single electrical unit (Schönknecht et al. 1990) with equipotential phases adjacent to the membrane. Figure 5-3 shows the effect of far-red background illumination (+FR, > 715 nm) on the P515 response (cf. also Fig. 5-7). Far-red illumination causes major oxidation of P700 and the P515 response will depend predominantly on PS II charge separation (Chylla et al. 1987). It was verified by chlorophyll fluorescence yield analysis that the far-red background illumination caused no more than 10 % closure of PS II reaction centers. It is evident that the amplitude of R1/RC$_f$ is hardly affected whereas the amplitude of R1/RC$_S$ is approximately halved (Fig. 5-3B). The difference between the traces of control and +FR demonstrates this effect more clearly (Fig. 5-3C). These results would suggest that charges from PS II only are involved in the occurrence of R1/RC$_f$ which would exclude damaged thylakoids as a possible explanation unless they would exclusively contain PS II reaction centers.

From several experiments of this kind an average PS II/PS I ratio of 1.35 was calculated from the initial amplitude with and without far-red background illumination.
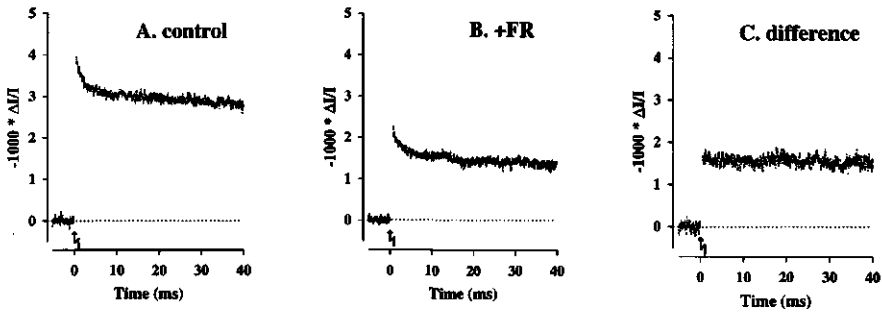
Fig. 5-3   Far-red light has little or no effect on Reaction 1/RC$_f$. (A) Control. (B) Presence of saturating far-red light (+FR, > 715 nm). (C) Difference response between A and B. Experimental conditions the same as for Fig. 5-1.

The PS II inhibitor DCMU caused a marked reduction of R1/RC$_f$ concomitant with a 70 % suppression of the total initial P515 amplitude (Fig. 5-4). From the joined results of Figs 5-3 and 5-4 we may conclude that the occurrence of R1/RC$_f$ is exclusively associated with photosystem II electrogenesis and not with that of photosystem I. The data of Table 5-1 then imply that as much as about 35 % of PS II electrogenesis is quickly lost in dark-adapted chloroplasts or thylakoids assuming a PS II/PS I ratio of 1.35.
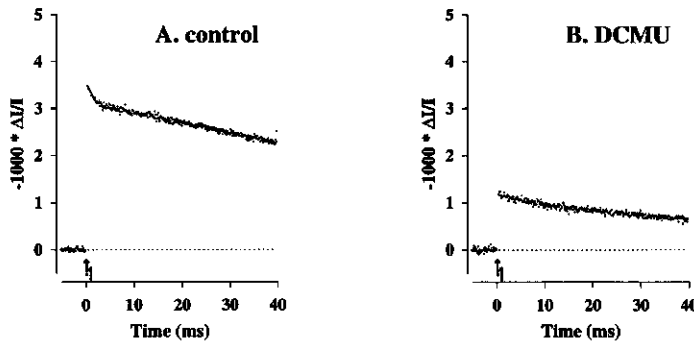
Fig. 5-4   Inhibition of R1/RC$_f$ by DCMU. (A) Control. (B) Presence of 2 μM DCMU. Experimental conditions: intact spinach chloroplasts (25 μg ml^{-1}), assay medium as given in Table 2-4, electronic filter 10 kHz, sample frequency 10 kHz, average of 100 sweeps with a dark time of 1 s. t = 10 °C.

Summary 1

The P515 response of spinach chloroplasts and thylakoids contains an essentially electrochromic component called R1/RC$_f$ with a fast unresolved rise of less than 0.25 ms and a comparatively fast dark decay with a relaxation time of 1 - 2 ms. The extent of R1/RC$_f$ is most probably associated with a fraction of the transmembrane electrical field as generated by photosystem II charge separation. About 35 % of the

electrical field set up by photosystem II charge separation is quickly dissipated on a first flash given to dark-adapted chloroplasts and thylakoids. For chloroplast in vivo this fraction will be 10 % or less. Charge recombination within PS I is not a likely cause for R1/RC$_f$.

5.3 Light saturation of R1/RC$_f$

In the preceding paragraph it was concluded that the occurrence of R1/RC$_f$ depends predominantly, if not exclusively, on photosystem II photochemistry or its ensuing reactions. Many types of functionally distinct PS II centers have been described in the past (van Gorkom 1985, Govindjee 1990), although recent evidence agitates against these many PS II heterogeneities (Hemelrijk and van Gorkom 1996). It was interesting to examine R1/RC$_f$ in relation to two possible types of PS II centers: inactive centers (Chylla and Whitmarsh 1990) and PS II$_\beta$ centers (Melis and Homann 1975, Melis and Anderson 1983). With respect to their decreased efficiency of light capture and/or primary energy conversion this was done by recording a flash intensity saturation curve of R1/RC$_f$ and R1/RC$_S$ (Fig. 5-5). Furthermore, it has been proposed that the fast ms-component is caused by an unspecific discharge of the membrane potential which would be enhanced upon overloading the thylakoid membrane, e.g. upon multiple flashes (Farineau *et al.* 1980). A flash saturation curve can also verify this proposal.
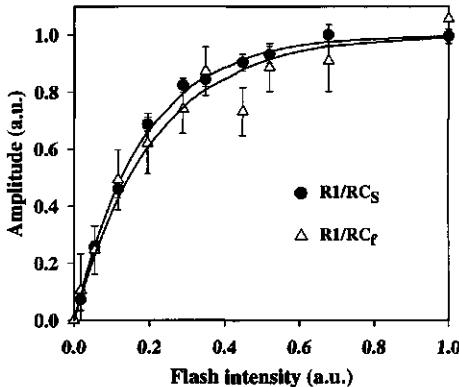
Fig. 5-5 Flash light saturation curve of R1/RC$_S$ and R1/RC$_f$. Intact spinach chloroplasts (10 µg ml^{-1}). The data were analysed according to Poisson statistics (eq. 5-2) which resulted in an effective absorption cross-sectional area of 5.6 ± 0.2 and 4.7 ± 0.8 for R1/RC$_S$ and R1/RC$_f$, respectively. A$_{max}$ (see eq. 5-2) of both R1/RC$_S$ and R1/RC$_f$ was set to 1.

The saturation behaviour of the amplitude (A) of a P515 component as a function of incident energy per unit area (E), which is proportional to the incident photon flux density (I), was analysed by a cumulative single hit Poisson probability distribution (Mauzerall and Greenbaum 1989, Chylla and Whitmarsh 1990),

$$A(E) = A_{max} \cdot (1 - e^{-\sigma \cdot E}) \tag{5-2}$$

with A_{max} the limiting amplitude at saturation, and σ the effective absorption cross-sectional area of a reaction center. The cross-sectional area depends both on the antenna size and the quantum yield of photochemistry. The effective absorption cross-sections calculated from the data of Fig. 5-5 were 5.6 ± 0.2 and 4.7 ± 0.8 for $R1/RC_S$ and $R1/RC_f$, respectively, a difference which is not significant. Since the initial amplitude of $R1/RC_S$ has a contribution of both PS I and II the single-exponential distribution function 5-2 presumes that σ_{PSI} equals σ_{PSII}, including any heterogeneities in the latter. Obviously, this need not be true in general, for example the size of the PS II antenna has been reported to be 1.1 - 1.3 times that of PS I (Melis and Anderson 1983). However, the experimental data of Fig. 5-5 allow no accurate discrimination between a single-exponential or double-exponential saturation curve. In addition, a saturation curve for PS I only was determined (not shown) from the difference signal of the control P515 response and of the P515 response measured in the presence of saturating far-red background light, similar as shown in Fig. 5-3. Here also single-exponential kinetics provided a satisfactory fit which resulted in $\sigma_{PSI} = 5.4 \pm 0.6$ which is not significantly different from σ_{R1/RC_S}, too.

The insignificant difference between the cross-sectional areas of $R1/RC_S$ and $R1/RC_f$ makes the relation to inactive PS II reaction centers (Chylla and Whitmarsh 1990) or to PS II$_\beta$ centers (Melis and Homann 1975, Melis and Anderson 1983) unlikely since both were reported to have decreased antenna sizes. Furthermore, $R1/RC_f$ does not seem to arise from an electrical break-down of the transmembrane field above a certain threshold value (high flash energies) because the ms-component is equally observed at low and high flash energies.

Equal effective absorption cross-sections might imply at least two possibilities. First, it could mean that both antenna and quantum yield of photochemistry of PS II for $R1/RC_S$ and $R1/RC_f$ are indistinguishable within our measuring precision. Second, charges generated by any PS II center have equal access to the fast dissipative route, which places this route after PS II.

5.4 Further characterisation of $R1/RC_f$

Magnesium and pH
Absence of magnesium ions in the assay medium (Fig. 5-6) and a lowering of the pH of the assay medium (Fig. 5-7) were found to increase the amplitude of $R1/RC_f$. The total initial amplitude of the P515 response was unaffected by both treatments which indicates that primary charge separation was not significantly inhibited. However, the fraction $R1/RC_f$ was substantially increased at the expense of $R1/RC_S$. Magnesium appears to be an obligatory cation for stabilising part of the transmembrane electrical field.

The difference response between control and +FR at pH = 6.0 (Fig. 5-7) indicates that only PS II-dependent charge separation is dissipated to a larger extent and not that of PS I. The fraction of PS II-dependent charges which are quickly dissipated amounts 63 % of the total PS II charge separation at pH = 6.0. No significant acceleration of the
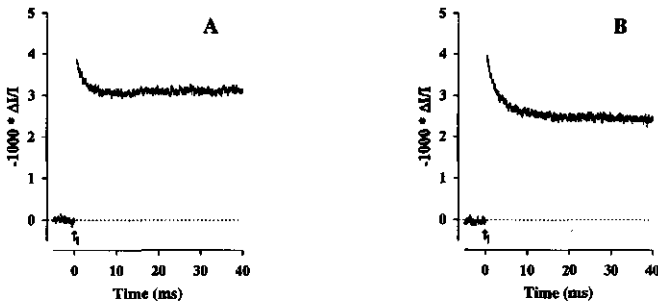
Fig. 5-6   P515 response of broken spinach chloroplasts incubated in the presence (**A**) or absence (**B**) of 5 mM MgCl₂. Broken chloroplasts were prepared from freshly isolated intact chloroplasts by incubating the chloroplasts for 2 minutes in dimineralised water plus 50 mM HEPES, pH 7.5 on ice. Thereafter, an equal volume of double strength assay medium was added (Table 2-4) and the preparation was allowed to incubate for another 15 minutes on ice before starting the experiment. Other experimental conditions: see Fig. 5-1.

decay of $R1/RC_f$ could be detected (at most somewhat slower) from which we conclude that an elevated concentration of protons causes the fraction of photosystem II-dependent charge separation to increase but leaves the conductance of a putative dissipative route unaffected. Therefore, the putative dissipative route is unlikely a simple bulk-to-bulk conductance channel for protons.

Artificial PS II donors
Incubation (10 minutes) of thylakoids with 0.1 - 5 mM hydroxylamine (not shown) was without detectable effect. Likewise, exogenous PS II donors like diphenylcarbazide (DPC) (500 μM) and *p*PD (100 μM) were without effect. This shows that electrochromism related to the PS II donor side (Saygin and Witt 1985) are probably not involved. Charge recombination reactions between Q_A^- or Q_B^- and the S_2 and S_3-states of the OEC (Rutherford *et al.* 1982) would then also be excluded. This conclusion is corroborated by the much faster kinetics of $R1/RC_f$ compared to the rate of charge recombination with the S-states which is in the order of seconds (Robinson and Crofts 1983, Vermaas *et al.* 1984).

DCCD
No inhibition was found of $R1/RC_f$ by DCCD, a reagent which closes the proton channel CF_0 of the ATP synthase (Linnett and Beechy 1979). Instead DCCD caused an increase of $R1/RC_f$ with increasing concentration, similar as was reported in Jahns *et al.* (1988). This suggests that a rapid proton back-flow through the ATP synthase is not involved. A relation to CF_0 proton conductance is not expected *a priori* because of the long diffusion pathway between the proton source at the OEC inside the grana and the ATP synthases in the stroma lamellae.
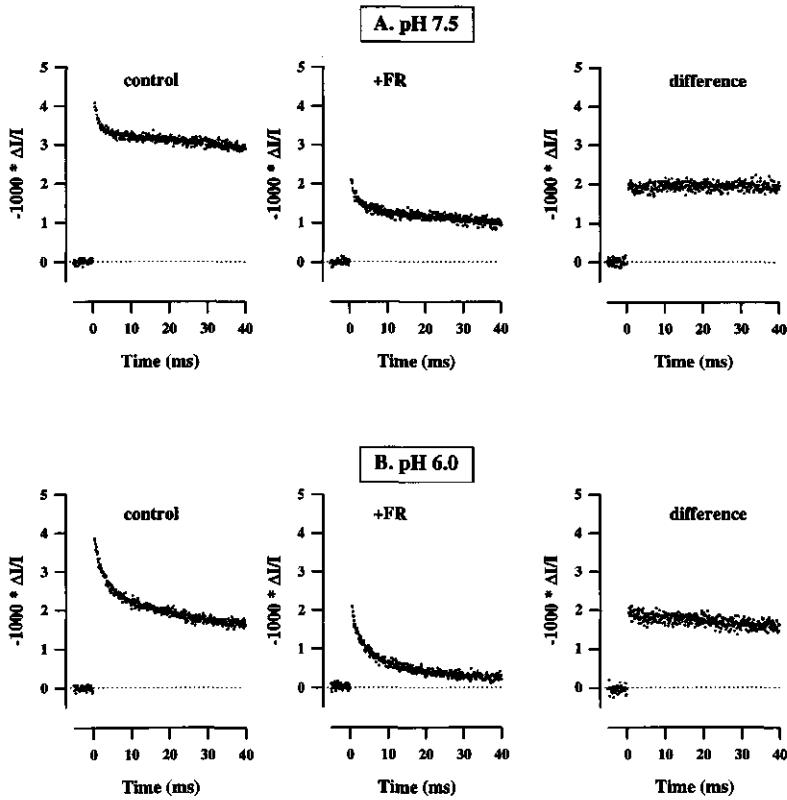
Fig. 5-7 Increase of $R1/RC_f$ in spinach thylakoids upon lowering the pH of the assay medium. Spinach thylakoids (20 μg ml⁻¹) were incubated for 5 minutes in assay medium (Table 2-4) with the following modifications: the buffer HEPES (50 mM) was replaced by the buffer combination HEPES/MES (25 mM/25 mM) and adjusted to pH 7.5 (**A**) or 6.0 (**B**). The difference signals were calculated from a subtraction of the control and +FR responses. An analysis as described in § 5.1 of the +FR response at pH = 6.0 gave amplitudes of 1.44 and 0.83 for $R1/RC_f$ and $R1/RC_S$, respectively. The relaxation time of $R1/RC_f$ was 2.3 ms.

Temperature

The relaxation time of $R1/RC_f$ showed a strong temperature dependence in the range 5 - 35 °C while the amplitude was unaffected in agreement with Farineau *et al.* (1980). The corresponding enthalpy and entropy changes as calculated from an Arrhenius plot were $\Delta H_{act} = 20.2 \pm 1.3$ kJ mol⁻¹ and $\Delta S_{act} = -179 \pm 10$ J mol⁻¹ K⁻¹, respectively.

5.5 Decrease of R1/RC_f by efficient drainage of electrons

It was observed that sufficient amounts (> 25 μM) of 2,6-dichloro-*p*-benzoquinone (2,6-DCBQ) could effectively diminish the amplitude of R1/RC_f (Fig. 5-8). The decrease of R1/RC_f was paralleled by a disappearance of the slow secondary rise of the P515 response which probably reflects an inhibition of R1/Q caused by an extensive oxidation of the PQ-pool by 2,6-DCBQ (Oettmeier *et al.* 1978). The reduction of the initial P515 amplitude (Fig. 5-8) may be explained on similar grounds to a decreased PS I charge separation. This is supported by the observation that the couple 2,6-DCBQ/FeCy was shown to retard the re-reduction of P700+ between flashes (Dennenberg *et al.* 1986). Other quinones like *p*-benzoquinone (*p*BQ) and duroquinone (DQ) were less effective but showed similar effects (data not shown). Thylakoids in the presence of 1 mM ferri-
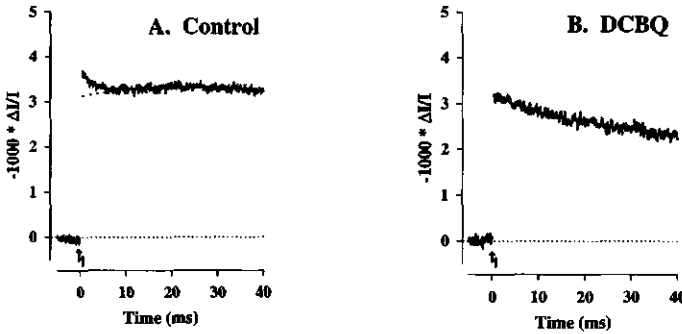
Fig. 5-8 Disappearance of R1/RC_f by 2,6-dichloro-*p*-benzoquinone (DCBQ). (A) Control. The smooth line is a summation of a single-exponential fit with amplitude 0.61 and relaxation time 2.8 ms and a second order polynomial P$^{(2)}$(t) (dotted line) (see § 5.1). (B) Presence of 100 μM 2,6-DCBQ. Responses were corrected for the valinomycin-insensitive residue as described in § 5.1. Experimental conditions: see Fig. 5-1.
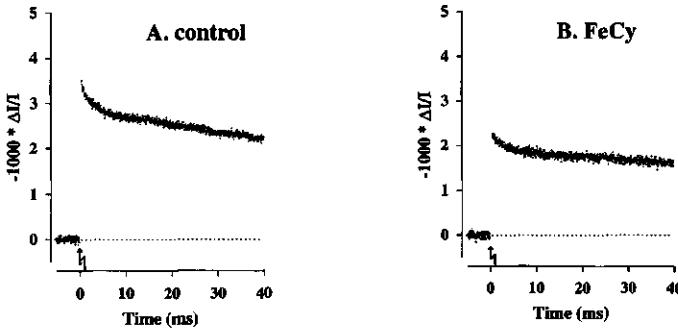
Fig. 5-9 Effect of ferricyanide (FeCy) on the P515 response. (A) Control. (B) Presence of 1 mM FeCy. Experimental conditions the same as for Fig. 5-1 except that broken chloroplasts were used and the sample frequency was set to 30 kHz.
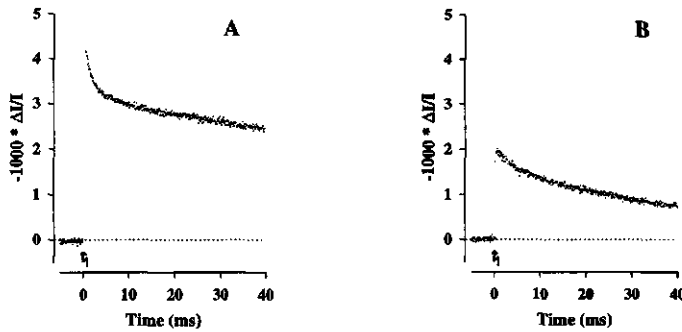
Fig. 5-10 (A) Control P515 response in spinach thylakoids. (B) Spinach thylakoids incubated with 1 mM FeCy, 0.4 mM pBQ, 1 µM DBMIB and 20 µM methylviologen.

cyanide, a hydrophilic oxidant, showed a somewhat larger decrease in $R1/RC_S$ than in $R1/RC_f$ (Fig. 5-9). The decrease in the amplitude of $R1/RC_S$ is again likely due to a diminished PS I-dependent charge separation because of the dark oxidation of the plastoquinone pool and of a fraction of P700 by FeCy (Joliot and Joliot 1984, Joliot and Joliot 1992). 2,6-DCBQ is more hydrophobic and has a high affinity for the Q_B niche of PS II as was found in *Synechococcus* cyanobacteria where the quinone was discussed to accepts electrons directly from reduced Q_A (Satoh *et al.* 1992, Satoh *et al.* 1995). Lavergne and Leci (1993) advanced that 2,6-DCBQ acts by relieving a blocking step involved in the reoxidation of a fraction of the PQ-pool.

Far-red light, FeCy and the exogenous quinones used here all oxidise the intersystem electron transport chain. Only in the latter case a significant, specific reduction of $R1/RC_f$ is seen. Although $R1/RC_f$ has been exclusively assigned to photosystem II-dependent charge separation Fig. 5-10 shows that the rapid loss of the electrical field might also be prevented in the PS II-dependent electron transport system from water to FeCy via pBQ, thus by-passing the endogenous PQ-pool and following electron transport chain components. Since $R1/RC_f$ is not associated with PS I-dependent charge separation (§ 5.2) these results demonstrate that the energy transduction between Q_A and plastocyanin is involved in the cascade of reactions giving rise to $R1/RC_f$. FeCy or +FR light alone apparently causes a too slow oxidation of Q_A^- and Q_B^- which may be substantially accelerated by the more hydrophobic quinones. Most likely, the site for electron acceptance of added quinones is in the membrane environment of the PS II reducing site and probably the Q_B binding niche is involved.

Summary 2

Reaction 1/RC_f is insensitive to PS II donor side reactions and could not be identified with inactive centers or with so-called PS II_β centers. Absence of Mg²⁺ or lowering the pH of the assay medium caused an increase of R1/RC_f of up to 60 %. When a sufficient fast reoxidation of the PS II reduction side is guaranteed, as facilitated by added benzoquinones in the presence of FeCy, R1/RC_f is decreased suggesting that stabilisation of PS II-dependent charge separation has improved.

5.6 Discussion. PS II charge stabilisation: necessity for superclusters?

Reaction $1/RC_f$ seems specific with respect to its association with PS II activity but unspecific with respect to heterogeneities therein like differences in the effective absorption cross-sectional area. Furthermore, $R1/RC_f$ is insensitive to the PS II donor side. However, a mere unspecific discharge of membrane potential is considered unlikely inasmuch as PS I-dependent energisation does not add to the amplitude of $R1/RC_f$ (Fig. 5-3). This would suggest that $R1/RC_f$ is related to a localised dissipative pathway for recombination of charges and not to a delocalised dissipation mediated by ion fluxes across the membrane. This would also exclude a bulk-to-bulk conductance of protons (§ 5.4).

The stimulating effects of both elevated proton concentrations and absence of magnesium are of interest (Figs 5-6 and 5-7). Both treatments are known to cause large rearrangements in the macro-organisational structure of the thylakoids (Murakami and Packer 1970, Dilley and Rothstein 1967, Briantais *et al.* 1984). Magnesium would be necessary to prevent electrostatic repulsion between PS II and the cyt. b_6f complex by shielding the negative surface charges (Joliot and Joliot 1992). We speculate that a macro-structural domain organisation is essential for stabilising PS II-dependent charge separation. Fast equilibration between PS II units and a plastoquinone pool which is mobile may not be met for efficient electron transfer and this might only be ensured for more restricted plastoquinone shared within the domains (Joliot *et al.* 1992). Domains lacking the cyt b_6f complex, as hypothesised to exist by Joliot and Joliot (1992), would further restrict electron drainage from PS II.

As to the nature of the electrogenic back-reaction we have no direct evidence. Among the possible candidates is a back-reaction from Q_B^- to $P680^+$. This could be facilitated by a redox intermediate like cyt. b_{559} or a carotenoid (Velthuys 1981b, Schreiber and Neubauer 1987, 1990). The low-potential (LP) form of cyt. b_{559}, which is more prevalent at low pH (Horton and Cramer 1975, De Las Rivas *et al.* 1995), is generally considered essential for electron donation to $P680^+$ (Schreiber and Neubauer 1987). It is tempting to speculate that superclusters guarantee the maintenance of a protected hydrophobic niche necessary to keep the b-heme in the native high-potential (HP) form (Cramer *et al.* 1993, McNamara and Gounaris 1995). Upon disintegration of PS II and cyt. b_6f protein complexes the niche might disrupt, thus exposing the b-heme to a more hydrophilic environment which converts it into the LP form. The HP $\rightarrow$ LP conversion was shown to be involved with damage to the structural integrity of thylakoid membranes (Cramer and Whitmarsh 1977, McNamara and Gounaris 1995).

In an alternative view the clustering of PS II and b_6f complexes could be essential for stabilising a semiquinone anion (PQ^-) in a pocket shared by the Q_B binding niche and the Q_n-site of the b_6f complex (Joliot and Joliot 1992). Upon disintegration the PQ^- may become unstable and transverse electrogenically to the lumenal site of the membrane, an energetically favourable movement along the transmembrane potential created after the flash. A third possible explanation for $R1/RC_f$ could be a reduction of the high potential b-heme in the b_6f complex by PQH_2, the reverse reaction being proposed to be electrogenic (Jones and Whitmarsh 1988).

The effect of the couple pBQ/FeCy (Fig. 5-10) and in particular of 2,6-DCBQ (Fig. 5-8) most likely is an efficient drainage of electrons away from the reducing side of PS II. This reaction will be competitive with a charge recombination reaction and thus stabilise primary charge separation. The semiquinone form of added benzoquinones, formed after flash reduction of the bound quinone, was assumed to have a lower affinity for the Q_B binding niche than does plastosemiquinone (Tanaka-Kitatani *et al.* 1990). Then, a rapid release of the reductant, the semiquinone, would make a charge recombination with an oxidant less favourable. Most interestingly, 2,6-DCBQ was found to inhibit cyt. b_{559} reduction in barley thylakoids whose PS II donor side was destabilised by the ADRY[†] agent carbonyl cyanide *m*-chlorophenylhydrazone (CCCP) (Samson and Fork 1992).

An alternative interpretation of $R1/RC_f$ concerns the physical origin of electrochromism. A strong permanent field perpendicular to the membrane was introduced to account for the observed linearity between the transmembrane electrical potential and the absorbance band shift of P515 (Sewe and Reich 1977, Witt 1979). A decrease or increase in the strength of this permanent field would cause a change in the proportionality constant relating the magnitude of the transmembrane electrical field to the extent of the electrochromic absorbance band-shift (Witt 1979). A significant change in localised fields inside the membrane may happen upon movement of localised charges. When such a field change occurs upon flash excitation of the photosynthetic membrane and extends to the environment of a putative P515 moiety a decrease in sensitivity of P515 to the transmembrane electrical field might occur and would then expose itself as a virtual decrease in absorbance bandshift similar to $R1/RC_f$. Alternatively, a reorientation of a putative P515 moiety may cause a similar change in sensitivity. The pools of pigments showing electrochromism may not be completely homogeneous (De Grooth and Amesz 1977) and specific chlorophylls associated with PS II (Schapendonk 1980) or with the cyt. b_6f complex (Joliot and Joliot 1995) may respond differently from other pigments. A careful study of the electrochromic spectrum of $R1/RC_f$ might discriminate between such different pigment moieties (Schapendonk 1980). The reorientation of localised charges or of the putative P515 moiety must agree with the time-scale of the decay relation time of $R1/RC_f$, i.e. several ms. In this context the charge rearrangement associated with electron transport from Q_A to Q_B and with proton uptake from stroma to the Q_B niche (Fig. 1-3, ❽) might result in a significantly altered localised field in the environment of an electrochromic responsive chlorophyll and corresponding decrease in field sensitivity. The time scale of the proton uptake (Table 1-1) is not inconsistent with the decay time of $R1/RC_f$. It should be recognised that a direct association of the decay of $R1/RC_f$ with the proton uptake reaction at the Q_B niche can be excluded because the electrogenicity of the proton uptake is equal to primary charge separation and hence opposite to the decay of $R1/RC_f$ (Fig. 1-3, ❽).

If Reaction $1/RC_f$ represents a futile recycling of reducing equivalents to some oxidant at the lumenal side it will lower the quantum efficiency of linear electron transport to PS I. Upon single-turnovers of PS II this would amount about a 35 % decreased efficiency in chloroplasts and thylakoids (§ 5.2). The energetic loss during

---

† = Acceleration of the Deactivation Reactions of the water splitting system Y

continuous illumination cannot be concluded from this work. However, it was observed that $R1/RC_f$ did not saturate upon successive flashes given every 50 ms (not shown, but see also Fig. 5-2C). Saturation might hence be expected only if the turnover rate of PS II approaches the characteristic turnover rate of $R1/RC_f$ which is in the order of 0.67 ms^{-1} (Table 5-1) and which shows no substantial energisation-dependent acceleration or deceleration (Figs 5-7 and 6-11 in the next Chapter). The turnover rate of active PS II in saturating continuous light is about 0.2 - 0.33 ms^{-1} at room temperature (Lee and Whitmarsh 1989). Therefore, this kinetic deduction might suggest that $R1/RC_f$ will decrease the efficiency of linear electron flow for most common irradiances but is likely to have less effect at irradiances approaching saturation. For photosynthetic electron flow *in vivo* the energetic loss by $R1/RC_f$ is predicted to be lower (Table 5-1).

A fast dissipative process as suggested for $R1/RC_f$ will decrease the rate at which the PQ-pool can be photochemically reduced. We therefore predict that part of the I-P fluorescence induction (Govindjee 1995) contains the counterpart of $R1/RC_f$. The decrease in the rate of the I-P rise upon transition of thylakoids from pH = 7.5 to a low pH around 6 (Schreiber and Neubauer 1987, Krieger *et al.* 1992, Meunier and Bendall 1993) could (partly) be explained by our observed increase in the fraction $R1/RC_f$ (Fig. 5-7). Conversely, the Q_A^- reoxidation after a single-turnover flash as monitored by fluorescence decay contains an exponential phase of about 5 ms (Crofts and Wraight 1983, Renger *et al.* 1995). Its origin is still debated but believed to be typical for PS II complexes where Q_A^- reoxidation is limited by diffusion and subsequent binding of PQ molecules to an empty Q_B site (Renger *et al.* 1995). A similar ms component was observed in the flash-induced absorbance change at 319 nm monitoring the formation and decay of PQ^- (Velthuys 1981a). Here again, this ms component might be related to $R1/RC_f$. Further studies of real time fluorescence measurements are required to verify these suggested correlations

Summary 3   *It is hypothesised that stabilisation of PS II charge separation depends critically on the intactness of superclusters composed of PS II and cyt. b$_6$f protein complexes. Upon disintegration of these clusters ($-Mg^{2+}$, low pH) a back-reaction from the PS II reducing side to an oxidant at the lumenal side is favoured, thus diminishing electron transport to PS I. This back-reaction might be envisioned as a localised dissipative pathway in proximity of photosystem II.*

Chapter 6   Reversible suppression of photosystem II-dependent electrogenesis after illumination

Photosynthetic charge separation and subsequent electron transfer initiate redox reactions involving binding and release of protons at the membrane/water interfaces of chloroplast thylakoids. The protonation and de-protonation reactions contribute to the delocalisation of the initially localised dipole fields in the membrane and establish the transthylakoid proton gradient (ΔpH), acidic inside. The dominant processes that occur concurrently with membrane energisation and which are of importance for understanding the regulation of electron transport are: (i) closing of a fraction of PS II reaction centers due to reduction of Q_A (Krause *et al.* 1982, Walker 1992); (ii) phosphorylation and subsequent lateral migration of LHC II (Allen 1992); (iii) inactivation and reactivation of RC II (Chylla and Whitmarsh 1989, Snel *et al.* 1992); (iv) decrease of intrinsic PS II efficiency, defined as the quantum efficiency for converting photon energy into a stable charge separated state. The decrease of PS II efficiency of the open reaction centers is ascribed to an increase in non-radiative thermal dissipation of (excess) absorbed energy and referred to as non-photochemical quenching (q_N) (Krause *et al.* 1982, Horton and Ruban 1992). The q_N has been proposed to be associated with structural changes in the LHC II (Horton *et al.* 1991, Horton and Ruban 1992) and/or an increase in charge recombination reactions at the PS II reaction center, most likely between P680$^+$ and Q_A^- (Weis and Berry 1987). The latter dissipation is favoured under conditions of PS II donor side inactivation (Schreiber and Neubauer 1987, Weis and Berry 1987, Schreiber and Neubauer 1990, Krieger *et al.* 1992, Krieger and Weis 1993). Part of the absorbed energy may also be dissipated as excess energy in a futile electron transport cycle around PS II, that will as well contribute to the non-photochemical quenching (Schreiber and Neubauer 1990). The thermal dissipation of excitation energy is believed to reflect an important regulatory mechanism of photosynthetic electron transport (Foyer *et al.* 1990, Horton *et al.* 1994).

Besides the role of ΔpH in regulating PS II photochemistry the re-oxidation rate of plastoquinol at the cytochrome b_6f complex is also under control of the lumenal pH (Siggel 1976, Bendall 1982, Foyer *et al.* 1990, Nishio and Whitmarsh 1993). This pH-dependent down-regulation is reflected by a decrease in electron donation rate to oxidised cyt. f and P700$^+$. The ΔpH-related dissipation of excess excitation energy may therefore occur from PS I as well as from PS II. The relationship between energy-dependent quenching and lumenal pH has been shown to be variable (Oxborough and

Horton 1987, Rees *et al.* 1989) and the dark relaxation of the proton gradient with a half time ($t_{1/2}$) of about 5 s (van Voorthuysen *et al.* 1996a) is significantly faster than the dark relaxation of q_N with a $t_{1/2}$ of about 45 s (Bilger *et al.* 1988). This shows that protons are involved but need not necessarily be the primary cause. Other membrane related phenomena which have been suggested to be associated with changes in the proton concentration are light scattering (Bilger *et al.* 1988) and changes in the dielectric properties of the thylakoid membrane (Vredenberg *et al.* 1992).

In this chapter we present experiments on the dark recovery characteristics (de-energisation) of the energised thylakoid membrane of *Peperomia metallica* chloroplasts. The amplitude and dark relaxation kinetics of the transmembrane electrical potential, induced by saturating single-turnover light flashes, were measured in the course of de-energisation in the dark after 2 minutes pre-illumination. Microelectrode and patch-clamp potential measurements were complemented with measurements of the flash-induced electrochromic absorbance band shift at 518 nm. Chlorophyll fluorescence and P700 redox changes were measured in the same leaf and set-up to obtain information on the redox state of the primary electron acceptor Q_A of PS II and the primary electron donor P700 of PS I. It will be argued that inactivation of PS II by a low pH in the lumen is a primary trigger for the suppression of PS II-dependent photochemistry.

6.1 Reversible suppression of flash-induced electrical potential after illumination

Peperomia chloroplasts were energised by 2 minutes illumination with red actinic light. Fluorescence measurements showed that an illumination period of 2 minutes was sufficient to obtain a steady-state level of energisation (cf. Fig. 2-4). Figure 6-1 shows the time course of the flash-induced transmembrane electrical potential, recorded with an impaled microelectrode, before (A) and after (C) 2 minutes actinic illumination. The potential transient during energisation (Fig. 6-1B) shows the well known kinetics with characteristic phases that have been documented extensively elsewhere (Vredenberg 1976, Bulychev *et al.* 1976). The flash-induced transmembrane potential of a dark-adapted chloroplast (A) has an amplitude of about 20 mV and is generated within the 1 - 3 ms response time of the detecting system (Vredenberg 1976). The decay shows single-exponential kinetics with a decay rate of about 30 s^{-1} and is caused by the passive movements of cations and anions across the thylakoid membrane (Bulychev and Vreden-berg 1976a). The flash-induced potential change measured 10 s after the end of the actinic illumination is shown in Fig. 6-1C.

Two principal changes of the flash-induced potential caused by pre-illumination can be observed: (i) a decrease in the half-time of the potential decay, which has been interpreted mainly to be due to the higher proton conductance of the membrane caused by the low lumenal pH during and briefly after energisation (Bulychev and Vredenberg 1976a) and (ii) a suppression of the amplitude of the potential. The energisation-dependent change in the magnitude of the electrical potential response hitherto has not
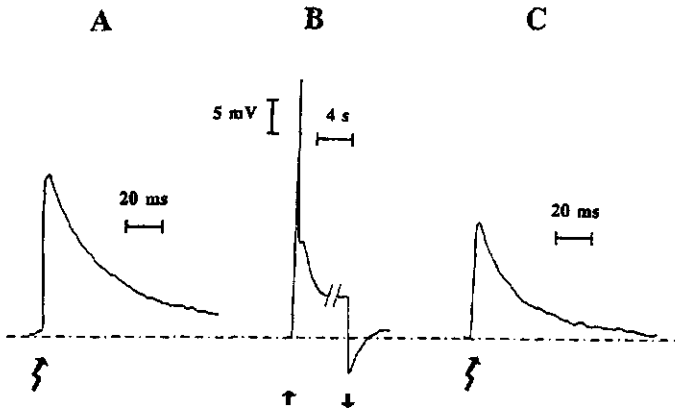
Fig. 6-1 Transmembrane electrical potential response in a *P. metallica* chloroplast upon a saturating single-turnover flash before (**A**) and 10 s after (**C**) 2 minutes illumination with red actinic light (**B**). The electrical potential is measured with an electrode impaled in a Peperomia chloroplast *in situ*. Flash arrows denote the saturating single-turnover flashes. Note the different time-scale for response B. Time resolution was 1 - 3 ms.

received close attention. As this suppression appeared to be partially reversible, the amplitude of the flash-induced electrical potential was measured as a function of the dark time after pre-illumination (Fig. 6-2). Figure 6-2 shows that initially the decrease in the amplitude of the flash-induced potential after pre-illumination (measured under current-clamp) is about 50 % of the amplitude in the dark-adapted state. The potential suppression clearly shows a fast recovery within about 60 - 90 s, followed by a much slower recovery phase, if at all (the experiment of Fig. 6-2 was halted after 120 s dark time). If a second recovery phase is neglected the fast recovery occurs with a relaxation time of 28 ± 6 s to a steady-state which is about 15 % below the amplitude in the dark-adapted state. The reversible part of the energisation-dependent suppression thus amounts about 35 %. The permanent or slowly recovering suppression might be associated with a fraction of PS II centers which were photo-inhibited during the pre-illumination (see also fluorescence induction of Fig. 2-4) and/or with a light-induced change in the chloroplast network conductance (see Fig. 7-7). Measurements of the electrochromic absorbance band shift at 518 nm, attributable to the transmembrane electrical potential, gave similar results with respect to a suppression of the initial amplitude and the relaxation kinetics after pre-illumination (Fig. 6-2). The temporary suppression of the P515 signal is about 25 % and has a recovery relaxation time of 20 ± 4 s. It was observed that even low intensities of background measuring light during the dark period following pre-illumination could already inhibit a full recovery of the amplitude of the flash-induced P515 response (data not shown). The discrepancy in the extent of the potential suppression between patch-clamped chloroplasts and leaves is likely a consequence of the P515 signal-averaging method which will mask any P515 component which does not reverse in the dark time between two measuring sweeps. An additional
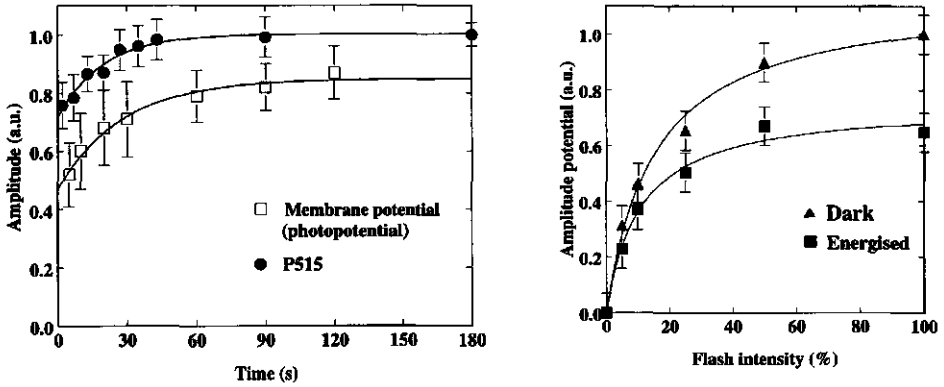
Fig. 6-2 **(left)** Relaxation of amplitude of the flash-induced potential (□) and of the P515 response (●) after 2 minutes pre-illumination with red actinic light. Curves are single-exponential fits with relaxation times of 28 ± 6 s and 20 ± 4 s for potential and P515 respectively. The relative change in the amplitude of the potential (as compared to the dark value) of 10 flash-induced responses like Fig. 6-1C. were averaged. The maximum potential value was taken as the amplitude. The potential was measured by a patch-clamp technique in current-clamp mode (Bulychev *et al.* 1992, Vredenberg *et al.* 1995a). The relative change of the P515 amplitude as compared to the dark-adapted amplitude of 30 flash-induced responses were averaged.

Fig. 6-3 **(right)** Flash-light saturation curve of the amplitude of the flash-induced electrical potential of a chloroplast in the dark (▲) and 10 s after pre-illumination (■). For both conditions the amplitude is expressed as a fraction of the amplitude in the dark-adapted state at maximal flash-light intensity. The relative changes of 5 flash-induced responses were averaged. The potential was measured by the patch-clamp technique in current-clamp mode (Bulychev *et al.* 1992, Vredenberg *et al.* 1995a).

likely cause is the presence of light-induced changes in the chloroplast network conductances causing an increased attenuation of the thylakoid membrane potential (see Fig. 7-7).

If we represent the thylakoid membrane by an electrical capacitor, the decrease of the potential can be explained either by an increase of the membrane capacitance or by a decrease of the actual number of charges that are separated and stabilised in the reactions centers of PS I and PS II. Changes in membrane capacitance are experimentally difficult to verify with our present techniques. Therefore, we concentrated on the second possible cause, which might include at least three different mechanisms:

(1) A decrease of intrinsic PS I/PS II efficiency.
(2) A temporary closure of a fraction of PS I/PS II reaction centers.
(3) An increase of energy dissipation in PS I/PS II reaction centers.

The first mechanism can be excluded because the intensity of the exciting flash was established to be saturating, both in dark-adapted and in energised chloroplasts (Fig. 6-3).

Summary 1   *Energisation of the thylakoid membrane of Peperomia metallica chloroplasts causes a reversible suppression of the amplitude of the flash-induced electrical transmembrane potential. This was detected by the patch-clamp technique (or impalement) and by the electrochromic bandshift and showed about 35 % and 25 % reversible amplitude suppression with recovery relaxation times in the dark of 28 ± 6 s and 20 ± 4 s, respectively. The phenomenon cannot be explained by a decrease in intrinsic efficiencies of PS I and PS II since the flashes used were saturating.*

6.2   Re-opening of PS II reaction centers after pre-illumination

The second mechanism was examined by measuring the chlorophyll *a* fluorescence kinetics of infiltrated intact *P. metallica* leaves. A typical fluorescence transient before, during and after 2 minutes actinic illumination has been shown in Chapter 2, Fig. 2-4. Photochemical quenching (q_P, eq. 2-1), which is a direct measure of the reduction state of the primary stable electron acceptor Q_A of PS II (Krause *et al.* 1982), was calculated for each saturating light pulse after actinic illumination. Figure 6-4 shows the average result of several experiments of this kind ($\square$). This figure shows that after pre-illumination q_P restores in the dark to a value of 1 within a few seconds (relaxation time of q_P equals 2 - 3 s), i.e. the PS II reaction centers closed during energisation re-open within a few seconds and can perform full charge separation. This is much faster than the observed relaxation rate of the energisation-dependent suppression of the flash-induced potential (Fig. 6-2). Thus, the second mechanism of § 6.1 concerning the closure of RC II can be excluded.
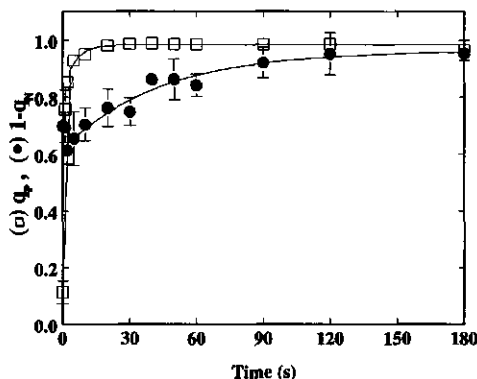
Fig. 6-4   Relaxation of photochemical q_P ($\square$) and non-photochemical ($1-q_N$) ($\bullet$) quenching after 2 minutes red actinic illumination. The values of q_P and q_N at different times after illumination were obtained from separate experiments on fresh dark-adapted leaves in which only one saturating light pulse was given, to ensure no perturbation of the pulse on the relaxation kinetics of q_N. The biphasic kinetics of the curve for ($1-q_N$) has been analysed by a double exponential fit to include the initial decrease of ($1-q_N$) briefly after pre-illumination. The slow component that describes the relaxation of q_N has a relaxation time of 44 ± 9 s. Standard deviations for q_P were less than the dimensions of the data symbols.

6.3 Re-opening of PS I reaction centers after pre-illumination

A temporary decrease in the number of charges transferred across the thylakoid membrane could equally well be caused by inactivation of PS I centers due to an accumulation of the P700$^+$ cation, which is known to be as effective a quencher of excitation energy as P700 (Nuijs *et al.* 1986). Figure 6-5A shows the light-induced absorbance change at 820 nm of an infiltrated *P. metallica* leaf upon a far-red light pulse of 60 s, in order to determine the maximal amount of oxidisable P700. Far-red light induces a fast absorbance increase within 1 s, reaching a quasi saturation level in about 30 s, which constitutes the maximum amount of P700 that could be oxidised. However, there may still be a fraction of P700 centers that has not been oxidised by the far-red light-pulse, for instance due to fast cyclic electron flow around PS I (Schreiber *et al.* 1988). After far-red light the rate of re-reduction of P700$^+$ is limited by a shortage of electron donors when the plastoquinone pool is almost completely oxidised (Schreiber *et al.* 1988). Figure 6-5B shows the 820 nm absorbance change during and after 2 minutes energisation with red actinic light of a leaf that has had several dark-light transitions in order to obtain a stable oxidation-reduction pattern. It was observed that the 820 nm absorbance change of fully dark-adapted leaves exhibited more complex kinetics, probably caused by slow absorbance changes due to light scattering (data not shown). Figure 6-5B shows that after 2 minutes actinic illumination P700 becomes fully reduced within 1 s, which implies that all PS I reaction centers are open again and can perform a charge separation. This excludes PS I reaction center closure as a possible cause for the reversible potential suppression.
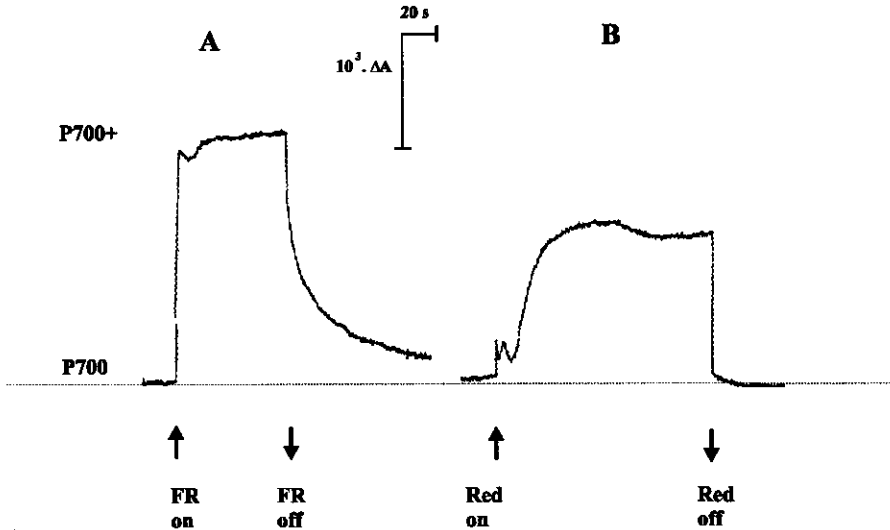

Fig. 6-5   Light-induced 820 nm absorbance changes of an intact *P. metallica* leaf infiltrated with standard isolation medium (§ 2.2) monitoring the formation and decay of the P700$^+$ cation. (A) Far-red (FR) light was given to determine the maximal amount of oxidisable P700; (B) energisation with 2 minutes red light.

6.4 Energy dissipation at photosystem II

The decline and recovery of F_M' during and after energisation (see Fig. 2-4 in Chapter 2) predominantly reflects the increase and relaxation of non-photochemical quenching. The dark reversion of non-photochemical quenching after energisation consists of multiphasic kinetics that contains a fast component attributed to the acidification-related high-energy state quenching (Walters and Horton 1991). In Fig. 6-4 the average result for the dark kinetics of the de-energisation as expressed by 1-q_N is incorporated. After an initial lag period of about 5 s 1-q_N starts to recover with a relaxation time of 44 ± 9 s. The recovery of the non-photochemical quenching bears resemblance to that of the amplitude of the suppressed electrical potential, the latter being somewhat faster. This lead us to the hypothesis that the energisation-dependent suppression of the amplitude of the transmembrane potential and the concomitant increase of the non-photochemical quenching might have a common cause. This can either be viewed as conformational changes in LHC II (Horton *et al.* 1991), or related to proposed changes in membrane capacitance (Vredenberg *et al.* 1992), or viewed as a fast charge recombination in RC II (Schreiber and Neubauer 1990) and/or RC I leading to energy dissipation (mechanism 3 of § 6.1).

Summary 2   *Photosystem I and II reaction centers reopen within 1 - 3 s after pre-illumination and reaction center closure can therefore not be responsible for the reversible energisation-dependent suppression of the flash-induced electrical potential. Rather, the potential suppression is caused by either the formation of a fraction of PS I and/or PS II reaction centers with fast charge recombination or by an increase of the membrane capacitance. The kinetics of the dark recovery of the amplitude of the transmembrane electrical potential and of non-photochemical fluorescence quenching in pre-energised chloroplasts were found to be comparable, which suggests a common cause for both phenomena.*

6.5 Involvement of proton and/or cation gradients

Figure 6-6 shows electrical potential responses upon an actinic light pulse of 15 s duration as measured with a microelectrode impaled in a single *P. metallica* chloroplast *in situ*. The quasi steady-state potential in the light is determined by the balance of the light-driven electrogenic proton current and the passive ion currents through the membrane. The transient undershoot in the rapid light-off reaction of the control (Fig. 6-6A) has been interpreted to be caused by the negative diffusion potential associated with the proton gradient created in the preceding light period (Vredenberg 1976, Bulychev *et al.* 1980). This interpretation is corroborated by the observation that nigericin prevents the formation of the undershoot (Fig. 6-6B). The dark relaxation of the undershoot in Fig. 6-6A results from the passive dissipation of the proton gradient and has a half-time of about 5 s. The rate of linear electron transport was substantially increased in the presence
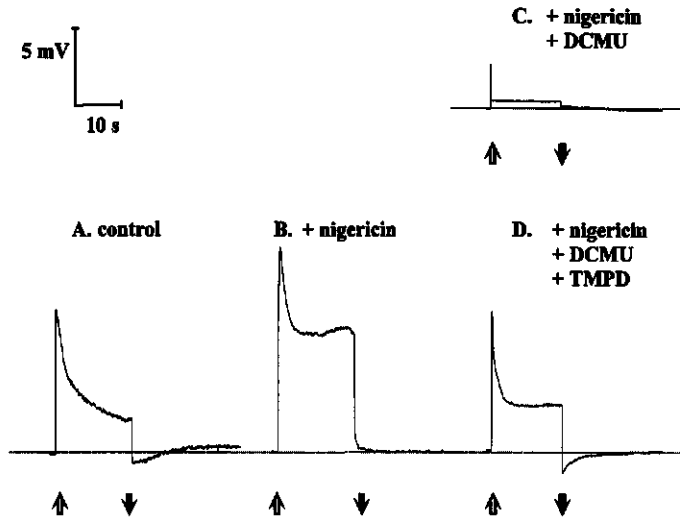
Fig. 6-6   Light-induced potential responses measured with a thin capillary microelectrode brought into a single *Peperomia metallica* chloroplast *in situ*. The following treatments were given: control without any additions (**A**), 0.2 µM nigericin added to the reaction medium (**B**), followed by the addition of 25 µM DCMU (**C**) and finally 0.1 mM TMPD (**D**). The up-and-downward pointing arrows mark the begin and end of illumination with actinic light, respectively.

of nigericin as reflected by the higher steady-state potential in the light (Fig. 6-6B). This stimulation is likely caused by the removal of photosynthetic control at the quinol oxidation site Q_p of the cyt b_6f complex (Bendall 1982, Weis *et al.* 1990) and at the PS II site (Foyer *et al.* 1990, Horton and Ruban 1992, Ehrenheim *et al.* 1994).

Figure 6-7A shows the effect of 2 minutes pre-illumination on the flash-induced electrical potential (expressed relatively to the value measured in the dark-adapted state) in the absence and presence of 1 µM nigericin. The control values, absence of nigericin, are identical to those of Fig. 6-2 and are included for easy comparison. Energisation in the presence of nigericin results in the prevention of the potential suppression or an accelerated temporary potential suppression resulting in complete recovery within 5 s. This observation suggests a decisive role for protons and/or for cation gradients in the energisation-dependent suppression of the flash-induced electrical potential. The effect of nigericin has been confirmed by a similar P515 experiment done with young intact *P. metallica* leaves (Fig. 6-7B).

To examine the involvement of PS I and of cation gradients in the reversible energisation-dependent suppression of the flash-induced potential, *P. metallica* chloroplasts were incubated in standard isolation medium supplemented with 20 µM DCMU and one of the two exogenous mediators N,N,N',N'-tetramethylphenylene-diamine (TMPD) or N-methylphenazonium methosulfate (PMS). Upon illumination the artificial mediator will, after being reduced at the acceptor side of PS I, penetrate into the lumen where it is oxidised by donating electrons to either plastocyanin or directly to $P700^+$ which results in accumulation of $TMPD^+$ or PMS^+ inside the lumenal space
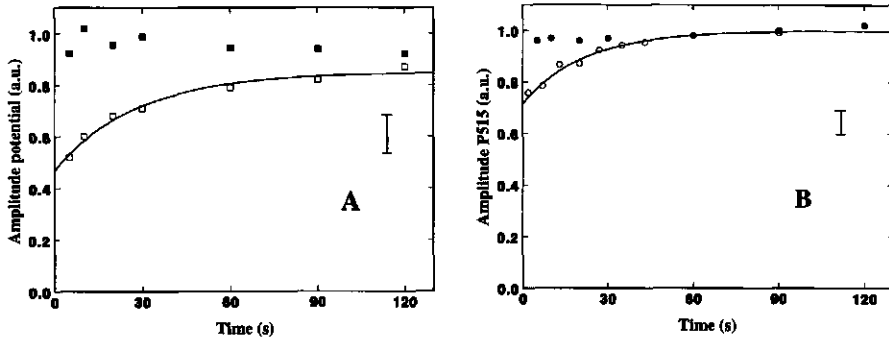
Fig. 6-7 Recovery of the amplitude of the flash-induced transmembrane electrical potential in *P. metallica* chloroplasts after 2 minutes pre-illumination in the absence (open symbols) or presence (closed symbols) of 1 µM nigericin. The amplitude was normalised to the amplitude obtained in the dark before pre-illumination. The curves of the control are single-exponential fits (cf. Fig. 6-2) (A) Patch-clamp recordings. The data are an average of n = 10 and n = 5 measurements for the control (□) and in the presence of nigericin (■), respectively. (B) P515 recordings. The data are an average of 30 and 21 flash-induced responses in a leaf for control (O) and after infiltration with nigericin (●), respectively. Error bars indicates average SE.

(Braun *et al.* 1992, Bulychev *et al.* 1994). TMPD is a one electron carrier, non-proton redox agent (above pH = 6.5) and forms a stable radical ($TMPD^+$) upon oxidation (Prince *et al.* 1981). PMS supports fast cyclic electron transport around PS I which is accompanied by proton translocation from stroma to lumen with a stoichiometry of H^+ : e^- = 1 : 2 at neutral pH (Prince *et al.* 1981), and is thus energy-conserving like the native plastoquinone shuttle (Hauska *et al.* 1974).

Figures 6-6C and D show the inhibition of the light-induced potential by DCMU and the release of inhibition after adding TMPD, respectively. The transient undershoot shown in Fig. 6-6D has routinely been observed with both the impalement and the patch-clamp technique and is suggested to be caused by the negative diffusion potential associated with the $TMPD^+$ gradient across the thylakoid membrane. The absence of a proton diffusion potential is supported by the observation that the undershoot is preserved in the presence of nigericin (Fig. 6-6D). Somewhat different results were obtained for electrogenic ion pumping assisted by PMS (Fig. 6-8, upper part). The negative potential V_d observed immediately after cessation of illumination is most likely caused by the diffusion potential resulting from both a PMS^+ and a H^+ gradient (Bulychev *et al.* 1994). Nigericin brings about a stimulation of cyclic electron transport as can be read from the increase of the initial electrical potential response V_i and of the magnitude of the final potential drop V_f at the light-dark transition. V_d is also increased, giving evidence for the creation of a larger PMS^+ gradient. These stimulations can be explained by a nigericin-induced release of the proton back-pressure on PMS oxidation by $P700^+$ at the lumenal membrane interface. This release is likely to increase the turnover rate of PMS conversion resulting in an enhanced accumulation of PMS^+ in the lumen. Figure 6-8 (lower part) demonstrates that nigericin does not significantly stimulate the magnitude of the potential undershoot in TMPD-assisted cyclic electron transport.

97
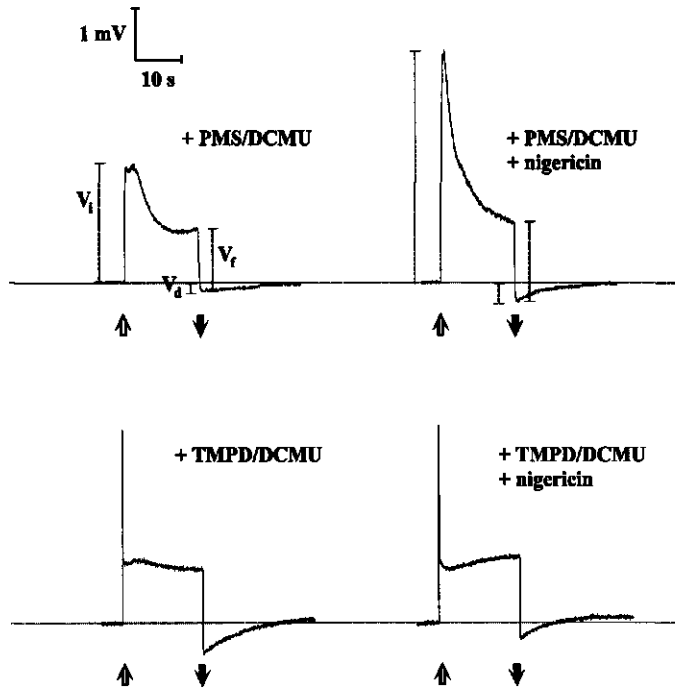
Fig. 6-8 Generation of electrical potential upon 15 s light exposures in two PS I-dependent cyclic electron transport systems as monitored with the patch-clamp technique on single isolated *P. metallica* chloroplasts. Note that 1 μM nigericin stimulates the magnitude of the potential undershoot (V_d) immediately after illumination in PMS-assisted cyclic electron transport (5 μM PMS and 20 μM DCMU) but not in TMPD-assisted electron transport (0.1 mM TMPD and 20 μM DCMU). V_i and V_f refer to the amplitude of the initial and final fast potential changes at light-on and light-off, respectively.

Subsequently the de-energisation kinetics of the two cyclic PS I-dependent electron transport systems were examined after 2 minutes pre-illumination. In order to avoid a contribution of PS II activity to the amplitude of the flash-induced electrical potential while monitoring the de-energisation kinetics, two saturating single-turnover flashes were given 500 ms apart for each measuring time point after pre-illumination. The first flash served to close the fraction of PS II reaction centers that might have been re-opened during the dark period after pre-illumination; the amplitude upon the second flash was taken to represent PS I-dependent potential generation. The time separation of 500 ms between two successive flashes was derived from the results presented in Fig. 6-9. This figure shows the decrease of the amplitude of the flash-induced electrical potential upon 5 successive flashes given after prolonged dark-adaptation and measured in the presence of DCMU and PMS. Under our conditions the recovery of PS II centers is negligible during 500 ms after a saturating flash. In the absence of DCMU and PMS the decrease in the amplitude of the flash-induced electrical potential on the second flash given after a dark interval of 500 ms was about 10 %. This decrease was not affected by 1 μM nigericin (data not shown).
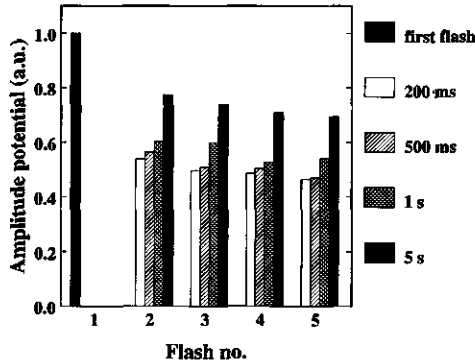
Fig. 6-9 Reduction of the amplitude of the flash-induced photopotential in a dark-adapted *P. metallica* chloroplast upon 5 successive saturating flashes measured in the presence of 20 μM DCMU and 5 μM PMS. The time between flashes was varied from 200 ms to 5 s. The amplitude was normalised to that of the first flash.

In the presence of DCMU and TMPD (Fig. 6-10, open circles) energisation causes a substantial suppression of the flash-induced potential generated by the second of a double flash. However, this suppression shows no recovery during de-energisation. The large non-reversible potential suppression can be mainly attributed to the fraction PS II reaction centers which have been closed by the preceding actinic illumination and by the first of the two flashes, as described above. Addition of nigericin prior to energisation (Fig. 6-10, closed circles) causes a systematic increase of the amplitude in the second flash but no significant change in the de-energisation kinetics. Pre-illumination in the presence of DCMU and PMS but without nigericin causes a distinct but relatively slowly
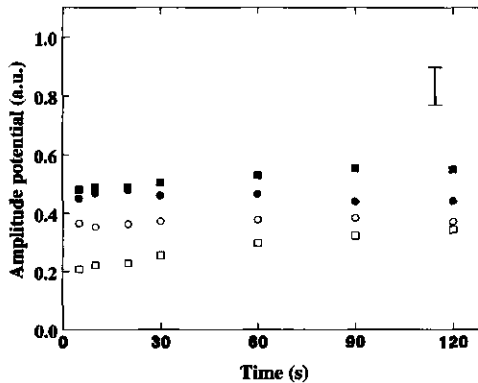
Fig. 6-10 Amplitudes of the electrical potential generated by the 2nd flash of 2 successive flashes, given at each time point (5, 10, 20, ... s) after 2 minutes pre-illumination in the presence of 0.1 mM TMPD (circles) or 5 μM PMS (squares). Open symbols and filled symbols refer to the absence and presence of 1 μM nigericin, respectively. DCMU (20 μM) was always added to the standard isolation medium. Amplitudes are given relatively to the amplitude measured in the dark-adapted state. Average result from n = 6 (TMPD) or n = 9 (PMS) experiments. Error bar indicates average SE.

recovering suppression of the potential (Fig. 6-10, open squares). However, the results for energisation in the presence of PMS must be approached with prudence. The recovery kinetics of the energisation-dependent potential suppression were also measured with the P515 technique on *P. metallica* leaves infiltrated with isolation medium supplemented with 50 μM PMS and 50 μM DCMU and this showed no significant reversible amplitude suppression (data not shown). The much slower recovery kinetics of the photopotential amplitude in the presence of PMS and DCMU (Fig. 6-10) as compared to the control (Fig. 6-7) suggest a different mechanism which might be related to light-induced changes in chloroplast conductances (see Chapter 7).

Summary 3   *Energisation of P. metallica chloroplasts in the presence of nigericin was without a reversible suppression of the flash-induced electrical potential which suggests a decisive role for protons in the phenomenon. Light-induced cyclic electron flow around PS I in the presence of DCMU and one of the two co-factors PMS or TMPD results in an accumulation of the cationic form of the cyclic co-factor in the lumen with an additionally co-transport of protons in the PMS-assisted cyclic flow. Energisation in both cyclic PS I-dependent electron transport systems was without a reversible potential suppression comparable to the control. This suggests that the energisation-dependent potential suppression is not caused by: (1) a cation-induced reversible increase of the membrane capacitance and (2) a low pH-induced reversible suppression of PS I-dependent electrogenesis. Most probably, PS II-dependent electrogenesis is reversibly suppressed by lumenal acidification.*

6.6   Amplitude suppression of the P515 response in spinach thylakoids in relation to pH

A more direct approach to examine the effect of pH on the potential suppression is to measure the photopotential amplitude upon a change of the external pH. For this purpose the patch-clamp technique in combination with the superfusion system was used (§ 2.3). This would allow a controlled decrease of the medium pH followed by a subsequent return to the starting pH, thus providing a test for the proposed reversibility of the low-pH-induced potential suppression. This method, however, was hampered by an irreversible and unpredictable change of the flash-induced photopotential below pH 6, presumably caused by alterations in the seal configuration of the patched chloroplast. Therefore, the effect of a low medium pH was examined on the amplitude of the P515 response in spinach thylakoids. Figure 6-11A shows a P515 response in the first 40 ms of spinach chloroplasts incubated at pH 7.5 and pH 5.0. Lowering the medium pH caused a suppression of the initial P515 amplitude in addition to a drastic change of the decay kinetics. The latter can been ascribed to an inhibition of a slow component of P515 (Reaction 2) and to an increase of the membrane conductance at lower pH (Vredenberg 1976, Junge 1977, Snel 1985, Ooms *et al.* 1989). The pH-induced alteration of the P515 response compares well with the energisation-induced change in the P515 response (Fig. 6-11B). The recovery kinetics of the suppressed P515 amplitude in spinach thylakoids
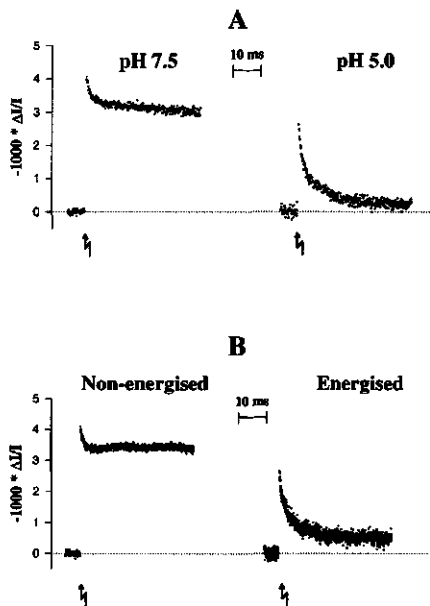
Fig. 6-11 (A) Flash-induced P515 response of dark-adapted spinach thylakoids incubated for 5 minutes in reaction medium at pH 7.5 and pH 5.0. Sample frequency 10 kHz, electronic filter 3 kHz, average of 50 responses with 20 s dark interval, 10 °C. (B) Flash-induced P515 response of spinach thylakoids before (Non-energised) and 5 s after (Energised) 2 minutes pre-illumination. Sample frequency 30 kHz, filter 3 kHz, average of 50 (non-energised) and 15 responses (energised); temperature was 20 - 25 °C. The first 0.25 ms of all responses were discarded for reasons discussed in § 2.4.

(data not shown) are comparable to that of *P. metallica* chloroplasts. The change in the amplitude of the P515 response of spinach thylakoids in the pH-range 5.0 to 7.5 is shown in Fig. 6-12. This shows that a decrease of the external pH below pH 5.5 causes a suppression of the initial P515 amplitude of about 40 %. The same experiment
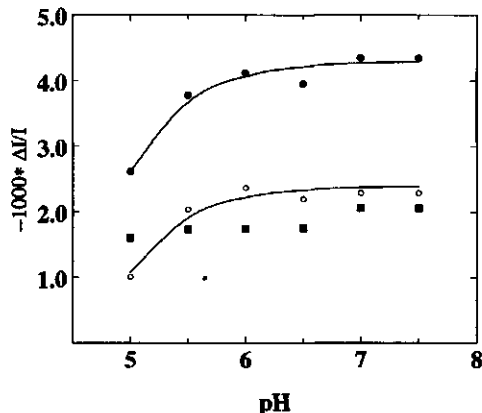
Fig. 6-12 Effect of external pH on the amplitude of the P515 response in spinach thylakoids. The amplitude of the P515 response at 0.25 ms was taken to represent the flash-induced transmembrane potential. At each pH the amplitude was determined in the dark-adapted state (●) and in the presence of saturating far-red light (○) to eliminate the contribution of PS I charge separation to the total response. The difference between dark and plus far-red light (■) was taken to represent PS I-dependent potential generation.

101

was repeated in the presence of far-red background illumination (> 715 nm) to close all PS I reaction centers. The initial amplitude of the P515 response will then depend predominantly, if not exclusively on PS II activity (Chylla *et al.* 1987). It was verified by chlorophyll fluorescence quenching analysis that the far-red background illumination caused only a minor energisation and no more than 10 % closure of PS II reaction centers. Figure 6-12 shows that the far-red background illumination caused an approximately pH-independent reduction of the P515 amplitude. This leads us to conclude that acidification of the thylakoid lumen causes partial inactivation of PS II but not of PS I.

The question was addressed whether the pH-dependent potential suppression is reversible. Therefore the effect of an applied pH gradient across the spinach thylakoid membranes was examined on the P515 response which allows a reversal of ΔpH upon addition of nigericin. A dark ΔpH was created by ATP hydrolysis catalysed by light-activated ATP synthase as described in § 2.7. Figure 6-13 demonstrates that a ΔpH = 2.5, as determined from a calibration of the 9-aminoacridine fluorescence quenching (Lohse *et al.* 1989), caused an amplitude suppression of about 20 %. Approximately 16 % appeared to be nigericin-reversible (Fig. 6-13C) which is the part assumed to be caused by the proton gradient. The nigericin facilitated H^+/K^+ exchange ($\Delta\mu_{H+} = \Delta\mu_{K+}$) is expected to lower the pH gradient below ΔpH = 0.1 assuming a lumenal potassium concentration equal to that of the assay medium, i.e. equal to 0.5 mM K^+ (Table 2-4, 1 : 1 mixture of double assay medium and break medium). In case that a higher potassium concentrations in the lumen is taken, which likely approaches a more realistic value (Bulychev and Vredenberg 1976a, Vredenberg 1976), an even lower equilibrium ΔpH after nigericin addition is calculated.
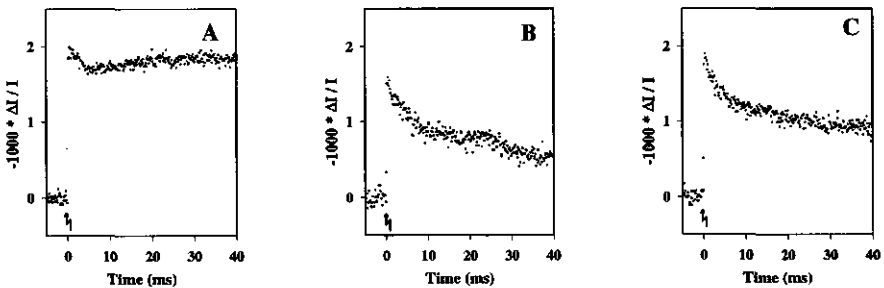
Fig. 6-13 Test for reversibility of low pH induced potential suppression. P515 responses of spinach thylakoids (10 μg Chl ml⁻¹) in the presence of 10 mM dithiothreitol (DTT) and 0.1 mM methylviologen. The ATP synthase was activated by 30 s pre-illumination. **(A)** Control response 60 s after the activating pre-illumination, without ATP addition. **(B)** Response in the presence of 0.2 mM ATP added 60 s after the activating pre-illumination. ΔpH = 2.5. **(C)** Same as B but after subsequent addition of 2 μM nigericin. Sample frequency 20 kHz, electronic filter 3 kHz, average of 3 samples which were given 15 flashes each with a dark interval of 5 s.

Summary 4   *The amplitude of the flash-induced P515 response of spinach thylakoids can be reversibly suppressed by a low lumenal pH. The P515 response pattern of a dark-adapted thylakoid sample at an assay pH 5.0 shows resemblance to that found at 5 s after pre-illumination of the thylakoid sample at neutral pH. These observations support the conclusion that light-driven acidification of the lumen causes the reversible suppression of the flash-induced transmembrane electrical potential.*

6.7   Discussion. Low-pH induced charge recombination in PS II

Measurement of the flash-induced electrical potential by either electrode impalement, patch-clamp technique or the flash-induced P515 absorbance shift shows a reversible decrease in the potential amplitude upon energisation (Figs 6-1, 6-2). The phenomenon cannot be explained by a decrease in the efficiency of excitation energy transfer in the antennae of PS I and II (Horton *et al.* 1991, Horton and Ruban 1992) since saturating flashes were used (Fig. 6-3).

A possible explanation for the reversible reduction of the electrical potential could be a decrease in the total number of charges that are separated and stabilised in RC I and RC II on a millisecond time-scale, which was our time resolution for the experimental detection of the potential. The relaxation of photochemical quenching q_P, an indicator for the number of open PS II reaction centers, showed that PS II centers are reopened within several seconds (Fig. 6-4), including inactive PS II reaction centers (Chylla and Whitmarsh 1989, Snel *et al.* 1992). The fast decrease of the 820 nm absorbance change after red actinic illumination (Fig. 6-5B) shows no evidence for the existence of a population of long-lived (10 - 20 s) $P700^+$ radicals. As formation of the $P680^+$ radical will equally contribute to the absorbance change in this wavelength region (Van Best and Mathis 1978), it can be concluded from Fig. 6-5B that there will be no fraction of long-lived $P680^+$ radicals as well. These observations are in accordance with the fast re-reduction times as was found for $P700^+$ (Harbinson and Hedley 1989, Laisk and Oja 1994) and $P680^+$ (Van Best and Mathis 1978) and indicate that within seconds after energisation the same amount of net charges will initially be separated as in the dark-state.

The potential suppression is likely the result of the acidification of the lumenal space of chloroplast thylakoids. If proton accumulation during energisation is prevented by rapid proton-potassium exchange facilitated by nigericin the potential suppression is not observed (Fig. 6-7). When the generation of the transmembrane potential depends solely on PS I activity associated with the electrogenic pumping of $TMPD^+$ or PMS^+ and H^+ no reversible potential suppression similar to the control is observed (Fig. 6-10), suggesting that PS II activity is required. The latter observation poses two additional constraints on a possible explanation of the phenomenon. First, the energisation-dependent potential suppression cannot be explained by a mechanism that operates on both potential generators PS I and PS II. For example, a membrane capacitance increase that might have been induced by proton release in the lumen associated with the PMS

reoxidation reaction should have been sensed by a transmembrane electrical field. Therefore, the proposed increase of the membrane capacitance upon energisation (van Voorthuysen *et al.* 1995) has to be considered unlikely. Still, proton evolution at the OEC of PS II from within the extensively folded grana thylakoids may be quit different from proton pumping associated with PMS oxidation at the PS I complex which is located in the grana margins and stroma thylakoids. Acidification of the lumen was shown to cause a decrease in cyt. b_{559} redox midpoint potential (Horton and Cramer 1975, De Las Rivas *et al.* 1995), an increase in Q_A midpoint redox potential (Krieger *et al.* 1993), liberation of Ca^{2+} (Krieger and Weis 1992) and dissociation of the 23 kDa protein. These events demonstrate that alterations in the structural integrity of the thylakoid membrane may occur upon acidification and the thylakoid membrane and its imbedded proteins would then be more exposed to the hydrophilic aqueous phase resulting in an increase of the effective membrane dielectric constant (increase in membrane capacitance). Therefore, capacitance changes strictly dependent on PS II proton evolution cannot be completely excluded. Secondly, the light-induced accumulation of the lipophylic cations $TMPD^+$ or PMS^+ is apparently not equivalent to the proton accumulation with respect to potential suppression. This suggests that protonation reactions of lumen-exposed carboxyl groups with pK values in the pH range 5 to 7 are involved as was postulated for the energisation-dependent changes in LHC II aggregation (Horton *et al.* 1994). The results obtained with spinach thylakoids (Figs 6-11, 6-12, 6-13) demonstrate that a low pH can indeed (reversibly) suppress the amplitude of the field indicating absorbance change. The absence of a pH-dependence of the P515 amplitude generated by PS I (Fig. 6-12) implies that only PS II-dependent potential generation is susceptible to a low pH.

We propose that the proton accumulation inside the lumen causes secondary reactions which might eventually result in the observed reversible suppression of the flash-induced electrical potential. The transmembrane proton equilibration after pre-illumination occurs with a half-time of about $t_{1/2} = 5$ s, as judged from the relaxation of the potential undershoot after the light-dark transition (Fig. 6-6A). This is much faster than the dark relaxation of the flash-induced potential suppression which occurs with $t_{1/2} = 14 - 20$ s (Fig. 6-2). Furthermore, the dark recovery after pre-illumination of energy-dependent chlorophyll fluorescence quenching was reported to occur with an even more slower recovery relaxation of $t_{1/2} = 32$ s (Fig. 6-4, Bilger *et al.* 1988, van Voorthuysen *et al.* 1995). The absence of a kinetic relationship between these two phenomena and the potential suppression supports the view that a cascade of reactions is involved rather than a single process.

It is conceivable that in a fraction of PS I and/or PS II centers the primary charge separation will not lead to a stabilisation of the charges but will instead be followed by fast charge recombination, either directly from a primary acceptor to the primary donor or by a futile electron transport cycle involving other redox mediators. If occurring on a time-scale below 1 ms, these dissipative processes will not contribute to the delocalised transmembrane potential and will neither be detected by our instruments as formation of a stable charge separated state is prevented by the fast charge recombination.

An energisation-dependent formation of charge dissipating PS I reaction centers appears here to be unlikely. An enhancement of dissipative charge recombination processes in the reaction center of PS I due to an accumulation of reduced acceptors at the reducing site is unlikely to occur under our experimental conditions of no shortage of CO_2 or O_2 (Foyer *et al.* 1990, Laisk and Oja 1994). PS I-dependent electrogenesis catalysed by TMPD showed no reversible potential suppression (Fig. 6-10, circles). The results obtained in the presence of PMS (Fig. 6-10, squares) are less straightforward but are probably not correlated to the phenomenon studied here. This conclusion is supported by P515 measurements with *P. metallica* leaves infiltrated with PMS and DCMU, which did not reveal any significant energisation-induced reversible potential suppression comparable to the control. Furthermore, the recovery relaxation kinetics for PMS shown in Fig. 6-10 are many times slower than what was found in the control (Fig. 6-2) which points to the interference of a novel phenomenon, e.g. light-induced changes in the chloroplast resistances. Energisation-dependent changes in the chloroplast resistances, presumably of the narrow partitions regions, have been proposed to exist (Vredenberg *et al.* 1995a, b). The absence of PS I inactivation, as judged from suppression of potential generation by H^+ and/or $TMPD^+$ and PMS^+ accumulation, suggests that energisation-dependent inactivation of this kind is restricted to PS II. Moreover, the magnitude of the reversible part of the potential suppression in the presence of DCMU and PMS (Fig. 6-10) is about half of that found for the control (Fig. 6-2), thus excluding a unique assignation to PS I.

An energy-dependent down-regulation of PS II performance resulting in non-photochemical quenching of chlorophyll fluorescence has been proposed to be caused by a fast dissipative charge recombination within a fraction of PS II reaction centers of which the donor side was impaired (Schreiber and Neubauer 1987, Weis and Berry 1987, Krieger and Weis 1993). Inhibition of the water splitting complex in photosystem II membranes by calcium depletion was demonstrated to cause a slowing down of $P680^+$ reduction from the submicrosecond time range into the microsecond time range (Boussac *et al.* 1992). The inactivation of the water splitting system by calcium release is suggested to occur at a low lumenal pH concomitantly with a shift of the redox potential of Q_A to higher values (Krieger and Weis 1993, Krieger *et al.* 1993). Both the decreased re-reduction rate of $P680^+$ and the Q_A redox shift favour a back-reaction of Q_A^- with $P680^+$, a charge recombination which competes with the forward charge stabilising reaction in which Q_A^- becomes oxidised by the secondary quinone Q_B. The inactivation of PS II measured in thylakoids and PS II particles at low pH was abolished upon restoration of the PS II donor side by the addition of excess Ca^{2+} or an efficient electron donor to P680 illustrating the reversible character of this type of PS II inactivation (Krieger and Weis 1993). The energisation-dependent suppression of the flash-induced electrical potential could thus in principle be described with the above charge recombination model. This conclusion is supported by the comparable transition pH around 5.5 at which both P515 suppression (Fig. 6-12) and variable chlorophyll fluorescence (Krieger and Weis 1993) start to decline. Figure 6-9 indicates that the fraction of PS II reaction centers in *P. metallica* chloroplasts is about 0.45 - 0.55. This

would imply that in Fig. 6-2 PS II performance is reversibly suppressed by about 55 - 65 %. Quenching of the variable PS II fluorescence and inhibition of oxygen evolution at pH 5.0 was about 60 % in spinach (Meunier and Bendall 1993) which corresponds nicely with our results.

Further experiments are required to elucidate whether membrane energisation leading to non-photochemical quenching transforms a fraction of PS II reaction centers into a state favourable for futile charge recombination induced by a donor site limitation .

Summary 5   *The reversible energisation-dependent suppression of the flash-induced electrical potential is best explained by rapid charge recombination in a fraction of photosystem II reaction centers induced by a low lumenal pH. In this view the initially charge separated state $P680^+Q_A^-$ is rapidly (< 0.25 ms) lost in these centers, thus escaping detection by our methods. This model finds its closest match with the reaction center quenching model of Weis and Berry (1987) and more extensively investigated in Krieger and Weis (1993).*

6

Chapter 7
Light-induced conductances changes in chloroplast lamellae

The intensively folded architecture of the chloroplast thylakoids has many structural implications regarding domain organisation and the existence of microscopic spaces between closely opposed membranes (Albertsson 1995). In particular, the two-dimensional sheets of the appressed grana membranes form alternating partitions and lumenal spaces of narrow dimensions with widths of about 5 nm (Haehnel 1984, Junge and Polle 1986). This is the scenery where transverse and lateral currents flow of mainly H^+, K^+, Cl^- and Mg^+ ions (Bulychev and Vredenberg 1976b, Barber 1980, Van Kooten 1988) along their respective electrochemical gradients associated with photosynthetic proton pumping. In the act of counterbalancing the proton pump, a redistribution of H^+, K^+, Cl^- and Mg^+ will take place which will affect the local ion concentrations. Surely, ion redistributions in the microscopic spaces like the grana partitions and the lumen will have their feedback on the membrane conductances as well as on the conductances of the phases adjacent to the membrane.

Several studies have addressed the problem of hindered ion diffusion along membrane/water interfaces. Conductivity measurements to examine the electrical properties of the membrane/water interface seem to indicate a decrease in anionic and cationic conductances along membranes (Menger *et al.* 1989, Gutman and Nachliel 1995). Charge gradients, both laterally between subcompartments from stroma to inner grana and transversely between top and bottom of grana stacks were inferred from photovoltage experiments (Osváth *et al.* 1994) and imply that low conductance phases in chloroplast thylakoids are likely to exist. The ion mobility of the proton forms an exceptional case inasmuch as only slight differences were found for proton diffusion along membrane surfaces and in bulk water (Polle and Junge 1989, Gutman *et al.* 1992, Gutman and Nachliel 1995). However, as soon as proton binding surface groups are considered the diffusion of protons is greatly reduced which results in a loss of the proton-motive-force (Junge and Polle 1986). Energetic losses were also proposed for proton exchange between the bulk phase and a membrane-localised phase (Sigalat *et al.* 1985). These examples demonstrate the involvement of lateral resistances in photosynthetic energy coupling (Haraux and de Kouchkovsky 1983, Allnut *et al.* 1991).

In recent reports the chloroplast patching technique was illustrated to be useful for studying electrogenic events in the thylakoid membrane of *Peperomia metallica* chloroplasts (Vredenberg *et al.* 1995a, van Voorthuysen *et al.* 1996b). In general, the light-induced

current (photocurrent) at zero holding potential as measured with the patch-clamp technique is directly proportional to the transthylakoid electrical potential difference (V_M) except for an attenuation factor determined by a voltage-dividing network, see Fig. 3-7 (Vredenberg *et al.* 1995a). This attenuation depends on the chloroplast resistive pathways and this dependency can likely provide us with new insights into (changes in) the lateral conductances of the narrow membrane/water interfaces.

In voltage-clamp mode the patch-clamp method would in principle allow to study the effects of externally applied electrical fields on chloroplast bioenergetics *in situ* (Bulychev *et al.* 1992). This may concern a broad field of interest ranging from primary charge separation in photosynthetic reaction centers (Meiburg *et al.* 1983, Bulychev *et al.* 1986, Dau and Sauer 1992, Boxer 1993) and the interheme electron transport in the cyt. *b6f* complex (Bouges-Bocquet 1981, Hope *et al.* 1992) to the translocation of proteins across the thylakoid membrane (Mould and Robinson 1991). Still little is known on how the imposed electrical fields might affect light-induced ion fluxes in intact chloroplasts and how they relate to electrogenic H^+ pumping.

A previous study on photocurrent kinetics in continuous light showed an additional component in the presence of a holding potential that might be related to a light-induced change in the chloroplast (input) seal conductance (Bulychev *et al.* 1992). Light-induced conductance changes show interesting prospects with regard to an understanding of thylakoid architecture and ion movements. Therefore, in this study we monitored direct changes in the chloroplast network conductances under the action of light. We show for the first time that a single turnover of PS I and PS II causes a transient decrease in the low conductance phases between the patch electrode and the thylakoid membrane.

7.1 Alteration of photocurrent by holding potential

A representative photocurrent measured at zero holding potential is shown in Fig. 7-1, V_h = 0 mV. The photocurrent has an initial amplitude of -300 pA, originating from fast charge separation in the reaction centers of PS I and PS II, and a single-exponential decay with a relaxation time of about 71 ms. A Q-cycle, which is associated with a slow secondary rising current at zero holding potential (van Voorthuysen *et al.* 1996b), is apparently not operational in this particular chloroplast. The seal conductance of this whole-thylakoid configuration was 33 nS (R_{seal} = 30 MΩ). The decay of the photocurrent is completed within 400 - 500 ms and reflects the discharge of the thylakoid membrane capacitance through the chloroplast network resistances, including R_A and R_L (Fig. 3-7). A holding potential of + 45 mV or - 45 mV substantially modified the kinetics of the photocurrent (Fig. 7-1). It should be noted that the corresponding positive and negative dark currents of about 1.5 nA have been set to zero for reasons of clarity. The voltage-dependence of the photocurrents induced by single-turnover flashes as shown in Fig. 7-1 show similarities with those induced by long light pulses (not shown, but see Bulychev *et al.* 1992). After both a flash and a light pulse the photocurrent returns more slower to the zero baseline in the presence of a holding potential. Secondary electron transfer (Q-cycle
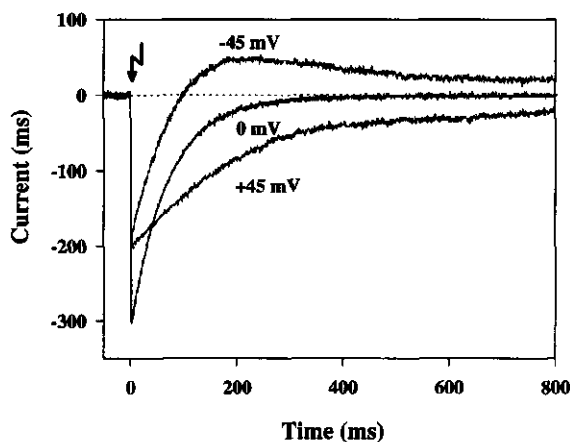
Fig. 7-1 Flash-induced photocurrents of a dark-adapted *P. metallica* chloroplast in the presence of 20 nM nigericin monitored in voltage-clamp mode at three different holding potentials: $V_h = 0$, $\pm$ 45 mV. The seal conductance g_{seal} at $V_h = 0$ mV was 33 nS. The dark positive and negative currents (about 1.5 nA) corresponding to + 45 and - 45 mV, respectively, have been set to zero. The photocurrent at $V_h = 0$ mV shows single-exponential kinetics with a decay relaxation time of 71 ms.

driven) has been found of no important qualitative effect on the photocurrent changes at holding potentials different from zero (see also Vredenberg 1996). Photocurrents measured at holding potentials smaller than 45 mV showed similar behaviour but with different magnitudes, in general with less effect for lower off-set potentials. The voltage-dependency, however, was in most cases nonlinear. The photocurrents shown in Fig. 7-1 should therefore be taken as representative responses giving a semi-quantitative description of the phenomenon .

The holding potential modifies three aspects of the photocurrent (Fig. 7-1): i) at a negative holding potential the current rapidly intersects the baseline whereas at a positive holding potential the current decay is retarded, ii) the complete relaxation of the photocurrent at both negative and positive holding potentials takes a longer time than at $V_h = 0$ mV and iii) the initial amplitude is altered. In Fig. 7-1 the initial amplitude is suppressed; other chloroplasts may show an amplitude increase (cf. Fig. 7-4). In general, the application of a holding potential caused photocurrent amplitude variations of approximately 0 - 60 % in different chloroplasts. Photocurrents in the presence of a holding potential were measured after the dark current had reached a steady-state and the amplitude variations are likely related to current-induced changes in the chloroplast network conductances. This interpretation is strengthened by the regularly observed 0 - 20 % increase of the chloroplast seal resistance upon application of V_h and illustrates again the nonlinear behaviour of the measuring configuration in the - 45 to + 45 mV range. The first two modifications are likely a manifestation of a flash-induced change in the chloroplast network conductances.

109

7.2 Flash-induced conductance changes calculated from photocurrents

A flash-induced change in the chloroplast seal conductance can be inferred from the photocurrents at $V_h = \pm$ 45 mV by subtracting the photocurrent measured at zero holding potential. Such a subtraction procedure is only valid when other processes contributing to the flash-induced current are voltage-independent. This is not quite the case considering the above mentioned nonlinearities. But for the purpose of illustration we will assume these effects to be negligible. Because of the amplitude variations, the photocurrents at different holding potentials were scaled to the same initial amplitude for further data analysis.

In voltage-clamp the current in the circuit (= current through tip resistance R_T, Fig. 3-7) is composed of the clamping current (I_C) and the transient photosystem-generated current (I_M) starting at t = 0, the moment of flash firing. The clamping current is given by the product of the seal conductance (g_{seal}) and the holding potential (V_h) while I_M originates from the generation and subsequent decay of the transthylakoid membrane potential ($V_M(t)$). The photocurrent at $V_h = 0$ (I_0) contains no contribution from I_C in which case it follows that,

$$V_h = 0: \qquad \begin{array}{ll} I_0(t) = 0 & \text{for} \quad t < 0 \\[2mm] I_0(t) = I_M[V_M(t)] & \text{for} \quad t \geq 0 \end{array} \qquad (7\text{-}1)$$

If $V_h = h \neq 0$ the (changing) seal conductance $g_{seal}(t)$ will contribute to the photocurrent (I_h),

$$V_h \neq 0: \qquad \begin{array}{ll} I_h(t) = g^0_{seal} \cdot V_h & \text{for} \quad t < 0 \\[2mm] I_h(t) = [g^0_{seal} + \Delta g_{seal}(t)] \cdot V_h + I_M[V_M(t)] & \text{for} \quad t \geq 0 \end{array} \qquad (7\text{-}2)$$

with g^0_{seal} the dark seal conductance and $\Delta g_{seal}(t)$ the flash-induced change in the seal conductance.

In equation 7-2 it has been assumed that I_M is independent of external voltages. Voltage-dependent changes in charge separation yield in RC I and II are probably insignificantly small within the range of V_h values used here (Dau and Sauer 1992). The function describing the time-dependent seal conductance for $t \geq 0$ can now be calculated by subtracting eq. 7-1 from eq. 7-2 which yields,

$$g_{seal}(t) = g^0_{seal} + \Delta g_{seal}(t) \;\; = \;\; \frac{I_h(t) - I_0(t)}{V_h} \qquad (7\text{-}3)$$
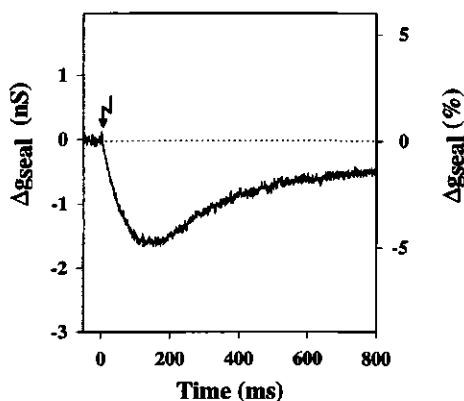
Fig. 7-2 Flash-induced decrease in the seal conductance (Δg_{seal}) obtained from a subtraction of the flash-induced current responses of Fig. 7-1 for $V_h = 0$ and $+45$ mV after normalisation of the $V_h = 0$ response to the $V_h = +45$ mV response. The dark seal conductance g^0_{seal} at $V_h = 0$ was 33 nS.

Figure 7-2 shows the flash-induced change in seal conductance ($\Delta g_{seal}(t)$) obtained according to this subtraction procedure using the photocurrents at $V_h = +45$ mV and $V_h = 0$ (scaled to the amplitude of the photocurrent at $V_h = +45$ mV) of Fig. 7-1. After the flash the seal conductance decreases within 150 ms by about 1.6 nS, or about 5 % of the dark seal conductance, and the subsequent reversal to the pre-flash dark level takes more than 0.8 s. Several experiments performed on different chloroplasts showed flash-induced decreases in g_{seal} having its minimum at 50 - 200 ms after the flash and ranging between 0.3 % and 5 % of the dark seal conductance.

Summary 1   *Measurements of flash-induced photocurrents at different holding potentials modified the kinetics of the photocurrents dramatically. At a negative holding potential the current rapidly intersects the baseline whereas at a positive holding potential the current decay is retarded. These modifications are likely a manifestation of a flash-induced change in the chloroplast conductance network. The kinetics of the flash-induced seal conductance change can be obtained by subtracting the photocurrents measured in the absence and presence of a holding potential, respectively. A partially, transient decrease of about 0.3 - 5% in seal conductance was observed with a minimum at 50 - 200 ms after the flash followed by a slow relaxation in 1 - 10 s.*

7.3 Direct recording of flash-induced conductance changes by phase-sensitive detection

In order to circumvent the nonlinear effects of the holding potential, which interfere with the kinetics of the light-induced conductance changes, we used a phase-sensitive detection technique as a second means for monitoring the flash-induced conductance changes. By virtue of the sine-wave modulation this technique allows the detection of conductance changes around zero holding potential albeit that the time response is reduced to 100 or 300 ms. Figure 7-3 compares a flash-induced conductance change on a

111

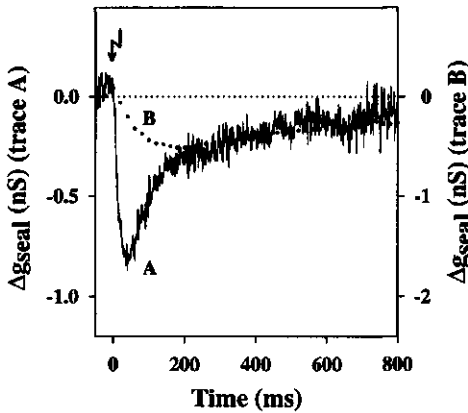**Fig. 7-3** Flash-induced change in seal conductance (Δg_{seal}) of a *P. metallica* chloroplast in the presence of 20 nM nigericin obtained by two alternative methods as discussed in detail in the text: **(A)** subtraction of the flash-induced current responses at $V_h = 0$ and $+ 25$ mV (original current traces not shown) and **(B)** direct recording of g_{seal} at $V_h = 0$ mV by phase-sensitive detection (rms amplitude 3.5 mV, 100 Hz, time constant 100 ms) with a lock-in amplifier. The latter signal is an average of 3 flash-induced responses which were sampled with a sampling rate of 40 Hz.

different chloroplast as obtained by phase-sensitive detection (100 ms time constant) and by the subtraction method. For an appropriate comparison of the kinetics the two conductance changes were normalised to an equal amplitude at $t = 400$ ms ($= 4 *$ time constant, > 98 % of signal transmitted). The maximum conductance changes were found to be -0.8 nS and -0.5 nS for subtraction (trace A) and phase-sensitive detection (trace B), respectively (Fig. 7-3). This difference in magnitude may again be related to the nonlinear behaviour of the chloroplast conductance network. Both methods give comparable kinetics on a slow time scale (> 300 ms) but diverge for smaller times as expected from the electronic filtering of the lock-in amplifier. Clearly, light-dependent changes in seal conductance do also occur at zero holding potential and demonstrate that the phenomenon is not a mere artefact of applying relatively high positive or negative holding potentials.

The effect of voltage-dependent modifications on photocurrents was found to be more pronounced in the presence of submicromolar concentrations of nigericin (10 - 50 nM) as was also found in experiments with continuous illumination (Bulychev *et al.* 1992). Other characteristics of the flash-induced conductance changes were (data not shown): valinomycin (1 μM) inhibited the conductance changes; addition of tentoxin, a specific blocker of ATP synthesis (Growth and Junge 1995), was without detectable effects which excludes the involvement of a voltage-activated ATP synthase; and light-induced conductance changes measured with or without nigericin were completely inhibited by 10 μM DCMU, thus demonstrating the intimate relationship of the phenomenon with photosynthetic activity.

Summary 2

Flash-induced changes in seal conductance were also recorded by a phase-sensitive detection technique at $V_h = 0$. The kinetics obtained in this way were comparable to those obtained by taking the difference between the photocurrents in the absence or

presence of a holding potential, respectively. Flash-induced changes in seal conductance were inhibited by 10 μM DCMU and 1 μM valinomycin indicating its intimate relationship with photochemistry and subsequent ion transport in the photosynthetic membrane.

7.4 Conductance decrease of the chloroplast network

The light-induced decrease in seal conductance reflects changes in one or more of the individual conductances g_A, g_L or g_M corresponding to the respective resistances of Fig. 3-7 which constitute the chloroplast network. Can something be said about the individual changes in any of these conductances? To address this question the change in the amplitude of the photocurrent and of the P515 response upon 8 closely spaced flashes was compared, Figs 7-4 and 7-5 respectively.

The rationale for this experiment is the following: the amplitude of the photosystem-generated current ($I_M(t = 0)$) upon a single turnover of the RC's is determined by both $V_M(t=0)$ and by the voltage-dividing network made up of the conductances g_A and g_L(plus the constant g_T in voltage-clamp) (Fig. 3-7),

$$I_M(t = 0) = \frac{g_A}{g_A + g_L + g_T} \cdot g_T \cdot V_M(t = 0) \qquad (7\text{-}4)$$

Fig. 7-4A shows photocurrent responses measured at zero holding potential upon 8 flashes separated by 250 ms. The dark relaxation time of the photocurrent was 80 ms and consequently the current was close to zero upon the next flash firing. The amplitude of
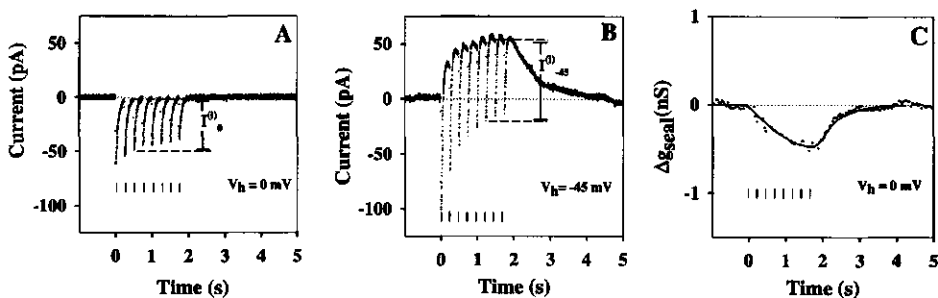
Fig. 7-4 Illustration of the parallel decrease of the initial amplitude of the photocurrents and of the seal conductance of *P. metallica* chloroplasts upon 8 successive single-turnover flashes spaced by 250 ms. Presence of 20 nM nigericin. (**A**) photocurrents at $V_h = 0$ mV. (**B**) photocurrents at $V_h = -45$ mV. The initial amplitude upon flash number i ($i = 1, 2, ..., 8$) for $V_h = 0$ and -45 mV is designated by $I^{(i)}_0$ and $I^{(i)}_{-45}$, respectively. (**C**) direct recording of flash-induced change in seal conductance by sine-wave modulated phase-sensitive detection (rms amplitude 1 mV, 100 Hz, time constant 300 ms) at $V_h = 0$ mV. The 8 vertical lines mark the times of flash firing. The dark seal conductance g^0_{seal} was 43 nS.

113
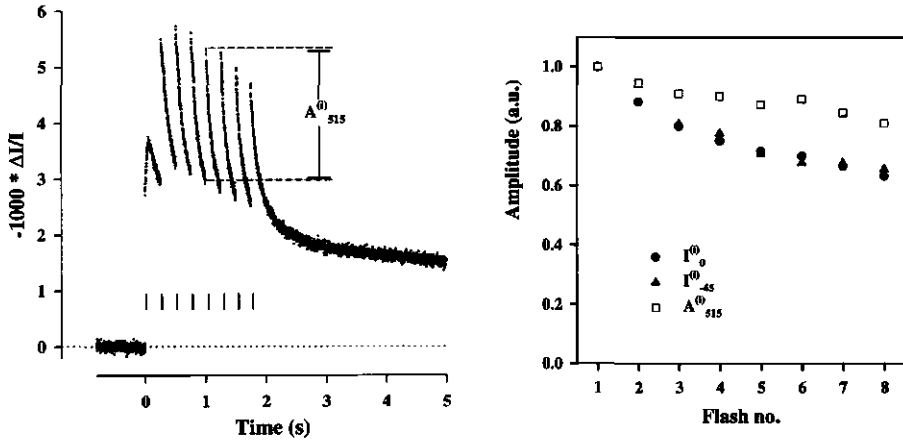
Fig. 7-5 (left) P515 response of *P. metallica* leaves upon 8 successive single-turnover flashes spaced 250 ms apart. The initial amplitude upon flash number i (i = 1, 2, ..., 8) is designated by $A^{(i)}_{515}$ and is a relative measure of the thylakoid membrane voltage. Time resolution was set to 1 ms and the response is an average of 150 sweeps with a dark time of 60 s between the 8-flash sequences. The leaves were infiltrated with standard isolation medium (§ 2.2) supplemented with 200 nM nigericin. The 8 vertical lines mark the times of flash firing. Room temperature.

Fig. 7-6 (right) Comparison of the relative decrease in the initial amplitude of the photocurrents at V_h = 0 and -45 mV (Fig. 7-4) and of the P515 response (Fig. 7-5) upon 8 successive flashes. The time between flashes was 250 ms. Amplitudes were normalised to that of the first flash.

the photocurrent upon flash number i ($I^{(i)}_0$; i = 1, 2, ..., 8) decreased to about 63 % of the initial value (Fig. 7-6). At the same time the seal conductance at V_h = 0 was found to decrease by about 0.48 nS in an additive fashion (Fig. 7-4C). At V_h = - 45 mV a temporarily sustained alteration in current is apparent (Fig. 7-4B) corresponding to a decrease in seal conductance as was discussed for Fig. 7-1. Again, when analysing the 8 successive photocurrents at V_h = - 45 mV a decrease of the initial amplitude is found, similar to that observed for V_h = 0 mV (Fig. 7-6).

The same experimental protocol was repeated by monitoring the P515 response on leaves of *P. metallica*. The initial amplitude of the P515 response was taken as a relative measure of V_M generated by a single turnover of the reaction centers. Figure 7-5 shows the result of this experiment and an amplitude decrease of about 18 % is measured for the 8th flash, significantly less than that found for the photocurrent responses (Fig. 7-6). The amplitude decrease of the P515 response is probably due to a temporary closure of inactive PS II centers (Chylla and Whitmarsh 1989) and to an accumulation of the primary PS II electron acceptor Q_A^- accompanying plastoquinone-pool reduction. The more prominent suppression of the amplitude of the flash-induced photocurrents is best explained by an increased attenuation according to eq. 7-4 due to a flash-induced conductance change within the thylakoid voltage-dividing network, either of g_A or g_L or both.

Summary 3   *A comparison between the reduction of the thylakoid transmembrane voltage (V_M, amplitude of P515 response) and the photocurrent amplitude upon 8 successive flashes showed that the latter was increasingly more reduces than the first. This is interpreted to indicate that V_M is increasingly more attenuated due to a change in either one of the network conductances g_A or g_L or both.*

7.5   Continuous light-induced conductance changes

Continuous actinic illumination of a patch-clamped chloroplast caused changes in the seal conductance which were about one order of magnitude larger than its flash-induced counterpart (Fig. 7-7). The extent of this conductance decrease was, however, observed to be variable among different chloroplasts ranging from a 0 to 50 % change in g_{seal}. The effects of ionophores and DCMU were similar as mentioned in § 7.3. In general, both rise and decay of the continuous light-induced conductance changes, which are not necessarily mirror images, were observed to be biphasic. The relative amplitude of fast and slow phases showed large variations among different chloroplasts and also in the course of experimentation of a single chloroplast (not shown): in some, the slowly recovering phase was absent and the conductances decrease was completely reversible while in others the conductance decrease was virtually irreversible.
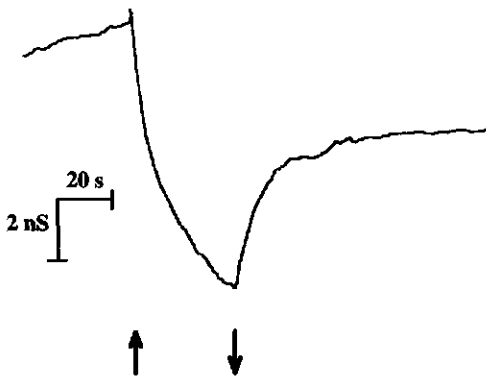
Fig. 7-7   Seal conductance change upon a 40 s continuous illumination with red (RG610) actinic light. Presence of 50 nM nigericin. Phase-sensitive detection (input 2 mV rms, 100 Hz, response time 300 ms) in voltage-clamp mode. The dark seal conductance was 79 nS.

Slowly reversible or even irreversible alterations of the chloroplast conductance network are of importance for understanding the long term effects of actinic illumination on the attenuation of the thylakoid voltage by the voltage-dividing network.

7.6 Discussion

The results shown here demonstrate that transient light-induced changes in the electrical properties of the chloroplast thylakoid network occur on a millisecond time-scale. A decline in seal conductance occurs which is completed within 50 - 200 ms (Figs 7-2 and 7-3) after the firing of a single-turnover flash. The elimination of the conductance changes by DCMU (not shown) reinforces the conclusion that photosynthetic charge separation is a primary event of the phenomenon. The conductance change is presumably the result of secondary ion transport through the extended thylakoid network of the chloroplast.

It is essential to distinguish between current changes which are caused by active ion pumping or those related to changes in the conductances of the chloroplast network. Concerning the first option the photocurrent measured at $V_h = 0$ mV (Fig. 7-1) demonstrates that the discharge current following primary charge separation in the reaction centers reverses in about 400 ms to the dark zero level. A Q-cycle mechanism which was shown to be operative in certain *P. metallica* chloroplasts under different conditions (i.e. in the absence of nigericin) has a transient activity which continues, however, for no more than 200 ms after the flash firing (van Voorthuysen *et al.* 1996b). The associated discharge current of this secondary electrogenic event will also practically have disappeared within about 400 ms. Hence, these two light-induced electrogenic events cannot be the origin of the prolonged current change observed at non-zero holding potentials (Fig. 7-1). Electrogenic proton pumping catalysed by a voltage-activated ATP synthase can be ruled out based on the ineffectiveness of tentoxin (data not shown). Therefore, the chloroplast electrical conductance network undergoes an apparent alteration in the light.

Evidence has been given (Vredenberg *et al.* 1995a) for the inclusion of an as yet unidentified conductance g_A in the electrical equivalence scheme (Fig. 3-7). In combination with the leak conductance g_L, persisting in the region where the glass surface of the pipette contacts with a chloroplast membrane, a voltage-divider is created which accounts for the attenuation of the flash-induced transthylakoid potential (V_M) (Fig. 3-7, Vredenberg *et al.* 1995a). In addition to g_L and g_A the thylakoid membrane conductance (g_M), which was in our experiments about 2 - 10 nS as inferred from current-induced potential responses (data not shown, but see Vredenberg *et al.* 1995a), contributes to the seal conductance. Yet the value of g_M is essentially smaller than g_{seal} (about 30 nS) and changes in g_{seal} can be attributed mainly to changes in g_L and g_A. Moreover, a light-induced increase in g_M is predicted due to the formation of ion diffusion potentials and activation of the ATP synthase (Bulychev and Vredenberg 1976a, Bulychev 1984, Ooms *et al.* 1991). The more pronounced decrease of the photocurrent amplitude compared with the P515 amplitude upon multiple flashes (Figs 7-4, 7-5 and 7-6) shows that V_M is increasingly attenuated. Considering eq. 7-4 this will happen when preceding flashes either cause a predominant *decrease* in g_A or a predominant *increase* in g_L. However, the accompanying light-induced decrease in g_{seal} makes the latter possibility less likely and we therefore conclude that the light-induced

conductance changes are, at least partially, due to a decrease in g_A. A small decrease in g_L is, however, still feasible as long as its effect on the voltage-divider (eq. 7-4) is small compared to the effect of a decrease in g_A.

As yet we can only speculate on the physiological nature of g_A. In general, any low conductance encountered in the current flow pathway from pipette or reference electrode to the thylakoid membrane may contribute to g_A. Considering the promotion and/or inhibition of the light-induced conductance changes by specific ionophores like nigericin and valinomycin we propose that a major part of the conductances in these phases is presumably governed by K^+. This would agree with the dominant role of the K^+ conductance in the total membrane conductance at neutral pH (Bulychev and Vredenberg 1976a) which is due to both the high abundance and the relatively high permeability coefficient of this cation in chloroplasts (Vredenberg 1976).

A predominant role of K^+ in the light-induced decrease in g_{seal} may be visualised as follows. In the absence of nigericin the light-induced transthylakoid potential difference, positive inside, forces K^+ out of the lumenal space by either K^+ transport across the thylakoid membrane to the stroma or, laterally, by K^+ flow out of the lumen along the thylakoid membrane/water interface (directed to the pipette). The resulting (small) depletion of K^+ in the lumen will cause a decrease of the conductance in these narrow microscopic spaces. In contrast, the stromal spaces including the grana partitions, will be enriched in K^+ and thus experience a conductance increase. But, because the lumenal and stromal conductances at opposing sides of the thylakoid membrane are in series with respect to the current flowing between electrode and reference (Fig. 3-7) g_A, defined as a substitute resistance including both lumenal and stromal conductances, is expected to decrease. This argumentation presumes no significant changes in other parameters that may be of importance, e.g. lumenal and stromal volume changes. Nigericin converts photosynthetic proton pumps into virtual K^+ pumps causing a depletion of K^+ at the opposite site, i.e. the stromal spaces and in particular the thylakoid partitions. The stimulatory effect of nigericin on the light-induced conductance changes might thus indicate that the intermembrane spaces of the partitions are significantly smaller than the lumenal spaces: the same amount of K^+ depleted in a smaller volume will be more effective.

The magnitude of the conductance change expected upon a single-turnover of the RC's can be roughly estimated based on the above discussed depletion-model. A single turnover of the reaction centers translocates 2 H^+ per electron transport chain (ETC). Assuming an ETC density of $7 * 10^{14}$ (PS I + PS II) m^{-2} (Van Kooten et al. 1986) and an intermembrane distance of about 5 nm in the grana partitions (Heahnel 1984) this would cause a decrease of 0.47 mM in proton concentration. If this proton pumping is stoichiometrically balanced by nigericin-facilitated K^+-transport from stroma to lumen the calculated decrease in K^+ level in the stroma is about 0.9 % if a K^+ concentration equal to the medium K^+ concentration (50 mM) is assumed. This number is of the same order of magnitude of what is experimentally found.

Other factors, such as electrostatic interactions between adjacent thylakoid membranes in relation to thylakoid shrinkage and swelling may affect the chloroplast

7

conductances. A light-induced swelling of the lumen was concluded from similar experiments in which a stimulation of flash-induced photocurrents was observed in the presence of NH₄Cl (Bulychev *et al.* 1996). A light-induced increase in the hindrance of an EPR spin-label rotational motion was found by Nesbitt and Berg (1982) which they related to the approaching of opposing thylakoid membranes when the thylakoid lumen shrinks in the light.

In conclusion, the application of the patch-clamp method for studying voltage regulation of electrogenic reactions in chloroplasts is promising but demands a more refined analysis of the electrical behaviour of the chloroplast conductance network. The first initiative given here has provided a semi-quantitative characterisation of the light-induced changes in the electrical conductances of the chloroplast and its regulation by ionophores. This demonstrates the unique power of the patch-clamp method for studying these effects in relation to chloroplast bioenergetics. The energisation-dependent regulation of ion mobility through the low conductance phases of the narrow spaces between thylakoids, if present, needs to be reconsidered in understanding photosynthetic energy transduction.

Summary 4   *A substantial part of the light-induced changes in seal conductance are caused by a decrease in the access conductance g_A which is suggested to be intimately related to alterations in the electrical properties of the lateral conductance phases along thylakoid lamellae. A simple model in which secondary K^+ transport across the thylakoid membrane causes a depletion of K^+ in a small domain, envisioned either as the lumen or the partition compartment, may account for the observed extent of the flash-induced conductance changes. The patch-clamp method is unique for quantifying these conductance changes in intact chloroplasts on a ms time-scale.*

7

Chapter 8   General discussion

8.1 Patch-clamp method and P515: two supplementing tools

Primary charge separation and ensuing energy conserving reactions in the photosynthetic membrane are inextricably bound up with electrical events. Studying changes in localised fields, but of more interest for this thesis changes in the delocalised, transmembrane electrical field, will therefore be a profitable challenge for expanding our knowledge about the bioenergetics of photosynthesis. Changes in the electrical field strength may not only occur upon charge separating reactions but equally well because of changes in (membrane) dielectric properties, membrane permeability, ionic composition or because of changes in distances between redox components.

    The two principle techniques used in this thesis, electrochromism (P515) and the patch-clamp method, form two supplementing tools with each having its own surplus information value. The common property of both techniques is their relationship with light-induced electrical fields but they differ on physical grounds in the way how and which fields are sensed. Being a dipole property of inner-membrane pigments the P515 pigment moiety senses, in addition to transmembrane fields, local charge redistributions and may react upon electrostatic interactions and induction. This additional information is illustrated e.g. by the non-electrogenic Reaction 2 which has been interpreted as alterations in the proton partitioning at the membrane/water interface (Ooms 1990, Ooms *et al.* 1991). A careful discrimination between electrogenic events and those events related to more localised phenomena is therefore essential for an unambiguous use of the P515 method.

    Although the patch-clamp method is free from interferences related to localised inner-membrane fields a new, but seemingly interesting property comes into play. This concerns the chloroplast conductance network and energisation-dependent changes therein. By virtue of the pipette-thylakoid contact an additional dissipative pathway competitive to the transmembrane flux is created and determines in part the magnitude and relaxation kinetics of the thylakoid potential. The patch-clamp method is unique for studying changes in proposed low conductance phases of thylakoids on a ms time-range which is difficult to realise with other techniques used so far in photosynthesis research. Yet unique in its own way the method as it is used here (Chapter 3) still needs support from other techniques as has clearly been demonstrated in Chapter 3 (P515 supplying τ_M), Chapter 6 (chlorophyll *a* fluorescence, P515 and P700 measurements giving information about reaction center closure) and in Chapter 7 (P515 showing the relative change in flash-induced thylakoid potential).

    In conclusion, the information obtained when both methods are combined is of

enhanced value for collecting quantitative and time-resolved data on the electrochemical and bioenergetic properties of the photosynthetic membrane. Using the model presented in Chapter 3, measurements of the amplitude and kinetics of flash-induced photocurrents and photopotentials have enabled to estimate:

- the number of PS I and PS II reaction centers active in charge separation;
- the transthylakoid potential generated upon a single-turnover flash;
- the electron transport chain density;
- the dissipation rate of the electrical field by current-injection, which will enhance the reliability of a deconvolution of flash-induced photocurrents/-potentials;
- a time-resolved secondary charge separation involving b_6f turnover;
- kinetics of changes in the chloroplast conductance network which are proposed to contain information about alterations of low conductances at the thylakoid/water interface, notably those of the intimately appressed grana thylakoids.

In combination with P515 the patch-clamp method has contributed to the important issue of how the efficiency of light utilisation in PS II is regulated upon energisation and it was shown that part of the energy dissipation may occur at the level of the reaction center (Chapter 6). An additional rapid loss of a fraction of PS II-dependent charge separation was resolved with the P515 technique thanks to its relatively high time resolution (Chapter 5).

A still complicating factor in the use of the patch-clamp method for obtaining absolute numerical data on electrical parameters concerns the *a priori* unknown value of the native diffusion-driven relaxation time τ_M of individual chloroplasts. Variations in this parameter may be related to differences between chloroplasts isolated from young or old leaves or even from different parts within the leaf itself. Light gradients in leaves were shown to induce differences in photosynthetic properties (Terashima and Inoue 1985). For a reliable utilisation of a τ_M as obtained from an independent technique like P515 the physico-chemical state of both thylakoids used for P515 and patch-clamp measurements needs equal and precise conditioning. An alteration of the H^+/K^+ equilibrium as induced upon addition of nigericin demonstrates that significant changes in τ_M may easily occur (Table 3-1). The uncertainty in the τ_M-value of a single chloroplast introduces a considerable uncertainty in the absolute numerical outcome of the model (Fig. 3-11). Nevertheless, when relative changes in model parameters are considered, based on an associated relative change in τ_M as determined by P515, the outcome will be more uniform.

Differences between P515 and patch-clamp data (Figs 6-2 and 7-6) have guided us into the new compelling realm of energisation-dependent changes in chloroplast conductances. Yet other differences remain unexplained, for example the apparent absence of Reaction $1/RC_f$ in flash-induced photocurrents/-potentials. A comprehensive analysis of energisation-dependent changes in photocurrents/-potentials should incorporate the changes in chloroplast conductances demonstrated in this thesis and the changes in the extent and dissipation kinetics of primary and secondary electrogenesis. Some of the differences between P515 and patch-clamp data will now be addressed.

8.2 Differences between P515 and patch-clamp method

Reaction 1/RC$_f$

While Reaction 1/RC$_f$ is a generally observed phenomenon in P515 recordings of both *S. oleracea* and *P. metallica* chloroplasts, this component is virtually absent in patch-clamp recordings. One exceptional photopotential registration (data not shown) did, however, clearly reveal a comparable fast component with a decay relaxation time of 7 ms which suggests that the phenomenon is not totally unfamiliar to the patch-clamp method. Sufficient grana stacking and accompanying association of PS II - cyt. *b$_6$f* protein complexes were proposed to reduce R1/RC$_f$ (§ 5.6). This condition might have been warranted by the standard electrophysiological isolation medium. Second, the absence of R1/RC$_f$ in patch-clamp recordings could indicate that the pipette has no electrical contact with that membrane moiety which exhibits the fast ms field dissipation. Reaction 1/RC$_f$ might then indeed be associated with a lost cluster of permeabilised thylakoid membranes which must, however, exclusively contain PS II reaction centers (see § 5.2). This would challenge the argumentation made in § 5.2 about the thylakoid membrane system being a single electrical unit as was proposed by Schönknecht *et al.* (1990). However, the 7 ms component of the exceptional photopotential was only observed in the flash-induced response and not in the current-induced response which excludes the involvement of two distinct membrane systems with one having a slow and the other a fast relaxation time. This provides little support for the hypothesis of a lost membrane cluster.

A possible induction of R1/RC$_f$ in photocurrents, as reflected by a fast transient current fraction, might be rationalised from a somewhat alternative interpretation of the lag phase of R1/Q seen in the energisation experiment of Fig. 4-5A. The lag phase of R1/Q emerged in Fig. 4-5A from the second, less constrained deconvolution method 2 as described in § 4.1. This lag phase is most prominent during the short time after pre-illumination (responses at 5 and 10 s after pre-illumination in Fig. 4-5A) when the lumenal pH is lowered. Similar energised conditions were also shown to promote R1/RC$_f$ (Figs 5-7 and 6-11). Therefore, part or all of the lag phase of R1/Q might be a manifestation of a fast decaying fraction R1/RC$_f$. There remains the observation that when R1/Q is absent in a flash-induced patch-clamp response, as in e.g. Fig. 7-1, a fast ms component is generally not detected suggesting that R1/Q and R1/RC$_f$ are closely related. The question whether or not the two phenomena R1/RC$_f$ and R1/Q are strictly related cannot be answered as yet. An accurate analysis into R1/RC$_f$ requires that the photocurrent is measured with a time resolution below 1 ms, which could not always be attained with an acceptable signal-to-noise ratio. In this alternative view (part of) the lag phase of R1/Q would then originate from a summation of R1/Q with a single-exponential rise and the fast decaying R1/RC$_f$. A hypothetical consecutive reaction sequence explaining a correlation between R1/RC$_f$ and R1/Q may be as follows. Upon a single turnover of PS II the plastosemiquinone formed at the Q$_B$-niche may translocate electrogenically to a cyt. *b$_6$f* complex giving rise to R1/RC$_f$. There the semiquinone initiates the Q-cycle by donating its electron to the high potential chain of *b*-

8

cytochromes, similarly as in the conventional Q-cycle model, producing R1/Q with a single exponential rise. This reaction sequence would also account for a turnover of the Q-cycle upon a first flash given in the dark contrary to the traditional reaction scheme where a plastoquinol molecule, which needs a double turnover of PS II for its formation, serves as the electron donor of the cyt. b_6f complex.

Still, the relaxation time τ_1 describing the lag phase of R1/Q (Table 4-1) is generally a factor 2 - 3 larger than the relaxation time of R1/RC$_f$ found for *P. metallica* (Table 5-1). This has the consequence that in an unprejudiced fit analysis of e.g. the photocurrent of Fig. 4-2, now assuming a single-exponential rise of R1/Q and incorporating a fast component R1/RC$_f$, still leads to a relaxation time of about 17 ms for the incorporated R1/RC$_f$. Therefore, in the most general approach we should seriously consider that both the lag phase of R1/Q and R1/RC$_f$ co-exist in flash-induced photocurrents/-potentials and whether or not there exists a causal relationship needs to be verified. More refined experiments using a higher time response are needed for an improved identification of both components.

Reaction 1/Q
Patch-clamp recordings clearly showed a variable contribution of Reaction 1/Q in dark-adapted chloroplasts (Table 4-1). In contrast, such a pronounced slow secondary rise was absent in P515 recordings of dark-adapted *P. metallica* leaves which were infiltrated with standard isolation medium. A secondary phase with a much more retarded rise may, however, be observed (e.g. in Fig. 1-2A) although this slow phase undoubtedly is for the major part composed of the non-electrogenic component R2 (Ooms *et al.* 1989). The P515 response originates from millions of chloroplasts. Considering the variation in the Q/RC-ratio among individual *P. metallica* chloroplasts (Table 4-1) an average R1/Q substantially smaller than the pronounced high performance Q-cycle (e.g. in Fig. 4-1) would then be a logical consequence.

No attempts have been made to identify the true contribution of the Q-cycle to the slow secondary phase of P515 as in Ooms *et al.* (1989). Interestingly, it was observed that a distinct large secondary rise with a half-time of about 40 ms showed up when nigericin was present in the infiltration medium (cf. Fig. 7-5, see also Garab *et al.* 1987). If part of this secondary rise originates from Q-cycle activity this observation suggests that nigericin releases the dark (or dim measuring light) H$^+$/K$^+$ equilibrium which seemingly acts adversely on the electrogenic steps of the Q-cycle in the control. In a most straightforward view this is explained by photosynthetic control at the b_6f complex. Hence, the lumenal pH presumably attains a low enough value in chloroplasts of dark-adapted, or more correctly, adapted to dim measuring light, infiltrated *P. metallica* leaves which will decelerate the onset of the Q-cycle as was discussed for Fig. 4-5. Infiltration of leaves introduces a diffusion-limited gas exchange and concomitant depletion of electron acceptors like O$_2$ and CO$_2$ which will induce photosynthetic control (Harbinson *et al.* 1990, Harbinson and Foyer 1991, Heber and Walker 1992). Loss of the slow phase of the P515 signal was reported in CO$_2$-depleted barley leaves (Garab *et al.* 1983) and suggests that a shortage of electron acceptors is involved indeed. In addition, the stroma

phosphate potential and redox state, under conditions when the reactions of the Calvin-Benson cycle are impaired, could also favour ATP hydrolysis in the dark, thus acidifying the lumen leading to photosynthetic control.

Energisation-dependent suppression of photopotential(-current) amplitudes and changes in chloroplast conductances

A significant difference was found in the extent of the energisation-dependent suppression of the flash-induced electrical potential and the P515 amplitude (Fig. 6-2). Although the common reversible part of the amplitude suppression is well explained by a temporary decrease of charge separation, the slowly or non-reversible potential suppression observed with the patch-clamp method deserves closer attention. Pre-illumination was generally observed to be accompanied by a decrease in the seal conductance (g_{seal}) whose magnitude was more pronounced in the presence of nigericin, as for example in Fig. 7-7. The magnitude of reversible and non-reversible components as well as their respective relaxation kinetics showed substantial variations among different chloroplasts. Part of changes in g_{seal} likely resides in an increased access resistance R_A (see Chapter 7) which inevitably leads to an attenuation of the measured photopotential $V_P(t)$ according to eq. 3-12 of Chapter 3. The slowly or non-reversible conductance recovery after pre-illumination (Fig. 7-7) may therefore be responsible for the sustained suppression of the amplitude of the flash-induced photopotential which is not observed with the P515 method (Fig. 6-2).

Consequently, concerning the energisation-dependent decrease in charge separation, I would assign more weight to the results obtained with the P515 method and propose that about 50 % of PS II undergoes a reversible energisation-dependent alteration with a dark recovery relaxation time of 20 s. These altered PS II centers behave different with respect to charge separation and may belong to the class of dissipative centers.

A last point of consideration in patch-clamp experiments is the extent of the light-induced ΔpH. In conformity with the stimulating effect of valinomycin on light-induced proton uptake (Graan and Ort 1983) the increased field dissipation rate caused by the additional dissipative branch R_A plus R_L (Fig. 3-7) may result in a higher steady-state proton gradient in patch-clamped chloroplasts under identical light intensities. A higher proton gradient favours more futile charge recombination in PS II (Krieger *et al.* 1992, Rees *et al.* 1992). Therefore, the somewhat larger extent of the reversible suppression of the photopotential amplitude (Fig. 6-2) might additionally be explained by a somewhat higher steady-state ΔpH during the pre-illumination in patch-clamped chloroplasts.

8.3 Some reflections on the regulation of the Q-cycle in *Peperomia metallica*

I like here to discuss a possible regulation of the Q-cycle in dark-adapted *P. metallica* chloroplasts rationalising the occasionally observed high extent of R1/Q. The observed diversity in the extent of R1/Q upon a first flash given to dark-adapted chloroplasts

(Table 4-1) is most likely related to a variation in the fraction of cyt. b_6f complexes which have a reduced plastoquinol molecule bound at their Q_P-site. This b_6f fraction will decrease when the average redox state of the PQ-pool decreases. Hence, under oxidising conditions, normally considered the dark-adapted condition, no Q-cycle activity is expected on a first flash (Velthuys 1978, Girvin and Cramer 1984, Joliot and Joliot 1984) and R1/Q should be small as for example in the photocurrent upon the first flash of Fig. 4-4A or absent as in Fig. 7-1. The actual occurrence of R1/Q upon a first flash in a dark-adapted *P. metallica* chloroplast and in particular those with a relatively high extent as for example in Fig. 4-1 or 4-2, undoubtedly implies the existence in the dark of a (partially) reduced PQ-pool. A non-photochemical or dark reduction of the PQ-pool was concluded from the relaxation kinetics of chlorophyll fluorescence decay in several C_3, but particularly C_4 plants (Groom *et al.* 1993). The rate of dark reduction was slow, 30 s to 4 minutes (Groom *et al.* 1993), which would agree nicely with our observation that flashes given in short succession suppressed the high performance R1/Q while it took tens of seconds before full recovery of R1/Q on a first flash was seen in such photocurrents/-potentials.

The precise pathway of electron donation to the intersystem chain is as yet not well understood (Bendall and Manasse 1995). Direct electron donation is possible from reduced Fd to the PQ-pool catalysed by a putative ferredoxin plastoquinone reductase (FQR) or indirectly from NADPH to the PQ-pool involving Fd-dependent $NADP^+$ reduction (Bendall and Manasse 1995). Stromal metabolites like malate, thioredoxin and ascorbate in addition to Fd and NADPH are assumed to constitute a pool of reducing equivalents for PQ reduction in chloroplasts (Groom *et al.* 1993). The (light) history of individual *P. metallica* chloroplasts and the extent and rates of supply and depletion of the stromal pool of reducing equivalents are then proposed to give rise to the observed variation in R1/Q upon a first flash in the dark (Table 4-1) .

The genus *Peperomia* has species that may be C_3, show Crassulacean Acid Metabolism (CAM), or modifications of CAM (Ting *et al.* 1994). It should therefore be seriously considered that the succulent *P. metallica* may not be a complete C_3 species. The species *P. camptotricha* has both a spatial separation, between spongy mesophyll and palisade mesophyll (Nishio and Ting 1987), as well as a temporal separation, between young and mature leaves (Sipes and Ting 1985, Ting *et al.* 1993), of C_3 and C_4 metabolism. The shade type *P. scandens* showed CAM activity in mature leaves (Ting *et al.* 1994). In this context the tentative observation (not shown) that *P. metallica* chloroplasts isolated from full-grown leaves showed a larger fraction R1/Q than those from young leaves should be reappraised. The energy requirements of CAM with 5.5 to 6.5 ATP/2 NADPH per CO_2 fixed (Edwards and Walker 1983) is higher than of C_3 metabolism with 3 ATP/2 NADPH per CO_2 fixed and the surplus ATP could be supplied by additional proton pumping via Q-cycle turnover (Bendall and Manasse 1995). The decarboxylation of L-malate by NADP-malic enzyme consuming $NADP^+$ and producing NADPH and H^+ may additionally provide dark PQ-pool reduction via the couple NADPH/Fd and hence promote Q-cycle activity (Leegood *et al.* 1983, Edwards and Walker 1983). That L-malate was indeed able to stimulate the slow P515 phase was shown by Leegood *et al.* (1983) in

maize bundle sheet chloroplasts.

The cyt. b_6f complex is believed to play a pivotal role in state 1 - state 2 transitions, maximising the efficiency of linear electron transport (Knaff 1991, Anderson 1992). Both the stimulation of PS I light capture upon state 1 - state 2 transition and of Q-cycle activity occur upon over-reduction of the intersystem chain. This correlation confronts us with the compelling question: "Does the site where the putative FQR binds to the cyt. b_6f complex act as a common redox sensor for controlling Q-cycle turnover and linear electron flow?". Further experiments are needed to answer this fascinating point (see also Allen 1995).

8.4 pH-dependent energy dissipation in PS II

A principal dispute on pH-dependent energy dissipation in PS II focuses on the discrimination between antennae quenching and reaction center quenching and in particular which of the two dominates *in vivo*. Both types of quenching were proposed to occur in spinach thylakoids (Rees *et al.* 1992) and spinach chloroplasts (Mohanty and Yamamoto 1996).

The energisation-dependent potential suppression (Fig. 6-2) can only be a vestige of a reaction center type of quenching since this suppression sustained at saturating flash intensities (Fig. 6-3) when the involvement of antennae processes can be neglected. The fast relaxing component of non-photochemical quenching (Fig. 6-4), supposed to reflect the ΔpH-associated high energy-state quenching q_E (Krause *et al.* 1982, Walters and Horton 1991), is likely composed of both types of ΔpH-dependent quenching in *P. metallica* chloroplasts. Therefore, I like to propose that the dark relaxations of reaction center and antennae quenching proceed with different kinetics: the first with a relaxation time of about 20 s (Fig. 6-2) and the latter with a relaxation time of about 45 s (Fig. 6-4). Furthermore, the results suggests that for *P. metallica* chloroplasts reaction center quenching *in vivo*, i.e. infiltrated leaves, is certainly not insignificant.

The dark relaxation of the proton gradient has a relaxation time of about 5 s (Figs 6-1B and 6-6A) which is faster than the dark relaxation of both types of ΔpH-dependent quenching. Apparently, the relaxation of ΔpH-dependent quenching responds in a retarded fashion to ΔpH and, moreover, the responsiveness of reaction center quenching seems faster than of antennae quenching. This reasoning would agree with the proposition made by Mohanty and Yamamoto (1996) that reaction center quenching is related to a delocalised proton pool while antennae quenching is related to more localised protons inside the membrane. Such would be expected from the structure of PS II with its LHC II and minor antennae proteins located in the hydrophobic membrane while the 17, 24 and 33 kDa subunits of the PS II donor side are more exposed to the bulk aqueous lumen (cf. Fig. 1-3). The faster dark relaxation of reaction center quenching than of antennae quenching is then explained by a faster equilibration with the bulk pH of protons associated with the lumen-exposed pool than of the more distant protons partitioned inside the membrane, respectively. A limited availability of free Ca^{2+} in the

lumen was shown to be involved in the restoration of low-pH induced inactivation of PS II (Krieger and Weis 1993, Johnson *et al.* 1995) and may be an additional factor responsible for the different recovery kinetics of ΔpH and reaction center quenching.

Differences in expression of the two types of ΔpH-dependent quenching may very well depend on the extent of the light-established ΔpH (Rees *et al.* 1992), with an increasing contribution of reaction center quenching when the lumen pH falls below 5.5 (Crofts and Horton 1991, Krieger *et al.* 1992), and on the pool and availability of reductants like ascorbate in the lumen (Crofts and Horton 1991, Krieger *et al.* 1992, Mohanty and Yamamoto 1996). The fact that *P. metallica* chloroplasts attain a high amount of reaction center quenching might suggest that one or both of these factors are of importance for this succulent shade plant. The lumen ascorbate pool may be small or quickly exhausted by e.g. synthesis of zeaxanthin (Yamamoto 1985) or by ascorbate consumption when this reductant acts as an alternative donor to already low-pH inactivated PS II complexes. The rate of replenishing the lumen ascorbate pool is limited by the slow diffusion (15 - 20 minutes) of ascorbate across the chloroplast membrane (Foyer 1993) and, if present, by the Mehler-ascorbate peroxidase reaction (Neubauer and Yamamoto 1993).

8.5 Recommendations for future research

Following on-line conductance changes
A continuous recording of changes in the chloroplast conductance network would give a better definition of the whole-thylakoid configuration at any time during a patch-clamp experiment. Slow or sudden changes in the measuring configuration can then be foreseen and can be consolidated in an analysis of light-induced responses. On-line recording of the seal conductance in the domain of seconds may be realised in voltage-clamp by phase sensitive detection using a sine-wave input voltage of small amplitude (< 0.1 mV) and at a sufficiently low modulation frequency ($f < \tau_{CC}/2\pi$) to detect the seal conductance g_{seal} ($= 1/R_{seal}$) at a level I_{SS} corresponding to level V_{SS} in current-clamp (Fig. 3-3B). The appropriate frequency depends on the relaxation time τ_{CC} of a particular whole-thylakoid configuration. A more sophisticated, but probably more elaborate method would make use of a double sine-wave function of a low (< 1 Hz, level I_{SS} (V_{SS})) and a frequency near resonance ($\sim 1/\tau_{CC}$). The sophisticated method would allow an on-line decoding of the first order approximations of R_L, R_A and C_M (§ 3.2.3) corresponding to R_1, R_2 and C_1, respectively, of scheme Fig. 3-4.

The a priori unknown value of τ_M of a single chloroplast
The reliability of the patch-clamp method can be improved when the measured parameters are dependent, i.e. when the control response and the response after a treatment are measured on the same single chloroplast. A relative change in τ_M is expected to be similar for chloroplasts used with P515 and with the patch-clamp method. The true τ_M of a particular patch-clamped chloroplast may alternatively be found when

one of the model parameters (Fig. 3-7) can be varied while leaving other parameters constant. For example, a predictable change of the tip resistance might be realised through superfusion with electrolyte solution of varying KCl concentrations inside the pipette tip. A predictable change in the flash-induced thylakoid potential V_M, e.g. by knowing the fraction of inactive PS II centers, would also be a possibility.

Reaction 1/RC_f

A more precise identification of R1/RC_f is desirable. The possible involvement of PS II acceptor side reactions as suggested in § 5.6 may be investigated by measuring chlorophyll *a* fluorescence decay after a single-turnover flash (Crofts and Wraight 1983, Renger *et al.* 1995) and chlorophyll *a* fluorescence induction upon continuous illumination (Govindjee 1995).

Reaction 1/Q

To verify the proposed involvement of Q_p-site and Q_n-site reactions in R1/Q of photocurrents/-potentials (van Voorthuysen *et al.* 1996b, § 4.5) the effects of the Q_n-site inhibitors 2-*n*-heptyl-4-hydroxyquinoline *N*-oxide (HQNO) and 2-*n*-nonyl-4-hydroxyquinoline *N*-oxide (NQNO) are of interest (Jones and Whitmarsh 1988, Rich *et al.* 1991). In relation to the lag phase of R1/Q this will offer an improved understanding of a possible relation or interference with R1/RC_f.

The proposed stimulating effect of stromal reducing equivalents on Q-cycle turnover (§ 8.3) can be tested by: i) addition of dihydroxyacetone phosphate (DHAP) which supplies equimolar concentrations of NADPH and ATP in the stroma of intact chloroplasts and causes dark reduction of the PQ-pool (Mano *et al.* 1995); ii) addition of L-malate which would verify the presence of the C_4 metabolic route involving NADP-malic enzyme (Leegood *et al.* 1983); iii) addition of antimycin A which was shown to inhibit dark reduction of the PQ-pool by Fd involving cyt. b_{559}(Fd) (Miyake *et al.* 1995, Heber *et al.* 1995).

The access resistance R_A

A differentiation of the composite access resistance R_A (§ 3.5) into lateral and transversal thylakoid conductances may be achieved by specifically increasing the transmembrane component. This might be realised through superfusing the pipette solution poised with either the transmembrane channel former gramicidin (Schönknecht *et al.* 1990) or EDTA. The magnesium complexing EDTA was shown to remove the CF_1 part of the ATP synthase leaving a non-regulated proton conductance channel (Schönknecht *et al.* 1990). A complicating factor may be that EDTA also induces destacking because of the removal of Mg^{2+}.

Application of an improved measuring configuration regarding geometry of the patch-pipette and the electrical tightness of the glass/membrane interaction (low leak currents, 'giga-ohm seals') would certainly improve the patch-clamp method.

Absorption measurements around 530 nm related to light scattering have been associated with structural changes in the thylakoid membrane and energisation (Bilger *et*

al. 1988, Horton *et al.* 1991). Comparative measurements of energisation-dependent changes in light scattering and chloroplast conductances might add towards an understanding of the involvement of structural changes in R_A.

8.6 Conclusions

The patch-clamp method has proven to be a useful tool to study the energisation-dependent electrochemical properties of the thylakoid membrane. The relative ease of establishing a good electrical contact favours this method over impalement. Noteworthy variations in electrical parameters of single chloroplasts have been demonstrated which remain hidden for other methods that usually measure an average response coming from millions of chloroplasts. Preliminary experiments on patching the much smaller pea or spinach chloroplasts were successful and as these species have significant interests in photosynthesis research further exploration on these chloroplasts is recommended. The applicability of the patch-clamp method to study conductance changes in relation to changes in thylakoid structure and ionic composition deserves closer attention in the near future. The patch-clamp method is unique for measuring the kinetics of these dynamic structural changes.

Nederlandse samenvatting

Voor groei en ontwikkeling is energie nodig die de groene plant betrekt uit het zonlicht. De zonne-energie wordt uiteindelijk vastgelegd in de vorm van de suiker glucose maar initieel in de vorm van een elektrisch potentiaalverschil ($\Delta\psi$) en een proton gradiënt (ΔpH) over het thylakoïdmembraan. Dit proefschrift gaat over lichtgeïnduceerde elektrische spanningen en stromen in chloroplasten en wat deze ons kunnen vertellen over de regulatie van deze eerste processen van de fotosynthese.

Het transmembraan potentiaalverschil of thylakoïdspanning werd met twee methoden bepaald: (i) als een snelle absorptieverandering bij 518 nm, veroorzaakt door een electrochrome bandverschuiving van chlorofyl- en caroteenpigmenten in het thylakoïdmembraan, en (ii) met een gemodificeerde patch-clamp methode. De eerste methode geeft, wanneer de nodige correcties zijn aangebracht, een relatieve maat voor het elektrische veld in het thylakoïdmembraan. De tweede methode meet een potentiaalverschil welke evenredig maar niet gelijk is aan de werkelijke thylakoïdpotentiaal. Deze twee methoden werden aangevuld met metingen van de variabele chlorofyl *a* fluorescentie en P700 absorptieveranderingen. Als modelplanten deden dienst de schaduwplant peperomia (*Peperomia metallica* G.) en de zonlicht-aangepaste plant spinazie (*Spinacia oleracea* L.). Patch-clamp metingen werden uitsluitend verricht aan *P. metallica.*

Een belangrijk deel van dit proefschrift is ingeruimd voor de ontwikkeling van de patch-clamp methode (hoofdstuk 3). Hoewel in 1976 geïntroduceerd als electrofysiologische techniek voor het meten van afzonderlijke ionkanalen in biomembranen (Neher and Sakman 1976) werd in 1992 de patch-clamp techniek aangewend voor de bestudering van relatief grote lichtgeïnduceerde stromen als funktie van een aangelegde spanning in een enkele *P. metallica* chloroplast (Bulychev *et al.* 1992). De pipet-chloroplast configuratie waarbij lichtgeïnduceerde stromen optreden blijkt zich te gedragen volgens een eenvoudig RC-circuit met een bijbehorende relaxatietijd die afhangt van de eigenschappen van de chloroplast en van het membraan-glas contact. Een elektrisch schema wordt geïntroduceerd waarin de capaciteit en weerstand van het thylakoïdmembraan alsmede een nieuw geïntroduceerde toegangsweerstand zijn opgenomen. Deze toegangsweerstand wordt verondersteld informatie te bevatten over relatief lage elektrische geleidingsfasen in de chloroplast. De weerstanden en capaciteit van het RC-circuit worden berekend uit het spanningspatroon als gevolg van een geïnjecteerde stroompuls. Na kwantificatie van het RC-circuit kunnen de lichtgeïnduceerde signalen worden terugvertaald naar de spanningsveranderingen over het thylakoïdmembraan. De berekende thylakoïdspanning geïnduceerd op een enkele lichtflits blijkt dan ongeveer 40 mV te bedragen. De simultane meting van stroomgeïnduceerde en lichtgeïnduceerde spanningen biedt de mogelijkheid om veranderingen in elektrische geleiding in de chloroplast te onderscheiden van elektrogene processen.

Bij de studie naar secundair elektronentransport onderhouden door de zogenaamde Q-cyclus in *P. metallica* (hoofdstuk 4) wordt juist dit verschil tussen stroom- en lichtgeïnduceerde patronen het duidelijkst geïllustreerd. Na een snelle initiële stijging van de lichtopgewekte spanning of stroom, gerelateerd aan primaire ladingsscheiding in PS I

en II (component R1/RC), kan het flitsgeïnduceerde signaal een tweede langzame stijging vertonen die niet is terug te voeren op veranderingen in stroomgeleiding in het elektrische netwerk in de chloroplast. Deze langzame fase in de stroom- of spanningsrespons wordt daarom toegeschreven aan een elektrogene component (R1/Q). De remming van R1/Q door DBMIB wijst op een betrokkenheid van het cytochroom b_6f complex, algemeen beschreven door de Q-cyclus. De goede kinetische correlatie tussen de relaxatietijden gevonden uit de stroominjectie en uit het langzame verval (t > 200 ms) van het flitsgeïnduceerde elektrische signaal waarborgt een betrouwbare deconvolutie van het flitsgeïnduceerde signaal in R1/RC en R1/Q. De stijging van R1/Q is een weinig sigmoïdaal. Dit gedrag wordt verklaard door twee populaties van b_6f complexen te postuleren waarbinnen een eerste populatie de ladingsscheiding direct start terwijl bij een tweede populatie dit volgens een consecutief reaktieschema verloopt. De twee hierbij behorende relaxatietijden zijn gemiddeld 13 en 28 ms en weerspiegelen mogelijk de oxydatie van plastochinol en reductie van plastochinon aan de lumen- en stromazijde van het cytochroom b_6f complex, respectievelijk. De omvang van R1/Q genormeerd op die van R1/RC blijkt sterk te variëren tussen chloroplasten. Ook in donker geadapteerde chloroplasten treedt R1/Q op wat wijst op een donkerreductie van de plastochinon-pool. Een uitzonderlijk hoge omvang van R1/Q waarbij 2 ladingen worden gescheiden per turnover kan een aanwijzing zijn voor het optreden van een semichinon-cyclus mechanisme in *P. metallica*. De waarde 2 kan echter overschat zijn wanneer een gelijktijdige reductie van Q_A optreedt bij donkerreduktie van de plastochinon-pool of wanneer de ladingsscheidingstoestand zich in een omgeving met een relatief lage diëlektrische constante bevindt.

Een fraktie (R1/RC$_f$) van ongeveer 20 % van het P515 signaal blijkt slecht te worden gestabiliseerd in donkergeadapteerde spinazie chloroplasten en thylakoïden en is het gevolg van een snelle dissipatie van fotosysteem II-afhankelijke ladingsscheiding (hoofdstuk 5). In intacte bladeren van spinazie of peperomia is deze fraktie lager, ongeveer 5 - 15 %. De relaxatietijd van de snelle ladingsdissipatie is 1 - 3 ms. Een lage pH of afwezigheid van magnesium in het reaktiemedium bevorderen R1/RC$_f$ terwijl een effectieve drainage van elektronen aan de acceptorzijde van fotosysteem II door exogene elektronenacceptoren R1/RC$_f$ doen afnemen. Er wordt gesuggereerd dat goede ladingsstabilisatie van een door fotosysteem II veroorzaakte ladingsscheiding samenhangt met een efficiënte interactie tussen fotosysteem II en cytochroom b_6f in supercomplexen. Het optreden van R1/RC$_f$ zou dan wijzen op een fractie fotosysteem II waarbij deze interactie slechter is geworden. Een speculatieve reaktieroute voor de snelle dissipatie is ladingsrecombinatie tussen Q_B^- en P680$^+$ waarbij cytochroom b_{559} als mogelijke redox intermediair kan optreden.

Energetisatie leidt tot een vermindering van fotosysteem II-afhankelijke ladingsscheiding in *P. metallica* en *S. oleracea* die omkeerbaar is door donkeradaptatie (hoofdstuk 6). Een belichting van 2 minuten met een lichtintensiteit van 175 μmol m^{-2} s^{-1} inactiveert ongeveer 50 % van de fotosysteem II reactiecentra in *P. metallica* en deze fractie hersteld zich in de donkerperiode na voorbelichting met een relaxatietijd van ongeveer 20 s. Een vergelijkbare omkeerbare onderdrukking van de fotosysteem II

afhankelijke ladingsscheiding werd gevonden in spinaziethylakoïden geïncubeerd bij een lage pH < 5,5 of in aanwezigheid van een pH-gradiënt aangelegd door middel van ATP hydrolyse. Deze bevindingen vinden goede aansluiting bij het reaktiecentrum-dovingmodel van Weis and Berry (1987). In dit model leidt lumenverzuring tot een vertraging van de reductie van P680$^+$ als gevolg van een geïnactiveerd watersplitsingscomplex en bevordert aldus een toename van een snelle ladingsrecombinatie tussen Q^-_A en P680$^+$ waarmee excitatieënergie verloren gaat als warmte. In de algemene discussie (Hoofdstuk 8) wordt een model besproken waarin het vóórkomen en de omvang van reaktiecentrumdoving wordt gerelateerd aan de beschikbaarheid van ascorbaat en vrij calcium in het lumen. Meting van de niet-fotochemische chlorofylfluorescentiedoving, een maat voor energiedissipatie in de antenne en het reaktiecentrum van fotosysteem II, laat een trager donkerherstel zien met een relaxatietijd van 44 s terwijl de donkerrelaxatietijd van de pH-gradiënt slechts 5 s bedraagt. De kinetische inconsistentie tussen herstel van de onderdrukte ladings-scheiding, pH gradiënt en niet-fotochemische chlorofylfluorescentiedoving leidt tot het postulaat dat de donkerrelaxatie van antennedoving trager is dan van reaktiecentrum-doving. Een tragere evenwichtsinstelling met de protonen in het lumen tussen de membraan-gelocaliseerde protonen betrokken bij antennedoving in vergelijking met de meer gedelocaliseerde protonen rond het watersplitsingscomplex betrokken bij reaktiecentrumdoving zou hier debet aan zijn.

Hoofdstuk 7 belicht de lichtgeïnduceerde veranderingen in het elektrische geleidingsnetwerk van de chloroplast. Een korte lichtflits geeft een tijdelijke verlaging in de sealgeleiding met een minimum van 0,3 - 5 % rond 50 tot 200 ms na de flits en een traag herstel binnen 1 tot 10 s. De verlaging in sealgeleiding kon waarden van 50 % bereiken bij continue belichting. De verscheidenheid in omvang en kinetiek van de lichtgeïnduceerde geleidingsveranderingen was groot bij verschillende chloroplasten en gevoelig voor ionoforen. De aanwezigheid van valinomycine verminderde de geleidingsveranderingen terwijl toevoeging van nigericine een stimulatie te zien gaf. In een eenvoudige voorstelling worden de geleidingsveranderingen verklaard door depletie van ladingsdragers, voornamelijk K$^+$, in stroma of lumen. Ook lichtgeïnduceerde zwelling of krimping van thylakoïden kan een rol spelen. Het wordt verondersteld dat een belangrijk deel van de geleidingsveranderingen nauw samenhangt met geleidbaarheidsveranderingen, waar-schijnlijk in de nauwe tussenruimten van grana-thylakoïden.

Deze drieledige studie betreffende de regulatie van primaire ladingsscheiding in fotosysteem II, secundair ladingstransport van het cytochroom b_6f complex en veranderingen in de laterale elektrische geleiding van thylakoïden zoals boven geschetst toont duidelijk de kracht van de patch-clamp methode in de bestudering van de bio-energetica van de fotosynthese in intacte chloroplasten. Fotosysteem II blijkt het meest kwetsbaar bij energetisatie wat dit fotosysteem tot een eerste aangrijpingspunt voor regulatie van lineair elektronentransport maakt. Eveneens legt deze studie een grote variatie in diverse grootheden tussen chloroplasten aan de dag welke uit metingen aan chloroplastsuspensies niet of moeilijk aan het licht komen.

Appendix A   Error analysis of the whole-thylakoid configuration

A1: Systematic errors

Time-dependent drift of seal

To investigate the stability and reproducibility in time of the patch-clamp method the whole-thylakoid configuration of a chloroplast was monitored during a prolonged dark period. Figure A-1 shows the changes in the measured quantities $\{V_{SS}, \beta, \tau_{CC}, V_P\}$ and in the calculated model parameters $\{R_L, R_A, R_M, C_M, V_M\}$. Since this figure shows the results of 2 experiments only, it can merely give the tendency of the time-effect. An accurate calculation of the model parameters was possible for 1 experiment only (Fig. A-1B).

The results suggest that a minimum dark time of about 5 - 15 minutes is necessary for attaining a quasi-stable measuring configuration. The increase in seal resistance, reflected by the increasing V_{SS} level, is generally observed when patching chloroplasts. The largest relative change is seen for the access resistance R_A which is one of the principle causes for the decrease in photocurrent/potential amplitude. The increase in dark relaxation time τ_{CC} is most likely related to the resistance of the branch $(R_A + R_L)$ whilst no significant changes in membrane capacitance or membrane resistance can be found.
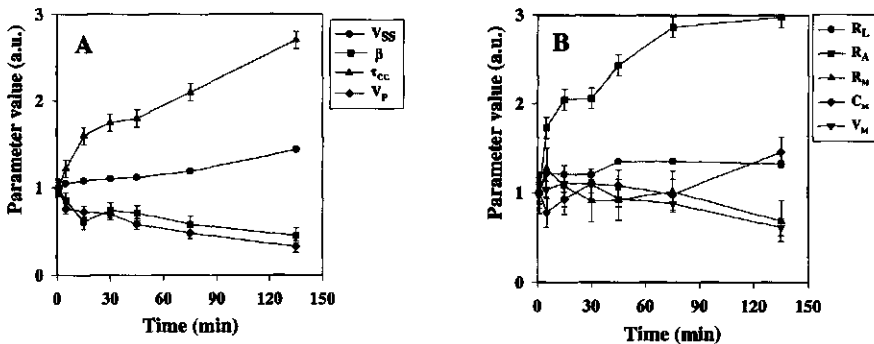
Fig. A-1   (A) Relative changes of V_{SS}, β, τ_{CC} and V_P (normalised on their value at the start of the experiment) during a prolonged dark-adaptation time. Average of $N = 2$ experiments. **(B)** Calculated change in the parameters describing the whole-thylakoid configuration during the same dark period. One experiment only. Standard errors, signifying experimental precision, of V_{SS} and R_L were less than the dimensions of the data symbols.

Polarisation: nonlinear current response

Employing large input currents with the current-injection technique introduces nonlinear effects which are caused by voltage-dependent alterations of the seal resistance. Part of these changes may be transient and part may be irreversible. It is therefore desirable to

133

work with low current amplitudes and with pulses of short duration but only to a level at which an adequate signal resolution is maintained. Figure A-2 shows the average result of V_{SS} determinations on 8 chloroplasts as a function of the input current I_{comm}. The pulse duration was set to 200 ms which was the most commonly used value in the experiments of this thesis. The potential V_{SS} was arbitrarily normalised on the value measured for $I_{comm} = +500$ pA, the input current routinely used, because the ideal value for the limiting case of $I_{comm} = 0$ pA could not unequivocally be determined (Fig. A-2). Apparently, the flow of large currents, both positive and negative, through the chloroplast network causes an increase in V_{SS}.
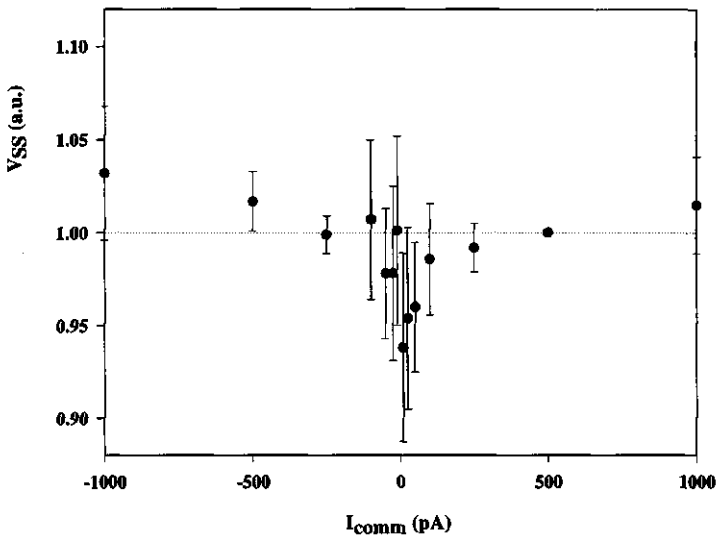
Fig. A-2   Test of linearity. Potential output V_{SS} upon current-injection by a square current pulse of 200 ms and variable amplitude I_{comm}. Average of 8 independent measurements on different chloroplasts. For every chloroplast V_{SS} was determined for all 2 x 7 different input currents starting with the lowest amplitude.

A2: Random errors

Any experimentally measured quantity (Q) is always an approximation of its true value with an uncertainty determined by the precision with which the quantity can be measured. The probability of measuring a certain value is assumed to be predicted by a Gaussian distribution function (Baird 1962, Squires 1968). The random error or standard deviation or precision E_Q of Q (Q ± E_Q) is then defined as the limits of a solution interval in which the probability of finding the true solution is 63 %.

To evaluate the random error in a final quantity of interest (e.g. R_A), which is a combination of measurements, the rule of combination of standard deviations was used (Baird 1962, Squires 1968). Any of the calculated quantities $\{R_T, R_1, R_2, C_1, R_L, R_A, R_M, C_M, A_{thyl}, V_M, Q, \text{ETCdens}\}$ was first explicitly expressed as a function of the measured quantities $\{V_T, V_{SS}, \beta, \tau_{CC}, \tau_M, I_{comm}\}$ according to the formula (3-1) through (3-12). The absolute random error in the calculated quantities $\{R_T, R_1, R_2, C_1, R_L, R_A, R_M, C_M, A_{thyl}, V_M, Q, \text{ETCdens}\}$ can then be expressed as (example given for R_A) (Baird 1962, Squires 1968):

$$E_{R_A}^2 = \left(\frac{\partial R_A}{\partial V_T}\right)^2 \cdot E_{V_T}^2 + \left(\frac{\partial R_A}{\partial V_{SS}}\right)^2 \cdot E_{V_{SS}}^2 + \left(\frac{\partial R_A}{\partial \beta}\right)^2 \cdot E_\beta^2 + \left(\frac{\partial R_A}{\partial \tau_{CC}}\right)^2 \cdot E_{\tau_{CC}}^2$$

$$(A-1)$$

$$+ \left(\frac{\partial R_A}{\partial \tau_M}\right)^2 \cdot E_{\tau_M}^2 + \left(\frac{\partial R_A}{\partial I_{comm}}\right)^2 \cdot E_{I_{comm}}^2$$

The relative random error in the calculated resistance R_A is then found by dividing equation A-1 by R_A,

Table A-1 Sensitivity coefficients used for estimation of relative error.

S(A,B) B→ A ↓	ΔV_T	ΔV_{SS}	$\Delta\beta$	$\Delta\tau_{CC}$	$\Delta\tau_M$	ΔI_{comm}
ΔR_T	1.00	-	-	-	-	-1.00
ΔR_L	-0.85	1.82	0.02	0.03	-0.03	-1.00
ΔR_A	-1.79	3.85	-1.06	-0.27	0.27	-1.00
ΔR_M	-1.69	3.64	-0.95	-1.55	1.55	-1.00
ΔC_M	1.69	-3.64	0.95	1.55	-0.55	1.00
ΔA_{thyl}	1.69	-3.64	0.95	1.55	-0.55	1.00
ΔV_M	-0.85	1.82	-0.98	-0.27	0.27	-
ΔQ	0.85	-1.82	-0.02	1.27	-0.27	1.00
ETCdens	-0.85	1.82	-0.98	-0.27	0.27	-

Coefficients $S(A,B)$ were calculated for the numerical example of § 3.3. A 1 % change in a measured quantity B results in a $S(A,B)$ % change in the calculated quantity A.

$$\left(\frac{E_{R_A}}{R_A}\right)^2 = \left(\frac{\partial R_A}{\partial V_T} \cdot \frac{V_T}{R_A}\right)^2 \cdot \left(\frac{E_{V_T}}{V_T}\right)^2 + \left(\frac{\partial R_A}{\partial V_{SS}} \cdot \frac{V_{SS}}{R_A}\right)^2 \cdot \left(\frac{E_{V_{SS}}}{V_{SS}}\right)^2 + \cdots$$

$$= S^2(R_A, V_T) \cdot \left(\frac{E_{V_T}}{V_T}\right)^2 + S^2(R_A, V_{SS}) \cdot \left(\frac{E_{V_{SS}}}{V_{SS}}\right)^2 + \cdots \qquad (A\text{-}2)$$

The sensitivity coefficient S thus introduced describes how much a calculated quantity changes relatively upon a relative change of an input measured quantity. For example, $S(R_A, V_T)$ gives the percentage change of R_A when V_T changes by 1 %. In table (A-1) all sensitivity coefficients are given based on the numerical example of § 3.3. This shows for instance that a change of +1.00 % in τ_{CC} introduces a change of -0.27 % in V_M.

Appendix B   The analytical solutions of a consecutive reaction scheme

In this appendix the analytical solution for the number of charges Q(t) displaced by cyt. *b₆f* turnover is derived using a kinetic model. Figure 4-6 of Chapter 4 shows two reaction sequences describing transient states A1, B1, etc. of the cyt. *b₆f* complex. A fraction A1 of *b₆f* complexes produces a charge separated state Q1 according to the consecutive reaction sequence 1 which involves two steps characterised by two rate constants k_1 and k_2. In a remaining fraction A2 a charge separated state Q2 is produced with a rate constant k_1. Subsequently, the electrogenic products Q1 and Q2 will be dissipated with a field dissipation rate constant (k_D) given by $1/\tau_D$, the same rate constant as was found upon current-injection.

The concentrations of the reactants A1, B1 and of the electrogenic product Q1 of the two-step reaction sequence 1 change in time according to,

$$\frac{dA1}{dt} = -k_1 \cdot A1 \tag{B1}$$

$$\frac{dB1}{dt} = k_1 \cdot A1 - k_2 \cdot B1 \tag{B2}$$

$$\frac{dQ1}{dt} = k_2 \cdot B1 - k_D \cdot Q1 \tag{B3}$$

with t the time. It is assumed that k_1, k_2 and k_D are independent of Q1 and Q2. These three differential equations were solved sequentially with initial conditions given by $A1(t = 0) = A1_0$, $B1(t = 0) = 0$ and $Q1(t = 0) = 0$ and the solution for Q1(t) results in a 3-exponential function,

$$Q1(t) = \alpha1 \cdot e^{-k_1 \cdot t} + \beta1 \cdot e^{-k_2 \cdot t} + \gamma1 \cdot e^{-k_D \cdot t} \tag{B4}$$

The coefficients $\alpha1$, $\beta1$ and $\gamma1$ are functions of the rate constants k_1, k_2 and k_D and of $A1_0$. In a similar way the solution for Q2(t) can be obtained as,

$$Q2(t) = \alpha2 \cdot e^{-k_1 \cdot t} + \gamma2 \cdot e^{-k_D \cdot t} \tag{B5}$$

The final fit-function was constructed out of Q1 and Q2 according to,

$$Q(t) = Q1(t) + Q2(t)$$

which results in the general expression,

$$Q(t) = \alpha \cdot e^{-k_1 \cdot t} + \beta \cdot e^{-k_2 \cdot t} + \gamma \cdot e^{-k_D \cdot t} \tag{B6}$$

Note that α, β and γ are functions of the four unknown variables $A1_0$, $A2_0$, k_1 and k_2 (k_D is taken from current-injection). Accordingly, equation B6 was fitted to the data of $R1/Q$ using the Marquardt-Levenberg algorithm (as implemented in SigmaPlot 2.01 for Windows) for finding the optimal solutions of the four variables $A1_0$, $A2_0$, k_1 and k_2.

List of publications

Papers

Voorthuysen, T. van, J.H.A. Dassen, J.F.H. Snel and W.J. Vredenberg (1995). Temporary suppression of the electrical potential across the thylakoid membrane upon energization. Physiol. Plant. 94: 729-735.

Voorthuysen, T. van, Bulychev, A.A., Dassen, J.H.A., Snel, J.F.H. and Vredenberg, W.J. (1996). Suppression of Photosystem II-dependent electrogenesis caused by proton pumping in chloroplasts. Physiol. Plant. 98: 156-164.

Voorthuysen, T. van, Dassen, J.H.A., Snel, J.F.H. and Vredenberg, W.J. (1996). Patch-clamp study on flash-induced secondary electrogenic transport in the thylakoid membrane. Interpretation in terms of a Q-cycle. Biochim. Biophys. Acta. 1277(3): 226-236.

Voorthuysen, T. van, Bulychev, A.A., Snel, J.F.H., Dassen, J.H.A. and Vredenberg, W.J. (1997). Flash-induced conductance changes in chloroplast thylakoid lamellae. A patch-clamp study. Bioelectrochem. Bioenerg., in press.

Vredenberg, W.J., Bulychev, A.A., Dassen, J.H.A., Snel, J.F.H. and T. van Voorthuysen (1995). A patch clamp method for determining single turnover charge separations in the chloroplast membrane. Biochim. Biophys. Acta 1230: 77-80.

Bulychev, A.A., van Voorthuysen, T. and Vredenberg, W.J. (1996). Transmembrane movements of artificial redox mediators in relation to electron transport and ionic currents in chloroplasts. Physiol. Plant. 98: 605-611.

Abstracts

Vredenberg, W.J., Snel, J.F.H., Dassen, J.H.A. and Voorthuysen, T. van (1992). Electrogenesis and energy regulation in the photosynthetic membrane. *In* Research in Photosynthesis. Proc. IXth International Congress on Photosynthesis, Nagoya, Japan. Vol. II, pp. 681-684.

Voorthuysen, T. van, J.H.A. Dassen, J.F.H. Snel and W.J. Vredenberg. A patch-clamp study on the regulation of electrogenesis by protons (1995). *In* Photosynthesis: from Light to Biosphere, Proc. Xth International Photosynthesis Congress, Montpellier, France. Vol III, pp. 79-82. ISBN 0-7923-3859-6.

References

Admon A, Y Shahak and M Avron (1982). Adenosine triphosphate-generated transmembrane electric potential in chloroplasts. Biochim Biophys Acta 681: 405-411.

Albertsson P- Å (1995). The structure and function of the chloroplast photosynthetic membrane - a model for the domain organization. Photosynth Res 46: 141-149.

Allen JF (1992). Protein phosphorylation in regulation of photosynthesis. Biochim Biophys Acta 1098: 275-335.

Allen JF (1995). Thylakoid protein phosphorylation, state 1-state 2 transitions, and photosystem stoichiometry adjustment: redox control at multiple levels of gene expression. Physiol Plant 93: 196-205.

Allnutt FCT, R Ewy, M Renganathan, RS Pan and RA Dilley (1991). Nigericin and hexylamine effects on localized proton gradients in thylakoids. Biochim Biophys Acta 1059: 28-36.

Anderson JM, WS Chow and DJ Goodchild (1988). Thylakoid membrane organization in sun/shade acclimation. Aust J Plant Physiol 15: 11-26.

Anderson JM (1992). Cytochrome b_6f complex: dynamic molecular organization, function and acclimation. Photosynth Res 34: 341-357.

Andréasson L-A, I Vass and S Styring (1995). Ca^{2+} depletion modifies the electron transfer on both donor and acceptor sides in photosystem II from spinach. Biochim Biophys Acta 1230: 155-164.

Arnold W and J Azzi (1971). The mechanism of delayed light production by photosynthetic organisms and a new effect of electric fields on chloroplasts. Photochem Photobiol 14: 233-240.

Baird DC (1964). Experimentation: an introduction to measurement theory and experiment design. Englewood Cliffs.

Barber J (1980). Membrane surface charges and potentials in relation to photosynthesis. Biochim Biophys Acta 594: 253-308.

Barber J (1982). Influence of surface charges on thylakoid structure and function. Ann Rev Plant Physiol 33: 261-295.

Becker JF, NE Geacintov and CE Swenberg (1978). Photovoltages in suspensions of magnetically oriented chloroplasts. Biochim Biophys Acta 503: 545-554.

Bendall DS (1982). Photosynthetic cytochromes of oxygenic organisms. Biochim Biophys Acta 683: 119-151.

Bendall DS and RS Manasse (1995). Cyclic photophosphorylation and electron transport. Biochim Biophys Acta 1229: 23-38.

Benyoucef M, JL Rigaud and CM Gary-Bobo (1978). Anion diffusion selectivity in pore model. The phosphatidylcholine-water lamellar phase. Biochim Biophys Acta 507: 219-229.

Bilger W, U Heber and U Schreiber (1988). Kinetic relationship between energy-dependent fluorescence quenching, light scattering, chlorophyll luminescence and proton pumping in intact leaves. Z Naturforsch 43c: 877-887.

Boekema EJ, JP Dekker, MG Van Heel, M Rögner, W Saenger, I Witt and HT Witt. (1987). Evidence for a trimeric organization of the photosystem I complex from the thermophyllic cyanobacterium *Synechococcus* sp. FEBS Lett 217: 283-286.

Boekema EJ, P Fromme and P Gräber (1988). On the structure of the ATP-synthase from chloroplasts. Ber Bunsenges Phys Chem 92: 1031-1036.

Boekema EJ, B Hankamer, D Bald, J Kruip, J Nield, AF Boonstra, J Barber and M Rögner (1995). Supramolecular structure of the photosystem II complex from green plants and cyanobacteria. Proc Natl Acad Sci USA 92: 175-179.

Bouges-Bocquet B (1981). Factors regulating the slow electrogenic phase in green algae and higher plants. Biochim Biophys Acta 635: 327-340.

Boussac A, P Sétif and AW Rutherford (1992). Inhibition of tyrosine Z photooxidation after formation of the S_3 state in Ca^{2+}-depleted and Cl^--depleted photosystem II. Biochem 31: 1224-1234.

Boxer SG (1993). Photosynthetic reaction center spectroscopy and electron transfer dynamics in applied electric fields. *In* The photosynthetic reaction center (J. Deisenhofer and J. R. Norris, eds), Vol. II, pp. 179-220. ISBN 0-12-208662-7.

Braun G, ARJ Driesenaar, E Shalgi and S Malkin (1992). Manipulation of the imbalance for linear electron flow activities between photosystems I and II of photosynthesis by cyclic electron flow cofactors.

141

Biochim Biophys Acta 1099: 57-66.

Briantais J-M, C Vernotte, J Olive and F-A Wollman (1984). Kinetics of cation-induced changes of photosystem II fluorescence and of lateral distribution of the two photosystems in the thylakoid membranes of pea chloroplasts. Biochim Biophys Acta 766: 1-8.

Bruinsma J (1963). The quantitative analysis of chlorophylls a and b in plant extracts. Photochem Photobiol 2: 241-249.

Bulychev AA, VK Andrianov, GA Kurella and FF Litvin (1971). Transmembrane potential of the cell and chloroplast in higher terrestrial plants. Soviet Plant Physiol 18: 204-210.

Bulychev AA, VK Andrianov, GA Kurella and FF Litvin (1972). Micro-electrode measurements of the transmembrane potential of chloroplasts and its photoinduced changes. Nature 236: 175-177.

Bulychev AA and WJ Vredenberg (1976a). The effect of cations and membrane permeability modifying agents on the dark kinetics of the photoelectric response in isolated chloroplasts. Biochim Biophys Acta 423: 548-556.

Bulychev AA and WJ Vredenberg (1976b). Effect of ionophores A23187 and nigericin on the light-induced redistribution of Mg^{2+}, K^+ and H^+ across the thylakoid membrane. Biochim Biophys Acta 449: 48-58.

Bulychev AA, VK Andrianov, GA Kurella and FF Litvin (1976). Photoinduction kinetics of electrical potential in a single chloroplast as studied with micro-electrode technique. Biochim Biophys Acta 420: 336-351.

Bulychev AA, VK Andrianov and GA Kurella (1980). Effect of dicyclohexylcarbodiimide on the proton conductance of thylakoid membranes in intact chloroplast. Biochim Biophys Acta 590: 300-308.

Bulychev AA (1984). Different kinetics of membrane potential formation in dark-adapted and preilluminated chloroplasts. Biochim Biophys Acta 766: 747-652.

Bulychev AA, MM Niyazova and VB Turovetsky (1986). Electro-induced changes of chlorophyll fluorescence in individual intact chloroplasts. Biochim Biophys Acta 850: 218-225.

Bulychev AA, VF Antonov and EV Schevchenko (1992). Patch-clamp studies of light-induced currents across the thylakoid membrane of isolated chloroplasts. Biochim Biophys Acta 1099: 16-24.

Bulychev AA, ES Cymbalyuk and EP Lukashev (1994). Use of irreversible electroporation and osmotic effects to prove photoinduced accumulation of methylphenazonium cations in the internal volume of thylakoids. Biol Mem 7(6): 567-578.

Bulychev AA, T van Voorthuysen and WJ Vredenberg (1996). Transmembrane movements of artificial redox mediators in relation to electron transport and ionic currents in chloroplasts. Physiol Plant 98: 605-611.

Byrd H, EP Suponeva, AB Bocarsly and ME Thompson (1996). Photocurrent generation in metal bisphosphonate multilayer thin films. Nature 380: 610-612.

Calvin M (1962). The path of carbon in photosynthesis. Science 135: 879-889.

Chain RK and R Malkin (1995). Functional activities of monomeric and dimeric forms of the chloroplast cytochrome b_6f complex. Photosynth Res 46: 419-426.

Chitnis PR, Q Xu, VP Chitnis and R Nechushtai (1995). Function and organisation of photosystem I polypeptides. Photosynth Res 44: 23-40.

Chylla RA, G Garab and J Whitmarsh (1987). Evidence for slow turnover in a fraction of photosystem II complexes in thylakoid membranes. Biochim Biophys Acta 894: 562-571.

Chylla RA and J Whitmarsh (1989). Inactive photosystem II complexes in leaves. Turnover rate and quantification. Plant Physiol 90: 765-772.

Chylla RA and J Whitmarsh (1990). Light saturation response of inactive photosystem II reaction centers in spinach. Photosynth Res 25: 39-48.

Corda D, C Pasternak and M Shinitzky (1982). Increase in lipid microviscosity of unilamellar vesicles upon the creation of transmembrane potential. J Membr Biol 65: 235-242.

Cramer WA and J Whitmarsh (1977). Photosynthetic cytochromes. Ann Rev Plant Physiol 28: 133-172.

Cramer WA, PN Furbacher, A Szczepaniak and G-S Tae (1991). Electron transport between photosystem II and photosystem I. Current Topics in Bioenergetics 16: 179-222.

Cramer WA, RM Everly, PN Furbacher, D Huang, G-S Tae, A Szczepaniak, DA Cherepanov and LI Krishtalik (1992). Structure-function-assembly of the cytochrome complexes in oxygenic photosynthesis. -*In* Research in Photosynthesis (N. Murata, ed.), Vol. II, pp. 447-454. Kluwer Academic

Publishers, Dordrecht, The Netherlands.

Cramer WA, G-S Tae, PN Furbacher and M Böttger (1993). The enigmatic cytochrome *b*-559 of oxygenic photosynthesis. Physiol Plant 88: 705-711.

Cramer WA, GM Soriano, M Ponomarev, D Huang, H Zhang, SE Martinez and JL Smith (1996). Some new structural aspects and old controversies concerning the cytochrome *b₆f* complex of oxygenic photosynthesis. Annu Rev Plant Physiol Plant Mol Biol 47: 477-508.

Crimi M, V Fregni, A Altimari and BA Melandri (1995). Unreliability of carotenoid electrochromism for the measure of electrical potential differences induced by ATP hydrolysis in bacterial chromatophores. FEBS Lett 367: 167-172.

Crofts J and P Horton (1991). Dissipation of excitation energy by photosystem II particles at low pH. Biochim Biophys Acta 1058: 187-193.

Crofts AR and CA Wraight (1983). The electrochemical domain of photosynthesis. Biochim Biophys Acta 726: 149-185.

Crofts AR and CT Yerkes (1994). A molecular mechanism for q_E-quenching. FEBS Lett 352: 265-270.

Dau H and K Sauer (1992). Electric field effect on the picosecond fluorescence of photosystem II and its relation to the energetics and kinetics of primar charge separation. Biochim Biophys Acta 1102: 91-106.

Dau H (1994). Molecular mechanisms and quantitative models of variable photosystem II fluorescence. Photochem Photobiol 60(1): 1-23.

Davenport JW and RE McCarty (1984). An analysis of proton fluxes coupled to electron transport and ATP synthesis in chloroplast thylakoids. Biochim Biophys Acta 766: 363-374.

Debus RJ, BA Barry, I Sithole, GT Babcock and L McIntosh (1988). Directed mutagenesis indicates that the donor to P680⁺ in photosystem II is tyrosine-161 of the D1 polypeptide. Biochem 27: 9071-9074.

De Grooth BG and J Amesz (1977). Electrochromic absorbance changes of photosynthetic pigments in *Rhodopseudomonas sphaeroides*. II. Analysis of the band shifts of carotenoid and bacteriochlorophyll. Biochim Biophys Acta 462: 247-258.

De Las Rivas J, J Klein and J Barber (1995). pH sensitivity of the redox state of cytochrome *b*559 may regulate its function as a protectant against donor and acceptor side photoinhibition. Photosynth Res 46: 193-202.

Demmig B, K Winter, A Krüger and F-C Czygan (1987). Photoinhibition and zeaxanthin formation in intact leaves. Plant Physiol 84: 218-224.

Demmig-Adams B (1990). Carotenoids and photoprotection in plants: a role for the xanthophyll zeaxanthin. Biochim Biophys Acta 1020:1-24.

Demmig-Adams B and WW Adams (1996). The role of xanthophyll cycle carotenoids in the protection of photosynthesis. Trends Plant Sci 1(1): 21-26.

Dennenberg RJ, PA Jursinic and SA McCarthy (1986). Intactness of the oxygen-evolving system in thylakoids and photosystem II particles. Biochim Biophys Acta 852: 222-233.

Dilley RA and A Rothstein (1967). Chloroplast membrane characteristics. Biochim Biophys Acta 135: 427-443.

Diner BA (1977). Dependence of the deactivation reactions of photosystem II on the redox state of plastoquinone pool A varied under anaerobic conditions. Biochim Biophys Acta 460: 247-258.

Dracheva SM, LA Drachev, AA Konstantinov, AYu Semenov, VP Skulachev, AM Arutjunjan, VA Shuvalov and SM Zaberezhnaya (1988). Electrogenic steps in the redox reactions catalyzed by photosynthetic reaction-centre complex from *Rhodopseudomonas viridis*. Eur J Biochem 171: 253-264.

Dreyfuss BW and JP Thornber (1994). Organization of the light-harvesting complex of photosystem I and its assembly during plastid development. Plant Physiol 106: 841-848.

Eckert HJ and G Renger (1980). Photochemistry of the reaction centers of system II under repetitive flash group excitation in isolated chloroplasts. Photochem Photobiol 31: 501-511.

Edwards G and D Walker (1983). C_3, C_4: mechansims, and cellular and environmental regulation, of photosynthesis. Blackwell Scientific Publications, London. Chapter 15. ISBN 0-632-00757-5.

Ehrenheim AM, G Finazzi and G Forti (1994). Inhibition of photosystem II activity by proton gradient. Biochim Biophys Acta 1185: 279-283.

Evans MCW and HA Nugent (1993). Structure and function of the reaction center cofactors in oxygenic organisms. -*In* The Photosynthetic Reaction Center (J Deisenhofer and JR Norris, ed), Vol. I, pp. 391-

References

415, Academic Press, San Diego. ISBN 0-12-208661-9.

Farineau J, Gy Garab, G Horváth and Á Faludi-Dániel (1980). Proton translocation in the slow rise of the flash-induced 515 nm absorbance change of intact chloroplasts. FEBS Lett 118(1): 119-122.

Fernández-Velasco JG, DA Berthold and R Malkin (1995). The mechanism of cyt b_6 photooxidation in *Chlamydomonas reinhardtii* - The possibility of a semiquinone cycle. *-In* Photosynthesis: from Light to Biosphere (P. Mathis, ed.) Vol II, pp. 555-558. Kluwer Academic Publishers. ISBN 0-7923-3858-8.

Forti G and G Elli (1995). The function of ascorbic acid in photosynthetic phosphorylation. Plant Physiol 109: 1207-1211.

Fowler CF and B Kok (1974). Direct observation of a light-induced electric field in chloroplasts. Biochim Biophys Acta 357: 308-318.

Foyer C, J Rowell and D Walker (1983). Measurement of the ascorbate content of spinach leaf protoplasts and chloroplasts during illumination. Planta 157: 239-244.

Foyer C, R Furbank, J Harbinson and P Horton (1990). The mechanisms contributing to photosynthetic control of electron transport by carbon assimilation in leaves. Photosynth Res 25: 83-100.

Foyer C (1993). Ascorbic acid. *-In* Antioxidants in Higher Plants (R Alscher and JL Hess, eds), CRC Press, Boca Raton, pp. 31-58.

Furbacher PN, ME Girvin and WA Cramer (1989). On the question of interheme electron transfer in the chloroplast cytochrome b_6 in situ. Biochem 28: 8990-8998.

Furbank RT, CLD Jenkins and MD Hatch (1990). C_4 photosynthesis: quantum requirement, C_4 acid overcycling and Q-cycle involvement. Aust J Plant Physiol 17: 1-7.

Garab Gy, AA Sanchez Burgos, L Zimányi and Á Faludi-Dániel (1983). Effect of CO_2 on the energization of thylakoids in leaves of higher plants. FEBS Lett 154(2): 323-327.

Garab Gy, J Farineau and G Hervo (1987). Dependence of energization of thylakoids on frequency of exciting flashes in intact chloroplasts. Photosynth Res 11: 15-27.

Genty B, J Harbinson, J-M Briantais and NR Baker (1990). The relationship between non-photochemical quenching of chlorophyll fluorescence and the rate of photosystem 2 photochemistry in leaves. Photosynth Res 25: 249-257.

Gerst U, G Schönknecht and U Heber (1994). ATP and NADPH as the driving force of carbon reduction in leaves in relation to thylakoid energization by light. Planta 193: 421-429.

Girvin ME and WA Cramer (1984). A redox study of the electron transport pathway resposible for generation of the slow electrochromic phase in chloroplasts. Biochim Biophys Acta 767: 29-38.

Golbeck JH and B Kok (1979). Redox titration of electron acceptor Q and the plastoquinone pool in photosystem II. Biochim Biophys Acta 547: 347-360.

Golbeck JH (1992). Structure and function of photosystem I. Annu Rev Plant Physiol Plant Mol Biol 43: 293-324.

Goldman DE (1943). *Potential, impedance, and rectification in membranes.* J Gen Physiol 27: 37-60.

Gorkom HJ van (1985). Electron transfer in photosystem II. Photosynth Res 6: 97-112.

Goss R, M Richter and A Wild (1995). Role of ΔpH in the mechanism of zeaxanthin-dependent amplification of q_E. J Photochem Photobiol 27: 147-152.

Govindjee (1990). Photosystem II heterogeneity: the acceptor side. Photosynth Res 25: 151-160.

Govindjee and JJS van Rensen (1993). Photosystem II reaction center and bicarbonate. *-In* The Photosynthetic Reaction Center (J Deisenhofer and JR Norris, eds), Academic Press, San Diego. Vol. I, pp. 357-389. ISBN 0-12-208661-9.

Govindjee (1995). Sixty-three years since Kautsky: chlorophyll *a* fluorescence. Aust J Plant Physiol 22: 131-160.

Graan T and DR Ort (1983). Initial events in the regulation of electron transfer in chloroplasts. The role of the membrane potential. J Biol Chem 258(5): 2831-2836.

Gräber P, E Schlodder and HT Witt (1977). Conformational change of the chloroplast ATPase induced by a transmembrane electric field and its correlation to phosphorylation. Biochim Biophys Acta 461: 426-440.

Groom QJ, DM Kramer, AR Crofts and DR Ort (1993). The non-photochemical reduction of plastoquinone in leaves. Photosynth Res 36: 205-215.

Groth G and W Junge (1995). ATP synthase: activating versus catalytic proton transfer. FEBS Lett 358(2): 142-144.

References

Gutman M, E Nachliel and S Kiryati (1992). Dynamic studies of proton diffusion in mesoscopic heterogeneous matrix. II. The interlayer space between phospholipid membranes. Biophys J 63: 281-290.

Gutman M and E Nachliel (1995). The dynamics of proton exchange between bulk and surface groups. Biochim Biophys Acta 1231: 123-138.

Haehnel W, A Pröpper and H Krause (1980). Evidence for complexed plastocyanin as the immediate electron donor to P-700. Biochim Biophys Acta 593: 384-399.

Haehnel W (1984). Photosynthetic electron transport in higher plants. Ann Rev Plant Physiol 35: 659-693.

Haraux F and Y de Kouchkovsky (1983). The energy-transduction theories: a microchemiosmotic approach in thylakoids. Physiol Vég 21(3): 563-576.

Harbinson J and CL Hedley (1989). The kinetics of P-700$^+$ reduction in leaves: a novel *in situ* probe of thylakoid functioning. Plant Cell Environ 12: 357-369.

Harbinson J, B Genty and CH Foyer (1990). Relationship between photosynthetic electron transport and stromal enzyme activity in pea leaves. Towards an understanding of the nature of photosynthetic control. Plant Physiol 94: 545-553.

Harbinson J and CH Foyer (1991). Relationships between the efficiencies of photosystems I and II and stromal redox state in CO_2-free air. Evidence for cyclic electron flow in vitro. Plant Physiol 97: 41-49.

Hauska G, S Reimer and A Trebst (1974). Native and artificial energy-conserving sites in cyclic photophosphorylation systems. Biochim Biophys Acta 357: 1-13.

Heber U and KA Santarius (1970). Direct and indirect transfer of ATP and ADP across the chloroplast envelope. Z. Naturforsch 25b: 718-728.

Heber U, H Egneus, U Hanck, M Jensen and S Köster (1978). Regulation of photosynthetic electron transport and photophosphorylation in intact chloroplasts and leaves of *Spinacia oleracea* L. Planta 143: 41-49.

Heber U and D Walker (1992). Concerning a dual function of coupled cyclic electron transport in leaves. Plant Physiol 100: 1621-1626.

Heber U, NG Bukhov, S Neimanis and Y Kobayashi (1995). Maximum $H^+/h\nu_{PSI}$ stoichiometry of proton transport during cyclic electron flow in intact chloroplasts is at least two, but probably higher than two. Plant Cell Physiol 36(8): 1639-1647.

Hecks B, K Wulf, J Breton, W Leibl and H-W Trissl (1994). Primary charge separation in photosystem I: A two-step electrogenic charge separation connected with $P700^+A_0^-$ and $P700^+A_1^-$ formation. Biochem 33(29): 8619-8624.

Hemelrijk PW and van Gorkom HJ (1996). Size-distributions of antenna and acceptor-pool of photosystem II. Biochim Biophys Acta 1274: 31-38.

Holzwarth AR, G Schatz, H Brock and E Bittersmann (1993). Energy transfer and charge separation kinetics in photosystem I. Part 1: picosecond transient absorption and fluorescence study of cyanobacterial photosystem I particles. Biophys J 64: 1813-1826.

Holzenburg A, MC Bewley, FH Wilson, WV Nicholson and RC Ford (1993). Three-dimensional structure of photosystem II. Nature 363: 470-472.

Holzenburg A, FH Shepherd and RC Ford (1994). Localization of the oxygen-evolving complex of photosystem II by fourier difference analysis. Micron 25: 447-451.

Höök F and P Brzezinski (1994). Light-induced voltage changes associated with electron and proton transfer in photosystem II core complexes reconstituted in phospholipid monolayers. Biophys J 66: 2066-2072.

Hope AB and DB Matthews (1987). The slow phase of the electrochromic shift in relation to the Q-cycle in thylakoids. Aust J Plant Physiol 14: 29-46.

Hope AB and PR Rich (1989). Proton uptake by the chloroplast cytochrome *bf* complex. Biochim Biophys Acta 975: 96-103.

Hope AB, RR Huilgol, M Panizza, M Thompson and DB Matthews (1992). The flash-induced turnover of cytochrome *b*-563, cytochrome *f* and plastocyanin in chloroplasts. Models and estimation of kinetic parameters. Biochim Biophys Acta 1100: 15-26.

Hope AB (1993). The chloroplast cytochrome *bf* complex: a critical focus on function. Biochim Biophys Acta 1143: 1-22.

Horton P and WA Cramer (1975). Acid-base induced redox changes of the chloroplast cytochrome b-559. FEBS Lett 56(2): 244-247.

145

References

Horton P, J Crofts, S Cordon, K Oxborough, D Rees and JD Scholes (1989). Regulation of photosystem II by metabolic and environmental factors. Phil Trans R Soc Lond B 323: 269-279.

Horton P, AV Ruban, D Rees, AA Pascal, G Noctor and AJ Young (1991). Control of the light-harvesting function of chloroplast membranes by aggregation of the LHCII chlorophyll-protein complex. FEBS Lett 292(1-2): 1-4.

Horton P and AV Ruban (1992). Regulation of photosystem II. Photosynth Res 34: 375-385.

Horton P, AV Ruban and RG Walters (1994). Regulation of light harvesting in green plants. Plant Physiol 106: 415-420.

Huang D, RM Everly, RH Cheng, JB Heymann, H Schägger, V Sled, T Ohnishi, TS Baker and WA Cramer (1994). Characterization of the chloroplast cyt b_6f complex as a structural and functional dimer. Biochem 33: 4401-4409.

Jahns P, A Polle and W Junge (1988). The photosynthetic water oxidase: its proton pumping activity is short-circuited within the protein by DCCD. EMBO J 7(3): 589-594.

Johnson G and A Krieger (1994). Thermoluminescence as a probe of photosystem II in intact leaves: non-photochemical fluorescence quenching in peas grown in an intermittant light regime. Photosynth Res 41: 371-379.

Johnson GN, AJ Young and P Horton (1994). Activation of non-photochemical quenching in thylakoids and leaves. Planta 194: 550-556.

Johnson GN, AW Rutherford and A Krieger (1995). A change in the midpoint potential of the quinone Q_A in photosystem II associated with photoactivation of oxygen evolution. Biochim Biophys Acta 1229: 202-207.

Joliot P and R Delosme (1974). Flash-induced 519 nm absorption change in green algae. Biochim Biophys Acta 357: 267-284.

Joliot P and A Joliot (1984). Electron transfer between the two photosystems. I. Flash excitation under oxidising conditions. Biochim Biophys Acta 765: 210-218.

Joliot P and A Joliot (1985). Slow electrogenic phase and intersystem electron transfer in algae. Biochim Biophys Acta 806: 398-409.

Joliot P and A Joliot (1986). Proton pumping and electron transfer in the cytochrome b/f complex of algae. Biochim Biophys Acta 849: 211-222.

Joliot P and A Joliot (1992). Electron transfer between photosystem II and the cytochrome b/f complex: mechanistic and structural implications. Biochim Biophys Acta 1102: 53-61.

Joliot P, J Lavergne and D Béal (1992). Plastoquinone compartmentation in chloroplasts. I. Evidence for domains with different rates of photo-reduction. Biochim Biophys Acta 1101: 1-12.

Joliot P and A Joliot (1994). Mechanism of electron transfer in the cytochrome b/f complex of algae: Evidence for a semiquinone cycle. Proc Natl Acad Sci USA 91: 1034-1038.

Joliot A and P Joliot (1995). A shift in a chlorophyll spectrum associated with electron transfer within the cytochrome b/f complex. -In Photosynthesis: from Light to Biosphere (P. Mathis, ed.), Vol. II. pp. 615-618. Kluwer Academic Publishers, Dordrecht, The Netherlands. ISBN 0-7923-3858-8.

Jones RW and J Whitmarsh (1985). Origin of the electrogenic reaction in the chloroplast cytochrome b/f complex. Photobiochem Photobiophys 9: 119-127.

Jones RW and J Whitmarsh (1988). Inhibition of electron transfer and the electrogenic reaction in the cytochrome b/f complex by 2-n-nonyl-4-hydroxyquinoline N-oxide (NQNO) and 2,5-dibromo-3-methyl-6-isopropyl-p-benzoquinone (DBMIB). Biochim Biophys Acta 933: 258-268.

Junge W and HT Witt (1968). On the ion transport system of photosynthesis. Investigations on a molecular level. Z Naturforsch 23b: 244-254.

Junge W (1970). The critical electric potential difference for photophosphorylation. Eur J Biochem 14: 582-592.

Junge W (1977). Membrane potentials in photosynthesis. Annu Rev Plant Physiol 28: 503-536.

Junge W and A Polle (1986). Theory of proton flow along appressed thylakoid membranes under both non-stationary and stationary conditions. Biochim Biophys Acta 848: 265-273.

Junge W and S McLaughlin (1987). The role of fixed and mobile buffers in the kinetics of proton movement. Biochim Biophys Acta 890:1-5.

Junge W (1989). Protons, the thylakoid membrane, and the chloroplast ATP synthase. -In Bicarbonate,

chloride, and proton transport systems, Annals of The New York Academy of Sciences (J.H. Durham and M.A. Hardy, eds), Vol. 574, pp 268-286. The New York Academy of Sciences, New York.

Junesch U and P Gräber (1991). The rate of ATP-synthesis as a function of ΔpH and $\Delta\psi$ catalyzed by the active, reduced H$^+$-ATPase from chloroplasts. FEBS Lett 294(3): 275-278.

Katona E, S Neimanis, G Schönknecht and U Heber (1992). Photosystem I-dependent cyclic electron transport is important in controlling photosystem II activity in leaves under conditions of water stress. Photosynth Res 34: 449-464.

Knaff DB (1991). Regulatory phosphorylation of chloroplast antenna proteins. Trends Biochem Sci 16: 82-83.

Kramer DM and AR Crofts (1994). Re-examination of the properties and function of the b cytochromes of the thylakoid cytochrome bf complex. Biochim Biophys Acta 1184: 193-201.

Kramer DM, A Joliot, P Joliot and AR Crofts (1994). Competition among plastoquinol and artificial quinone/quinol couples at the quinol oxidizing site of the cytochrome bf complex. Biochim Biophys Acta 1184: 251-262.

Krause GH, C Vernotte and J-M Briantais (1982). Photoinduced quenching of chlorophyll fluorescence in intact chloroplasts and algae. Resolution into two components. Biochim Biophys Acta 679: 116-124.

Krauss N, W Hinrichs, I Witt, P Fromme, W Pritzkow, Z Dauter, C Betzel, KS Wilson, HT Witt and W Saenger (1993). Three-dimensional structure of system I of photosynthesis at 6 Å resolution. Nature 361: 326-331.

Krieger A and E Weis (1992). Energy-dependent quenching of chlorophyll-a-fluorescence: the involvement of proton-calcium exchange at photosystem 2. Photosynthetica 27(1-2): 89-98.

Krieger A, I Moya and E Weis (1992). Energy-dependent quenching of chlorophyll a fluorescence: effect of pH on stationary fluorescence and picosecond-relaxation kinetics in thylakoid membranes and photosystem II preparations. Biochim Biophys Acta 1102: 167-176.

Krieger A and E Weis (1993). The role of calcium in the pH-dependent control of photosystem II. Photosynth Res 37: 117-130.

Krieger A, E Weis and S Demeter (1993). Low-pH-induced Ca^{2+} ion release in the water-splitting system is accompanied by a shift in the midpoint redox potential of the primary quinone acceptor Q$_A$. Biochim Biophys Acta 1144: 411-418.

Kruip J, D Bald, E Boekema and M Rögner (1994). Evidence for the existence of trimeric and monomeric photosystem I complexes in thylakoid membranes of cyanobacteria. Photosynth Res 40: 279-286.

Kühlbrandt W and DN Wang (1991). Three-dimensional structure of plant light-harvesting complex determined by electron crystallography. Nature 350: 130-134.

Laasch H, C Ihle and G Günther (1993). Detecting localized proton currents in photophosphorylation by procaine inhibition of the transthylakoid pH-gradient. Biochim Biophys Acta 1140: 251-261.

Laisk A, V Oja and U Heber (1992). Steady-state and induction kinetics of photosynthetic electron transport related to donor side oxidation and acceptor side reduction of photosystem I in sunflower leaves. Photosynthetica 27(4): 449-463.

Laisk A and V Oja (1994). Range of photosynthetic control of postillumination P700$^+$ reduction rate in sunflower leaves. Photosynth Res 39: 39-50.

Laisk A and V Oja (1995). Coregulation of electron transport through PS I by cyt b_6f, excitation capture by P700 and acceptor side reduction. Time kinetics and electron transport requirement. Photosynth Res 45: 11-19.

Lavergne J and E Leci (1993). Properties of inactive photosystem II centers. Photosynth Res 35: 323-343.

Lee WJ and J Whitmarsh (1989). Photosynthetic apparatus of pea thylakoid membranes: Response to growth light intensity. Plant Physiol 89: 932-940.

Leegood RC, D Crowther, DA Walker and G Hind (1983). Energetics of photosynthesis in *Zea mays*. I. Studies of the flash-induced electrochromic shift and fluorescence induction in bundle sheath cells. Biochim Biophys Acta 722: 116-126.

Leibl W, J Breton, J Deprez and H-W Trissl (1989). Photoelectric study on the kinetics of trapping and charge stabilization in oriented PS II membranes. Photosynth Res 22: 257-275.

Linden L and Rodigus (1892). *In* Illustration Horticole xxxix, 79 t.557.

Lohse D, R Thelen and H Strotmann (1989). Activity equilibria of the thiol-modulated chloroplast H$^+$-ATPase as a function of the proton gradient in the absence and presence of ADP and arsenate. Biochim

Biophys Acta 976: 85-93.

Mamedov MD, OE Beshta, VD Samuilov and AY Semenov (1994). Electrogenicity at the secondary quinone acceptor site of cyanobacterial photosystem II. FEBS Lett 350: 96-98.

Mano J, C Miyake, U Schreiber and K Asada (1995). Photoactivation of the electron flow from NADPH to plastoquinone in spinach chloroplasts. Plant Cell Physiol 36(8): 1589-1598.

Mauzerall D and NL Greenbaum (1989). The absolute size of a photosynthetic unit. Biochim Biophys Acta 974: 119-140.

McNamara VP and K Gounaris (1995). Granal photosystem II complexes contain only the high redox potential form of cytochrome *b*-559 which is stabilised by the ligation of calcium. Biochim Biophys Acta 1231: 289-296.

Meiburg RF, HJ van Gorkom and RJ van Dorssen (1983). Excitation trapping and charge separation in photosystem II in the presence of an electrical field. Biochim Biophys Acta 724: 352-358.

Melis A and PH Homann (1975). Kinetic analysis of the fluorescence induction in 3-(3,4-dichlorophenyl)-1,1-dimethylurea poisoned chloroplasts. Photochem Photobiol 21: 431-437.

Melis A and JM Anderson (1983). Structural and functional organization of the photosystems in spinach chloroplasts. Antenna size, relative electron-transport capacity, and chlorophyll composition. Biochim Biophys Acta 724: 473-484.

Menger FM, SD Richardson and GR Bromley (1989). Ion conductance along lipid monolayers. J Am Chem Soc 111: 6893-6894.

Meunier PC and DS Bendall (1993). On the rates of cyclic electron transport around photosystem II in the presence of donor side limitation. Photosynth Res 37: 147-158.

Michel H and J Deisenhofer (1988). Relevance of the photosynthetic reaction center from purple bacteria to the structure of photosystem II. Biochem 27: 1-7.

Mitchell P (1976). Possible molecular mechanisms of the protonmotive function of cytochrome systems. J Theor Biol 62: 327-367.

Miyake C, U Schreiber and K Asada (1995). Ferredoxin-dependent and antimycin A-sensitive reduction of cytochrome *b*-559 by far-red light in maize thylakoids; participation of a menadiol-reducible cytochrome *b*-559 in cyclic electron flow. Plant Cell Physiol 36(4): 743-748.

Mohanty N and HY Yamamoto (1995). Mechanism of non-photochemical chlorophyll fluorescence quenching. I. The role of de-epoxidised xanthophylls and sequestered thylakoid membrane protons as probed by dibucaine. Aust J Plant Physiol 22: 231-238.

Mohanty N and HY Yamamoto (1996). Induction of two types of non-photochemical chlorophyll fluorescence quenching in carbon-assimilating intact spinach chloroplasts: the effects of ascorbate, de-epoxidation, and dibucaine. Plant Science 115: 267-275.

Morgan H, DM Taylor and ON Oliveira Jr (1991). Proton transport at the monolayer-water interface. Biochim Biophys Acta 1062: 149-156.

Moss DA and DS Bendall (1984). Cyclic electron transport in chloroplasts. The Q-cycle and the site of action of antimycin. Biochim Biophys Acta 767: 389-395.

Mould RM and C Robinson (1991). A proton gradient is required for the transport of two lumenal oxygen-evolving proteins across the thylakoid membrane. J Biological Chem 266(19): 12189-12193.

Mullet JE and CJ Arntzen (1980). Simulation of grana stacking in a model membrane system. Mediation by a purified light-harvesting pigment-protein complex from chloroplasts. Biochim Biophys Acta 589: 100-117.

Murakami S and L Packer (1970). Protonation and chloroplast membrane structure. J Cell Biol 47: 332-351.

Neher E and B Sakman (1976). Single channel currents recorded from membrane of denerved frog muscles. Nature 260: 799-802.

Nesbitt DM and SP Berg (1982). The influence of spinach thylakoid lumen volume and membrane proximity on the rotational motion of the spin label tempamine. Biochim Biophys Acta 679: 169-174.

Neubauer C and HY Yamamoto (1994). Membrane barriers and Mehler-peroxidase reaction limit the ascorbate available for violaxanthin de-epoxidase activity in intact chloroplasts. Photosynth Res 39: 137-147.

Nishio JN and IP Ting (1987). Carbon flow and metabolic specialization in the tissue layers of the crassulacean acid metabolism plant, *Peperomia camptotricha*. Plant Physiol 84: 600-604.

Nishio JN and J Whitmarsh (1993). Dissipation of the proton electrochemical potential in intact chloroplasts.

II. The pH gradient monitored by cytochrome *f* reduction kinetics. Plant Physiol 101: 89-96.

Noctor G, D Rees, A Young and P Horton (1991). The relationship between zeaxanthin, energy-dependent quenching of chlorophyll fluorescence, and trans-thylakoid pH gradient in isolated chloroplasts. Biochim Biophys Acta 1057: 320-330.

Noctor G, AV Ruban and P Horton (1993). Modulation of ΔpH-dependent nonphotochemical quenching of chlorophyll fluorescence in spinach chloroplasts. Biochim Biophys Acta 1183: 339-344.

Nuijs AM, VA Shuvalov, HJ van Gorkom, JJ Plijter and LNM Duysens (1986). Picosecond absorbance difference spectroscopy on the primary reactions and the antenna-excited states in photosystem I particles. Biochim Biophys Acta 850: 310-318.

Oettmeier W, S Reimer and K Link (1978). Quantitative structure-activity relationship of substituted benzoquinones as inhibitors of photosynthetic electron transport. Z Naturforsch 33c: 695-703.

Olive J, O Vallon, FA Wollman, M Recouvreur and P Bennoun (1986). Studies on the cytochrome *b₆/f* complex. II. Localization of the complex in the thylakoid membranes from spinach and *Chlamydomonas reinhardtii* by immunocytochemistry and freeze-fracture analysis of *b₆/f* mutants. Biochim Biophys Acta 851: 239-248.

Ooms JJJ, WJ Vredenberg and WF Buurmeijer (1989). Evidence for an electrogenic and a non-electrogenic component in the slow phase of the P515 response in chloroplasts. Photosynth Res 20: 119-128.

Ooms JJJ (1990). Electrochromic absorbance changes in relation to electron transport and energy coupling in thylakoid membranes. Thesis Wageningen Agricultural University.

Ooms JJJ, W Versluis, PH van Vliet and WJ Vredenberg (1991). The flash-induced P515 shift in relation to ATPase activity in chloroplasts. Biochim Biophys Acta 1056: 293-300.

Ort DR and K Oxborough (1992). In situ regulation of chloroplast coupling factor activity. Annu Rev Plant Physiol Plant Mol Biol 43: 269-291.

Oxborough K and P Horton (1987). Characterisation of the effects of antimycin A upon high energy state quenching of chlorophyll fluorescence (qE) in spinach and pea chloroplasts. Photosynth Res 12: 119-128.

Osváth Sz, G Meszéna, V Barzda and G Garab (1994). Trapping magnetically oriented chloroplast thylakoid membranes in gels for electric measurements. J Photochem Photobiol 26: 287-292.

Pace RJ, AB Hope and P Smith (1992). Detection of flash-induced quinone radicals in spinach chloroplasts. Biochim Biophys Acta 1098: 209-216.

Peter GF and JP Thornber (1991). Biochemical composition and organization of higher plant photosystem II light-harvesting pigment-proteins. J Biol Chem 266: 16745-16754.

Pokorny A, K Wulf and H-W Trissl (1994). An electrogenic reaction assiciated with the re-reduction of P680 by Tyr Z in photosystem II. Biochim Biophys Acta 1184: 65-70.

Polle A and W Junge (1986). The slow rise of the flash-light-induced alkalization by photosystem II of the suspending medium of thylakoids is reversibly related to thylakoid stacking. Biochim Biophys Acta 848: 257-264.

Polle A and W Junge (1989). Proton diffusion along the membrane surface of thylakoids is not enhanced over that in bulk water. Biophys J 56: 27-31.

Prince RC, SJG Linkletter and PL Dutton (1981). The thermodynamic properties of some commonly used oxidation-reduction mediators, inhibitors and dyes, as determined by polarography. Biochim Biophys Acta 635: 132-148.

Racker E (1976). Phosphorylation and membranology. -*In* A New Look at Mechanisms in Bioenergetics (E. Racker, ed.). Academic Press, New York, USA, p. 62. ISBN 0-12-574670-9.

Raghavan K, M Rami Reddy and ML Berkowitz (1992). A molecular dynamics study of the structure and dynamics of water between dilauroylphosphadidylethanolamine bilayers. Langmuir 8: 233-240.

Rees D, A Young, G Noctor, G Britton and P Horton (1989). Enhancement of the ΔpH-dependent dissipation of excitation energy in spinach chloroplasts by light-activation: correlation with the synthesis of zeaxanthin. FEBS Lett 256(1,2): 85-90.

Rees D and P Horton (1990). The mechanisms of changes in photosystem II efficiency in spinach thylakoids. Biochim Biophys Acta 1016: 219-227.

Rees D, GD Noctor and P Horton (1990). The effect of high-energy-state excitation quenching on maximum and dark level chlorophyll fluorescence yield. Photosynth Res 25: 199-211.

Rees D, GD Noctor, AV Ruban, J Crofts, A Young and P Horton (1992). pH dependent chlorophyll

fluorescence quenching in spinach thylakoids from light treated or dark adapted leaves. Photosynt Res 31: 11-19.

Renger G, H-J Eckert, A Bergmann, J Bernarding, B Liu, A Napiwotzki, F Reifarth and HJ Eichler (1995). Fluorescence and spectroscopic studies of exciton trapping and electron transfer in photosystem II of higher plants. Aust J Plant Physiol 22: 167-181.

Rich PR and DS Bendall (1980). The kinetics and thermodynamics of the reduction of cytochrome c by substituted p-benzoquinols in solution. Biochim Biophys Acta 592: 506-518.

Rich PR and M Wikström (1986). Evidence for a mobile semiquinone in the redox cycle of the mammalian cytochrome bc_1 complex. FEBS Lett 194(1): 176-182.

Rich PR (1988). A critical examination of the supposed variable proton stoichiometry of the chloroplast cytochrome bf complex. Biochim Biophys Acta 932: 33-42.

Rich PR, SA Madgwick and DA Moss (1991). The interactions of duroquinol, DBMIB and NQNO with the chloroplast cytochrome bf complex. Biochim Biophys Acta 1058: 312-328.

Rich PR, SA Madgwick, S Brown, G von Jagow and U Brandt (1992). MOA-stilbene: A new tool for investigation of the reactions of the chloroplast cytochrome bf complex. Photosynth Res 34: 465-477.

Rigaud JL and CM Gary-Bobo (1977). Cation diffusion selectivity in pore model. The phosphatidylcholine/water lamellar phase. Biochim Biophys Acta 469: 246-256.

Robertson DE and PL Dutton (1988). The nature and magnitude of the charge-separation reactions of ubiquinol cytochrome c_2 oxidoreductase. Biochim Biophys Acta 935: 273-291.

Robinson HH and AR Crofts (1983). Kinetics of the oxidation-reduction reactions of the photosystem II quinone acceptor complex, and the pathway for deactivation. FEBS Lett 153(1): 221-226.

Rögner M, JP Dekker, EJ Boekema and HT Witt (1987). Size, shape and mass of the oxygen-evolving photosystem II complex from the thermophilic cyanobacterium *Synechococcus* sp. FEBS Lett 219: 207-211.

Rögner M, EJ Boekema and J Barber (1996). How does photosystem 2 split water? The structural basis of efficient energy conversion. Trends Biochem Sci 21: 44-49.

Romanowska E and P-Å Albertsson (1994). Isolation and characterization of the cytochrome bf complex from whole thylakoids, grana and stroma lamellae vesicles from spinach chloroplast. Plant Cell Physiol 35: 557-568.

Rosing J and EC Slater (1972). The value of $\Delta G°$ for the hydrolysis of ATP. Biochim Biophys Acta 267: 275-286.

Rottenberg H, T Grunwald and M Avron (1972). Determination of ΔpH in chloroplasts. 1. Distribution of [^{14}C]methylamine. Eur J Biochem 25: 54-63.

Ruban AV and P Horton (1992). Mehanism of ΔpH-dependent dissipation of absorbed excitation energy by photosynthetic membranes. 1. Spectroscopic analysis of isolated light-harvesting complexes. Biochim Biophys Acta 1102: 30-38.

Ruban AV, RG Walters and P Horton (1992a). The molecular mechanism of the control of excitation energy dissipation in chloroplast membranes. Inhibition of ΔpH-dependent quenching of chlorophyll fluorescence by dicyclohexylcarbodiimide. FEBS Lett 309(2): 175-179.

Ruban AV, D Rees, AA Pascal and P Horton (1992b). Mechanism of ΔpH-dependent dissipation of absorbed excitation energy by photosynthetic membranes. II. The relationship between LHCII aggregation in vitro and qE in isolated thylakoids. Biochim Biophys Acta 1101: 39-44.

Ruban AV, AJ Young and P Horton (1993). Induction of nonphotochemical energy dissipation and absorbance changes in leaves. Evidence for changes in the state of the light-harvesting system of photosystem II in vivo. Plant Physiol 102: 741-750.

Ruban AV, A Young and P Horton (1994). Modulation of chlorophyll fluorescence quenching in isolated light harvesting complex of photosystem II. Biochim Biophys Acta 1186: 123-127.

Rumberg B and A Berry (1995). Refined measurement of the H^+/ATP coupling ratio at the ATP synthase of chloroplasts. -*In* Photosynthesis: from Light to Biosphere (P. Mathis, ed.), Kluwer Academic Press. Vol III, pp. 139-142. ISBN 0-7923-3859-6.

Rutherford AW, AR Crofts and Y Inoue (1982). Thermoluminescence as a probe of photosystem II photochemistry. The origin of the flash-induced glow peaks. Biochim Biophys Acta 682: 457-465.

Sailaja MV and VS Rama Das (1995). Photosystem II acclimation to limiting growth light in fully developed

leaves of *Amaranthus hypochondriacus* L., an NAD-ME C$_4$ plant. Photosynth Res 46: 227-233.

Sakurai I and Y Kawamura (1989). Effect of a magnetic field on charge flow along the interface between phosphatidylcholine monolayer and water. Biochim Biophys Acta 985: 347-350.

Samson G and DC Fork (1992). Simultaneous photoreduction and photooxidation of cytochrome *b*-559 in photosystem II treated with carbonylcyanide-*m*-chlorophenylhydrazone. Photosynth Res 33: 203-212.

Santini C, V Tidu, G Tognon, G Magaldi and R Bassi (1994). Three-dimensional structure of the higher-plant photosystem II reaction centre and evidence for its dimeric organisation *in vivo*. Eur J Biochem 221: 307-315.

Satoh K, Ö Hansson and P Mathis (1990). Charge recombination between stabilized P-680$^+$ and reduced cytochrome *b*-559 in quinone-reconstituted PS II reaction center. Biochim Biophys Acta 1016: 121-126.

Satoh K, H Koike, T Ichimura and S Katoh (1992). Binding affinities of benzoquinones to the Q$_B$ site of photosystem II in *Synechococcus* oxygen-evolving preparation. Biochim Biophys Acta 1102: 45-52.

Satoh K, M Oh-hashi, Y Kashino and H Koike (1995). Mechanism of electron flow through the Q$_B$ site in photosystem II. 1. Kinetics of the reduction of electron acceptors at the Q$_B$ and plastoquinone sites in photosystem II particles from the cyanobacterium *Synechococcus vulcanus*. Plant Cell Physiol 36(4): 597-605.

Saygin Ö and HT Witt (1985). Evidence for the electrochromic identification of the change of charges in the four oxidation steps of the photoinduced water cleavage in photosynthesis. FEBS 187(2): 224-226.

Schapendonk AHCM and WJ Vredenberg (1977). Salt-induced absorbance changes of *P*-515 in broken chloroplasts. Biochim Biophys Acta 462: 613-621.

Schapendonk AHCM, WJ Vredenberg and WJM Tonk (1979). Studies on the kinetics of the 515 nm absorbance changes in chloroplasts. Evidence for the induction of a fast and a slow P515 response upon saturating light flashes. FEBS Lett 100(2): 325- 330.

Schapendonk AHCM (1980). Electrical events associated with primary photosynthetic reactions in chloroplast membranes. Thesis, Agric Univ Wageningen, The Netherlands.

Schliephake W, W Junge and HT Witt (1968). Correlation between field formation, proton translocation, and the light reactions in photosynthesis. Z Naturforsch 23b: 1571-1578.

Schlodder E and B Meyer (1987). pH dependence of oxygen evolution and reduction kinetics of photooxidized chlorophyll *a*$_{II}$ (P-680) in photosystem II particles from *Synechococcus* sp. Biochim Biophys Acta 890: 23-31.

Schönknecht G, R Hedrich, W Junge and K Raschke (1988). A voltage-dependent chloride channel in the photosynthetic membrane of a higher plant. Nature 336: 589-592.

Schönknecht G, G Althoff and W Junge (1990). The electrical unit size of thylakoid membranes. FEBS Lett 277(1,2): 65-68.

Schönknecht G, S Neimanis, E Katona, U Gerst and U Heber (1995). Relationship between photosynthetic electron transport and pH gradient across the thylakoid membrane in intact leaves. Proc Natl Acad Sci USA 92: 12185-12189.

Schreiber U (1986). Detection of rapid induction kinetics with a new type of high-frequency modulated chlorophyll fluorometer. Photosynth Res 9: 261-272.

Schreiber U, U Schliwa and W Bilger (1986).Continuous recording of photochemical and non-photochemical chlorophyll fluorescence quenching with a new type of modulation fluorometer. Photosynth 10: 51-62.

Schreiber U and C Neubauer (1987). The polyphasic rise of chlorophyll fluorescence upon onset of strong continuous illumination: II. Partial control by the photosystem II donor side and possible ways of interpretation. Z Naturforsch 42c: 1255-1264.

Schreiber U, C Klughammer and C Neubauer (1988). Measuring P700 absorbance changes around 830nm with a new type of pulse modulation system. Z Naturforsch 43c: 686-698.

Schreiber U and C Neubauer (1989). Correlation between dissipative fluorescence quenching at photosystem II and 50 µs recombination luminescence. FEBS Lett 258(2): 339-342.

Schreiber U and C Neubauer (1990). O$_2$-dependent electron flow, membrane energization and the mechanism of non-photochemical quenching of chlorophyll fluorescence. Photosynth Res 25: 279-293.

Schürmann P, BB Buchanan and DI Arnon (1971). Role of cyclic photophosphorylation in photosynthetic carbon dioxide assimilation by isolated chloroplasts. Biochim Biophys Acta 267: 111-124.

Schuurmans JJ, RP Casey and R Kraayenhof (1978). Transmembrane electrical potential formation in

spinach chloroplasts. FEBS Lett 94(2): 405-409.

Sewe K-U and R Reich (1977). Influence of the chlorophylls on the electrochromism of carotenoids in the membranes of photosynthesis. FEBS Lett 80(1): 30-34.

Shahak Y, A Admon and M Avron (1982). Transmembrane electrical potential formation by chloroplast ATPase complex (CF_1-CF_0) proteoliposomes. FEBS Lett 150(1): 27-31.

Sigalat C, F Haraux, F de Kouchkovsky, SPN Hung and Y de Kouchkovsky (1985). Adjustable microchemiosmotic character of the proton gradient generated by systems I and II for photosynthetic phosphorylation in thylakoids. Biochim Biophys Acta 809: 403-413.

Siggel U (1976). The function of plastoquinone as a electron and proton carrier in photosynthesis. Bioelectrochem Bioenerg 3: 302-318.

Sigfridsson K, Ö Hansson and P Brzezinski (1995). Electrogenic light reactions in photosystem I: resolution of electron-transfer rates between the iron-sulfur centers. Proc Natl Acad Sci USA 92: 3458-3462.

Sipes DL and IP Ting (1985). Crassulacean acid metabolism and crassulacean acid metabolism modifications in *Peperomia camptotricha*. Plant Physiol 77: 59-63.

Skulachev VP (1982). The localized $\Delta\mu_{H+}$ problem. The possible role of the local electric field in ATP synthesis. FEBS Lett 146(1): 1-4.

Snel JFH (1985). Regulation of photosynthetic electron flow in isolated chloroplasts by bicarbonate, formate and herbicides. Thesis, Agric Univ Wageningen, The Netherlands.

Snel JFH, H Boumans and WJ Vredenberg (1992). Formation of inactive PS2 centers in spinach leaves during light adaptation. -*In* Research in Photosynthesis (N. Murata, ed.), Vol. IV. pp. 615-818. Kluwer Academic Publishers, Dordrecht, The Netherlands.

Squires GL (1976). Practical physics. McGraw-Hill, London.

Steinhoff H-J, B Kramm, G Hess, C Owerdieck and A Redhardt (1993). Rotational and translational water diffusion in the hemoglobin hydration shell: dielectric and proton nuclear relaxation measurements. Biophys J 65: 1486-1495.

Stys D (1995). Stacking and separation of photosystem I and photosystem II in plant thylakoid membranes: A physico-chemical view. Physiol Plant 95: 651-657.

Tanaka-Kitatani Y, K Satoh and S Satoh (1990). Interaction of benzoquinones with Q_A^- and Q_B^- in oxygen-evolving photosystem II particles from the thermophilic cyanobacterium *Synechococcus elongatus*. Plant Cell Physiol 31(7): 1039-1047.

Terashima I and Y Inoue (1985). Vertical gradient in photosynthetic properties of spinach chloroplasts dependent on intra-leaf light environment. Plant Cell Physiol 26: 781-785.

Ting IP, J Hann, D Sipes, A Patel and LL Walling (1993). Expression of p-enolpyruvate carboxylase and other aspects of CAM during the development of *Peperomia camptotricha* leaves. Bot Acta 106: 313-319.

Ting IP, A Patel, DL Sipes, PD Reid and LL Walling (1994). Differential expression of photosynthesis genes in leaf tissue layers of *Peperomia* as revealed by tissue printing. Am J Bot 81(4): 414-422.

Trebst A (1980). Inhibitors in electron flow: tools for the functional and structural localization of carriers and energy conservation sites. -*In* Methods Enzymol, Academic press, Inc, Vol. 69, pp. 675-715. ISBN 0-12-181969-8.

Trissl H-W, J Breton, J Deprez and W Leibl (1987). Primary electrogenic reactions of photosystem II as probed by the light-gradient method. Biochim Biophys Acta 893: 305-319.

Trissl H-W and W Leibl (1989). Primary charge separation in photosystem II involves two electrogenic steps. FEBS Lett 244(1): 85-88.

Vallon O, FA Wollman and J Olive (1986). Lateral distribution of the main protein complexes of the photosynthetic apparatus in *Chlamydomonas reinhardtii* and in spinach: An immunocytochemical study using intact thylakoid membranes and a PS II enriched membrane preparation. Photobiochem Photobiophys 12: 203-220.

Van Best JA and P Mathis (1978). Kinetics of reduction of the oxidized primary electron donor of photosystem II in spinach chloroplasts and in Chlorella cells in the microsecond and nanosecond time ranges following flash excitation. Biochim Biophys Acta 503: 178-188.

Van Kooten O, AGM Gloudemand and WJ Vredenberg (1983). On the slow component of P-515 and the flash-induced reduction of cytochrome *b*-563 in chloroplast membranes. Photobiochem Photobiophys 6:

9-14.

Van Kooten O, JFH Snel and WJ Vredenberg (1986). Photosynthetic free energy transduction related to the electric potential changes across the thylakoid membrane. Photosynth Res 9: 211-227.

Van Kooten O (1988). Photosynthetic Free Energy Transduction. Thesis Wageningen Agricultural University.

Van Kooten O and JFH Snel (1990). The use of chlorophyll fluorescence nomenclature in plant stress physiology. Photosynth Res 25: 147-150

Velthuys BR (1978). A third site of proton translocation in green plant photosynthetic electron transport. Proc Natl Acad Sci USA 75(12): 6031-6034.

Velthuys BR (1981a). Electron-dependent competition between plastoquinone and inhibitors for binding to photosystem II. FEBS Lett 126(2): 277-281.

Velthuys BR (1981b). Carotenoid and cytochrome b 559 reactions in photosystem II in the presence of tetraphenylboron. FEBS Lett 126(2): 272-276.

Vermaas WFJ, G Renger and G Dohnt (1984). The reduction of the oxygen-evolving system in chloroplasts by thylakoid components. Biochim Biophys Acta 764: 194-202.

Voorthuysen T van, JHA Dassen, JFH Snel and WJ Vredenberg (1995). Temporary suppression of the flash-induced electrical potential across the thylakoid membrane upon energization. Physiol Plant 94: 729-735.

Voorthuysen T van, AA Bulychev, JHA Dassen, JFH Snel and WJ Vredenberg (1996a). Suppression of flash-induced PSII-dependent electrogenesis caused by proton pumping in chloroplasts. Physiol Plant 98: 156-164.

Voorthuysen T van, JHA Dassen, JFH Snel and WJ Vredenberg (1996b). Patch-clamp study on flash-induced secondary electrogenic transport in the thylakoid membrane. Interpretation in terms of a Q-cycle. Biochim Biophys Acta. 1277: 226-236.

Voorthuysen T van, AA Bulychev, JFH Snel, JHA Dassen and WJ Vredenberg (1997). Flash-induced conductance changes in chloroplast thylakoid lamellae. A patch-clamp study. Bioelectrochem Bioenerg, in press.

Vos MH and HJ van Gorkom (1990). Thermodynamical and structural information on photosynthetic systems obtained from electroluminescence kinetics. Biophys J 58: 1547-1555.

Vos MH, HJ van Gorkom and PJ van Leeuwen (1991). An electroluminescence study of stabilization reactions in the oxygen-evolving complex of photosystem II. Biochim Biophys Acta 1056: 27-39.

Vredenberg WJ and WJM Tonk (1975). On the steady-state electrical potential difference across the thylakoid membranes of chloroplasts in illuminated plant cells. Biochim Biophys Acta 387: 580-587.

Vredenberg WJ (1976). Electrical interactions and gradients between chloroplast compartments and cytoplasm. -In The Intact Chloroplast (J. Barber, ed.). Elsevier/North-Holland Biomedical Press, The Netherlands, pp. 54-88. ISBN 0-444-41451-7.

Vredenberg WJ and AA Bulychev (1976). Changes in the electrical potential across the thylakoid membranes of illuminated intact chloroplasts in the presence of membrane-modifying agents. Plant Science Lett 7: 101-107.

Vredenberg WJ (1981). P515: A monitor of photosynthetic energization in chloroplast membranes. Physiol Plant 53: 598-602.

Vredenberg WJ, JFH Snel, HJ Dassen and T van Voorthuysen (1992). Electrogenesis and energy regulation in the photosynthetic membrane. -In Research in photosynthesis (N. Murata, ed.), Vol. II, pp. 681-684. Kluwer Academic Publishers, Dordrecht. ISBN 0-7923-2091-3.

Vredenberg W, A Bulychev, H Dassen, J Snel and T van Voorthuysen (1995a). A patch clamp method for determining single turnover charge separation in the chloroplast membrane. Biochim Biophys Acta 1230: 77-80.

Vredenberg WJ, AA Bulychev, Voorthuysen T van and JFH Snel (1995b). The electrical properties of the thylakoid membrane and its partitions ('brush borders') in relation to energy supply. -In Photosynthesis: from Light to Biosphere (P. Mathis, ed.), Vol. III. pp. 269-272. Kluwer Academic Publishers, Dordrecht, The Netherlands. ISBN 0-7923-3859-6.

Vredenberg WJ (1996). Electrogenesis in the photosynthetic membrane: Fields, Facts and Features. Bioelectrochem Bioenerg, in press.

Walker DA (1992). Excited leaves. New Phytol 121: 325-345.

References

Walters RG and P Horton (1991). Resolution of components of non-photochemical chlorophyll fluorescence quenching in barley leaves. Photosynth Res 27: 121-133.

Walraven HS van and RHA Bakels (1996). Function, structure and regulation of cyanobacterial and chloroplast ATP synthase. Physiol Planta 96: 526-532.

Wasielewski MR, DG Johnson, M Seibert and Govindjee (1989). Determination of the primary charge separation rate in isolated photosystem II reaction centers with 500-fs time resolution. Proc Natl Acad Sci USA 86: 524-528.

Weis E and JA Berry (1987). Quantum efficiency of photosystem II in relation to 'energy'-dependent quenching of chlorophyll fluorescence. Biochim Biophys Acta 894: 198-208.

Weis E and D Lechtenberg (1989). Fluorescence analysis during steady-state photosynthesis. Phil Trans R Soc Lond B 323: 253-268.

Weis E, D Lechtenberg and A Krieger (1990). Physiological control of primary photochemical energy conversion in higher plants. *-In* Current Research in Photosynthesis (M. Baltscheffsky, ed.), Vol. IV, pp. 307-312. Kluwer Academic Publishers, The Netherlands. ISBN 0-7923-0591-4.

Wikström M and K Krab (1986). The semiquinone cycle. A hypothesis of electron transfer and proton translocation in cytochrome *bc*-type complexes. J Bioenerg Biomembr 18(3): 181-193.

Witt HT (1967). *-In* Fast Reactions and Primary Processes in Chemical Kinetics (Claesson, S., ed.), Nobel Symposium V, Almqvist and Wiksell, Stockholm, Interscience Publ., New York, pp. 261-316.

Witt HT (1979). Energy conversion in the functional membrane of photosynthesis. Analysis by light pulse and electric pulse methods. The central role of the electric field. Biochim Biophys Acta 505: 355-427.

Wolff Ch, H-E Buchwald, H Rüppel, K Witt and HT Witt (1969). Rise time of the light induced electrical field across the function membrane of photosynthesis. Z Naturforsch 24B: 1038-1041.

Yamamoto HY (1985). Xanthophyll cycles. Method Enzymol 110: 303-312.

Yu S-G, G Björn and P-Å Albertsson (1993). Characterization of a non-detergent PS II - cytochrome *b/f* preparation (BS). Photosynth Res 37: 227-236.

Zickler A, HT Witt and G Boheim (1976). Estimation of the light-induced electrical potential at the functional membrane of photosynthesis using a voltage-dependent ionophore. FEBS Lett 66(1): 142-148.

Curriculum vitae

Tijmen van Voorthuysen werd op 4 augustus 1966 geboren te Helmond. In 1984 behaalde hij het VWO diploma aan het Dr.-Knippenbergcollege te Helmond en begon in september van hetzelfde jaar met de studie Moleculaire Wetenschappen aan de Landbouwuniversiteit te Wageningen. Het doctoraalexamen met fysisch-chemische oriëntatie werd in 1990 behaald met als hoofdvakken kolloid- en grensvlakchemie bij de vakgroep Fysische- en Kolloidchemie (prof. Lyklema) en moleculaire fysica bij de vakgroep Moleculaire Fysica (prof. Schaafsma). De praktijktijd Fysische- en Kolloidchemie werd doorgebracht bij het Institut Français du Pétrole (Paris, F.) op het gebied van de grensvlakchemie. In 1985 werd gestart met de studie Natuurkunde aan de Katholieke Universiteit te Nijmegen. Het propaedeuse examen werd behaald in 1987 waarna nog enkele tweede en derde jaars vakken werden gevolgd. Van 15 oktober 1990 tot 15 april 1996 was hij werkzaam als tijdelijk projectmedewerker (oio) in dienst van de Nederlandse organisatie voor Wetenschappelijk Onderzoek (NWO) en gestationeerd bij de vakgroep Plantenfysiologie van de Landbouwuniversiteit te Wageningen. Het project getiteld 'Energy Regulation in the Chloroplast Membrane' betrof biofysisch onderzoek onder auspiciën van prof. Vredenberg en heeft geleid tot dit proefschrift. Sinds 1 april 1997 verricht hij in het kader van een EG-project onderzoek naar het fosfaat-metabolisme in planten bij de vakgroep Plantenfysiologie in samenwerking met de vakgroep Moleculaire Fysica van de Landbouwuniversiteit in Wageningen.